TECHNISCHE UNIVERSITÄT MÜNCHEN

Lehrstuhl für Bioverfahrenstechnik

Biphasic whole-cell synthesis of *R*-2-octanol with recycling of the ionic liquid

Danielle Dennewald

Vollständiger Abdruck der von der Fakultät für Maschinenwesen der Technischen Universität München zur Erlangung des akademischen Grades eines

Doktor-Ingenieurs

genehmigten Dissertation.

Vorsitzende:		Univ.-Prof. Dr. rer. nat. Sonja Berensmeier
Prüfer der Dissertation:	1.	Univ.-Prof. Dr.-Ing. Dirk Weuster-Botz
	2.	Univ.-Prof. Dr. sc. tech. Urs von Stockar, em. Eidgenössische Technische Hochschule Lausanne / Schweiz

Die Dissertation wurde am 19.04.2011 bei der Technischen Universität München eingereicht und durch die Fakultät für Maschinenwesen am 29.07.2011 angenommen.

Preface

Many people have contributed to the present thesis in many different ways. I would like to express my gratitude to the following:

Prof. Dr.-Ing. Dirk Weuster-Botz for giving me the opportunity to do my PhD at his institute, for the excellent supervision of the project and for his great support during the last years.

Prof. Dr. sc. tech. Urs von Stockar for accepting to be co-examiner and Prof. Dr. rer. nat. Sonja Berensmeier for taking over the position of the chairman of the jury.

The National Research Fund, Luxembourg (grant no. PHD-09-064) and the German Federal Ministry of Education and Research (grant no. 03X2011C) for the financial support of this project.

My cooperation partners during the project PRAKTIBIOKAT: Dr. William Pitner (Merck KGaA) for kindly providing the ionic liquids used during this project. Dr. Jeffrey Lutje-Spelberg (Julich Chiral Solutions, Codexis Company) for providing the biocatalyst (*Escherichia coli* BL21 (DE3) T1r(pET24a-adhL.brevis-fdhC.boidinii)). Prof. Dr.-Ing. Jörg Thöming (UFT Bremen) and his staff for their contribution to the project.

Dr. Stefan Bräutigam for the introduction into the subject of whole-cell biocatalysis in biphasic ionic liquid-water systems.

My students Florian Baumgärtner, Anna Groher, Nico Jäger, Florian Loga, and Julia Tröndle for their contribution to this project and for the good times we spent together in the lab.

All my colleagues and former colleagues for the great work atmosphere and the good times we had outside the working hours. A special thank you to those who were more closely involved in my project through many interesting and very helpful discussions: Michael

Weiner, Gabi Gebhardt, Torben Höfel, Clara Delhomme and Kathrin Hölsch. Thank you for your invaluable advice, for sharing your knowledge - and brain power - and for being so generous with your time.

Thank you Clara, Kathrin and Ralph for proof-reading my thesis and for the helpful comments. Thank you Jens, for your great help with LaTeX.

Thank you Clara for the moments we shared together in our office. Thank you for your 24/7 support in absolutely everything, for your critical sense and your amazing gift to structure even the most confusing slide shows and manuscripts. Torben, thank you for making the tough moments better with your great sense of (black) humour.

Special thanks to my dear friends from Germany, Luxembourg and Switzerland, as well as to my sisters Martine and Isabelle, and to my brother François. Thank you for your great support and for making my life so much more interesting and fun.

Thank you to my parents for their support during all these years.

Ralph, thank you for your support, your patience and your love.

Contents

1 Introduction

Today, many areas of our every day life rely on chiral substances. A chiral molecule is a molecule lacking an internal plane of symmetry (Fig. 1.1). The same chiral molecule can thus occur under two different three-dimensional forms, called (*S*- and *R*-) enantiomers. They are a special form of stereoisomers, defined as 'a pair of molecular entities which are mirror images of each other and non-superposable' (Moss, 1996).

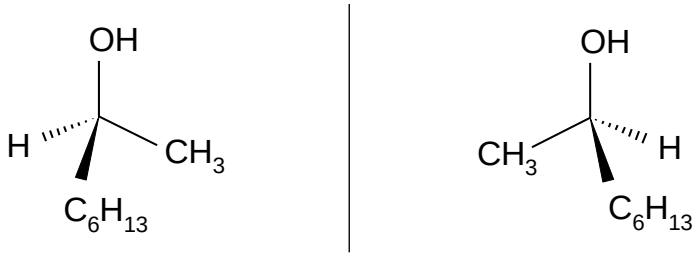

Figure 1.1: *S*-enantiomer (left) and *R*-enantiomer (right) of the chiral compound 2-octanol.

Enantiomers have very similar physical properties and the same chemical reactivity towards other achiral molecules. However, their respective interaction with other chiral compounds is different. For certain applications, involving the interaction of these chiral compounds with other chiral entities, enantiopure substances are therefore required, instead of a mix of both enantiomers. This requirement is then not only crucial for the correct functioning of these products, but the presence of both the *S*- and the *R*-enantiomer can even have dramatic consequences, as was illustrated by the Contergan scandal in the 1950s (Nguyen *et al.*, 2006). In order to avoid such scenarios, there is thus a strong demand for the production of enantiopure substances.

If the synthesis of the chiral entity is not enantioselective, a mix of both enantiomers is produced. As two enantiomers have such similar physical properties, a separation of the *S*-

and the *R*-enantiomer after their synthesis is very time and cost intensive. The preferred alternative is therefore to directly produce these substances at very high enantioselectivity. For several years, this has been successfully conducted by relying on biotechnology. Due to the high enantioselectivity of enzymes, these biological entities are indeed very suitable catalysts for asymmetric syntheses. In contrast to chemical catalyses, biocatalyses are in most cases one-step reactions and they generally occur in mild reaction conditions (e.g. room temperature and neutral pH). These factors are part of the reason why the industrial application of biotechnology ('White Biotechnology') showed such a large success during the last few decades.

One very frequently used group of chiral chemicals are chiral alcohols. They are building blocks for fine chemicals, agrochemicals and precursor molecules for pharmaceuticals, but they are also used in technical applications, such as liquid crystal displays. The production of enantiopure chiral alcohols is thus of large interest and the application of biocatalysis to produce these substances would permit to profit of the favourable features of this approach. However, chiral short-chain alcohols present a number of challenges to biocatalysis, which have not all been resolved to date. Efforts are therefore ongoing to develop new processes for the production of these chiral compounds at high enantioselectivity, and if possible, at reduced environmental impact.

2 Motivation and objectives

While many substrates can be successfully transformed by biocatalytic means, some substances still constitute a challenge. This is particularly true when the substrates and/or the products of interest are toxic towards the biocatalyst, when they show low water solubility or when they decompose in aqueous solutions. In many cases, the outcome of these biotransformations can be significantly improved by using a biphasic reaction setup, where the second phase acts as substrate reservoir and *in situ* product extractant.

Traditionally, biphasic setups were formed by adding a non-water miscible organic solvent to the aqueous phase containing the biocatalyst. Today, increased interest is given towards a new class of solvents: ionic liquids. Ionic liquids are salts with a melting point below 100 °C. They possess many interesting features, such as non-volatility and non-flammability, making them an attractive alternative to organic solvents. Using ionic liquids, the security and toxicity issues arising through the use of organic solvents and their fugitive emission could be reduced. While more and more biotransformations performed in biphasic setups with an ionic liquid were published during the last decade, most authors only demonstrated the feasibility of such reactions, but did not proceed to a detailed characterisation of the respective reaction systems. In order to take full advantage of the potential of these applications, more information on these biphasic reaction systems is however required. Only then, an optimisation of the productivity of the reaction and an evaluation for a possible industrial implementation of the process is possible.

This project was therefore concerned with a detailed characterisation of such a biphasic whole-cell biotransformation involving an ionic liquid as a non-water miscible second phase. To this aim, the asymmetric reduction of 2-octanone to *R*-2-octanol was considered, because it can figure as a model reaction for this kind of applications. Both the substrate and the product of this reaction are indeed toxic to living organisms (Tanaka *et al.*, 1987; Chen and Chiou, 1995), they show low water solubility (~ 1.1 g L^{-1} at 20 °C), and they inhibit some enzymes when present at large concentrations (Kohlmann *et al.*, 2011a). This biotransformation can thus only be successful when performed in a biphasic setup. Bräutigam *et al.* (2009) showed that this reduction could be performed by a recombinant

Escherichia coli in a biphasic ionic liquid-water reaction system. At 600 mM substrate in the ionic liquid, a conversion of 95 % was reached at an enantiomeric excess > 99.5 % (*R*) after 6 h. This demonstrated the feasibility of the reaction at a small scale and showed relatively good results in non-optimised conditions.

Taking this promising reaction setup as a starting point, the aim of this project was to further optimise and characterise the biphasic whole-cell biotransformation and to assess its suitability for an industrial application. To this aim, the following points were investigated:

1. Characterisation of the biotransformation:
    a) Evaluation of the biocompatibility of the system components and of the stability of the enzymes in the reaction conditions.
    b) Analysis of the effect of varying reaction conditions on the reaction outcome and parallel optimisation of the productivity of the reaction system.
    c) Investigation of the possibility to perform a scale-up in the optimised reaction conditions.
    d) Evaluation of the applicability of a high-throughput platform for the process development of biphasic reactions involving non-water miscible ionic liquids.
2. Characterisation of the biphasic reaction system:
    a) Evaluation of the physical properties of the different system components.
    b) Characterisation of the different mass transfers taking place during the biotransformation.
    c) Modelling of the reaction system.
3. Evaluation of the recyclability:
    a) Recycling of the ionic liquid.
    b) Recycling of the biocatalyst.

3 Fundamentals of whole-cell biocatalysis with ionic liquids

The first two sections of this chapter present a short introduction to whole-cell biocatalysis, its advantages and its limitations, and to a new class of solvents called ionic liquids. The following two sections focus on the use of these solvents in whole-cell biocatalysis: first, a general overview of what properties an ionic liquid should present to constitute a suitable solvent for applications in whole-cell biocatalysis will be given. Then, the state of the art of whole-cell biocatalysis in ionic liquids is presented.

3.1 Whole-cell biocatalysis

Biocatalysis has become a method of choice for producing fine chemicals, building blocks for the pharmaceutical industry and agrochemicals (Liese and Filho, 1999; Schmid *et al.*, 2001; Straathof *et al.*, 2002; Patel, 2002). Biocatalysis usually permits to reach higher yields and excellent (enantio)selectivities under milder reaction conditions than usually found in chemical catalysis. In addition, the use of enzymes as catalysts sometimes permits to reduce the number of steps required in comparison to the chemical approach. This simplifies the process and avoids waste products and subsequent purification steps (Nakamura *et al.*, 2003; Bommarius and Riebel-Bommarius, 2004).

Biocatalysis can be performed using either whole cells, or only the (purified) enzymes. Whole-cell biocatalysis presents two main advantages in comparison to the purely enzymatic approach: (1) the biocatalyst production is more rapid and less expensive because there is no need for enzyme purification steps after the cultivation; (2) using whole cells, a cell-internal cofactor regeneration system can be used, making an addition of these very costly substances not necessary. On the downside, the natural presence of other enzymes in the whole cell also accepting the substrate or the product might interfere with the wanted reaction and decreases the selectivity for the target product. This can be avoided by a strong overexpression of the enzymes of interest and a careful choice of the host cell.

In whole-cell biocatalysis, the cell-internal cofactor regeneration can either rely on an substrate-coupled or on an enzyme-coupled approach (Kroutil *et al.*, 2004). In the

substrate-coupled approach, the same enzyme as performing the main reaction of interest is used to regenerate the cofactor by transforming a co-substrate to the corresponding co-product. For example, if the reaction of interest is the reduction of a given ketone to its corresponding *R*- or *S*-alcohol through an alcohol dehydrogenase by consumption of NAD(P)H, then the cofactor could be regenerated by the oxidation of another alcohol to its corresponding ketone, consuming the oxidized form of the cofactor (NAD(P)) and restoring its reduced form (NAD(P)H) (Fig. 3.1).
The enzyme-coupled approach, in contrast, makes use of a different enzyme than the enzyme catalysing the main reaction for the regeneration of the cofactor (Fig. 3.2).

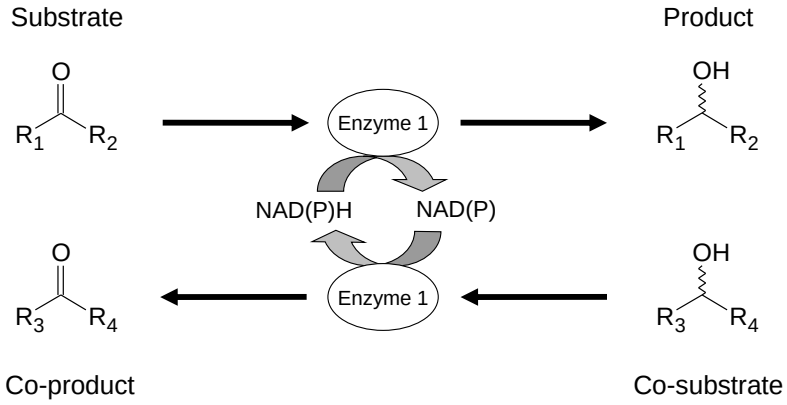

Figure 3.1: Substrate coupled cofactor regeneration: the same enzyme that performs the reaction of interest is used to regenerate the cofactor by transforming a co-substrate to its corresponding co-product.

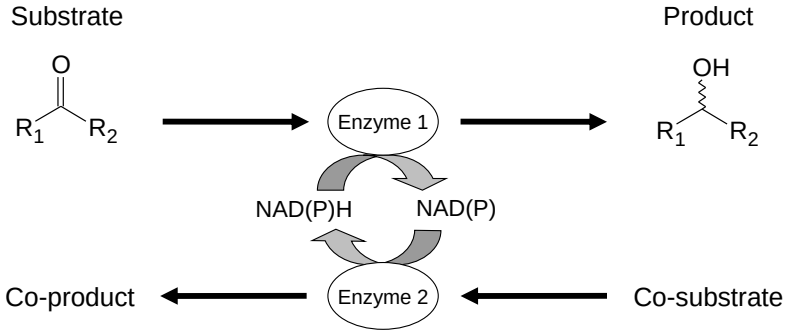

Figure 3.2: Enzyme coupled cofactor regeneration: the cofactor is regenerated by a second enzyme transforming a co-substrate to its corresponding co-product.

Organic compounds presenting low water solubility and/or toxicity to the biocatalyst make the application of whole-cell biocatalysis difficult (Straathof *et al.*, 2002). These substrate/products cannot be added in large quantities into the reaction system, or not without risking to intoxicate and damage the biocatalyst. The productivity will thus remain low. Several techniques have been developed to overcome these limitations.

The solubility of a substance can be increased by adding solubilizers, like short chain alcohols, dimethyl sulfoxide (DMSO) or cyclodextrines. The drawback of these methods is that either the solubilizers are toxic or they form too strong complexes and thereby limit the reaction rate.

Microemulsions formed by the addition of surfactants, encapsulation of the biocatalyst in alginate beads and the use of membrane reactors have the same goal: protect the biocatalyst from too intense contact with the toxic substances, either by isolating the biocatalyst or the substrate from the rest of the reaction system. Unfortunately, microemulsions are often not very stable, and they constitute a supplemental component added to the system, difficult to get rid off once the biotransformation is finished. Alginate beads often limit the mass transfer, and enzyme membrane reactors significantly increase the cost of the equipment and its maintenance.

Often, a more elegant solution is to use a biphasic reaction mode. These reaction systems are composed of an aqueous buffer, in which the biocatalyst is suspended, and a second, non-water miscible solvent. The solvent is chosen on basis of three criteria: (1) non-water miscibility, (2) biocompatibility, and (3) large partition coefficients of the substrate and the product in the solvent-buffer system. This way, the solvent phase can act as a substrate reservoir and *in situ* product extractant (Lye and Woodley, 1999): the substrate and the product will be found in majority in the solvent phase, and only in very low concentrations in the aqueous phase (Fig. 3.3). These very low concentrations of toxic substances in the aqueous phase limit the damage done to the biocatalyst, and, still, large quantities of substrate are available for the biotransformation.
For substrates and products, which are toxic, of low water solubility, or decomposing in the presence of water, the conversion reached during the process can be significantly increased by choosing a biphasic reaction mode. In addition, the product isolation is facilitated in a biphasic setup, because it is continuously extracted during the biotransformation, and thus already present at relatively large concentration in the solvent phase. This makes the down stream processing more cost-efficient.

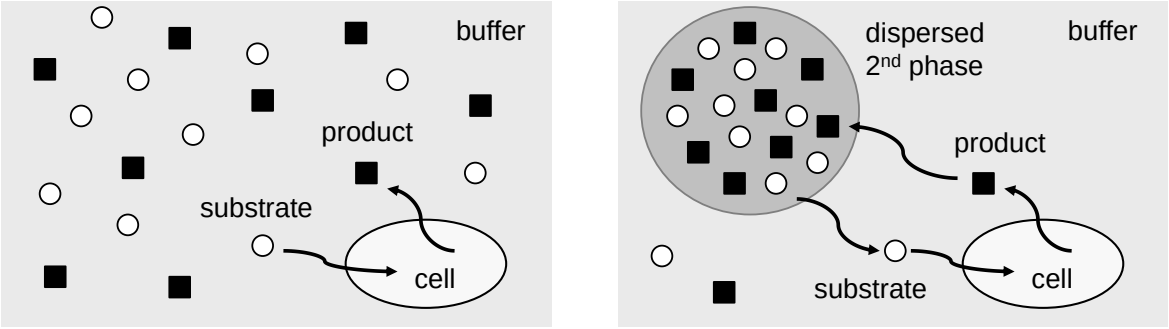

Figure 3.3: Monophasic and biphasic reaction modes for a biotransformation: the biocatalyst is suspended in the aqueous buffer. In the monophasic setup (left), the substrate is directly added into the buffer. In the biphasic setup (right), the majority of the substrate and the product is in the non-water miscible dispersed phase, and only low concentrations of both substances are found in the aqueous phase.

Traditionally, the second phases used in biphasic systems were organic solvents. However, their very volatile nature, the low flash point and the often toxic character make their use relatively inconvenient (Vermuë *et al.*, 1993). Today, a new class of solvents is seen as a more secure and potentially more environmentally friendly alternative to organic solvents: ionic liquids (IL).

3.2 Ionic liquids

Ionic liquids are commonly defined as salts with a melting point below 100 °C (Wasserscheid and Welton, 2003). They are totally ionic, nonaqueous solvents. Even though the specific composition of these solvents, and consequently their chemical and physical properties vary significantly, ionic liquids are almost invariably composed of an organic cation and an inorganic polyatomic anion (Wasserscheid and Welton, 2003). The relatively low melting point of these salts is due to the large and asymmetric structure of the composing anion and cation (Holbrey and Rogers, 2003). One of the main characteristics of ionic liquids is their very wide liquidus range of typically 300 K and sometimes even larger than 400 K (Seddon *et al.*, 2000; Jacquemin *et al.*, 2006). Almost no other molecular solvent presents such a wide span of temperatures between the melting point and the boiling point. Salts which are even fluid at room temperature are frequently called 'room temperature ionic liquids' (RTILs).

The reason why ionic liquids gained increasing attention during the last two decades is that ionic liquids show an interesting set of characteristics: they have very low vapour pressure, they are non-flammable and show generally high chemical and thermal stability (Wasserscheid and Keim, 2000; van Rantwijk *et al.*, 2003). Moreover, they solve both polar

and non-polar substances extraordinarily well. Ionic liquids thus constitute a welcome alternative to common used organic solvents, which often cause security and toxicity issues. Ionic liquids also present a wide electrochemical window, high conductivity, and a low dielectric constant. All of these properties led to a large range of applications of ionic liquids, including e.g. their use as solvents in catalysis, as extractant in liquid-liquid and gas separations, as lubricants and heat transfer fluids, or as electrolytes in batteries and fuel cells (Brennecke and Maginn, 2001).
Another interesting property of ionic liquids is that, by modifying the structure of the composing anions and cations, their physical characteristics such as e.g. the hydrophobicity, the viscosity, the acidity/basicity, or the co-ordination properties can be influenced. This led to the name 'designer solvents' (Seddon, 1997; Brennecke and Maginn, 2001), because 'task-specific' ionic liquids may indeed be designed to match the requirements imposed by the application of interest by choosing a different anion or cation or varying the substituents on either of them. The almost unlimited number of possible cation and anion combinations - according to estimations up to 10^{18} (Carmichael and Seddon, 2000) - offers thus an enormous range of varying properties, e.g. from hydrophobic to completely water-miscible ionic liquids, with densities higher or lower than water, and solvents with largely varying viscosity and acidic/basic properties. Similarly, while some ionic liquids are toxic to living organisms, others show particularly good biocompatibility (Pfruender *et al.*, 2004). This makes ionic liquids also very suitable as solvents in whole-cell biocatalysis.

The first report of the preparation of an ionic liquid was published by Walden (1914). They reported the preparation of ethylammonium nitrate, a salt with a melting point at 12 °C. However, the interest in ionic liquids only started developing in the 1970s and 1980s, when it was discovered that binary mixtures of alumininum(III) chloride and n-akylpyridinium or 1,3-dialkylimidazolium chloride were liquids at room temperature (Gale *et al.*, 1978; Wilkes *et al.*, 1982). These compounds had been developed for application as electrolytes in batteries. These first generation ionic liquids are however very unstable in the presence of water, and thus difficult to handle.
At the beginning of the 21st century, a new generation of air and moisture stable ionic liquids was developed. They mostly still contained imidazolium and pyridinium based cations, but the anions were formed by tetrafluoroborate ([BF4]), hexafluorophosphate ([PF6]), nitrate ([NO3]), tosylate ([TOS]), trifluoromethanesulfonate ([CF3SO3]) or halides such as bromide ([Br]) and iodate ([I]). These second generation ionic liquids permitted a much larger range of applications, which led to the increased attention they are receiving since the last two decades.

Today, increased effort is made to further expand the panel of available ionic liquids. The aims are to satisfy the requirements for an even broader range of possible applications and to produce less toxic and more environmentally friendly (third generation) ionic liquids. These are ionic liquids without halides, or including anions such as ethyl- and octylsulfate, which are more desirable from an (eco)toxicological point of view (Jacquemin *et al.*, 2006; Ranke *et al.*, 2007b). Ionic liquids based on naturally-derived moieties such as lactic acid, acetic acid, sugars and sugar substitutes, or on basis of amino acids have also been presented (Handy *et al.*, 2003; Carter *et al.*, 2004; Pernak *et al.*, 2004; Fukumoto *et al.*, 2005; Kagimoto *et al.*, 2006; Ou *et al.*, 2006). Such building blocks would make the largely synthetic ionic liquids bio-renewable and further reduce their hazard potential.

3.3 Ionic liquids for whole-cell biocatalysis

As discussed above (section 3.2), ionic liquids present many interesting features making them suitable solvents for whole-cell biocatalysis. However, several factors should be taken into account when choosing an ionic liquid for this kind of applications. In the following, the most important features will be discussed.

3.3.1 Biocompatibility

The first condition a solvent must satisfy to be considered for whole-cell biocatalysis is biocompatibility. This notion includes not only the impact of the solvent on cell growth and cell division, but also on the activity of the organism in presence of the solvent or after exposure to it. If the solvent is toxic to the biocatalyst, the biotransformation can hardly be successful, because the biocatalyst will rapidly be damaged and lose its activity. The biocompatibility of the ionic liquid depends on the nature of its composing anion and cation. To date, only one observation was consistently made in each of the biocompatibility studies: a significant effect of the length of the alkyl substituents on the cation. It was repeatedly noticed that, the longer these side chains are, the lower the tolerance of the organisms towards the solvent (Matsumoto *et al.*, 2004; Docherty and Kulpa, 2005; Evans, 2006; Yang *et al.*, 2009). This 'side chain effect' was observed for many different organisms covering a large variety of physiological and respiratory capabilities (aerobe, facultative anaerobe, Gram positive and Gram negative), including cocci, fungi and bacilli strains, and it was independent of the cation head group or the anion used (Pernak, 2001; Pernak *et al.*, 2003, 2004; Docherty and Kulpa, 2005; Pernak *et al.*, 2006; Lou *et al.*, 2009a,b). It is thus indeed a very general effect.

The explanation to these observation is the surfactant-like structure of cations with long alkyl chains (Evans, 2008a). Cations with relatively long alkyl chains are more lipophilic than cations with shorter alkyl chains, and undergo stronger interactions with the cell membrane. The consequences are facilitated insertion of the cation into the phospholipid bilayer and (partial) disintegration of the membrane, as well as accumulation of the toxic molecules inside the cells (Evans, 2006, 2008b; Cromie *et al.*, 2009). In contrast, the introduction of hydrophilic groups into the cation side chains reduces the overall toxicity of the ionic liquid under consideration (Lou *et al.*, 2009a,b). Based on the data currently available, it seems that the cation head group has only moderate influence on the biocompatibility.

Concerning the anion, a general influence of the anion's potential to hydrolyse or undergo other degradation reactions on toxicity has been observed. One example is [BF4], which frequently decreases the biocompatibility of the ionic liquid in comparison to other anions (Ganske and Bornscheuer, 2006; Lou *et al.*, 2006, 2009a; Zhang *et al.*, 2008). This increased toxicity is due to the decomposition of [BF4] in presence of water, forming hydrofluoric acid (Swatloski *et al.*, 2003; van Rantwijk and Sheldon, 2007). In addition, as for the cation, a slight influence of lipophilic side chains of the anion on the solvent's toxicity has been postulated (Cromie *et al.*, 2009). This might also be the reason for the toxicity that was observed in some cases for the [NTF] moiety (Bräutigam *et al.*, 2007; Cornmell *et al.*, 2008b; Wang *et al.*, 2009), even though not all sources confirmed the detrimental effect of this anion (Pfruender *et al.*, 2004, 2006).

The type of organism used is also, to some degree, of importance when considering the biocompatibility of an ionic liquid. Differences in the tolerance of the solvent have indeed been observed when using different cell types (Pernak, 2001; Pernak *et al.*, 2003; Baumann *et al.*, 2004; Matsumoto *et al.*, 2004; Docherty and Kulpa, 2005; Ganske and Bornscheuer, 2006; Pernak *et al.*, 2006; Hussain *et al.*, 2007; Dipeolu *et al.*, 2009). Still, to date, no reference was found describing that specific physiological properties provide particular tolerance or susceptibility to a given class of ionic liquids. The type of organism used is probably a parameter of smaller impact than the composition of the ionic liquid itself. More pronounced effects have been observed when comparing immobilized biocatalyst to the corresponding free cells: immobilization provides increased tolerance towards the solvent (Yang *et al.*, 2009).

The duration of the exposure and the concentration at which the solvent is present are also factors of major importance concerning the effect ionic liquids have on an organism (Yang *et al.*, 2009). Other parameters of influence are the effect of the solvent on the pH of the cell suspension (Lou *et al.*, 2009a), its water content (Li *et al.*, 2007; Zhang *et al.*,

2008; He *et al.*, 2009; Wang *et al.*, 2009; Yang *et al.*, 2009), as well as in some cases the ionic liquid's miscibility to water (Lee *et al.*, 2005; Ganske and Bornscheuer, 2006; Zhang *et al.*, 2008).

The mechanisms of action of the ionic liquids on given organisms is not yet fully elucidated, but the cell membrane is probably the primary target of the solvent toxicity. The interaction of ionic liquids with the phospholipid bilayer has been confirmed, as well as an increased permeability of the membrane when the biocatalyst is exposed to them (Pfruender *et al.*, 2004; Bräutigam *et al.*, 2007; Cornmell *et al.*, 2008b; Lou *et al.*, 2009a). Membrane-similar structures have been used to simulate the effect of different ionic liquid cations and anions on the cell membrane (Evans, 2006, 2008a,b; Cromie *et al.*, 2009). These analyses showed that the 1-alklyl-3-methyl imidazolium cations created small hole like defects in the membrane by inserting into the bilayer, provoking leakage (butyl- side chains) and in some cases even causing the complete disruption of the membrane (hexyl- and octyl side chains). The authors observed a partial incorporation of the alkyl chain of the cation and an accumulation of some ionic liquids at the water-membrane interface, giving rise to a nanometer thick deposit of ionic liquid. The anions did not show significant interaction with the membrane, except for [NTF] which contains slightly lipophilic side chains.
Accumulation of ionic liquid inside the cells was also observed. For these analyses, the authors relied on Fourier transform infrared (FT-IR) spectroscopy to analyse the chemical composition of the cells after exposition to ionic liquids (Cornmell *et al.*, 2008b) or made use of the fluorescent properties of dialkylimidazolium-based ionic liquids (Lou *et al.*, 2009a).

3.3.2 Availability and purity

To be considered for application in a given process, the solvent must be available at sufficient volume, but also at sufficient purity and affordable costs. Purity is a factor of major importance, because impurities resulting from the synthesis, such as halides or unreacted organic salts, easily accumulate in the ionic liquid and might not only influence the physical properties of the solvent, but also affect the reaction and the biocatalyst (Scammells *et al.*, 2005). The most common contaminant, however, is water, as even water immiscible ionic liquids are hygroscopic and can absorb a significant quantity up to a few weight percent (van Rantwijk and Sheldon, 2007). This does generally not harm the biocatalyst, but it can significantly affect the viscosity as well as other physical properties (Seddon *et al.*, 2000; Marsh, 2004), and it might interfere with the biotransformation under

investigation (Ghatee and Zolghadr, 2008). Consistent purity is also of high importance because only then reliable comparisons and analyses of existing data, as well as persistent process productivities are possible.

3.3.3 Stability

The ionic liquid of choice needs to be stable. The chemical stability of the solvent is a crucial feature and necessary to allow consistent quality of the solvent during the process, as well as during the storage before and possibly after it. Depending on the process, thermal stability might also be decisive. Thermal stability of ionic liquids is depending on the composing anions and cations, as well as on the presence of impurities, and might thus vary significantly from one case to another (Kosmulski *et al.*, 2004). The trend is leading away from ionic liquids containing [BF4] anions, as these tend to hydrolyse over time when in contact with humidity, and even more under heating conditions, forming hydrofluoric acid (Huddleston *et al.*, 2001; Swatloski *et al.*, 2003; Scammells *et al.*, 2005; Ohtani *et al.*, 2008). Generally, ionic liquids are however reported to present good thermal stability, showing little or no degradation up to temperature ranges of 150–200 °C (Awad, 2004; Kosmulski *et al.*, 2004; Bösmann *et al.*, 2007) . Sometimes, even values larger than 400 °C are indicated (Chiappe and Pieraccini, 2005; Wooster *et al.*, 2006; Ohtani *et al.*, 2008).

3.3.4 Process design criteria

Besides the previously cited factors, a range of process design criteria such as viscosity, density, corrosiveness and water miscibility have to be taken into account when choosing a suitable ionic liquid. These properties will be part of determining which reaction setup is applied.

Viscosity, density and corrosiveness

Ionic liquids generally show relatively large viscosity in comparison to their commonly used organic counterparts, but the values vary roughly within a range of 15–500 mPa s (Mantz and Trulove, 2003). Viscosity should be taken into consideration when choosing a suitable solvent, because too large viscosity might affect the homogenisation and the mass transfer during the process. However, it should be kept in mind that the viscosity of ionic liquids is dramatically decreased by the presence of already low amounts of water (Seddon *et al.*, 2000; Jacquemin *et al.*, 2006; Hussain *et al.*, 2007). Hence, many of the current applications involving ionic liquids along with an aqueous phase should not suffer

from mass transfer limitations due to the viscosity of the solvent.
Most ionic liquids available to date are denser than water, with typical values ranging from 1 g cm^{-3} to 1.6 g cm^{-3} (Marsh, 2004; Zhang *et al.*, 2006). Density of the solvent is generally only a matter of concern for biphasic ionic liquid-aqueous phase systems. In these cases, a minimal relative density difference of 20 % between the two phases is often desired, as this facilitates the phase separation at the end of the process by gravitational forces.
Corrosiveness was mainly observed for ionic liquids containing halides (Brennecke and Maginn, 2001). With the development of new second and third generation ionic liquids, this problem seems to be widely resolved.

Water miscibility

The miscibility of ionic liquids with water varies from fully miscible to virtually immiscible (Roosen *et al.*, 2008). It is known that this property depends largely on the anion-cation combination (Hussain *et al.*, 2007), but, nevertheless, the miscibility of ionic liquids with water is still perceived as varying widely and unpredictably (van Rantwijk and Sheldon, 2007). In contrast to organic solvents, where the concept of solvent polarity is relatively useful to predict the miscibility behaviour with water, this concept is too elusive to permit predictions concerning the water miscibility of ionic liquids (Dupont *et al.*, 2002). In fact, solvent-solute interactions in ionic liquids obey a dual interaction model: ionic liquids act like polar solvents towards polar molecules, but display non-polar character towards non-polar compounds (Armstrong *et al.*, 1999). As water miscibility is however such a decisive property in terms of process design, the development of structure-property relationships is a topic constantly investigated.
Recently, Ranke *et al.* (2009) tried to distinguish the contribution of the composing entities to the overall water solubility by splitting the activity coefficient of ionic liquids in water into anion and cation contributions. This was achieved by deriving the effect of the anion on overall water solubility by regression against experimentally determined cation hydrophobicity parameters. The derived anion hydrophobicity data, together with the measured cation hydrophobicity values, would then permit to predict the water solubility for not yet analyzed anion-cation combinations. The future will show if the proposed method will indeed facilitate the directed molecular design of ionic liquids and be accurate enough to match the expectations.

Monophasic vs. biphasic reaction mode

Depending on the solvent's miscibility with water, ionic liquids can either be used as solvents, cosolvents, or as second phase in biphasic reaction modes. While applications as solvent are not usual in whole-cell biocatalysis, both other types of applications are common. The choice for one of these reaction modes is mainly a question of reaction design, and less a matter of productivity. At least to date, the published data does not permit to generally relate water miscibility to better or worse biocompatibility or to larger productivity at the end of the whole-cell biotransformation (Matsuda *et al.*, 2006; Hussain *et al.*, 2007). In literature, examples of both types of reaction mode reaching good process productivities are found.
When used as a cosolvent, the reason for adding ionic liquid to whole-cell applications is generally its solubilising effect, i.e. that larger quantities of a given compound can be dissolved in the reaction system when water miscible ionic liquid is added to the aqueous buffer than without it. This permits to reach larger productivities than in a purely aqueous setup. However, one of the disadvantages of using water miscible ionic liquids is that the biocatalyst is exposed to increased molecular toxicity in comparison to biphasic reaction modes, where it is mainly affected by the phase toxicity. Similarly, the recovery of the ionic liquid from the monophasic reaction system after the biotransformation is relatively complicated and more elaborate separation techniques are necessary, as e.g. extraction by an organic solvent or nanofiltration. These involve not only a supplemental process step, but also generate larger costs and increased environmental pollution.

When relying on a biphasic reaction mode, the disadvantages of monophasic systems can be avoided, while larger substrate loading is still possible. This is why most of today's applications involve biphasic reaction systems with water immiscible ionic liquids rather than monophasic setups. Only a water immiscible solvent with sufficiently large partition coefficients (D) for the substrate and the product in the ionic liquid-buffer system will be able to act as a substrate reservoir and *in situ* product extractant. This limits the exposure of the cell to the toxic substrate and/or product and thus still permits higher substrate loading without risking inhibition and damage of the biocatalyst. Additionally, extracting the product from the reactive phase will shift the thermodynamic equilibrium towards the desired direction. As water miscible ionic liquids do not form a second phase, monophasic setups expose the biocatalyst to the complete amount of substrate and product present in the reaction system. The biotransformation might thus be limited both because of toxic effects and for thermodynamic reasons.

When choosing water immiscible ionic liquids for biphasic applications, solvents with partition coefficients in the ionic liquid-water system of log D ≥ 2 for the substrate and the product in the ionic liquid-aqueous phase system are generally preferred (Pfruender *et al.*, 2006). Such values would roughly permit to add substrate concentrations of the order of magnitude of several 100 mM to the ionic liquid, while still not surpassing substrate and product concentrations of only a few mM in the aqueous phase. This guarantees relatively low substrate concentrations in the aqueous phase, limiting the inhibition of the biocatalyst, and relatively large product concentration in the ionic liquid phase, making downstream processing more cost-efficient than in the corresponding monophasic reaction modes with relatively dilute product solutions at the end.
Non-miscibility with water also permits an uncomplicated recovery of the ionic liquid from the rest of the biotransformation media, as simple phase separation through gravitational forces is possible. This facilitates the possible recycling of the ionic liquid and decreases material loss, not only reducing the process costs, but also limiting the impact on the environment. Product recovery is also facilitated by a biphasic reaction mode. Once the ionic liquid phase is isolated from the rest of the reaction broth, the product can be recovered from the solvent using common separation techniques, such as distillation (if the product is thermally stable), pervaporation or extraction. These recovery methods are facilitated by the low vapor pressure and non flammability of ionic liquids in comparison to their organic analogues.

3.3.5 Hazard potential

As more and more effort is invested to make the production of fine chemicals more sustainable, relying on biocatalysis and replacing volatile organic solvents by non volatile ionic liquids is very attractive. Still, it cannot be completely excluded that some of the solvent will be lost during the process and will reach the environment, either by small quantities dissolving in the waste waters of the process, or when disposing of the solvent. Low hazard potential should therefore also be a criterion when choosing or designing an ionic liquid for a given application. Evaluations of the ionic liquids' hazard potential should include two factors: ecotoxicity and biodegradability of the solvent. The latter describes the persistence in the environment and thus on which time scale a spilling into the environment will have consequences, while the former gives an indication about the immediate severity of it.

From an ecotoxicological point of view, solvents composed of lipophilic entities should be avoided. Lipophilic cations and anions are indeed more harmful towards living organisms because these molecules undergo stronger interaction with the phospholipid bilayer composing the cell membrane, potentially distroying it by (partial) insertion into it (Ranke *et al.*, 2004, 2007b; Stolte *et al.*, 2007a,b; Ranke *et al.*, 2007a). For some applications, lipophilicity of the solvent is however a desired feature, e.g. when a biphasic reaction mode is wanted, because this feature often also means low water solubility. In these cases, a compromise has to be reached between reaction design criteria on one hand side and biocompatibility and environmentally safe solvents on the other hand side.

The biodegradability of a solvent is generally linked to the compound's chemical and thermal stability: more stable molecules - wished for in industrial applications - show longer persistence in the environment. This leads to a conflict, because large chemical and thermal stability are properties wanted for industrial applications, while they are undesired from an ecological point of view.
One possible strategy to increase the biodegradability is trying to create supplemental sites for enzymatic attacks during the biodegradation process by modifying the side chain structure. Including an ester function into the side chains could for example increase the degradation rate and level of some ionic liquids (Gathergood *et al.*, 2004; Garcia *et al.*, 2005; Harjani *et al.*, 2008, 2009). It should also be noted that, when modifying the structure of an ionic liquid to fit ecological purposes, the variation of physico-chemical properties this might induce has to be taken into account, and it should be verified afterwards if the ionic liquid is still suitable for the application under consideration.

Finally, the synthesis of the solvent under investigation should also be included into the previous considerations. Materials produced from non-toxic and biodegradable starting components are preferable, as e.g. ionic liquids synthesized on the basis of naturally-derived moieties such as lactic acid, acetic acid, sugars or amino acids (Handy *et al.*, 2003; Carter *et al.*, 2004; Pernak *et al.*, 2004; Fukumoto *et al.*, 2005; Kagimoto *et al.*, 2006; Ou *et al.*, 2006).

3.3.6 Recyclability

The recyclability of the solvent would not only limit waste production and thus be favourable from an ecological point of view, but it would also significantly reduce the process costs, especially considering the still very large expenses of ionic liquids. The

conditions for re-using the same ionic liquid batch are (1) stability of the material and (2) no accumulation of impurities in this phase over the different process cycles. Only then, constant productivity can be guaranteed. As mentioned above, most second generation ionic liquids present very good thermal and chemical stability. Accumulation of impurities other than degradation products from the ionic liquid might occur due to the process itself. This can be avoided by redesigning part of the process or by applying specific purification steps at the end of each cycle.
To date, little data is published about the recyclability of ionic liquids in whole-cell biocatalysis, even though this is surely a matter of great importance to industry. Only Zhang *et al.* (2008) showed data where the ionic liquid [BMIM][PF6] was reused for six subsequent biotransformations. As the large cost of ionic liquids is still holding back their application at large scale, it would however be important to investigate their recyclability over a large number of cycles. If ionic liquids can be re-used during many subsequent biotransformations without loss of productivity, this might help further trigger the interest in this class of materials.

3.4 State of the art

In 2000, Cull *et al.* (2000) were the first to publish the application of a room temperature ionic liquid in whole-cell biocatalysis. The authors considered a transformation that was limited by the low water solubility of the substrate. To overcome this limitation, a biphasic reaction mode was chosen (20 % v/v solvent), and the ionic liquid [BMIM][PF6] was used to avoid the standard implication of an organic solvent for such applications (here, toluene). After 20 min raction time, the product concentration detected in the reaction system with ionic liquid was larger than in the organic reference. This was the first demonstration of a successful application of ionic liquids in whole-cell biocatalysis.

Since then, several research groups have entered this promising field, and the number of applications of ionic liquids in whole-cell biocatalysis showed an impressive increase over the last decade. Most of the work involves biphasic reaction systems formed by a hydrophobic ionic liquid with an aqueous phase, as used in the pioneering work by Cull *et al.* (2000), because these present certain advantages over monophasic reaction modes (subsection 3.3.4). Nevertheless, some applications also involve hydrophilic ionic liquids as a cosolvent with the aqueous phase.
Most of the reactions studied in whole-cell biocatalysis involving ionic liquids are asymmetric reductions of ketones by oxidoreductases for the production of chiral alcohols. This

class of enzymes takes particular advantage of the whole-cell approach due to its need of cofactors to perform the reduction. Oxidoreductases are also one of the enzyme classes most used in industry (Jeromin, 2005), and thus the subject of ongoing research. Their large substrate spectrum involves toxic and low water soluble compounds, making biphasic reaction modes particularly attractive. Still, the applications involving ionic liquids are getting more and more diverse, already also including e.g. the deracemization of racemic alcohol mixtures (Tanaka *et al.*, 2009), the hydrogenation of C-C double bonds (Lenourry *et al.*, 2005), the degradation of xenobiotics (Baumann *et al.*, 2004) or even biodiesel fuel production (Arai *et al.*, 2010).
The cells used as biocatalyst cover a great diversity of microorganisms, ranging from the very commonly used (recombinant) *E. coli* and many different yeast species, to cocci, bacilli, or even strictly anaerobe organisms.
The ionic liquids studied are to date mostly those of the second generation, due to the larger amount of data available for these solvents. They are most of all (di)alkyl-imidazolium ionic liquids with fluorinated anions such as [PF6] or [NTF], but the diversity of ionic liquids found in literature increases.

In the following, some examples of interesting applications will be shortly described.

3.4.1 Asymmetric reductions by whole cells with ionic liquids

After Cull *et al.* (2000), Howarth *et al.* (2001) were the second group to present an application of ionic liquids in whole-cell biocatalysis. Bakers yeast immobilized in alginate beads was used to reduce different aliphatic and cyclic ketones in water-[BMIM][PF6] (1:10) mixtures (Howarth *et al.*, 2001). In comparison to literature data for biphasic systems composed of water and organic solvents, the ionic liquid involving systems performed generally better, with yields increased by up to 20 %. The enantiomeric excesses, however, were lower by up to 15 %. After Cull et al., this study showed that whole cells could indeed be active in biphasic reaction systems involving ionic liquids.

Pfruender *et al.* (2004, 2006) used three different hydrophobic ionic liquids ([BMIM][PF6], [BMIM][NTF] and [Oc3MeN][NTF]) in biphasic setups for the reduction of 4-chloro-acetophenone, tert-butyl-6-chloro-3,5-dioxohexanoate and 4-chloroacetoacetate to their corresponding alcohols by three different organisms (*Lactobacillus kefir* DSM20587, *E. coli* K12 (DSM 498) and *S. cerevisiae* FasB His6). The aim of this study was to demonstrate the possibility to increase the yield of such asymmetric reductions by using hydrophobic

ionic liquids instead of monophasic aqueous systems or biphasic reaction systems with organic solvents. All three model reactions confirmed the beneficial effect of involving ionic liquids in the biphasic whole-cell biotransformations. In addition to the significantly improved conversions observed, it could be demonstrated that the mass transfer between the ionic liquid and the aqueous phase was not limiting, even though the ionic liquid has a relatively large viscosity in comparison to commonly used organic solvents.

Matsuda *et al.* (2006) investigated the importance of the presence of minimal quantities of water in whole-cell reaction systems with ionic liquids. *Geotrichum candidum* IFO 5767 was used to reduce *(*-fluoroacetophenone to *S*-1-(o-fluorophenyl)ethanol in assays containing either the hydrophobic [BMIM][PF6] or the hydrophilic [EMIM][BF4]. When the dried cells were added into the pure ionic liquid, neither of the reaction systems showed conversion of the substrate after 16 h. To improve the activity, it was decided to add water to the assays. Interestingly, the outcome was different for both ionic liquids tested: while the assay containing the water immiscible ionic liquid [BMIM][PF6] showed a dramatic increase of yield (84 %), the assay with the water miscible solvent [EMIM][BF4] still led to only very small quantities of product ($<$ 1 % yield). The authors concluded that a water layer around the cells is essential for the biocatalyst to work properly. In order to permit the formation of a water layer in the water miscible ionic liquid, a water absorbing polymer was used to immobilize the biocatalyst. This guaranteed the presence of a minimal quantity of water near the biocatalyst. Indeed, using this setup, the reaction system with [EMIM][BF4] reached very satisfying 96 % yield. To confirm the success of this reaction setup, other ionic liquids and substrates were tested. In addition to the two ionic liquids cited above, the following solvents were introduced: [BMIM][BF4], [BMIM][NTF], [BMIM][CF3SO3], [EMIM][PF6], [EMIM][NTF], [EMIM][CF3SO3], [EMIM][NO3], [EMIM][MeSO4], [EMIM][EtSO4] and [OMIM][PF6]. The resulting conversions could however not be linked to the hydrophobic or hydrophilic properties of the different solvents.

Many authors presented optimisation studies where the effect of the ionic liquid volume fraction, the buffer pH, the reaction temperature, the initial substrate concentration on the reaction outcome was analysed (Lou *et al.*, 2006; Zhang *et al.*, 2008; He *et al.*, 2009; Wang *et al.*, 2009; Lou *et al.*, 2009a). Most of these studies evaluated a pool of ionic liquids, mostly including alkyl-1-methylimidazolium cations and [BF4] and [PF6] anions, and a large variation of different organisms. The optimal conditions reached varied depending on the organism, the ionic liquids, and the substrates used. However, all of the setups

performed better than their corresponding monophasic or biphasic organic counterparts. Similarly to the biocompatibility, a negative influence of the increasing length of the side chains of the cation on the final conversion of the biotransformation was observed (Wang *et al.*, 2009).

Hussain *et al.* (2007) attempted to link the conversion and the reaction rates observed during the biotransformation to physical properties of the ionic liquid such as the water miscibility, the density and the viscosity, its biocompatibility and the substrate solubility. Exemplarily, the reduction of a β-tetralone by *Trichosporon capitatum* MY1890 and *Rhodcoccus erythropolis* MA7213 was considered. The authors evaluated two hydrophobic ([BMIM][PF6] and [Oc3MeN][NTF]) and five hydrophilic ionic liquids ([EMIM][TOS], [BMIM][BF4], [BMIM][OcSO4], [BMIM][MDEGSO4] and [CABHEM][MeSO4]), chosen to represent a large diversity of possible anions and cations.
The observations made during the study correlated only partially with the viability measurements and the substrate solubility. This indicated that these parameters are probably part of the reasons for the observed variations in biocatalyst efficiency, but not the only ones. No predictable relationship between the physical properties and the activity data could be established. With the current lack of knowledge concerning the interaction of ionic liquids with the cells and the resulting effect on the reaction rate, the authors concluded that the screening of ionic liquids was currently still a more reliable method for applications in industry than rational selection.

Bräutigam *et al.* (2007, 2009) presented an extensive study including 21 different ionic liquids forming biphasic systems with aqueous phosphate buffer. The goal of this study was to determine guidelines permitting to reduce the number of ionic liquids that could be employed in biphasic whole-cell biocatalysis to the few most appropriate ones for a given reaction system. This should be achieved by applying a systematic procedure based on physical properties, as well as on the conversion reached in small scale screening experiments. The physical criteria include the ionic liquid melting point (< 30 °C), the density (> 1.2 g cm^{-3}), and the viscosity (< 400 mm^2 s^{-1}). Then, the solvents were rated according to their biocompatibility, the corresponding distribution coefficients of the substrate and the product in the biphasic buffer-ionic liquid systems, as well as on basis of the yields reached during biotransformations at the milliliter scale. The authors demonstrated the applicability of this procedure using three model reactions with a recombinant *E. coli* as biocatalyst.

Schroer *et al.* (2007) applied a biphasic setup with [BMIM][NTF] to overcome thermodynamic limitations in the reduction of 2,5-hexadione to (2R,5R)-hexanediol and compared this approach to two other *in situ* removal techniques (stripping and pervaporation) and a biphasic setup with methyl tert-butylether (MTBE). Together with the stripping method, the biphasic setup with ionic liquid permitted to reach the most satisfying yields (> 95 %). Kratzer *et al.* (2008) used a biphasic system to overcome three different limitations in the synthesis of ethyl *R*-4-cyanomandelate through reduction of ethyl 4-cyanobenzoylformate: the low solubility of the substrate, its low stability in the phosphate buffer used, as well as its toxicity towards the biocatalyst, a recombinant *E. coli*.

Finally, two groups investigated the recycling of the biocatalyst in biotransformations in ionic liquid-water systems. Lou *et al.* (2006) and Wang *et al.* (2009) used *S. cerevisiae* and *Rhodotorula* sp. AS2.2241, respectively, immobilized in alginate beads. After 8 batch biotransformations (corresponding to 96 h of operation), the immobilized *S. cerevisiae* showed a decrease of their relative activity to 81 % in biphasic systems with [BMIM][PF6] and 63 % in monphasic systems with [BMIM][BF4]. The repeated use of the immobilized *Rhodotorula* sp. AS2.2241 also provoked a significant decrease in relative activity, but it remained above 90 % after 7 recyclings.

3.4.2 Other whole-cell biotransformations with ionic liquids

Cornmell *et al.* (2008a) were the first to investigate the oxidation of aromatic compounds by whole-cell biocatalysis in biphasic reaction media with ionic liquids. The biphasic reaction mode was chosen here due to the strong toxicity of the substrate, toluene (Phumathon, 1999). The authors turned to ionic liquids for this application because organic solvents had previously shown only moderate success (Tsai *et al.*, 1996; Phumathon, 1999).

Baumann *et al.* (2004) used biphasic ionic liquid-buffer systems for the same reason when investigating the degradation of phenol by three xenobiotic degrading bacteria (*Pseudomonas putida*, *Achromobacter xylosoxidans* and *Sphingomonas aromaticivorans*). The biphasic setup permitted significantly larger substrate loading, while still limiting the damage to the biocatalyst: after a reaction duration of 12 h, the complete degradation of the xenobiotic by *P. putida* was observed.

Tanaka *et al.* (2009) applied water miscible ionic liquids in the optical resolution of racemic secondary alcohols. *Geotrichum candidum* NBRC 5767 was used to oxidise the *S*-form

of the alcohol to the corresponding ketone, leaving the *R*-enantiomer unchanged. To guarantee the necessary presence of given amounts of water (Matsuda *et al.*, 2006), the biocatalyst was immobilized on water absorbing polymer.

Arai *et al.* (2010) presented a novel application of ionic liquids as second phases in the production of biodiesel fuels by whole-cell biocatalysis. In the reaction considered, fatty acid methyl esters were produced by transesterification of triglycerides with methanol in biphasic reaction systems. The triglycerides were provided by soy bean oil, and the transesterification was performed by different lipase producing biocatalysts. A biphasic reaction mode was applied to avoid deactivation of the biocatalyst by methanol. In addition to their protective effect, ionic liquids can dissolve glycerol, a by-product of the process having a negative effect on biodiesel production and on the lipase activity (Dossat, 1999; Abbott *et al.*, 2004). The ionic liquids tested were [BMIM][BF4], [EMIM][BF4], and [EMIM][CF3SO3]. When comparing the production of methyl esters in the different solvent-oil systems (at volume ratios of 1:1), the results were unequivocal: the monophasic reaction system showed very poor yields for almost all of the biocatalysts tested, due to their intoxication by methanol. The use of a second ionic liquid phase, however, permitted a clear improvement of the reaction outcome for three out of the four biocatalysts tested, with final methyl ester contents of up to ~ 45 %.

4 Presentation of the reaction system and theoretical background

In this chapter, the reaction system considered during this project and the relevant theoretical background are presented. First, a general view of the reaction system is given. Following this, each of its different components are described in more detail. The theoretical considerations related to each subject are given in each of these sections. Finally, the variables used to characterise the biotransformation are defined in the last section of this chapter.

4.1 The biphasic whole-cell reaction system

The reaction under consideration in this project is the asymmetric reduction of 2-octanone to *R*-2-octanol using a recombinant *Escherichia coli* (*E. coli*). Like many other asymmetric reductions, this reaction would profit from the large enantiomeric excesses that can be reached without the addition of costly cofactors using a whole-cell biocatalyst. However, as both the substrate and the product are toxic to *E. coli* (Tanaka *et al.*, 1987; Chen and Chiou, 1995) and show low water solubility (~ 1.1 g L^{-1} at 20 °C), the application of a whole-cell biotransformation is difficult with this substrate/product pair. Bräutigam *et al.* (2009) showed that this biotransformation can nevertheless be performed with very satisfying conversion and enantiomeric excess, if a biphasic reaction setup is chosen. Instead of using a flammable and volatile organic solvent, the authors used a non-water miscible ionic liquid as second phase. During this project, the reduction of 2-octanone to *R*-2-octanol is thus also considered in a biphasic ionic liquid-water setup.

The aqueous phase is a phosphate buffer (0.5 M potassium phosphate, pH 6.5) in which the biocatalyst is suspended. The second phase is a non-water miscible ionic liquid, in which the substrate is initially dissolved. The role of the ionic liquid is to act as a substrate reservoir and an *in situ* product extractant, thereby protecting the biocatalyst from the toxic effect of large substrate or product concentrations. It is thus important that the substrate and the product both show large partition coefficients in the ionic liquid-water system chosen. During the reaction, the ionic liquid and the aqueous phase are intensely

mixed to allow an efficient mass transfer between the ionic liquid and the aqueous phase (Fig. 4.1). As both phases are not miscible, an emulsion is formed, where the dispersed phase is present as drops in the continuous phase. Which solvent takes over which role in the emulsion depends on the respective phase fraction, but also on the physical properties of the liquids, such as the interfacial tension.

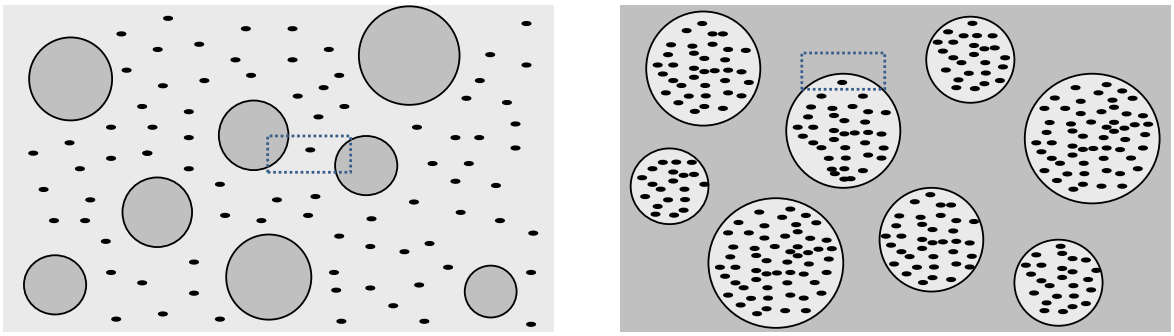

Figure 4.1: Schematic representation of the emulsion formed in a biphasic reaction setup: ionic liquid (▬), aqueous phase (▭) and biocatalyst (•). Two different scenarios are possible: either the ionic liquid forms the dispersed phase surrounded by the aqueous phase containing the biocatalyst (left) or the aqueous phase forms the dispersed phase surrounded by the ionic liquid, while the biocatalyst is suspended in the dispersed aqueous drops (right).

The biotransformation is performed by the *Lactobacillus brevis* alcohol dehydrogenase (LB ADH) overexpressed in the recombinant *E. coli*. This enzyme reduces 2-octanone to its corresponding *R*-alcohol (Fig. 4.2). However, to perform this transformation, the enzyme needs a cofactor: NADH. This cofactor is stoichiometrically consumed during the reaction within the cell. To guarantee a constant supply of NADH for the main reaction, a second enzyme was introduced into the biocatalyst: the *Candida boidinii* formate dehydrogenase (CB FDH). It is responsible for the cofactor regeneration. This regeneration results from the transformation of the co-substrate formate to carbon dioxide, consuming NAD^+ and producing NADH.

The reason why this reaction system is of such large interest is explained in the following section.

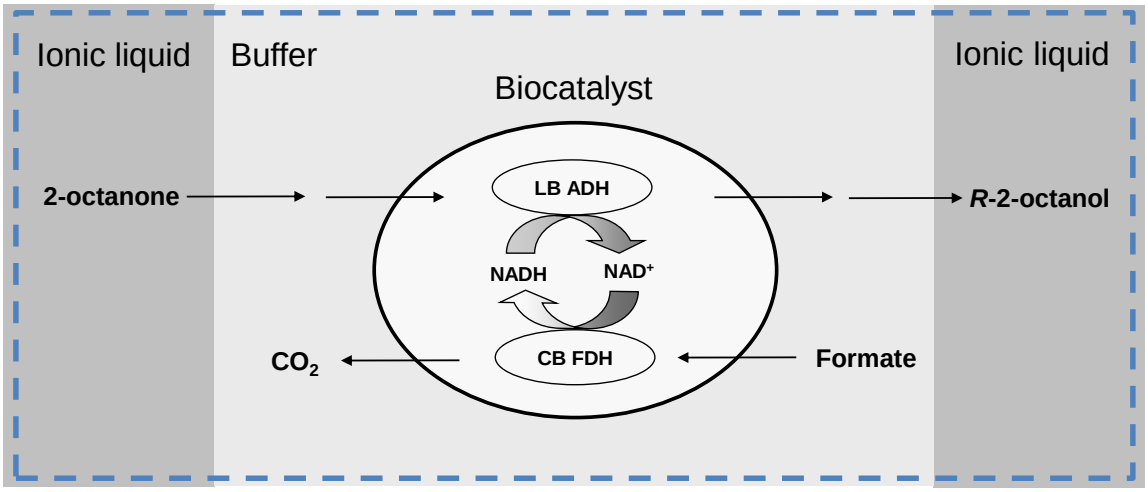

Figure 4.2: Schematic representation of the biphasic reaction system and the different steps of the biotransformation: zoom of Fig. 4.1.

4.2 State of the art of the production of *R*-2-octanol

2-octanol is an important chiral chemical. It serves as building block for fine chemicals, and figures as precursor for the production of pharmaceuticals, agrochemicals and pheromones (Faber and Franssen, 1993; Öhrner *et al.*, 1996; Nie *et al.*, 2005; Hu and Xu, 2006). In addition, it constitutes a versatile starting material in the production of ferroelectric and anitferroelectric liquid crystals with intrinsic optical activity (Liese, 1998; Shi *et al.*, 2008). Besides these interesting applications, there is supplemental reason why the production of enantiopure 2-octanol is so intensely analysed: the asymmetric reduction of small aliphatic ketones still constitutes a major challenge in both organic chemistry and biocatalysis, and the reduction of 2-octanone to *S*- or *R*-2-octanol figures as a model reaction for this type of reductions (Nakamura and Matsuda, 1998; Hu and Xu, 2006). Consequently, if suitable techniques and reaction conditions are found for this reaction, a large number of similar transformations may be considered, too.

2-octanol is mostly produced by reduction of the corresponding ketone, 2-octanone. As the applications involving this substance have very strict requirements concerning the enantiomeric purity, it is crucial that the reduction be enantio-differentiating. An enantio-selective reduction of 2-octanone can be reached relying on (1) traditional chemical catalysis, or (2) biocatalysis, distinguishing again between (i) the purely enzymatic method and (ii) the whole-cell approach. The resulting enantiomer (*S* or *R*) depends on the catalyst used.

The reduction of 2-octanone by chemical routes mostly involves modified Raney Nickel catalysts (Osawa *et al.*, 2004, 2006; Mebane *et al.*, 2007), but some examples are also found using polyvinylpyridines or PEG-armed Ru(III)-bearing microgel core star polymers (Terashima *et al.*, 2010). Azcan and Demirel (2008) chose an interesting alternative to these processes, producing 2-octanol from castor oil. The multi-step process however leads to a mixture of 2-octanol and 2-octanone, which would have to be separated eventually, a difficult and costly procedure.
Most of these chemical routes are based on a transfer hydrogenation with chiral catalysts involving transition metals, and often high pressure and high temperatures. Similarly, the asymmetric reduction according to Corey-Bakshi-Shibata (CBS reduction) makes use of harmful borane and costly chiral oxazaborolidine catalysts (Li, 2006). This makes these production methods not very attractive.
More importantly, however, the yields reached by these processes are only moderate, and generally no indications are made at which enantiomeric excess the product is recovered. As the separation of rests of non-converted substrate or of a mix of both enantiomers is however very cost and time intensive, high yield at a maximal enantiomeric excess are decisive criteria for this reduction. This is the reason why biocatalysis is an interesting alternative.

Biocatalysis is indeed often characterised by very high (enantio)selectivity and can, in appropriate conditions, reach very large conversion. Another advantage of biocatalytic pathways are the mostly mild reaction conditions involved (temperatures between 20 °C and 37 °C, neutral pH, ambient pressure).
However, when trying to produce enantiopure 2-octanol by biocatalytic means, a number of challenges appear, which reside (1) in the low water solubility of the substrate (~ 1.1 g L^{-1} at 20 °C), (2) in the toxicity of both the substrate and the product towards living organisms, and (3) in the fact that the enzymatic transformation often suffers from an inhibition by the substrate and by the product if either of them is present in too large quantities (Kohlmann *et al.*, 2011a).

One way to avoid an inhibition by large concentrations of substrate and/or product during an enzymatic transformation, while still being able to add the substrate in large quantities into the reaction system, is the use of an enzyme membrane reactor (EMB). Liese (1998) and Kohlmann *et al.* (2011a) applied such a system with different enzymes (*Candida parapsilosis* carbonyl reductase and *Lactobacillus brevis* alcoholdehydrogenase, respectively) and reached satisfying conversion (> 95 %) and enantiomeric excesses

(> 99.5 %). However, the space-time yield reached in these setups was only between 9.4 g L^{-1} d^{-1} and 21.2 g L^{-1} d^{-1}, and the proposed processes suffer from a relatively complex setup. More satisfying results were observed in the work published a year earlier by (Kohlmann *et al.*, 2011b). In this work, the addition of different water miscible ionic liquids was tested to increase the solubility of the substrate in the reaction system. In one of these setups, the biotransformation of 2-octanone by the *Lactobacillus brevis* alcohol dehydrogenase reached a conversion of 99 % at excellent enantioselectivity after ~ 20 h. The space-time yield in this setup was 350 mmol L^{-1} day^{-1} (~ 45.6 g L^{-1} d^{-1}). Eckstein *et al.* (2004) used a biphasic setup with an ionic liquid ([BMIM][NTF]) to overcome an inhibition of the enzymes, but reached only 88% conversion of 2-octanone with the *Lactobacillus brevis* alcohol dehydrogenase.

Most of the biocatalytic production of 2-octanone published is however performed using whole cells rather than purified enzymes. This is probably due to the advantages the use of whole cells confers during such biotransformations (section 3.1). Many different organisms were used as whole-cell biocatalysts: *Sulfolobus solfactaricus* (Trincone *et al.*, 1990), *Gluconobacter oxydans* (Adlercreutz, 1991), *Geotrichum candidum* (Nakamura and Matsuda, 1998), *Saccharomyces cerevisiae* (Heidlas *et al.*, 1991; Gervais *et al.*, 2000; Shi *et al.*, 2008; Wolfson *et al.*, 2006; Li *et al.*, 2007), *Escherichia coli* (de Gonzalo *et al.*, 2007; Bräutigam *et al.*, 2009) and *Oenococcus oeni* (Hu and Xu, 2006). Some authors used encapsulated biocatalysts, permeabilised cells, resting cells in monophasic setups, or acetone powder of the corresponding cells to limit the damage and/or inhibition by the toxic substrate and product. These approaches did however not permit to reach very satisfying conversion and enantiomeric excesses (Trincone *et al.*, 1990; Adlercreutz, 1991; Nakamura and Matsuda, 1998; Gervais *et al.*, 2000). In contrast, biphasic reaction setups with either non-water miscible organic solvents or non-water miscible ionic liquids led to more satisfying results. The best results in terms of conversion and enantiomeric excess were published by Hu and Xu (2006): the reduction of 2-octanone by *O. oeni* in a biphasic system composed of n-nonane and buffer (1:1) permitted to reach a conversion of 99 % after 48 h, with an enantiomeric excess > 99 % (*R*). However, in terms of productivity, Bräutigam *et al.* (2009) presented a setup that was more efficient. The use of a recombinant *E. coli* in a biphasic setup with ionic liquid (20 % v/v) ([HMPL][NTF]) produced 180 g *R*-2-octanol L^{-1} day^{-1}, at a chemical yield of 95 % and an enantiomeric excess of 99.7 %.

Some work has also been published on the resolution of mixtures of *S*- and *R*-2-octanol (Nie *et al.*, 2005; Yu *et al.*, 2007a,b; Voss *et al.*, 2008). The approach presented by Voss *et al.*

(2008) permitted to reach 99 % yield at an enantiomeric excess of 99 % (*S*). If no other way can be found to directly produce enantiopure 2-octanol, these methods thus surely constitute a good solution. However, a resolution of the mix of enantiomers produced means a supplementary step in the process after the biotransformation, increasing the necessary time and resources investment. The priviledged procedure is thus still the direct production of 2-octanol at maximal enantiomeric excess.

4.3 The whole-cell biocatalyst

The whole-cell biocatalyst used to perform the reduction of 2-octanone to *R*-2-octanol is a recombinant *E. coli*. *E. coli* is a microorganism that was discovered in 1885 by the German paediatrician and bacteriologist Theodor Escherich and named after him in 1919. It is a Gram-negative non-sporulating rod-shaped bacterium (Fig. 4.3) commonly found in the lower intestine of warm-blooded organisms (endotherms) and it is now classified as part of the *Enterobacteriaceae* family of gamma-proteobacteria.

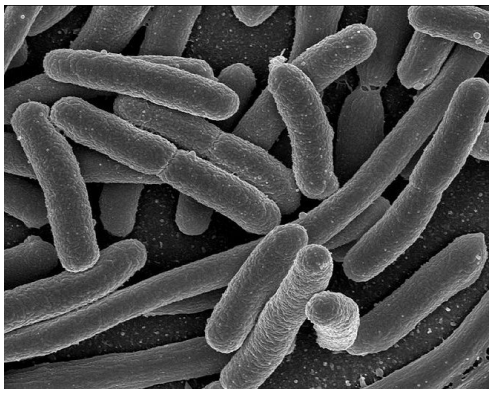

Figure 4.3: Scanning electron micrograph of *Escherichia coli*. Courtesy of the National Institutes of Health, United States Department of Health and Human Services.

E. coli is a facultative aerobic organism, which means that it can gain energy by aerobic respiration if oxygen is present but that it is also capable of switching to fermentation in the absence of oxygen. It is a chemoheterotroph organism growing on complex as well as on minimal media and it can consume a large variety of sugars and amino acids. In optimal conditions, *E. coli* has a doubling time of 20 min. Glucose is the preferred substrate, and the optimal growth temperature is 37 °C. However, depending on the strain, *E. coli* growth can take place between temperatures of 8 °C and 48 °C, and within a pH range of pH 6 to pH 8 (Lederberg and Bloom, 2000).

Over the last decades, *E. coli* has become one of the most used microorganisms in microbiology and biochemical engineering. This is due to the ease of manipulation and its rapid growth, but also because *E. coli* is a very versatile host for the production of heterologous proteins. By introducing the corresponding genes, it allows to produce many proteins at the large scale. The easy and largely successful (over)expression of heterologous enzymes in *E. coli* makes it a very attractive tool in biotechnology. The use of *E. coli* as host for the expression of heterologous proteins is however limited by the fact that it cannot reliably produce complex proteins requiring post-translational modifications for activity.

Finally, there is a supplemental reason why this organism is especially interesting as whole-cell biocatalyst in biotransformations involving alcohol dehydrogenases: the endogenous alcohol dehydrogenases of *E. coli* show relatively low activity. This means that an exogenous alcohol dehydrogenase expressed in *E. coli* for a given biotransformation will not have to compete with other alcohol dehydrogenases also present, which might form unwanted by-products. Consequently, the use of *E. coli* cells instead of e.g. recombinant yeast allows a more specific production of only the wanted enantiomer, reaching higher enantiomeric excesses, and thus also larger yields and product purities (Hildebrandt *et al.*, 2002). This makes *E. coli* a particularly suitable biocatalyst for this kind of biotransformations.

4.3.1 Characteristics of the *E. coli* cell growth

The cultivation of the recombinant *E. coli* is performed either in batch or in fed-batch mode, depending on the biocatalyst quantities required. When no other limitations or inhibitions occur, the batch growth of *E. coli* in presence of limited amounts of substrate evolves as depicted in Fig. 4.4.

After a short lag phase (1), during which the cells adapt to the culture conditions, the cells start slowly to divide (2). The growth is still only moderate, but increases with time. The growth rate is defined as given by equation 4.1.

The following phase, the exponential growth (3), is characterised by a cell growth at a constant, maximal growth rate (μ_{max}). Then, after some time, the substrate slowly becomes limiting (4), and the specific growth rate decreases. During these phases, the growth rate can be defined as a function of the concentration of the growth limiting substrate, according to an expression developed by Monod in 1942 (equation 4.2). This

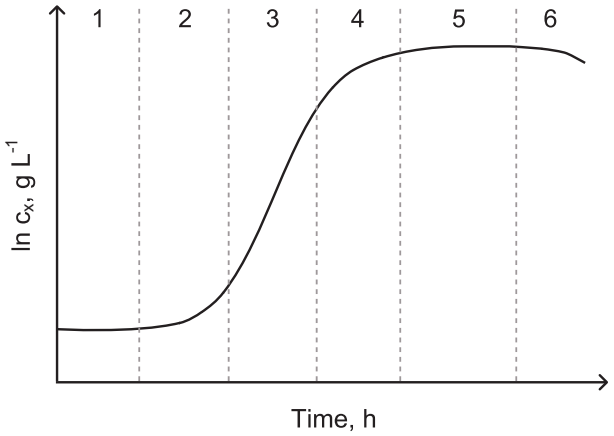

Figure 4.4: Schematic representation of the different growth phases (1-6) of *Escherichia coli* in substrate limited conditions.

expression is only valid if only one substrate is growth limiting, and all the other culture parameters - such as the pH, the oxygen availability and the temperature - can be supposed constant. When almost no substrate is available anymore, the cells stop dividing, and the stationary phase is reached (5) ($\mu = 0$). Finally, when all the substrate is consumed, and the cells cannot even perform the necessary maintenance anymore, they die and their number starts decreasing (death phase) (6).

$$\mu \equiv \frac{1}{c_X} \cdot \frac{dc_X}{dt} \tag{4.1}$$

μ	growth rate, h^{-1}
c_X	cell concentration, g_{DCW} L^{-1}
t	time, h

$$\mu = \mu_{max} \cdot \frac{c_S}{K_S + c_S} \tag{4.2}$$

μ_{max}	growth rate under non-limiting conditions, h^{-1}
c_S	concentration of the limiting substrates, mol L^{-1}
K_S	half-saturation constant, mol L^{-1}

When sufficiently large cell concentrations cannot be reached in a batch cultivation mode due to substrate limitations, a fed-batch mode can be used to produce larger cell densities

through the supplemental addition of substrate. Adding the substrate through a feed can also be a method to control the substrate concentration in the medium, because the substrate can be added at a determined rate. Deliberately fixing low concentrations in the medium might e.g. be interesting to avoid an excessive production of acetate or an inhibition of the protein expression due to large substrate concentrations. An exponential feeding profile fixes the growth rate of the cells to a fixed value chosen for μ (μ_{set}). When the substrate quantities necessary for the cell maintenance is neglected, the exponential feeding profile is given by equation 4.3. The evolution of the biomass concentration as a function of time in a fed-batch cultivation mode is then given by equation 4.4.

$$\dot{V}(t) = \frac{\mu_{set} \cdot V(t_{0,feed}) \cdot c_X(t_{0,feed})}{Y_{X,S} \cdot c_{S,feed}} \cdot \exp(\mu_{set} \cdot (t - t_{0,feed})) \tag{4.3}$$

$$\frac{dc_X}{dt} = -\frac{\dot{V}(t)}{V(t)} \cdot c_X + \mu \cdot c_X \tag{4.4}$$

$\dot{V}$	feeding rate, L h^{-1}
μ_{set}	specific growth rate fixed, h^{-1}
V	culture volume, L
$t_{0,feed}$	cultivation time when the feeding is started, h
$Y_{X,S}$	biomass to substrate yield, g_{DCW} g_S^{-1}
$c_{S,feed}$	concentration of the limiting substrate in the feed, g L^{-1}

The expressions given by equation 4.3 and equation 4.4 are only valid for so-called 'ideal' stirred tank reactors, where complete spatial homogeneity is supposed, excluding concentration gradients or local differences in the physical parameters.

4.3.2 Transport across the cell membrane

When using whole cells rather than isolated enzymes for a biotransformation, the substrate has to cross the cell membrane before it can be transformed by the enzymes within the cell. There are different mechanisms permitting a substance to pass the cell membrane. The simplest mechanism is the transfer by simple diffusion. It occurs spontaneously and only in the direction of the chemical gradient. The diffusion rate across the lipid bilayer depends strongly on the size and on the lipophilicity of the molecule (Alberts *et al.*, 2002). Small nonpolar molecules such as O_2 or CO_2 dissolve very well in the membrane and cross the membrane rapidly. Small uncharged polar molecules like water or ethanol also diffuse relatively rapidly. Larger uncharged polar molecules like glycerol diffuse not very well, and charged molecules can almost not enter the cell by diffusion, independently of their size. Even very small ions like K^+ or Na^+ cannot cross the membrane.

As the cell however also needs e.g. ions and sugars, these substances also have to be able to enter in some way. Their transport into the cell is assured by membrane transport proteins (Fig. 4.5). There are two main classes of membrane proteins: carrier proteins, binding to specific solutes only, and channel proteins, not binding to the solute transported. This transport mechanism is called 'passive transport' or 'facilitated diffusion'.

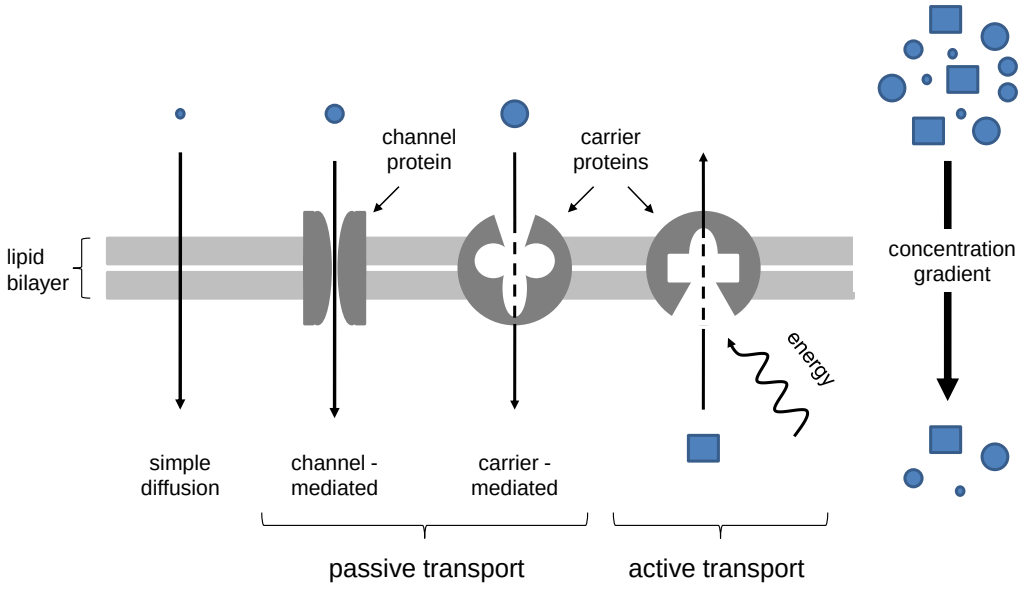

Figure 4.5: Schematic representation of the different transport modes through the membrane, according to Alberts *et al.* (2002): passive and active transport.

Both the simple diffusion and the facilitated diffusion occur only in the direction of the chemical gradient. Sometimes, however, a transport against the direction of the electrochemical gradient is required. This can only be done with an input of metabolic energy and through a carrier protein. This type of transport is called 'active transport'.

In the current project, the substances of interest (2-octanone and 2-octanol) are supposed to cross the cell membrane by simple diffusion. For this transport mechanism, the following assumptions can be made:

- the cell membrane can be represented as a homogeneous liquid film, in which the diffusing substance has a constant partition coefficient ($K_{i,\ extracellular} = K_{i,\ intracellular} = K_i$) and a constant diffusion coefficient ($D_{i,m}$)
- the diffusion across the cell membrane is supposed to be the rate limiting step, so that a constant state of equilibrium can be assumed at the interface between the surrounding liquid and the cell membrane

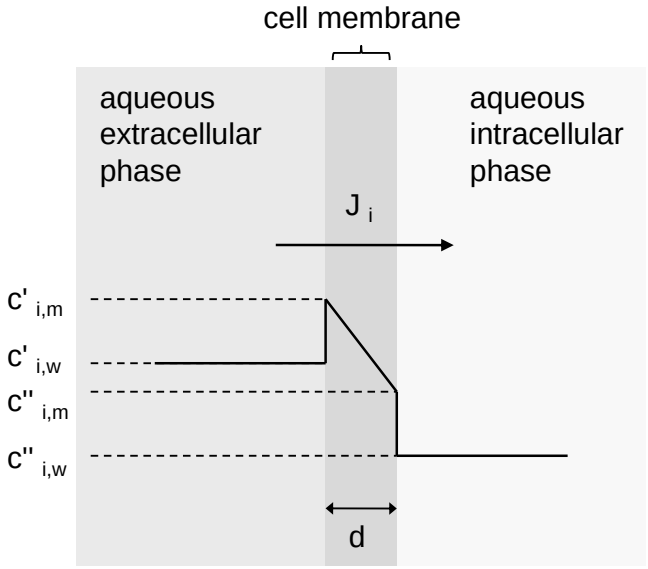

Figure 4.6: Scematic representation of the diffusion of a lipophilic substance (i) from the extracellular liquid through the cell membrane into the cell.

As a consequence, under steady state conditions, a linear concentration profile can be assumed in the cell membrane (Fig. 4.6). If the mass transfer through the membrane is the rate limiting step, the corresponding flux can be described by equation 4.5.

$$J_i = -D_{i,m} \cdot \frac{(c''_{i,m} - c'_{i,m})}{d} \tag{4.5}$$

J_i	mass transfer flux density, mol s^{-1} m^{-2}
$D_{i,m}$	diffusion coefficient of i in the membrane, m^2 s^{-1}
$c_{i,m}$	concentration of i in the membrane, mol m^{-3}
d	thickness of the membrane, m

The partitioning of the diffusing substance between the membrane and the surrounding liquid is defined by the corresponding coefficient K_i (equation 4.6).

$$K_i = \frac{c'_{i,m}}{c'_{i,w}} = \frac{c''_{i,m}}{c''_{i,w}} \tag{4.6}$$

K_i	partition coefficient of i between the surrounding liquid and the membrane, -
$c_{i,w}$	concentration of i in the surrounding liquid, mol m^{-3}

This means that the concentration gradient occurring in the membrane can also be expressed by equation 4.7.

$$c'_{i,m} - c''_{i,m} = K_i \cdot (c'_{i,w} - c''_{i,w}) \tag{4.7}$$

Replacing equation 4.7 in equation 4.5, the expression for the flux gives equation 4.8.

$$J_i = \frac{K_i \cdot D_{i,m}}{d} \cdot (c'_{i,w} - c''_{i,w}) \tag{4.8}$$

Merging all the factors into one coefficient, the 'membrane permeability' (P_i) (equation 4.9), the mass transfer across the cell membrane is given by equation 4.10.

$$P_i = \frac{K_i \cdot D_{i,m}}{d} \tag{4.9}$$

$$J_i = P_i \cdot (c'_{i,w} - c''_{i,w}) \tag{4.10}$$

P_i membrane permeability of i, m s^{-1}

In literature, only very little data is published concerning the membrane permeability of given organisms towards various substances. Table 4.2 gives the membrane permeability of some substances published for *Chara ceratophylla* (Nielsen and Villadsen, 1994). Alberts *et al.* (2002) indicated a membrane permeability for sodium of $1 \cdot 10^{-14}$ m s^{-1}.

Table 4.2: Membrane permeability of various substances for *Chara ceratophylla* (source Nielsen and Villadsen (1994)).

Substance	Membrane permeability, m s^{-1}
Carbon dioxide	$4.5 \cdot 10^{-3}$
Methanol	$2.5 \cdot 10^{-6}$
Ethanol	$1.4 \cdot 10^{-6}$
Urea	$2.8 \cdot 10^{-9}$
Glucose	$5.0 \cdot 10^{-10}$

4.4 The enzymes used for the biotransformation and their characterisation

To be able to perform the biotransformation of interest sucessfully, two enzymes are overexpressed in the whole-cell biocatalyst: the *Lactobacillus brevis* alcohol dehydrogenase and the *Candida boidinii* formate dehydrogenase. In this section, these two enzymes will be described in more detail. Then, the theoretical background related to the quantification of their activity, the evaluation of their stability and the determination of their kinetic parameters is presented.

4.4.1 The *Lactobacillus brevis* alcohol dehydrogenase (EC 1.1.1.2)

The *Lactobacillus brevis* alcohol dehydrogenase (LB ADH) is an oxidoreductase catalysing the reduction of ketones to secondary alcohols (Fig. 4.7). It accepts both NAD(H) and NADP(H) as cofactor.

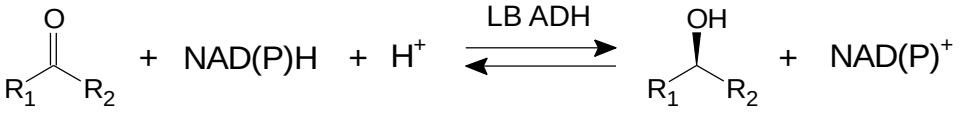

Figure 4.7: Reduction of a ketone to its corresponding *R*-alcohol by the *Lactobacillus brevis* alcohol dehydrogenase with NAD(P)H as cofactor.

The LB ADH is a homotetramer, where each subunit has a molecular weight of 26.6 kDa and 251 amino acids. It belongs to the extended family of the short chain dehydrogenases/reductases (SDR), a large family of NAD(P)(H)-dependent oxidoreductases sharing sequence motifs - a 'Rossmann-fold' dinucleotide cofactor binding motif - and presenting similar mechanisms (Kavanagh *et al.*, 2008). Members of the SRD family are normally independent of the presence of metal ions. The LB ADH, however, constitutes the first exception to this rule: it contains two divalent magnesium ions per tetramer, and the removal of these ions by chelating substances inactivates the enzyme (Niefind *et al.*, 2003). The LB ADH is a bacterial, cytosolic protein. It does not contain disulfide bridges, it is not glycosilated and does not undergo any other posttranslational modifications (Müller, 2000). It can thus be correctly expressed in *E. coli*.

Even though the LB ADH accepts both NADH and NADPH as cofactors, it has a strong preference for the phosphorylated cofactor: using NADH as cofactor, the specific activity of LB ADH is 10 times lower than with NADPH (Ernst *et al.*, 2004). Still, the acceptance of both cofactors allows larger flexibility for the cofactor regeneration because both NADH and NADPH dependent enzymes can be used. Like most oxidoreductases, the LB ADH is able to catalyse the reaction in both ways. The enzyme mechanism is supposed to correspond to an ordered bi-bi mechanism, with the cofactor binding first and only then the substrate (Kavanagh *et al.*, 2008). Similarly, the product first leaves the enzyme after the transformation, followed by the reduced or oxidized cofactor. With a specific activity of 490 U mg^{-1} in the reduction of acetophenone with NADPH (Hummel, 1997), it is known to be a highly efficient enzyme.

The LB ADH has a large spectrum of possible substrates, but its preferred *in vitro* substrates are prochiral ketones like acetophenone with almost invariably a small methyl group as one substituent (R_1, Fig. 4.7) and a bulky (often aromatic) moiety as the other (R_2, Fig. 4.7) (Schlieben *et al.*, 2005). Like the other members of the SDR family, the LB ADH also shows large stereo- and regioselectivity. In fact, the hydride transfer of SDRs is strictly stereospecific: each enzyme reduces the ketone only to either the *R*- or the *S*-alcohol, and only oxidises either the *R*- or *S*-alcohol. The LB ADH attacks the substrate from the *si*-side according to an anti-Prelog-rule (Prelog, 1964; Faber, 1997). It is therefore one of the rare alcoholdehydrogenases forming the *R*-enantiomer during the reduction and being strictly *R*-specific for the oxidation process (Hummel and Riebel, 2000).

The activity and the stability of the LB ADH are both strongly dependent on the pH and on temperature. For oxidations, the maximal activity with NADP(H) is reached at pH 8 and for reductions around pH 6.5–7 (Filho, 2007; Machielsen *et al.*, 2009). With NAD(H) as cofactor, the optimal pH for reductions is significantly lower (pH 5.5) (Machielsen *et al.*, 2009). The maximal enzyme activity of LB ADH is reached at a temperature of 50 °C (Hummel and Riebel, 2000). The maximal enzyme stability is obtained at pH 7, and it decreases dramatically with increasing temperature (Filho, 2007).

4.4.2 The *Candida boidinii* formate dehydrogenase (EC 1.2.1.2)

The *Candida boidinii* formate dehydrogenase (CB FDH) is a dehydrogenase catalysing the oxidation of formate to carbon dioxide (CO_2) using NAD^+ as cofactor (Fig. 4.8). It is a homodimer, where each subunit has a molecuar weight of 40.6 kDa (Bommarius and Karau, 2005). This enzyme belongs to the family of the D-specific 2-hydroxyacid dehydrogenases acting on D-stereoisomers of their respective substrate (Mesentsev *et al.*, 1997). The CB FDH presents large similarities with these dehydrogenases, both concerning its amino acid sequence and its three-dimensional structure.

Figure 4.8: Oxidation of formate to CO_2 by the *Candida boidinii* formate dehydrogenase with NAD^+ as cofactor.

The CB FDH is an enzyme frequently and very successfully used for the regeneration of the cofactor in many different reaction systems, including the production of optically active amino acids, esters, alcohols and other fine chemicals (Hummel and Kula, 1989; Kragl *et al.*, 1996; Galkin *et al.*, 1997; Liese, 1998). In fact, many factors make its application particularly attractive: (1) the catalysed reaction is essentially irreversible (Schütte *et al.*, 1976) and strongly favours the production of CO_2 and NADH, which makes the cofactor regeneration particularly efficient (Faber, 1997; Weuster-Botz, 1999) (2) the product (CO_2) is easily removed from the reaction system, (3) the substrate is inexpensive and (4) neither the substrate nor the product have a negative influence on the enzyme activity. Drawbacks of this enzyme are (1) that the CB FDH does not accept $NADP^+$ as cofactor (Schütte *et al.*, 1976), and its application for the cofactor regeneration is thus limited to reactions involving NAD(H), and (2) its relatively low specific activity (4–6 U mg^{-1}, at 30 °C, pH 7.5) (Hummel, 1997; Slusarczyk *et al.*, 2000).

The CB FDH specifically only accepts formate as substrate. The enzyme mechanism follows an ordered bi-bi mechanism, where the cofactor binds first to the enzyme, and leaves the active site last (Kato *et al.*, 1979). Its main reason for deactivation is its sensitivity to oxidation due to its cysteine side chains (Bommarius and Karau, 2005). Its optimal temperature and pH are 55 °C and pH 7 (Bommarius and Karau, 2005).

4.4.3 Enzyme characterisation

Enzyme activity

In the present project, the LB ADH performs the reduction of the prochiral ketone while stoechiometrically consuming NADH to produce the corresponding *R*-alcohol and NAD^+ (Fig. 4.7). The CB FDH, on the other hand side, is responsible for the cell-internal regeneration of NADH through oxidation of formate to CO_2, consuming the NAD^+ produced by the LB ADH and forming NADH (Fig. 4.8). The activity of both enzymes can thus be evaluated on basis of the rate of the consumption or the formation, respectively, of NADH. The decrease or the increase of NADH can be monitored photometrically, by evaluating the absorption at a wavelength of 340 nm. On basis of the recorded data, the enzyme activity is then determined using the Lambert-Beer relation as described by equation 4.11.

$$EA_x = \frac{\Delta c_{NADH} \cdot V_R}{\Delta t \cdot V_x \cdot c_X} = \frac{\Delta A_{340} \cdot V_R \cdot 10^6}{\Delta t \cdot \varepsilon_{NADH} \cdot b \cdot V_x \cdot c_X} \tag{4.11}$$

EA_x	enzyme activity, U g_{DCW}^{-1}
$\frac{\Delta c_{NADH}}{\Delta t}$	variation of the NADH concentration over time, μM min^{-1}
V_R	reaction volume, L
V_x	sample volume, L
c_X	cell concentration, g_{DCW} L^{-1}
$\frac{\Delta A_{340}}{\Delta t}$	variation of the absorption at 340 nm over time, min^{-1}
ε_{NADH}	molar extinction coefficient of NADH, 6300 L mol^{-1} cm^{-1}
b	path length of the sample, cm

Enzyme stability

The evaluation of the stability of the enzymes performing the transformation in varying conditions is important for the process development. The stability of an enzyme is given by its half-life in the conditions under consideration. When the deactivation kinetic is of first order, the enzyme activity decreases according to equation 4.12. The enzyme half-life is then obtained by measuring the enzyme activity over a given period of time when exposed to given conditions.

$$A = A_0 \cdot e^{-k_i t} \tag{4.12}$$

A	enzyme activity at time t, U mg^{-1}
A_0	enzyme activity at time t = 0, U mg^{-1}
k_i	inactivation constant, h^{-1}
t	time, h

When plotting the natural logarithm of the activities measured as a function of time, the slope of the line gives the inactivation constant (k_i). The half-life ($t_{1/2}$) of the enzyme can then be determined using equation 4.13.

$$t_{1/2} = \frac{ln\,2}{k_i} \tag{4.13}$$

$t_{1/2}$ half-life, h

Enzyme kinetics

A thorough characterisation of the enzymes of interest includes the determination of their kinetic parameters. Therefore, in a first step, the reaction mechanism of the enzyme must be known. The simplest reaction mechanism possible is a one-substrate-one-product reaction. In this kinetic model, the substrate binds to the enzyme to form the enzyme-substrate complex (ES). This complex can either dissociate to return to the initial situation, the free substrate and the free enzyme, or to give the free product and the free enzyme as a result of the biotransformation (Fig. 4.9).

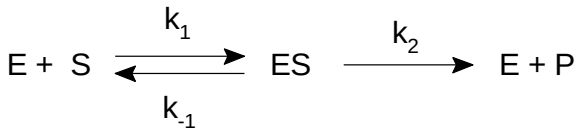

Figure 4.9: Scheme of an irreversible one-substrate-one-product reaction. The substrate (S) binds to the enzyme (E) to form the enzyme-substrate complex (ES). This complex dissociates either into the free enzyme and the un-transformed substrate, or into the free enzyme and the product (P). The constants k_i are the rate constants of the individual steps forming the overall reaction.

The kinetic model corresponding to this reaction mechanism was developed by Leonor Michaelis and Maud Menten in 1913. It is based on several assumptions:

- One enzyme entity and one substrate molecule form the activated enzyme-substrate-complex (ES).
- The pseudo-steady-state assumption, i.e. that the concentration of the enzyme-substrate-complex changes much more slowly than those of the substrate (S) and the product (P). Consequently, it can be supposed that its concentration is constant: $\frac{d[ES]}{dt} = 0$.
- The overall reaction evolves far from the thermodynamic equilibrium, and a possible reverse evolution of the last step of the overall reaction is negligible. This is the case when initial reaction rates are determined: $[P] \cong 0$.
- The dissociation of the product from the enzyme (k_2) is the rate limiting step.

In these conditions, the reaction rate (v) can be described by equation 4.14, the so-called 'Michaelis-Menten kinetic'.

$$v = v_{max} \cdot \frac{[S]}{K_m + [S]} \tag{4.14}$$

v	reaction rate, mol s^{-1}
v_{max}	maximal reaction rate, mol s^{-1}
[S]	substrate concentration, mol L^{-1}
K_m	half saturation constant, mol L^{-1}

The half saturation constant (K_m) is given by the ratio of the rate constants of the individual steps forming the overall reaction (equation 4.15). It corresponds to the substrate concentration at which the reaction rate is half the maximal reaction rate (v_{max}).

$$K_m = \frac{k_2 + k_{-1}}{k_1} \tag{4.15}$$

As mentioned above, these considerations are only valid for a one-substrate-one-product reaction. Most enzymatic transformations, however, do not occur according to such a simple mechanism and involve two or more substrates. This is also the case for the enzymes of importance in this project, the LB ADH and the CB FDH. For both enzymes, a so-called 'ordered bi-bi mechanism' was indicated (subsection 4.4.1 and subsection 4.4.2). This mechanism is based on the binding of two substrates and on the dissociation of the two products in a defined and fixed order: substrate A has to bind to the enzyme before substrate B can bind to it. Similarly, product P has to leave the enzyme complex first, before product Q can leave (Fig. 4.10) (Cleland, 1963a,b,c). For both the LB ADH and the CB FDH, the cofactor (A) binds first to the enzyme, and then the substrate (B). After the biotransformation, the product (P) leaves the enzyme first, and only then the transformed cofactor (Q) leaves it, too.

The reaction rate for an ordered bi-bi mechanism is represented by the expression given by equation 4.16 (Bisswanger, 2000). The corresponding parameters are defined in Table 4.4.

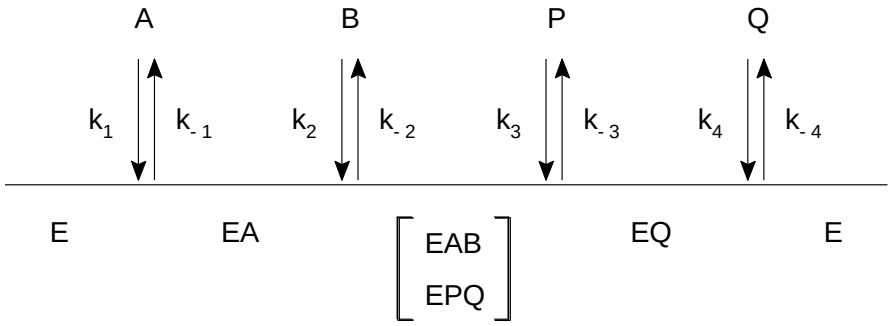

Figure 4.10: Scheme of the ordered bi-bi mechanism of the LB ADH and the CB FDH, according to Cleland (1963a,b,c). First, the cofactor (A) binds to the enzyme, and then the substrate (B). After the transformation, the product (P) leaves the enzyme first, and only then the transformed cofactor (Q).

$$v = \frac{v_1 v_2([A][B] - \frac{[P][Q]}{K_g})}{K_{iA}K_{mB}v_2 + K_{mB}v_2[A] + K_{mA}v_2[B] + \frac{K_{mQ}v_1[P]}{K_g} + \frac{K_{mP}v_1[Q]}{K_g} + v_2[A][B]} \\ + \frac{K_{mQ}v_1[A][P]}{K_{iA}K_g} + \frac{K_{mA}v_2[B][Q]}{K_{iQ}} + \frac{v_1[P][Q]}{K_g} + \frac{v_2[A][B][P]}{K_{iP}} + \frac{v_1[B][P][Q]}{K_{iB}K_g} \tag{4.16}$$

When initial reaction rates are determined, it can be assumed that the product and co-product concentrations are close to 0 ([P] = [Q] ≅ 0). In this case, equation 4.16 is simplified to equation 4.17.

$$v = \frac{v_1[A][B]}{K_{iA}K_{mB} + K_{mB}[A] + K_{mA}[B] + [A][B]} \tag{4.17}$$

Similarly, for the backward reaction, supposing that [A] = [B] ≅ 0, equation 4.16 can be expressed as equation 4.18.

$$v = \frac{v_2[P][Q]}{K_{iA}K_{mB} + K_{mQ}[P] + K_{mP}[Q] + [P][Q]} \tag{4.18}$$

Table 4.4: Kinetic parameters of an ordered bi-bi mechanism (Bisswanger, 2000), with E_0 corresponding to the total enzyme concentration in the reaction.

Symbol	Parameter	Definition
v_1	maximal rate of the forward reaction	$\frac{k_3 k_4 [E]_0}{k_3 + k_4}$
v_2	maximal rate of the backward reaction	$\frac{k_{-1} k_{-2} [E]_0}{k_{-1} + k_{-2}}$
K_{mA}	half saturation constant of the substrate A	$\frac{k_3 k_4}{k_1 (k_3 + k_4)}$
K_{mB}	half saturation constant of the substrate B	$\frac{k_4 (k_{-2} + k_3)}{k_2 (k_3 + k_4)}$
K_{mP}	half saturation constant of the product P	$\frac{k_{-1} (k_{-2} + k_3)}{k_{-3} (k_{-1} + k_{-2})}$
K_{mQ}	half saturation constant of the product Q	$\frac{k_{-1} k_{-2}}{k_{-4} (k_{-1} + k_{-2})}$
K_{iA}	dissociation constant of the substrate A	$\frac{k_{-1}}{k_1}$
K_{iB}	dissociation constant of the substrate B	$\frac{k_{-1} + k_{-2}}{k_2}$
K_{iP}	dissociation constant of the product P	$\frac{k_3 + k_4}{k_{-3}}$
K_{iQ}	dissociation constant of the product Q	$\frac{k_4}{k_{-4}}$
K_g	equilibrium constant of the reaction	$\frac{k_1 k_2 k_3 k_4}{k_{-1} k_{-2} k_{-3} k_{-4}}$

4.5 The biphasic setup

Due to the large toxicity and the low water solubility of both the substrate and the product, the reduction of 2-octanone to *R*-2-octanol is only successful if the biotransformation is performed in a biphasic setup. The second phase is a non-water miscible ionic liquid for which the substrate and the product show large partition coefficients in the ionic liquid-water system. The substrate is initially dissolved in the ionic liquid. To be transformed, it has to reach the cell, i.e. it has to be transferred to the aqueous phase phase. Similarly, the product is formed in the aqueous phase and it should be rapidly extracted by the ionic liquid. A good mass transfer between the ionic liquid and the aqueous phase thus has to be assured during the reaction, to avoid a limitation of the reaction rate as well as the intoxication of the biocatalyst by the toxic product, and a consequent decrease of the productivity of the biotransformation.

In this section, the theoretical considerations concerning the mass transfer between the ionic liquid and the aqueous phase are presented. First, the ionic liquid added as second phase is described. Then, the variables used to characterise an emulsion are indicated. Finally, the equations needed to determine the mass transfer in liquid-liquid dispersions are given.

4.5.1 The ionic liquid used: 1-hexyl-1-methyl-pyrrolidinium bis(trifluoromethylsulfonyl)imide

The ionic liquid used in this project is 1-hexyl-1-methyl-pyrrolidinium bis(trifluoromethylsulfonyl)imide ([HMPL][NTF]) (Fig. 4.11). It was chosen as second phase based on the methodology proposed by Bräutigam *et al.* (2007). It had indeed been shown that this ionic liquid showed favourable characteristics for the biotransformation of 2-octanone to *R*-2-octanol with a recombinant *E. coli* (Bräutigam *et al.*, 2009): large partition coefficients for the substrate (1230) and the product (172) in [HMPL][NTF]-water systems, relatively good biocompatibility and a sufficiently large density in comparison to water to allow an efficient phase separation after the biotransformation. As the solvent is relatively new, it has not been the subject of many investigations. The solvent's published properties are summarized in Table 4.5.

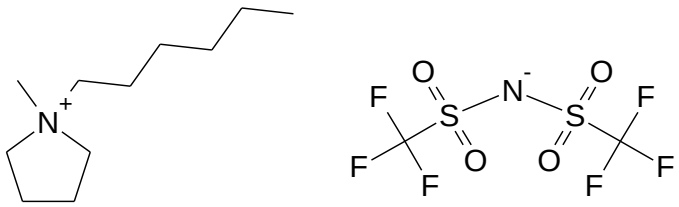

[HMPL] [NTF]

Figure 4.11: Structure of the ionic liquid used in this project, 1-hexyl-1-methyl-pyrrolidinium bis(trifluoromethylsulfonyl)imide ([HMPL][NTF]): the composing cation (left) and anion (right).

Table 4.5: Properties of 1-hexyl-1-methyl-pyrrolidinium bis(trifluoromethylsulfonyl)imide ([HMPL][NTF]) (source Merck KGaA).

Property	Value	Unit
CAS number	380497-19-8	-
Molecular weight	450.47	g mol^{-1}
Density	1.34	g cm^{-3}
pH (20 °C)	6	-
Partition coefficient 2-octanone[a,b]	1230	-
Partition coefficient 2-octanol[a,b]	172	-
Solubility in water[b]	1.9	g L^{-1}
Maximal water uptake	0.9	% wt

[a] partitioning [HMPL][NTF]-buffer; [b] source Bräutigam *et al.* (2009)

4.5.2 Characterisation of liquid-liquid dispersions

A dispersion is a mixture of at least two non-miscible liquids not reacting one with the other (Staak, 2010). In non-agitated form, both liquids are present as two separate phases, one above the other due to their respective different densities. When mixing, the hydrodynamic forces arising through the stirring provokes the dispersion of one of the liquids, while the other liquid remains as continuous phase around the drops of dispersed phase formed. Usually, the dispersed phase is formed by the liquid present in smaller volume, but under extreme conditions, the dispersed phase can also represent 99 % of the total volume (Paul *et al.*, 2004). The volume fraction alone is thus not sufficient to predict which phase will necessarily form the dispersed phase and which one the continuous phase. The physical properties of the liquids such as the viscosity play an important role. The transition of

dispersed phase to continuous phase is called phase inversion. It can occur as a result of several effects, such as changes in stabilisation, physical properties or phase ratios (Paul *et al.*, 2004).
Numerous processes in the chemical, the crude oil and the pharmaceutical industry involve liquid-liquid dispersions. Frequently, the overall reaction rate of the process is dependent on the mass transfer between the dispersed phase and the continuous phase. This mass transfer is predominantly a function of the interfacial area, and the interfacial area depends on the size of the drops of dispersed phase formed in the continuous phase: the smaller the drops formed, the larger the interfacial area. The drops of dispersed phase are not of uniform and unique size, they rather show a size distribution. For the process design, it is of importance to determine this drop size distribution to be able to characterise and evaluate the resulting mass transfer.

Drop size distribution

In a biphasic setup, the dispersion observed is the result of the equilibrium between two opposite phenomena: (1) the disruption of the phase, which is due to the shear stress applied on the drops through the stirrer and their consequent deformation, and (2) the coalescence of the drops produced through collision with other drops of dispersed phase. The drop size distribution is a result of the inhomogeneous distribution of the hydrodynamic forces in the reactor, leading to regions where the coalescence is predominant, and others, where the dispersion is prevalent. The maximum and minimum drop size observed largely depend on the stirrer speed and the stirrer type used. The drop size distribution is commonly described in terms of number frequency (equation 4.19), volume frequency (equation 4.20), cumulative number frequency (equation 4.21) or cumulative volume frequency (equation 4.22).

$$f_n(d_i) = \frac{n_i}{\sum_{j=1}^{m} n_j} \tag{4.19}$$

$$f_v(d_i) = \frac{n_i \cdot d_i^3}{\sum_{j=1}^{m} n_j \cdot d_j^3} \tag{4.20}$$

$$F_n(d_i) = \frac{\sum_{i=1}^{k} n_i \cdot d_i}{\sum_{j=1}^{m} n_j \cdot d_j} \tag{4.21}$$

$$F_v(d_i) = \frac{\sum_{i=1}^{k} n_i \cdot d_i^3}{\sum_{j=1}^{m} n_j \cdot d_j^3} \tag{4.22}$$

n_i number of drops in the size fraction i -

n_j number of drops in the size fraction j -

d_i average drop size of the size fraction i, m

d_j average drop size of the size fraction j, m

A parameter commonly used to represent the drop size distribution is the Sauter diameter (d_{32}). It is the ratio of the third to the second moment of the distribution and it is calculated according to equation 4.23. Physically, the Sauter diameter represents the diameter the drops would have if the entire volume of the dispersed phase was divided into spherical particles of the same size, whose total area is the same than the total area of the drop size distribution. Consequently, the Sauter diameter has the same ratio of surface area to volume than the drop size distribution. This is the reason why it is frequently used to represent the drop size distribution in mass transfer calculations (Paul *et al.*, 2004).

$$d_{32} = \frac{\sum_{j=1}^{m} n_j \cdot d_j^3}{\sum_{j=1}^{m} n_j \cdot d_j^2} \tag{4.23}$$

d_{32} Sauter diameter, m

Based on the Sauter diameter, the interfacial area (a_d) of the dispersion can be determined as indicated in equation 4.24.

$$a_d = \frac{6 \cdot \varphi_d}{d_{32}} \tag{4.24}$$

a_d interfacial area, m^{-1}

φ_d phase fraction of the dispersed phase, -

Experimental determination of the drop size distribution and the interfacial area

Various experimental methods are available to determine the drop size distribution of a dispersion. They can be divided into *in situ* measurement methods, directly applied to the dispersion in the reactor, and at-line measurement methods, requiring to retrieve samples. With the latter methods, it is crucial that the sampling procedure does not influence the state of the dispersion. These methods are therefore only recommended for stable and dilute dispersions.

The at-line methods include the static determination of the light scattering: a sample is taken from the dispersion, and the total drop surface is determined through the intensity and the angle of the scattered light. The Sauter diameter is then deduced using equation 4.24. Another means to determine the drop size distribution is to record pictures of a sample of the dispersion through a microscope, and evaluate the size of the drops with an image processing software.

The *in situ* methods require the introduction of a probe into the reactor. An endoscope equipped with a photosensor can record pictures on-line. The drop size distribution is obtained using an image processing software giving the size of each drop on the picture. The Phase-Doppler anemometry makes use of a light source and two photodetectors to determine the diameter of flowing drops based on the Doppler effect created through the movement. Finally, the three-dimensional optical laser reflexion measurement is based on the detection of the reflexion of a laser by the drops flowing by the lense of the sensor. The time elapsed while a reflexion is recorded is used to determine the corresponding drop diameter.

Estimation of the Sauter diameter and the interfacial area

In addition to the methods presented above, semi-empirical correlations have been developed that permit to estimate the Sauter diameter (d_{32}). The drop size distribution, and thus also the Sauter diameter are strongly dependent on many process characteristics, such as the density (ρ) and the viscosity (η) of both phases, the interfacial tension ($\sigma_{d,c}$), the phase fraction of the dispersed phase (φ_d), as well as the stirrer speed (N_R) and the stirrer diameter (d_R). The correlations established are however also only valid for given geometric characteristics of the reactor itself . They generally suppose a constant ratio between the reactor diameter, the reactor height, the height at which the stirrer is fixed and the stirrer diameter (Zlokarnik, 1999). In addition, each correlation is only valid for a given stirrer type. Concerning the reaction systems, it is generally distinguished between:

- Dispersed phase concentration:
  - dilute systems: $\varphi_d < 0.01$
  - moderately concentrated systems: $\varphi_d < 0.2$
  - concentrated systems: $\varphi_d > 0.2$
- Viscosity:
  - low-viscosity dispersed phases: $\eta_d < 10$ mPa s
  - moderate-viscosity dispersed phases: 10 mPa s $< \eta_d <$ 500 mPa s
  - large-viscosity dispersed phases: $\eta_d > 500$ mPa s
- Coalescence behaviour: visual observation after 5 min stirring
  - stable dispersion: appearance of a coalesced layer after only 5 min
  - strongly coalescing: complete phase separation after only 30 s

The drop formation in a dilute, low-viscosity and stable reaction system is relatively well described in literature (Paul *et al.*, 2004). In contrast, almost no information is found on reaction systems with $\varphi_d > 0.2$ or strongly coalescing reaction systems, due to the complexity of the phenomena occurring in these systems. For reaction systems with dispersed phase volume fraction up to $\varphi_d \cong 0.2$, and showing low coalescence behaviour, the expressions established for dilute systems are usually applied with empirical correction terms accounting for the larger dispersed phase concentrations and its consequences for the Sauter diameter.

Chen and Middleman (1967) established a correlation giving d_{32} for a stable reaction system with low dispersed phase concentration and low-viscosity dispersed phase in a cylindrical reactor with a six-blade Rushton turbine (equation 4.25). The relationship indicated is valid under the assumptions of local isotropy and constant power input in turbulent mixing conditions.

$$\frac{d_{32}}{d_R} = 0.053 \cdot We^{-0.6} \tag{4.25}$$

$$We = \frac{\rho_c \cdot N_R^2 \cdot d_R^3}{\sigma_{d,c}} \tag{4.26}$$

We Weber number, -

ρ_c density of the continuous phase, kg m^{-3}

N_R stirrer speed, s^{-1}

d_R stirrer diameter, m

$\sigma_{d,c}$ interfacial tension between the dispersed and the continuous phase, N m^{-1}

For dilute and stable reaction system, but with a moderate-viscosity dispersed phase, Calabrese *et al.* (1986a,b) and Wang and Calabrese (1986) presented a slightly modified version of equation 4.25, including a correction term for the increased viscosity (Vi). This 'viscosity group' represents the ratio of the viscous forces to the surface forces stabilising the drop. In the limit of Vi $\longrightarrow$ 0, equation 4.27 yields again equation 4.25.

$$\frac{d_{32}}{d_R} = 0.053 \cdot We^{-0.6} \cdot \left(1 + 0.91 \cdot Vi^{\,0.84}\right)^{0.6} \tag{4.27}$$

$$Vi = \left(\frac{\rho_c}{\rho_d}\right)^{0.5} \cdot \frac{\eta_d \cdot N_R \cdot d_R}{\sigma_{d,c}} \tag{4.28}$$

Vi viscosity group, -

ρ_d density of the dispersed phase, kg m^{-3}

η_d viscosity of the dispersed phase, Pa s

The same authors also adapted equation 4.27 to account for moderately concentrated and stable reaction system with moderate-viscosity dispersed phase (equation 4.29) (Calabrese *et al.*, 1986b). The expression presented was suggested valid for $\eta_{\mathrm{d}} < 500$ mPa s and $\varphi_{\mathrm{d}} < 0.3$. However, no experimental validation was presented.

$$\frac{d_{32}}{d_R} = 0.054 \cdot (1 + 3 \cdot \varphi_d) \cdot We^{-0.6} \cdot (1 + 4.42 \cdot (1 - 2.5 \cdot \varphi_d) \cdot Vi \cdot (\frac{d_{32}}{d_R})^{1/3})^{0.6} \tag{4.29}$$

4.5.3 Diffusion in dispersions

Once the drop size distribution, its corresponding Sauter diameter and thus also the interfacial area of the dispersion are known, the mass transfer between both phases can be estimated. The mass transfer between two liquid phases can be described on basis of several models. The most common are the two-film theory, the penetration theory and the surface renewal theory. The two-film model was first presented by Lewis and Whitman (1924). It assumes that the boundary layer at the interface is a stagnant fluid film of thickness δ (Fig. 4.12), on each side of the interface. The mass transfer in these films occurs only by molecular diffusion. This diffusion through both films on each side of the interface forms the rate limiting part of the mass transfer from one phase to the other. The interface is in a state of constant thermodynamic equilibrium.

In contrast to the two-film model, the penetration model and the surface renewal model suppose a non-steady state at the interface. Both describe an exchange of the surface elements in contact at the interface after a given amount of time. The penetration model developed by Higbie (1935) indicates a given time span, depending on the relative movement of both phases to each other, during which the two volume elements are in contact, and after which they are exchanged with other volume elements. The surface renewal model by Danckwerts (1951), is based on the assumption that the different liquid elements do not all stay at the interface the same amount of time. The contact time is not supposed to be solely dependent on the relative velocity of one phase to the other, but rather on the random movement of the turbulent flow around the volumes considered. In contrast to the penetration model, where each volume element is considered to be in contact during the same limited and fixed time span, this stochastic approach leads to a variable contact time between 0 and ∞.

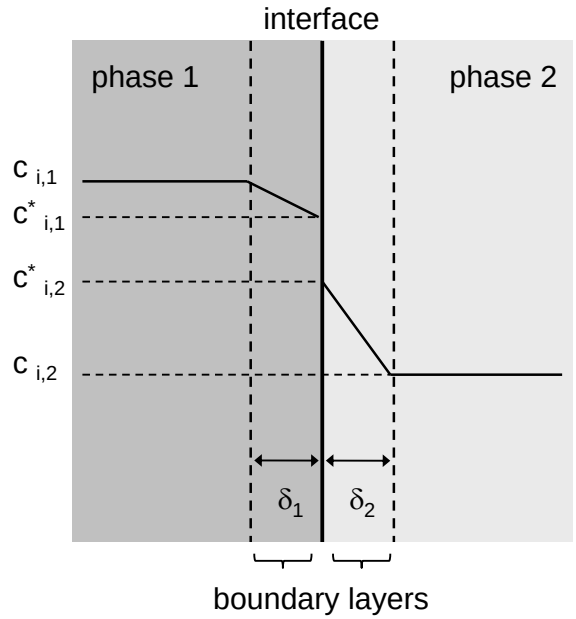

Figure 4.12: Diffusion in biphasic liquid systems according to the two-film model. Concentration of i in the bulk of phase 1 ($c_{i,1}$), equilibrium concentration of i at the interface in phase 1 ($c^*_{i,1}$), equilibrium concentration of i at the interface in phase 2 ($c^*_{i,2}$), concentration of i in the bulk of phase 2 ($c_{i,2}$) and thickness of the boundary layer (δ).

While the penetration model and the surface renewal model surely give a more realistic description of the processes taking place, the two-film model is generally applied when evaluating the mass transfer between two phases. It is a less complex model, but it still gives very similar results in comparison to the other two models (Perry, 1999).

When it can be assumed that the mass transfer resistance in one of the boundary layers on each side of the interface is negligible in comparison to the other, the two-film model is reduced to a one-film-model (Fig. 4.13). This assumption is e.g. valid when the diffusion coefficient of the substance of interest in one of the liquids is much larger than in the other phase, and when the partition coefficient of the compound is largely in favour of it, too (Brauer, 1978a,b; Schügerl, 2009).

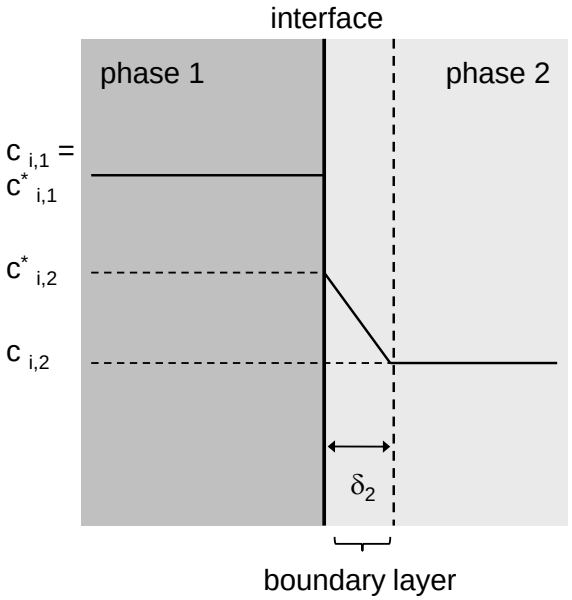

Figure 4.13: Diffusion in biphasic liquid systems according to the one-film model. Concentration of i in the bulk of phase 1 ($c_{i,1}$), equilibrium concentration of i at the interface in phase 1 ($c^*_{i,1}$), equilibrium concentration of i at the interface in phase 2 ($c^*_{i,2}$), concentration of i in the bulk of phase 2 ($c_{i,2}$) and thickness of the boundary layer (δ).

According to the one-film model, the mass transfer between two phases can be described by equation 4.30.

$$STR = \beta_i \cdot a_d \cdot (c^*_{i,c} - c_{i,c}) \tag{4.30}$$

STR	substrate transfer rate, mol L^{-1} s^{-1}
β_i	mass transfer coefficient of i, m s^{-1}
$c_{i,c}^*$	equilibrium concentration of i at the interface, mol L^{-1}
$c_{i,c}$	concentration of i in the bulk of the continuous phase, mol L^{-1}

The mass transfer coefficient in the mixing conditions fixed is usually not known. It can be deduced using the Sherwood number (Sh) and the diffusion coefficient of the substance under consideration (equation 4.31). However, these parameters are themselves often unknown. In that case, they have to be estimated using (semi-)empirical correlations.

$$Sh = \frac{\beta_i \cdot d_{32}}{D_{i,c}} \tag{4.31}$$

Sh	Sherwood number, -
$D_{i,c}$	diffusion coefficient of i in the continuous phase, $m^2\ s^{-1}$

The semi-empirical correlations giving Sh or β_i as a function of the process parameters are specific to a given setup and they are only valid in the conditions indicated. For the case of liquid drops in a baffled tank reactor with a six-blade turbine, three different correlation were presented by Skelland and Moeti (1990) (equation 4.32), Skelland and Tedder (1987) (equation 4.33) and Skelland and Lee (1981, 1982) (equation 4.34).

$$Sh = 1.237 \cdot 10^{-5} \cdot {Sc_c}^{1/3} \cdot Re^{\,2/3} \cdot Fr^{\,5/12} \cdot \left(\frac{d_R}{d_{32}}\right)^2 \cdot \left(\frac{d_R}{D_R}\right)^{0.5} \cdot \left(\frac{\rho_d \cdot {d_{32}}^2 \cdot g}{\sigma_{d,c}}\right)^{1.25} \cdot \varphi_d^{-0.5} \tag{4.32}$$

$$Sh = 2.621 \cdot 10^{-3} \cdot \frac{\left(N_R \cdot D_{i,c}\right)^{0.5}}{d_R} \cdot \varphi_d^{0.304} \cdot \left(\frac{d_R}{D_R}\right)^{1.582} \cdot Re^{\,1.929} \cdot Oh^{\,1.025} \tag{4.33}$$

$$\frac{\beta_i}{\left(N_R \cdot D_{i,c}\right)^{0.5}} = 2.932 \cdot 10^{-7} \cdot \varphi_d^{-0.508} \cdot \left(\frac{d_R}{D_R}\right)^{0.548} \cdot Re^{\,1.371} \tag{4.34}$$

Sc_c	Schmidt number of the continuous phase, -, given by equation 4.35
Re	Reynolds number, -, given by equation 4.38
Fr	Froude number, -, given by equation 4.36
g	gravity, $m\ s^2$
D_R	reactor diameter, m
Oh	Ohnesorge number, -, given by equation 4.37

$$Sc_c = \frac{\eta_c}{\rho_c \cdot D_{i,c}} \tag{4.35}$$

$$Fr = \frac{N_R^2 \cdot d_R}{g} \tag{4.36}$$

$$Oh = \frac{\eta_c}{(\rho_c \cdot d_R \cdot \sigma_{d,c})^{0.5}} \tag{4.37}$$

$$Re = \frac{d_R^2 \cdot N_R \cdot \bar{\rho}}{\bar{\eta}} \tag{4.38}$$

$\bar{\eta}$ combined viscosity, mPa s, given by equation 4.40

$\bar{\rho}$ combined density, g cm^{-3}, given by equation 4.39

$$\bar{\rho} = \varphi_d \cdot \rho_d + \varphi_c \cdot \rho_c \tag{4.39}$$

$$\bar{\eta} = \frac{\eta_c}{\varphi_c} \cdot (1 + \frac{1.5 \cdot \eta_d \cdot \varphi_d}{\eta_d + \eta_c}) \tag{4.40}$$

ρ_c density of the continuous phase, kg m^{-3}

η_c viscosity of the continuous phase, Pa s

The correlations presented above also necessitate the knowledge of the diffusion coefficient ($D_{i,c}$) of the compound considered in the continuous phase. If it cannot be determined experimentally, it has to be estimated by using a correlation giving the diffusion coefficient as a function of other, known, parameters.

The best known correlation for the estimation of the diffusion coefficient is the expression developed by Wilke and Chang (1955) (equation 4.41). It was established for the characterisation of the diffusion of a substance i in an aqueous liquid at infinite dilute concentrations of i (up 5 or 10 % mol/mol). The prediction for 251 solute-solvent pairs showed an error of ~ 10 % in comparison to the experimental data. To date, no validation of the expression for temperatures above 30 °C has been established (Sherwood *et al.*, 1975).

$$D_{i,c} = 7.4 \cdot 10^{-8} \cdot \frac{(\Phi_c \cdot M_c)^{0.5} \cdot T}{\eta_c \cdot MV_i^{0.6}} \tag{4.41}$$

Φ_c association coefficient of the solvent, -

M_c molar weight of the solvent, g mol^{-1}

T temperature, K

MV_i molar volume of i at its boiling temperature, cm^3 mol^{-1}

The model presented by Reddy and Doraiswamy (1967) was developed on basis of equation 4.41, replacing the association coefficient by the square root of the molar volume of the diffusing compound (equation 4.42). The constant k_{RS} is dependent on the ratio of the molar volume of the continuous phase (MV_c) to the molar volume of the diffusing substance (MV_i). If this ratio is ≤ 1.5, $k_{RS} = 1 \cdot 10^{-7}$. The correlation showed an average error of 13.5 % when tested on 76 different systems.

$$D_{i,c} = k_{RS} \cdot \frac{T}{\eta_c} \cdot \frac{M_c^{0.5}}{(MV_i \cdot MV_c)^{1/3}} \tag{4.42}$$

Hayduk and Laudie (1974) adapted a correlation presented by Othmer and Thakar (1955) on basis of the diffusion of 87 substances in diluted aqueous solutions (equation 4.43). This correlation should only be used for the diffusion in low-viscosity solvents.

$$D_{i,c} = 1.326 \cdot 10^{-4} \cdot \eta_c^{-1.4} \cdot {MV_i}^{-0.589} \tag{4.43}$$

The correlation established by Tyn and Calus (1975) is also only valid for low-viscosity solvents (equation 4.44). It leads to relatively good predictions of the diffusion coefficient at infinite dilution, with errors generally < 10 % (Reid, 1988) .

$$D_{i,c} = 8.93 \cdot 10^{-8} \cdot \left(\frac{MV_i}{{MV_c}^2}\right) \cdot \left(\frac{p_c}{p_i}\right)^{0.6} \cdot \frac{T}{\eta_c} \tag{4.44}$$

$$p = MV \cdot \sigma^{0.25} \tag{4.45}$$

P_c parachor of the solvent, $cm^3\ g^{0.25}\ mol^{-1}\ s^{-0.5}$

P_i parachor of the diffusing substance, $cm^3\ g^{0.25}\ mol^{-1}\ s^{-0.5}$

σ surface tension, $N\ m^{-1}$

Similarly, Hayduk and Minhas (1982) published a correlation for aqueous solutions (equation 4.46). According to the authors, it predicts the diffusion coefficient with less than 10 % error.

$$D_{i,c} = 1.25 \cdot 10^{-8} \cdot \left({MV_i}^{-0.19} - 0.292\right) \cdot T^{1.52} \cdot \eta_c^{\varepsilon^*} \tag{4.46}$$

$$\varepsilon^* = \frac{9.58\ cm^3\ mol^{-1}}{MV_i} - 1.12 \tag{4.47}$$

Finally, when the diffusion coefficient ($D_{i,c}$) of the substances of interest in the reaction system and the Sherwood number (Sh) have been determined according to the considerations above, the mass transfer coefficient (β_i) can be determined using equation 4.31. Once this parameter is known, the mass transfer between the two phases can then be estimated and this information can then be integrated into the process development.

4.6 Characterisation of the biotransformation

To characterise the evolution of a given biotransformation, several parameters are used. One of the most important variables is the conversion. It describes the quantity of substrate that was converted at a given point in time (equation 4.48).

$$X(t) = \frac{n_{S,0} - n_S}{n_{S,0}} \cdot 100\ \% \tag{4.48}$$

X	conversion, %
$n_{S,0}$	initial substrate quantity, mol
n_S	substrate quantity at time t, mol

Similarly, the yield of the product of interest at a given point in time is given by equation 4.49.

$$Y(t) = \frac{n_P - n_{P,0}}{n_{S,0}} \cdot \frac{|\nu_S|}{|\nu_P|} \cdot 100\ \% \tag{4.49}$$

Y	yield, %
n_P	product quantity at t, mol
ν_S	stoichiometric factor of the substrate
ν_P	stoichiometric factor of the product

If only one product is formed during the reaction and if side-products can thus be excluded, the conversion and the yield are the same, because in that case $(n_P - n_{P,0}) \cdot \frac{|\nu_S|}{|\nu_P|} = n_{S,0} - n_S$.

The success of a given process is also often evaluated by its productivity relative to the reaction volume. This variable is called the space-time yield (STY) and it is calculated as indicated in equation 4.50.

$$STY = \frac{n_P}{t \cdot V_R} \tag{4.50}$$

STY	space-time yield, mol L^{-1} h^{-1}
t	reaction duration, h
V_R	reaction volume, L

Finally, one of the crucial variables during the production of chiral compounds is the enantiomeric excess (ee). This variable indicates in which proportion the respective enantiomers were formed (equation 4.51). Ideally, an enantiomeric excess of 100 % is reached, meaning that only one of the two enantiomers was formed. If both enantiomers are formed in equal amounts, the enantiomeric excess will be 0.

$$ee = \frac{|n_R - n_S|}{n_R + n_S} \cdot 100\ \% \tag{4.51}$$

n_R	quantity of *R*-enantiomer, mol
n_S	quantity of *S*-enantiomer, mol

5 Materials and Methods

5.1 Materials

5.1.1 Chemicals and equipment

The ionic liquids used in this project were kindly provided by Merck KGaA (Darmstadt, Germany). Their full names and the abbreviations used are given in the appendix (Table A.3 and Table A.4). All other chemicals purchased from different producers, as well as the equipment and the different media and buffers used during this work are listed in the appendix (section B to section F).

5.1.2 The biocatalyst used: *Escherichia coli* LB ADH CB FDH

The biocatalyst used is a recombinant *Escherichia coli* strain (*E. coli*), which was kindly provided by Julich Chiral Solutions (Jülich, Germany): *E. coli* BL21 (DE3) T1r(pET24a-adhL.brevis-fdhC.boidinii) (*E. coli* LB ADH CB FDH). The BL21 strain contains a copy of the T7 polymerase gene (λ-DE3 lysogen). The T7 RNA polymerase activates the transcription from the T7 promoter of the pET-plasmid. The expression of this plasmid is consequently repressed until the T7 RNA polymerase is induced from its lac promoter. The pET-plasmid contains the two genes coding for the *Lactobacillus brevis* alcohol dehydrogenase (LB ADH) and the *Candida boidinii* formate dehydrogenase (CB FDH). The expression of both genes is thus controlled by the same promoter. The plasmid also confers a Kanamycin resistance.

5.2 Microbiological methods

5.2.1 Cell culture

Stocks

The biocatalyst was stored as cryogenic stocks. Cell banks were prepared by growing the biocatalyst in shake flasks as described below. The cells were harvested during the exponential growth phase and mixed to sterile glycerol at a ratio of 2:1 (v/v). The cell-

glycerol mix was poured in sterile Eppendorf vials and shock-frozen using liquid nitrogen. The cryogenic stocks were then kept at −80 °C until their further use.

Preculture

For the preculture of the biocatalyst, two cryogenic stocks were added into a 500 mL shake flask containing 50 mL cultivation medium (appendix, Table F.23). The shake flask was then incubated at 37 °C and 250 min^{-1} for 10 h.

Culture

The cultivation of the biocatalyst was performed in fed-batch mode in a stirred tank bioreactor of nominal volume 7.5 L (Fig. 5.1).

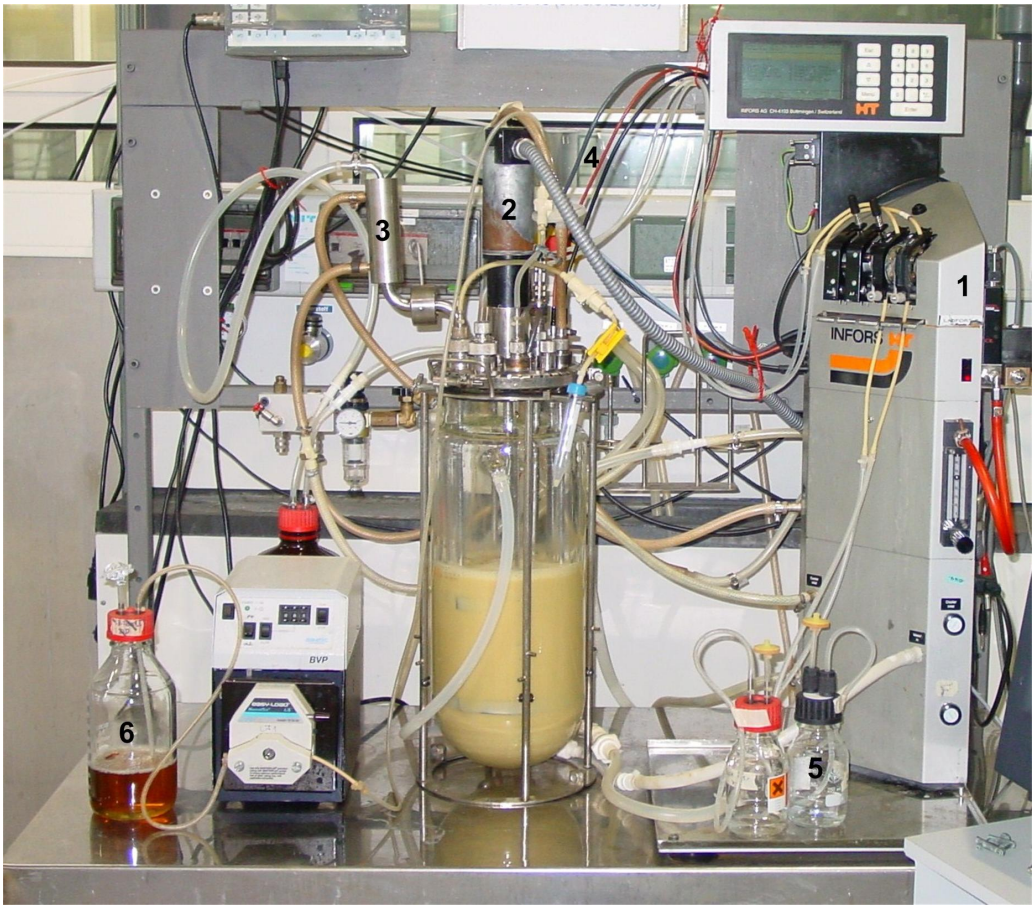

Figure 5.1: 7.5 L stirred tank reactor used for the cultivation of *E. coli* LB ADH CB FDH in fed-batch mode: control station (1), stirrer (2), air outlet (3), pH, pO_2 and temperature probes (4), acid and base for pH control (5), feed (6).

The reactor was filled with 4 L cultivation medium (appendix, Table F.24) and inoculated with a syringe with 50 mL of preculture cell suspension. The temperature was set to 37 °C and pH was fixed to 6.8. The pH was automatically controlled by addition of 25 % (v/v) NH_4OH or 18 % (v/v) H_3PO_4. The air flow was set to 6 L min^{-1} (1.5 vvm). The mixing speed was adjusted between 600 and 1200 min^{-1} by a control sequence keeping the dissolved oxygen (DO) between 25 % and 35 %. Once all the substrate was consumed, the temperature was decreased to 30 °C and a glucose containing feed (appendix, Table F.25) was added according to equation (equation 4.3), fixing the specific growth rate to 0.12 h^{-1}. 6 h after the start of the glucose feed, this first feeding phase was stopped. The cell culture was then induced by addition of 1 mM Isopropyl β-D-1-thiogalactopyranoside (IPTG). As the protein expression would be inhibited by glucose, a second exponential feeding phase was started after induction, now adding a glycerol feed (appendix, Table F.26). The specific growth rate was now fixed to 0.09 h^{-1}. 9 h after induction, the cells were harvested and kept at 4 °C until their further use.

5.2.2 Determination of the dry cell weight

The determination of the dry cell weight (DCW) of *E. coli* samples was made gravimetrically. A given volume of cell suspension was introduced in previously dried and weighted 2 mL-Eppendorf vials. The vials were then centrifuged at 13000 min^{-1} for 10 min. After drying again to constant weight, the vials were weighted again. The DCW of the sample was deduced using equation 5.1.

$$c_x = \frac{m_{full} - m_{empty}}{V} \tag{5.1}$$

c_x	cell concentration, g_{DCW} L^{-1}
m_{full}	weight of vial with cells after drying, g
m_{empty}	weight of empty vial, g
V	volume of the sample of the cell suspension , L

5.2.3 Determination of the optical density of cell suspensions

The dry cell weight of a cell suspension is directly proportional to the optical density (OD) of the sample (equation 5.2). The corresponding correlation factor (f_x) can be determined by calibration on a set of data for which both the OD and the DCW was measured. Once

this factor is known, the OD of the culture samples rather than the DCW is measured and the DCW is determined using equation 5.2. In this project, the OD of the various *E. coli* cell suspensions was determined in cuvettes with an optical path length of 10 mm using a single beam photometer at a wavelength of 600 nm.

$$c_x = OD_{600} \cdot f_x \tag{5.2}$$

OD_{600} optical density at 600 nm, -

f_x correlation factor, $g_{DCW}\ L^{-1}$

5.2.4 Biocompatibility evaluation

The evaluation of the biocompatibility is often made by determining the membrane integrity of the biocatalyst after exposure to the substances under investigation. The determination of the membrane integrity is ideally made using methods that rely on the photometric detection of various substances entering the cells only when the membrane is lysed (as used in e.g. the LIVE/DEAD Kit by Invitrogen). These methods showed however very low reproducibility when used in assays containing (traces) of ionic liquid. This is due to the fluorescence of some ionic liquids at the same wavelengths as used during the measurements, interfering with the signals that should be detected (data not shown). These methods were thus not further considered here. As an alternative to these techniques, an indirect indicator was chosen to evaluate the integrity of the cell membrane in varying conditions: the viability of the cell. It is indeed supposed that a cell with a (partially) permeabilised cell membrane cannot reproduce. The ability to reproduce should consequently be a sufficiently precise indication for the integrity of the cell membrane. In this project, the viability after exposure to given conditions and the growth in presence of the substances under investigation were therefore analysed.

Viability evaluation and agar plating

Resting cells of *E. coli* LB ADH CB FDH were first incubated in the various conditions of interest (e.g. in presence of different organic solvents or ionic liquids). The assays were prepared in 4 mL glass vials, at a total volume of 1.2 mL. They were incubated at room temperature, without stirring. After 5 h of incubation, samples were taken to be plated on Agar in order to evaluate the cell viability.

The composition of the Agar plates used is indicated in appendix (Table F.19). Before plating, the cell suspensions were diluted in sterile conditions with phosphate buffered saline to reach an estimated number of colony forming units (CFU) on the Agar plates between 10 and 100 after incubation for 24 h. The plates were incubated at 37 °C. After 24 h, the number of CFUs on each plate was counted. The comparison with a reference sample then permitted to evaluate the relative viability of the cells in each of the other samples.

Cell growth in presence of toxic compounds

To evaluate the toxicity of 2-octanone and 2-octanol to the biocatalyst, *E. coli* LB ADH CB FDH was grown in 250 mL flasks in 50 mL preculture medium (appendix, Table F.23) to which different concentrations of these substances were added. The concentrations of 2-octanone and 2-octanol were chosen inferior to their respective maximal solubility in water. A reference not containing any of the aforementioned substances was also established. The cells were incubated at 37 °C and 250 min^{-1}, for a duration of 7 h. Samples were taken at regular time intervals to monitor the evolution of the cell growth in the different growth conditions. The specific growth rates of each test culture were determined on basis of the cell concentrations measured at the different points of time using equation 4.1.

5.2.5 Cell lysis

Cell lysis with glass beads

Glass beads were added to the cell suspension of wanted cell density at a volume fraction of 50 %. The cells were lysed for 8 min at 1800 min^{-1} in a mixer mill and then centrifuged at 4 °C (20 min at 13000 min^{-1}) to separate the glass beads and the cell fractions from the rest. Only the supernatant was used in further experiments.

Cell lysis with PopCulture™

The reagent PopCulture™ is a concentrated mixture of detergents, which lyses the cell membrane without denaturing the proteins present in the cell. For this lysis procedure, the cell suspension was diluted to a cell density of 1 g_{DCW} L^{-1} with phosphate buffer (0.1 M, pH 6.5). PopCulture™ was added to the cell suspension at a concentration of 10 % (v/v). The assays were then incubated for 15 min at room temperature, whereafter the cell lysate was ready for further use.

5.3 Enzyme characterisation

5.3.1 Enzyme activity assay

The determination of the enzyme activity was performed in microtiter plates (MTPs) using cell lysate as described in subsection 5.2.5. The composition of the respective assays is given in Table 5.1. The total reaction volume and the sample volume (cell lysate) were fixed to 200 μL and 20 μL, respectively. The reaction was started by the addition of the cell lysate into the assay, at a final concentration equivalent to a cell concentration of 0.2 g_{DCW} L^{-1}. On basis of the recorded data, the enzyme activity was then determined using the Lambert-Beer relation as described by equation 4.11.

Table 5.1: Composition of the assays used for the photometric determination of the enzyme activity of the *Lactobacillus brevis* alcohol dehydrogenase (LB ADH) and the *Candida boidinii* formate dehydrogenase (CB FDH).

Reagent	LB ADH	CB FDH
Cofactor	NADH 0.88 mM	NAD^+ 0.94 mM
Substrate	2-octanone 6.67 mM	sodium formate 80 mM
Buffer	0.1 M phosphate pH 7.0	0.1 M phosphate pH 8.0

5.3.2 Determination of kinetic parameters

The kinetic parameters of both enzymes were estimated on basis of the initial reaction rates in varying reaction conditions. As both enzymes function according to a two-substrate mechanism, the determination of the half saturation concentration (K_m) of one enzyme for one of its substrates was determined in assays where the second substrate was present in excess, i.e. in concentrations larger than 10 times its K_m. In these conditions, the specific reaction rate can be described according to a classic Michaelis-Menten kinetic described by equation 4.14 (Bisswanger, 2000).

The evaluation of the kinetic parameters of both enzymes was performed using cell lysate prepared according to subsection 5.2.5 and not with the purified enzymes. This choice was made because the cell lysate better represents the conditions effectively found within the whole cell during the whole-cell biotransformation than the purified enzymes. The K_m determined here are thus more 'apparent K_m' values rather than true K_m commonly indicated in enzyme characterisation studies. For the same reason, the assays were prepared at pH 7, approximately the pH value generally found within *E. coli* cells and not at the optimal pH of each enzyme (pH 5.5 for the LB ADH (Machielsen *et al.*, 2009) and pH 7 for the CB FDH (Bommarius and Karau, 2005)).

When evaluating the initial reaction rates in given conditions, it is of great importance to be within an enzyme concentration range where the reaction rate is directly proportional to the quantity of enzyme present (Bisswanger, 2000). To guarantee that this condition was satisfied, the valid concentration range was determined afresh for each new biocatalyst batch and the cell lysate used for the K_m determinations was then prepared accordingly. For each K_m determination 10 different initial reaction rates were registered, varying the substrate concentration within a range of 0.2 to 5 times the (expected) K_m (Segel, 1993). The enzyme concentration was kept constant, as well as the co-substrate quantity, present in excess. The assays were prepared at a total reaction volume of 200 μL. First, the cell lysate was mixed with the cofactor. Then, the assay was diluted in 0.1 M phosphate buffer at pH 7. Finally the reaction was started by the addition of the substrate. The reactions were performed at a constant temperature of 30 °C.

For the CB FDH, the experiments were performed in a MTP, monitoring the increase of absorption in a photometer at 340 nm, analogous to subsection 5.3.1. The reaction rate was then determined using equation 4.11. For the LB ADH, the experiments could not be evaluated photometrically, as the range of concentrations of the cofactor (NADH) necessary to be in excess provoked absorptions above the linearity domain of the photometer (up to 0.8 mM NADH only). The determination of the reaction rate in these assays was thus performed in a different setup. The composition of the assays was the same as described above, but the reaction was performed in Eppendorf vials kept a constant temperature in a shaking thermomixer (600 min^{-1}). The duration of the reaction was chosen to be within a time frame where the measured reaction rate can still be considered as 'initial', i.e. a time range during which a conversion of 10 % would not be exceeded. After this reaction time, the reaction was stopped by addition of cold ethyl acetate (−20 °C), containing internal standard (7.2 mM 2-heptanone), at a volume ratio aqueous phase:ethyl acetate of 2:1.

The assays were then immediately treated for analysis by gas chromatography: the buffer phase was extracted with the organic phase added to stop the reaction in a mixer mill (10 min at 1800 min^{-1}), whereafter the phases were separated by centrifugation at room temperature (5 min at 13000 min^{-1}). After the phase separation, the organic phase was analysed by gas chromatography. The reaction rate of the enzyme was then determined on basis of the quantity of product formed over the fixed reaction duration.

Once 3–5 sets of at least 10 initial reaction rates had been registered using different initial substrate concentrations, the determination of the corresponding K_m was made by non-linear regression using the program SigmaPlot 8.0 (Systat Software Inc).

5.3.3 Enzyme stability evaluation

The stability of the LB ADH and the CB FDH in given conditions was evaluated by determining their corresponding half-life. To this aim, the enzymes were incubated in the conditions of interest, and the rest-activity was measured over a fixed period of time. The experiments were performed in 4 mL glass vials placed on a multistirrer plate. The assays were prepared at a total volume of 1.4 mL. When testing the stability of the enzymes in presence of various water soluble substances, these chemicals were dissolved in the buffer phase (0.5 M potassium phosphate, 1 M formate, pH 6.5) and no stirring was applied. The substances of interest were added in different concentrations below their maximal water solubility. When evaluating the stability of the enzymes in presence of a second phase, two different modes were applied: with stirring (250 min^{-1}), in order to evaluate the phase toxicity, and without stirring, to evaluate the molecular toxicity of this second phase. These biphasic assays contained 20 % non water miscible solvent and the aqueous phase was formed by phophate buffered saline (appendix, Table E.18).

The half-life of the enzyme in given conditions was evaluated by measuring the decrease of the enzyme activity over time and then determining the corresponding inactivation constant. When the inactivation kinetic is of first order, this constant is obtained as described in subsection 4.4.3, using equation 4.12. The half-life of the enzyme in these conditions is then given by equation 4.13.

5.4 Biotransformations

5.4.1 General proceeding

For the biotransformations, the cells stored at 4 °C were resuspended in the aqueous phase to the wanted biocatalyst concentration, varying from 50 g L^{-1} to 130 g L^{-1}. The aqueous phase was composed of a potassium phosphate buffer (0.5 M, pH 6.5), also containing the co-substrate (appendix, Table E.14 and Table E.15). The substrate was diluted to the wanted concentration in the ionic liquid ([HMPL][NTF]), varying from 150 mM to 1200 mM. Substrate concentrations indicated in the following as 'initial substrate concentration in the ionic liquid phase' refer to the concentrations of 2-octanone found in the ionic liquid before equilibration of the loaded ionic liquid with the aqueous phase. Varying volume ratios of aqueous phase to ionic liquid were used. The experiments were started by mixing the loaded ionic liquid phase with the aqueous phase containing the biocatalyst.

All the biotransformations were performed at room temperature and in sealed vessels to avoid loss of the organic substrate and product by evaporation. Samples of the ionic liquid phase were taken before starting each biotransformation in order to determine the exact amount of substrate initially present in the system. Samples of the emulsion formed after starting the reaction were continuously taken to monitor the evolution of the conversion and the enantiomeric excess during the biotransformation. The samples were treated according to subsection 5.7.1 and then analysed by gas chromatography. The data shown represent the average of two samples analysed per time point.

5.4.2 Biotransformations at the 200 mL scale

The biotransformations at the 200 mL scale were performed in a modified bubble column according to Weuster-Botz *et al.* (2002) (Fig. 5.2). It has a nominal volume of 400 mL and it is equipped with three baffles (width 15 mm) and a magnetically driven six-blade Rushton turbine. The blades have a square geometry of 8 x 8 mm. The stirrer speed was fixed to 600 min^{-1}, except mentioned otherwise. The relatively large volume of the reaction vessel allows frequent sampling and thus good monitoring of the evolution of the reaction over time.

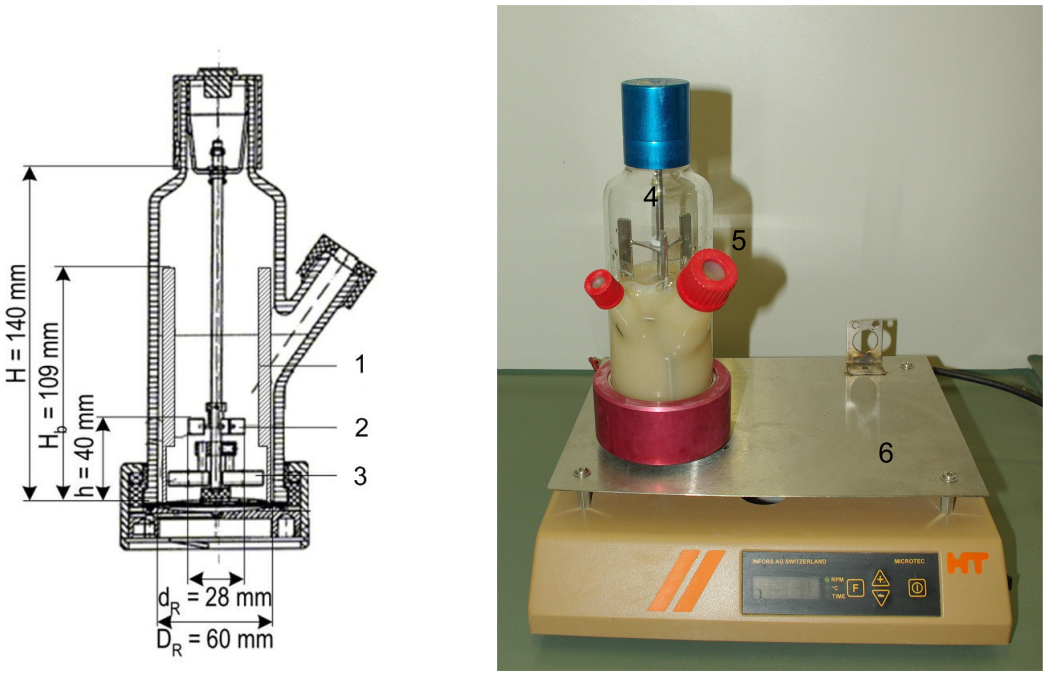

Figure 5.2: Drawing of the 200 mL stirred tank reactor (adapted from Pfründer (2005)) and picture of the reactor during a biotransformation: baffles (1), six-blade Rushton turbine (2), magnetic drive inside the reactor (3), stirrer axis (4), sampling opening (5), support with main magnetic drive (6).

5.4.3 Scale-up to the Liter scale

The scale-up of the biotransformation to Liter scale was performed in a stirred tank bioreactor with a nominal volume of 1.2 L (Fig. 5.3). It is equipped with two six-blade Rushton turbines, which were fixed at a height of 2 cm and 6 cm from the stirrer tip. During the reaction, the stirrer speed was set to 450 min^{-1}. This stirring speed was chosen to provide the same maximal local energy dissipation in the Liter scale reactor than in the 200 mL reactor at a mixing speed of 600 min^{-1}.

To guarantee that the experiments at the Liter scale and at the 200 mL scale would be performed in exact the same conditions, the biotransformations were performed in parallel, using the same biocatalyst batch. The reactions were performed at room temperature, with an initial substrate concentration of 300 mM 2-octanone in the ionic liquid phase, 50 g_{DCW} L^{-1} biocatalyst and 0.3 M sodium formate in the aqueous phase (appendix, Table E.15), and at an ionic liquid volume fraction of 20 %. The working volumes were 200 mL and 1 L, respectively. Samples were taken to monitor the evolution of the conversion and the enantiomeric excess over a duration of 6 h. Even though the Liter scale reactor permits pH and temperature control, these features were not used here.

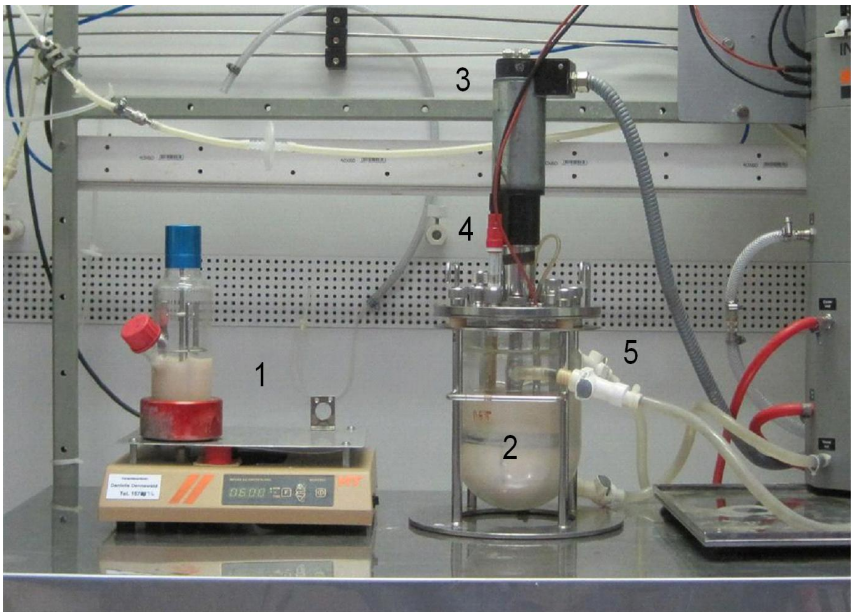

Figure 5.3: Scale-up of the biotransformation to the Liter scale: 200 mL reactor (1) and 1 L reactor (2), with its stirrer (3), a pH probe (4) and the possibility to control the temperature (5). The experiments were performed in parallel, and in the same reaction conditions.

5.4.4 Biotransformations at the 10 mL scale

When no continuous monitoring of the conversion was required and an end point determination was sufficient, the biotransformations were performed at smaller scale (10 mL). This allowed a significant reduction of the experimental effort and costs. The reaction vessels used for these experiments were glass vials of nominal volume 25 mL that can be sealed with a plastic cap (Fig. 5.4). For the biotransformations, the vials were placed on a multistirrer plate, where mixing was assured by a magnetic stirrer in the vial. To guarantee homogeneous mixing, the stirrer speeds was fixed to 350 min^{-1}. In this setup, a maximum of 5–7 samples could be taken. Experiments were performed as two parallel replicates. The results indicated are the average values obtained in each assay.

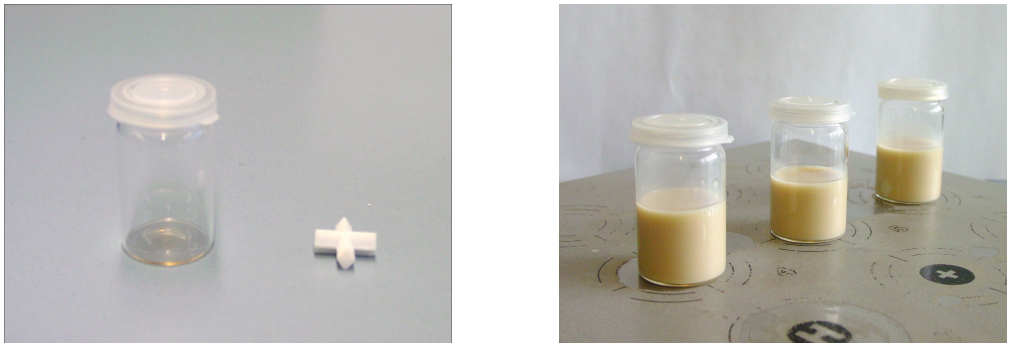

Figure 5.4: Biotransformations at reduced volume: glass vial of nominal volume 25 mL and the magnetic stirrer used for end point determinations of the conversion in biotransformations (left). Glass vials on the multistirrer plate during the biotransformations (right).

5.4.5 Biotransformations in the 'bioreactor unit'

The biotransformations were also performed in the bioreactor unit developed by Weuster-Botz *et al.* (2005). This tool was developed to overcome the common issue of scalability between small scale and large scale vessels. It is composed of a set of miniaturized stirred tank bioreactors, allowing the parallel operation of up to 48 reactors at the mL-scale (Puskeiler *et al.*, 2005; Weuster-Botz *et al.*, 2005). The system is equipped with magnetically driven impellers and shows similar process engineering characteristics compared to laboratory- and production-scale reactors (Hortsch and Weuster-Botz, 2010c). Through this, a reliable and robust scale-up of the processes from the small-scale to a larger-scale is assured. The bioreactor unit allows temperature and pH control, monitoring of the dissolved oxygen (DO), as well as sampling and feeding.

Biotransformations in the bioreactor unit were performed at a reaction volume of 14 mL in each bioreactor. The stirring was set to 1500 min^{-1} and the experiments were performed at room temperature. Three parallel assays were prepared for each reaction setup analysed. The results indicated are the average values obtained in the three parallel experiments.

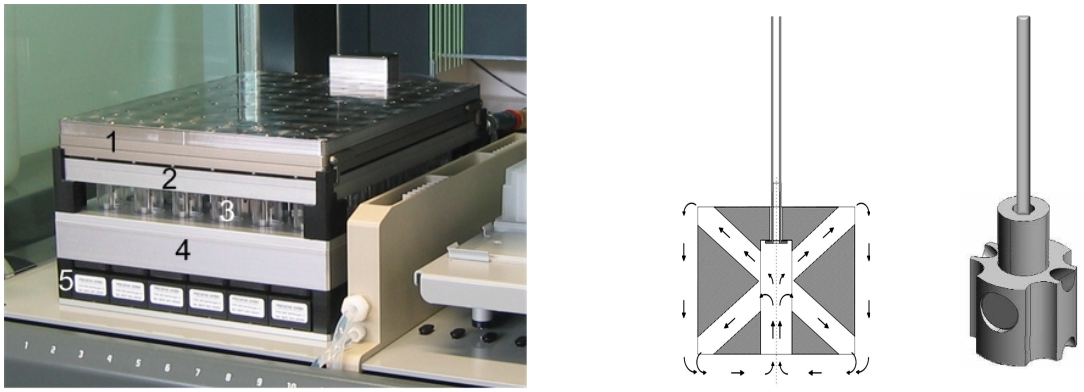

Figure 5.5: Biotransformations in the bioreactor unit: bioreactor unit with the 48 parallel miniaturized stirred tank bioreactors (left): sterile gas supply and outlet (1), head space cooling (2), bioreactor (3), magnetic stirrer drive (4), optical sensors for pH and dissolved oxygen monitoring (5). Scheme of the stirrer used in the bioreactors and the mixing induced (adapted from Michael Fischer, 2mag AG) (right).

5.5 Recycling of the ionic liquid

The recyclability of the ionic liquid phase was evaluated by using the same ionic liquid batch during 25 of the following cycles: (1) a biotransformation at the 200 mL scale, followed by (2) the phase separation by centrifugation and (3) the product isolation and ionic liquid purification by distillation.

The biotransformations were executed as described in subsection 5.4.1 and subsection 5.4.2. The reaction conditions were an initial substrate concentration of 300 mM 2-octanone in the ionic liquid phase, 50 g_{DCW} L^{-1} biocatalyst and 0.3 M sodium formate in the aqueous phase, and an ionic liquid volume fraction of 20 %.
After the biotransformation, the emulsion formed during the reaction was separated into its individual components by centrifugation (5 min, 2500 min^{-1}, room temperature). The ionic liquid was then isolated from the other components of the reaction system. While the aqueous phase and the used biocatalyst were discarded, the ionic liquid phase - containing the wanted product - was introduced into the next stage of the process.

In this next stage, the product, as well as any non converted substrate was withdrawn from the ionic liquid phase by distillation. This step thus constitutes both the product recovery and the purification of the ionic liquid phase. The distillation was performed in a rotary evaporator at a temperature of 130 °C under minimal pressure ($P < 5$ mbar) over a duration of 5 h. After the distillation, the purified ionic liquid was reused in a subsequent biotransformation.

The sampling and the transfer of ionic liquid between the different recipients resulted in a loss of ionic liquid in each cycle. Therefore, the ionic liquid volume was completed with fresh ionic liquid before each new biotransformation, in order to guarantee a constant volume ratio between the ionic liquid and the aqueous phase. New substrate was added at the beginning of each cycle to a concentration of 300 mM 2-octanone in the ionic liquid phase. Fresh aqueous phase containing fresh biocatalyst was introduced into the stirred tank reactor and mixed to the ionic liquid containing the substrate. The co-substrate (sodium formate) necessary for the cofactor regeneration was contained in the aqueous phase and was thus supplied simultaneously with the latter.

Samples were taken before starting the reaction, during the biotransformation, as well as before and after the distillation. The samples were treated according to subsection 5.7.1 and analysed by gas chromatography to determine their 2-octanone and 2-octanol content. This allowed to monitor the evolution of conversion during the biotransformation, as well as the recovery yield of the distillation. In addition, samples of ionic liquid were taken after each cycle, and analysed by ion ^{1}H NMR and ion chromatography according to subsection 5.7.3. The goal of these analyses was to verify if the anion or the cation composing the ionic liquid were degrading over the subsequent process cycles and to monitor a possible accumulation of potentially harmful substances in the ionic liquid.
The purity of the product recovered at the end of each cycle was determined by gas chromatography. The values indicated were calculated by comparison of the concentration of 2-octanol in the distillate to the concentration of 2-octanol determined in purchased samples of known analytical degree.

5.6 Recycling of the ionic liquid and the biocatalyst

In addition to the recyclability of the ionic liquid, the recyclability of the biocatalyst was investigated. For these experiments, the same procedure as described in section 5.5 was followed, except that the biocatalyst was not discarded. After the biotransformation and the phase separation by centrifugation, only the aqueous phase was discarded. The ionic liquid was introduced into the rotary evaporator for the product isolation and ionic liquid purification, and the biocatalyst was stored at 4 °C in phosphate buffered saline until the next biotransformation was started.
For the following biotransformation, the biocatalyst was then resuspended in fresh aqueous phase and mixed to the recycled ionic liquid containing new substrate. As the sampling and the transfer of the reaction mix during the different process steps resulted on average in a loss of ~ 12.5 % of the cells, these losses were compensated by addition of fresh cells to reach the fixed biocatalyst concentration (50 g_{DCW} L^{-1}).

5.7 Analytics

5.7.1 Sample treatment for the analysis by gas chromatography

As neither water nor ionic liquid can be injected onto the column for analysis by gas chromatography, the samples taken during the various experiments had to be pre-treated before proceeding to the determination of their 2-octanone and 2-octanol content.
Samples containing only an aqueous phase and no ionic liquid were extracted with ethyl acetate containing 36 mM 2-heptanone at a ratio of 1:1 (v/v) in a mixer mill (30 min, 1800 min^{-1}). Subsequently, the two phases were separated by centrifugation (15 min, 4500 min^{-1}, room temperature) and the organic phase was diluted if necessary with dry ethyl acetate. The samples were stored at −20 °C until their analysis by gas chromatography.
Samples containing both an aqueous phase and ionic liquid were first centrifuged (5 min, 13000 min^{-1}) to separate both phases. The ionic liquid phase was extracted with *n*-hexane at a ratio of 1:4 (v/v) in a mixer mill (1 h, 1800 min^{-1}). The organic phase and the ionic liquid were then separated by centrifugation (15 min, 4500 min^{-1}, room temperature). Finally, the organic phase was diluted with dry ethyl acetate and ethyl acetate containing 36 mM 2-heptanone at a volume ratio of 1:3:1. The samples were stored at −20 °C until their analysis by gas chromatography.

5.7.2 Gas chromatography methods

Once the samples were treated according to subsection 5.7.1, they were analysed by gas chromatography to determine their 2-octanone, *R*-2-octanol and *S*-2-octanol content. The analyses were performed on a CP-3800 gas chromatograph from Varian, Inc. (Darmstadt, Germany),using the following setup:

Column:	BGB-175
Internal standard:	7.2 mM 2-heptanone
Injection:	1 μL, split 40
Column flow:	2.5 mL min^{-1} helium 5.0
Oven temperatur:	50 °C, for 44 min; increase to 150 °C at 6 °C min^{-1}
Typical retention time:	2-heptanone: 15 min; 2-octanone: 29 min; *S*-2-octanol: 32 min; *R*-2-octanol: 33 min

The detector used is a flame ionisation detector (FID). The detector and the injector temperatures were fixed to 250 °C. The split was reduced to 10 before 0.01 min and after 0.5 min. Further equipment specifications are indicated in the appendix (Table B.8). The quantification of the sample content was done by calibration within a range of concentrations from 1 mM to 500 mM for each substance of interest.

5.7.3 Analysis of ionic liquid samples by ^{1}H NMR and ion chromatography

Samples of the ionic liquid phase were analysed by ^{1}H NMR to detect compounds resulting from the possible degradation of the cation due to the recycling procedure.

Accumulation of potentially harmful substances in the ionic liquid phase through contamination during the recycling procedure or through degradation of either the anion or the cation was also verified by ion chromatography. These analyses were carried out on a Metrohm system (Deutsche METROHM GmbH & Co. KG, Filderstadt, Germany), equipped with a model 820 IC separation center, a 819 IC detector, and a Metrosepp A Supp 5 column. The eluent was composed of an aqueous mixture containing $3.2 \cdot 10^{-3}$ M Na_2CO_3, $1.0 \cdot 10^{-3}$ M $NaHCO_3$ and 5 % (v/v) acetonitrile.

5.8 Reaction system characterisation

5.8.1 Partition coefficients

The partition coefficients of the relevant substances (2-octanone and 2-octanol) in two different systems had to be determined. First, the partition coefficient of 2-octanone and 2-octanol between the ionic liquid and the aqueous phase: the knowledge of this partition coefficient is of importance because it will permit to follow the evolution of conversion during the reaction by analysing only one of the phases (the ionic liquid) and deducing the concentration of each substance in the second phase (the buffer phase) through the known partition coefficient, instead of measuring the concentrations of each substance in both phases. In addition, it gives an indication of how much the ionic liquid reduces the exposure of the biocatalyst to the toxic substrate and product.
Second, the partition coefficient of 2-octanone and 2-octanol between the ionic liquid and *n*-hexane: the knowledge of this partition coefficient is important for the analytical determination of the substrate and product content of the ionic liquid: as the ionic liquid has an extremely low volatility, it cannot be introduced into the gas chromatograph directly. It needs to be extracted with a non-miscible, volatile organic solvent beforehand, e.g. *n*-hexane. This organic solvent is then introduced into the gas chromatograph to determine its substrate and product content instead of the ionic liquid. However, to be able to deduce the ionic liquid substrate and product content on basis of the results obtained during the analysis of the organic phase, the partition coefficient between the ionic liquid and this organic solvent has to be known. These partition coefficients were determined in a common set of experiments, based on three subsequent extraction steps.

In the first step, the substrate and the product were dissolved at a concentration of 300 mM in *n*-hexane. This loaded hexane phase was then extracted at a ratio of 4:1 (v/v) by ionic liquid in a mixer mill (1 h, 1800 min^{-1}, room temperature). After phase separation by centrifugation (15 min, 4500 min^{-1}, room temperature), the hexane phase was analysed by gas chromatography to determine its substrate and product content. The concentration of substrate and product in the ionic liquid after the extraction was then deduced using equation 5.3.

$$c_{IL} = (\varphi_{IL}^{-1} - 1) \cdot (c_{hexane,0} - c_{hexane}) \tag{5.3}$$

c_{IL}	concentration in the ionic liquid after extraction with *n*-hexane, mol L^{-1}
$c_{hexane,0}$	initial concentration in *n*-hexane, mol L^{-1}
c_{hexane}	equilibrium concentration in *n*-hexane after the extraction, mol L^{-1}
φ_{IL}	volume fraction of the ionic liquid in the extraction step, -

For the determination of the partition coefficient between the ionic liquid and the buffer (0.5 M potassium phosphate, 1 M formate, pH 6.5, appendix Table E.14), the now loaded ionic liquid was extracted with buffer at a phase ratio of 1:4 (1 h, 1800 min^{-1}, room temperature). After the phase separation by centrifugation (15 min, 4500 min^{-1}, room temperature), the substrate and product content of the buffer phase was analysed according to section 5.7. The equilibrium concentration of the substrate and product in the ionic liquid after extraction with the buffer phase was then determined by calculating the difference of the aqueous phase content to the previously determined concentration of the substance in the loaded ionic liquid phase before the extraction. The partition coefficient of the substrate or the product between the ionic liquid and the buffer phase is then calculated according to equation 5.4.

$$logD_{IL/aq} = log_{10} \frac{c_{IL} - (\varphi_{IL}^{-1} - 1) \cdot c_{aq}}{c_{aq}} \tag{5.4}$$

$\log D_{IL/aq}$	decadic logarithm of the partition coefficient of a substance between the ionic liquid and the aqueous phase, -
c_{aq}	equilibrium concentration in the aqueous buffer after the extraction, mol L^{-1}

Then, the ionic liquid obtained from the extraction with the buffer phase was again extracted with *n*-hexane at a phase ratio of 1:4 (1 h, 1800 min^{-1}, room temperature). After the phase separation (15 min, 4500 min^{-1}, room temperature), the organic phase

was analysed by gas chromatography. The goal of this step was to determine the partition coefficient of the substrate and the product between water saturated ionic liquid and *n*-hexane according to equation 5.5.

$$logD_{IL/hexane} = log_{10} \frac{(c_{IL} - (\varphi_{IL}^{-1} - 1) \cdot c_{buffer}) - (\varphi_{IL}^{-1} - 1) \cdot c_{hexane}}{c_{hexane}} \tag{5.5}$$

$\log D_{IL/hexane}$ decadic logarithm of the partition coefficient of a substance between the ionic liquid and *n*-hexane, -

5.8.2 Viscosity

The viscosities of various liquids were determined using a Searle-type rotational viscosimeter (Rheomat 115, Contraves, Zurich, Switzerland) with 15 previously set shear rates in a broad range from 22 s^{-1} to 3430 s^{-1}. The rheological measurements were made at a constant temperature of 30 °C.

5.8.3 Surface tension and interfacial tension

The surface tension and the interfacial tension were determined using a tensiometer K100C (A.KRÜSS Optronic, GmbH, Hamburg, Germany). The determination of the surface tension of different aqueous solutions and of ionic liquids were made using the De Noüy ring method as described by du Noüy (1925) and Harkins and Jordan (1930a,b). Due to the slightly unusual properties of the ionic liquid used - having larger density than the buffer phase, but lower surface tension than the latter - the interfacial tension of the biphasic system had to be determined using the less common ring-push method (du Noüy, 1925). The measurements were performed at room temperature.

5.8.4 Drop size distribution, Sauter diameter and interfacial area

The drop size distribution of the dispersed phase within the continuous phase was determined using a laser scanning probe with a rotating laser beam (3D ORM Sensor, MTS, Düsseldorf, Germany) with a measurement range from 10 μm to 1000 μm. The measurements were performed in the stirred tank reactor described in subsection 5.4.2.
The distributions were determined for biphasic reaction systems ionic liquid-buffer (0.5 M phosphate, 1 M sodium formate, pH 6.5) with and without cells. The measurements were

made varying both the stirrer speed (from 300 min^{-1} to 900 min^{-1}), as well as the phase fraction of the ionic liquid (from 10 % to 70 %). The cell concentrations used for the measurements with cells were 5 g_{DCW} L^{-1} and 50 g_{DCW} L^{-1}. The total measurement volume was fixed to 200 mL and the measurements were made at room temperature. The drop size distributions were only recorded once the system was stable, and then each 60 s for at least 20 min.
The Sauter diameter (d_{32}) and the interfacial area were calculated on basis of the recorded distributions, according to equation 4.23 and equation 4.24. The values indicated for each set of conditions are the average value obtained from all the spectra recorded for this setup.

5.8.5 Maximum local energy dissipation

The maximum local energy dissipation was measured by adapting the clay/polymer flocculation system (Hoffmann *et al.*, 1992) to the 200 mL-scale. It was shown that this system is suitable for the estimation of the maximum local energy dissipation in bioreactors (Henzler, 2000; Mahnke *et al.*, 2000). First, blue clay particles (Witterschlicker Blauton HFF, WBB-Fuchs, Ransbach-Baumbach, Germany) were suspended to a concentration of 5 g L^{-1} in deionized water in the reactor, at a given stirrer speed. Sodium chloride was added to the suspension (1 g L^{-1}), in order to reduce the repulsion forces of the clay particles. The floc accumulation was induced by adding 0.03 g L^{-1} of a cationic polymer (Preastol 650 BC, Ashland, Krefeld, Germany). The resulting floc size distribution was taken as starting point for all the floc break-up experiments. As a result of the shear forces provoked in the fluid by stirring, the particle size of the flocs then started decreasing until an equilibrium particle size was reached after an extended period of time. This equilibrium size distribution was determined as described in subsection 5.8.4. It is a function of the maximum local energy dissipation in the reactor and it can thus be used as a direct means of comparison (Hinze, 1955).

In this project, the equilibrium floc diameters were determined after 40 min of stirring at the various stirring speeds. This period of time was sufficient to reach the equilibrium floc size distribution in each of the setups evaluated. The obtained equilibrium drop size distribution can be represented by a logarithmic normal distribution. This means that the median value ($d_{3.50}$) of the volume sum distribution can be used as characteristic floc size. This floc size is consequently also a direct function of the maximum local energy dissipation in the reactor.

Once the characteristic floc size has been registered for each stirrer speed in the 200 mL reactor, the values obtained are compared with the $d_{3.50}$ values recorded for a standard laboratory stirred tank reactor. For such standard tank reactors, empiric correlations permit to calculate the maximal local energy dissipation as a function of the stirrer speed (equation 5.6).

$$\varepsilon_{\max} = \frac{c_D \cdot u_{tip}^3}{h} \tag{5.6}$$

$\varepsilon_{\max}$	maximum local energy dissipation, W kg^{-1}
u_{tip}	stirrer tip speed, m s^{-1}
h	height of the stirrer blade, m
c_D	dissipation constant, for standard stirred tank reactors with six-blade Rushton turbines $c_D = 0.1$ (Hinze, 1955; Brodkey, 1975; Henzler, 2000)

$$u_{tip} = d_R \cdot \pi \cdot N_R \tag{5.7}$$

d_R	stirrer diameter, m
N_R	stirrer speed, s^{-1}

As given $d_{3.50}$ values are due to the same maximal local energy dissipation (Hinze, 1955), the comparison between the $d_{3.50}$ values for the standard laboratory reactor - for which the maximal energy dissipation can be calculated - and the $d_{3.50}$ values for the 200 mL reactor permits to determine the corresponding maximal local energy dissipation for each stirring speed in the smaller reactor.

5.9 Modelling of the biphasic whole-cell reaction system

5.9.1 System equations

A mechanistic approach is chosen to establish a model of the reaction system. The variables of the model are the concentrations of the different substrates and products of the system - 2-octanone and 2-octanol, but also the co-substrate formate and its corresponding product CO_2, as well as the cofactors NADH and NAD^+ - in the different parts of the reaction system: the ionic liquid phase, the aqueous phase in which the cells are suspended and the space inside the cell. The system equations are the differential equations describing the evolution of these concentrations over time. They are obtained by mass balances and are defined as a function of the different mass fluxes occurring in the reaction system during the process.

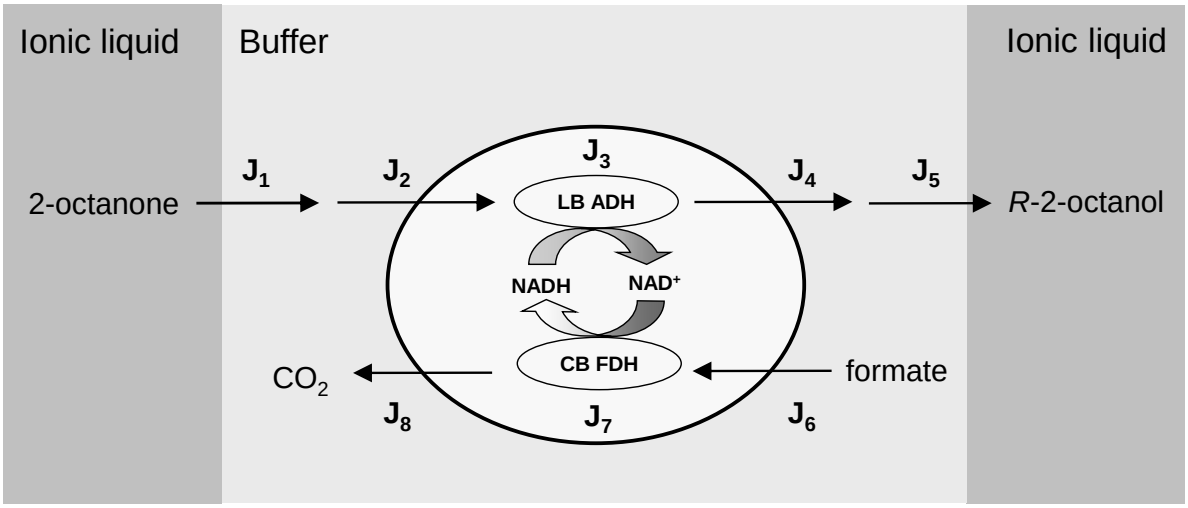

Figure 5.6: Scheme of the biphasic whole-cell biocatalysis with the mass transfers from the ionic liquid to the aqueous phase (J_1) and from the aqueous phase into the cell (J_2 and J_6); the enzymatic transformations (J_3 and J_7); and the mass transfers from the cell to the aqueous phase (J_4 and J_8) and from the aqueous phase to the ionic liquid (J_5).

In total, 8 different mass fluxes intervene in the reaction system (Fig. 5.6):

- The mass transfer between the ionic liquid phase and the aqueous phase:
  - The transfer of the substrate (2-octanone) from the ionic liquid phase to the aqueous phase (J1).
  - The transfer of the product (*R*-2-octanol) from the aqueous phase to the ionic liquid phase (J5).

- The mass transfer between the aqueous phase to the medium inside the cell:
  - The transfer of the substrate (2-octanone) from outside to inside the cell (J_2).
  - The transfer of the product (*R*-2-octanol) from inside the cell to outside (J_4).
  - The transfer of the co-substrate (formate) from outside to inside the cell (J_6).
  - The transfer of the co-product (CO_2) from inside the cell to the outside (J_8).
- The enzymatic reactions:
  - The reaction of interest, i.e. the transformation of the substrate (2-octanone) to the product of interest (*R*-2-octanol) by the LB ADH (J_3).
  - The reaction assuring the cofactor regeneration, i.e. the transformation of the co-substrate (formate) to the co-product (CO_2) by the CB FDH (J_7).

As the selectivity of the reduction of 2-octanone for *R*-2-octanol is maximal in the current process, no formation of by-products (e.g. the *S*-enantiomer) has to be taken into account.

If the reaction conditions are chosen carefully, conditions can be found in which the cofactor regeneration step by the CB FDH is not the rate limiting step of the biotransformation. In these conditions, the regeneration of NADH can be considered more rapid than its consumption. Consequently, it can be assumed: (1) that the cofactor in the cell is essentially present in its reduced form (NADH), and (2) that the influence of the CB FDH kinetic on the biotransformation can be neglected. In that case, the expression of the CB FDH kinetic does not have to be included into the model and the number of fluxes that have to be considered is significantly reduced (only J_1 to J_5). The enzymatic transformation during the biotransformation is then described by the LB ADH kinetic only.
In addition, in these conditions, the two-substrate model necessary to reliably describe the kinetic of the LB ADH is simplified. In fact, not only the product is constantly extracted through the aqueous phase into the ionic liquid, but also the oxidized cofactor produced by the LB ADH is very rapidly regenerated to NADH by the CB FDH. The backward reaction of the LB ADH - the oxidation of the alcohol formed using the oxidized form of the cofactor, NAD^+ - can thus be neglected and the kinetic is sufficiently well described by the expression given by equation 4.17 (subsection 4.4.3).
The number of variables considered is thus also considerably reduced: only 2-octanone and 2-octanol are now of importance. Indeed, the only other compound intervening in the equations is NADH. As it can be supposed that the cofactor is almost exclusively

present in its reduced form due to the rapid regeneration by the CB FDH, and the sum of NAD^+ and NADH is constant within a resting cell, the NADH concentration is supposed constant and equal to this sum (~ 1 mM, source Link (2009)).

Based on the equations for the corresponding mass transfer and the enzymatic reaction (equation 4.30, equation 4.10 and equation 4.17) presented in subsection 4.5.3, subsection 4.3.2 and subsection 4.4.3, the fluxes J_1 to J_5 are described by the following expressions:

$$J_1 = \beta_S \cdot a_d \cdot (C_S^* - C_{S,aq}) \tag{5.8}$$

$$J_2 = P_S \cdot \frac{A_{x,total}}{V_{x,total}} \cdot 10^3 \cdot (C_{S,aq} - C_{S,cell}) \tag{5.9}$$

$$J_3 = \frac{M_{x,total}}{V_{x,total}} \cdot \frac{v_{max} C_{NADH} C_{S,cell}}{K_{iNADH} K_{mS} + K_{mS} C_{NADH} + K_{mNADH} C_{S,cell} + C_{NADH} C_{S,cell}} \tag{5.10}$$

$$J_4 = P_P \cdot \frac{A_{x,total}}{V_{x,total}} \cdot 10^3 \cdot (C_{P,cell} - C_{P,aq}) \tag{5.11}$$

$$J_5 = \beta_P \cdot a_d \cdot (C_{P,aq} - C_P^*) \tag{5.12}$$

$$C_S^* = \frac{C_{S,IL}}{D_{IL/aq,S}} \tag{5.13}$$

$$C_P^* = \frac{C_{P,IL}}{D_{IL/aq,P}} \tag{5.14}$$

$$A_{x,total} = a_x \cdot M_{x,total} \tag{5.15}$$

$$V_{x,total} = v_x \cdot M_{x,total} \tag{5.16}$$

$$M_{x,total} = c_x \cdot V_{aq} \tag{5.17}$$

a_x	specific cell membrane surface, m^2 g_{DCW}^{-1}
$A_{x,total}$	total cell membrane surface, m^2
$C_{i,aq}$	concentration of i in the aqueous phase, mol L^{-1}
$C_{i,cell}$	concentration of i in the cell, mol L^{-1}
$C_{i,IL}$	concentration of i in the ionic liquid phase, mol L^{-1}
C^*_i	equilibrium concentration of i at the interface between the aqueous phase and the ionic liquid, mol L^{-1}
c_x	cell concentration in the aqueous phase, g_{DCW} L^{-1}
$D_{IL/aq,\ S,P}$	partition coefficient of S or P between the ionic liquid phase and the aqueous phase, -
J_n	mass flux, mol L^{-1} s^{-1}
K_m	half saturation concentration, mol L^{-1}
$M_{x,total}$	total cell mass, g_{DCW}
P_i	membrane permeability of i, m s^{-1}
subscript P	relative to the product (*R*-2-octanol)
subscript S	relative to the substrate (2-octanone)
V_{aq}	volume of the aqueous phase, L
v_{max}	maximal enzymatic reaction rate, mol s^{-1} g_{DCW}^{-1}
v_x	specific cell volume of *E. coli*, L g_{DCW}^{-1}
$V_{x,total}$	total cell volume, L

The expressions given by equation 5.8 to equation 5.17 are only valid in the conditions specified in subsection 4.5.3, subsection 4.3.2 and subsection 4.4.3, i.e.:

- the concentrations in the bulk of the ionic liquid, in the bulk of the aqueous phase and within the cells are homogeneous. There are no local concentration gradients.
- concerning the mass transfer between the ionic liquid and the aqueous phase: the resistance to the mass transfer in the ionic liquid can be neglected.

The mass balances giving the evolution over time of the substrate and product concentrations in the ionic liquid, in the aqueous phase and inside the cells are then defined by equation 5.18 to equation 5.23. These equations form the set of equations used to describe the reaction system under investigation. The simultaneous integration of these six differential equations gives the evolution of $C_{S,IL}$, $C_{S,aq}$, $C_{S,cell}$,$C_{P,cell}$, $C_{P,aq}$ and $C_{P,IL}$ with time during the process. However, all the parameters appearing in the equations have to be known.

$$\frac{dC_{S,IL}}{dt} = -J_1 \tag{5.18}$$

$$\frac{dC_{S,aq}}{dt} = J_1 \cdot \frac{V_{IL}}{V_{aq}} - J_2 \cdot \frac{V_{x,total}}{V_{aq}} \tag{5.19}$$

$$\frac{dC_{S,cell}}{dt} = J_2 - J_3 \tag{5.20}$$

$$\frac{dC_{P,cell}}{dt} = J_3 - J_4 \tag{5.21}$$

$$\frac{dC_{P,aq}}{dt} = J_4 \cdot \frac{V_{x,total}}{V_{aq}} - J_5 \cdot \frac{V_{IL}}{V_{aq}} \tag{5.22}$$

$$\frac{dC_{P,IL}}{dt} = J_5 \tag{5.23}$$

V_{IL} volume of the ionic liquid, L

5.9.2 Parameter determination

To be able to apply equation 5.18 to equation 5.23, the parameters appearing in the equations have to be determined. Most of the parameters can be determined experimentally (Table 5.6). The only exceptions are the mass transfer coefficients (β_i) of the substrate (2-octanone) and the product (*R*-2-octanol) defining the transfer between the ionic liquid to the aqueous phase and the respective membrane permeabilities (P_i).

Table 5.6: Symbol, description and determination methods for the different parameters of the biphasic whole-cell reaction model.

Symbol	Parameter	Determination
a_d	interfacial area between the ionic liquid and the aqueous phase per volume of dispersed phase, m^{-1}	experimental
a_x	specific cell membrane surface, $m^2\ g_{DCW}^{-1}$	experimental
β_i	mass transfer coefficient, $m\ s^{-1}$	estimation
$D_{IL/aq,\ i}$	partition coefficient of i between the ionic liquid phase and the aqueous phase, -	experimental
K_m	half saturation concentration, $mol\ L^{-1}$	experimental
$M_{x,total}$	total cell mass, g_{DCW}	experimental
P_i	membrane permeability of i, $m\ s^{-1}$	identification
v_{max}	maximal enzymatic reaction rate, $mol\ s^{-1}\ g_{DCW}^{-1}$	experimental
v_x	specific cell volume, $L\ g_{DCW}^{-1}$	experimental

The interfacial area, the partition coefficients, as well as the maximal enzymatic reaction rate and the half saturation constant were determined according to subsection 5.8.4, subsection 5.8.1 and subsection 5.3.2. The total cell mass used is given by the experimental conditions fixed. The total cell membrane area and the total cell volume are calculated on basis of literature data published for *E. coli*.

The mass transfer coefficients (β_i) for the substrate and the product can be determined if the respective Sherwood numbers (Sh) and diffusion coefficients (D_i) in the continuous phase are known (equation 4.31). These factors can be estimated using existing correlations giving the Sherwood number and the diffusion coefficient as a function of other system characteristics (a.o. viscosities, densities, molar volumes, temperature, stirrer diameter) (equation 4.32, equation 4.33 and equation 4.34).

Thus, only the membrane permeabilities can be neither measured nor estimated. These are the parameters that have to be identified by fitting the model to the experimental data recorded for the biotransformation.

5.9.3 Identification of the membrane permeability

The model established was used to identify the membrane permeability of the substrate and the product by fitting the model to the experimental data recorded during biotransformations. The experimental data is constituted by the concentrations of 2-octanone and *R*-2-octanol in the ionic liquid measured at different time intervals during the biotransformation. The identification of the two parameters (the membrane permeabilities of 2-octanone and *R*-2-octanol) was performed using the program MATLAB 7.8.0 (R2009a) (The MathWorks, Inc.). The integration of the set of differential equations was made with an ode15s solver. The model was fitted using a global search method, minimizing the sum of the squared errors (SSE) between the measured and the simulated substrate and product concentrations in the ionic liquid. The SSE is calculated as indicated in equation 5.24.

$$SSE = \sum_{i=1}^{m} (y_i - \hat{y}_i)^2 \tag{5.24}$$

SSE	sum of the squared errors, -
y_i	real (experimental) value of data point i, -
$\hat{y}_i$	estimated (simulated) value of data point i, -

The MATLAB codes used for the identification of the membrane permeabilities and the subsequent simulations are given in appendix (section H). The global search method was used over the range of 10^{-12} m s^{-1} to 1 m s^{-1} with a step of 80 values per decade. Nine different sets of biotransformation data were simultaneously fitted, each composed of seven values for the evolution of the substrate concentration and seven values for the evolution of the product concentration in the ionic liquid with time. These nine biotransformations were performed in different reaction conditions, with the initial substrate concentration varying between 200 mM and 750 mM 2-octanone in the ionic liquid and the ionic liquid volume fraction between 10 % and 40 %.

6 Process characterisation and parameter study for the asymmetric reduction of 2-octanone to *R*-2-octanol in biphasic ionic liquid/water systems

Bräutigam *et al.* (2009) applied biphasic ionic liquid-water systems to reduce 2-octanone to *R*-2-octanol using a recombinant *E. coli*. Even though very satisfying conversion (95 %) and enantiomeric excess (> 99.5 % (*R*)) were reached, the system had not been analysed in detail.

The aim of this chapter is therefore a more thorough investigation and characterisation of the asymmetric reduction of 2-octanone to *R*-2-octanol by *E. coli* LB ADH CB FDH, in order to assess its suitability for industrial applications. One of the major points of interest is the further optimisation of the reaction conditions to reach complete conversion. This might permit (1) to further increase the productivity and thus the financial success of the process, but more importantly (2) to avoid an additional purification of the product at the end of the process. This would require to reach a conversion > 99.0 % at an enantiomeric excess > 99.5 % (*R*). However, first, it is necessary to gain more information about the impact of the different system components on the biocatalyst activity and stability. Only then, the influence of varying reaction conditions on the reaction outcome can be better understood, making the outcome of the reaction more predictable.

Therefore, in the first section of this chapter, the effect of the various system components on the stability of the biocatalyst and the enzymes it contains are analysed. In the second section, various biotransformations performed in different reaction conditions are presented, with the aim to further elucidate the influence of the reaction conditions on the outcome of the reaction. The third section investigates the scale-up of the reaction to Liter scale. Finally, in the fourth and last part of this chapter, a tool for the parallel operation of 48 different setups is applied in order to evaluate its applicability for biphasic reaction systems involving ionic liquids.

6.1 Biocompatibility and enzyme stability in the biphasic whole-cell reaction system

The integrity of the biocatalyst and the activity of the enzymes are essential to the success of whole-cell biotransformations. If the cells are not integer, the cofactor necessary for the enzymatic transformation will leak from the cell, and the conversion will stop. Similarly, without active enzymes, no biotransformation can take place at all. The biocompatibility of the different system components as well as the enzyme stability within the reaction system are thus two very important aspects in whole-cell processes. They are therefore analysed in more detail for the process under consideration.

6.1.1 Toxicity of the substrate and the product

As demonstrated in the work by Bräutigam *et al.* (2009), the use of a biphasic reaction setup is essential to reach a satisfying conversion of 2-octanone and to avoid the stagnation of the biotransformation after only ~ 20 min reaction time, as it was observed in the monophasic setup. The early termination of the reaction in the monophasic setup is supposed to be due to the well-known toxicity of the substrate and the product towards the biocatalyst (Tanaka *et al.*, 1987; Chen and Chiou, 1995). To quantify this toxicity, the effect of the substrate and the product on the cell growth was monitored.

The range of concentrations tested were 4–7 mM 2-octanone and 2–5 mM 2-octanol. These concentrations are below the solubility limit of both substances in water (~ 8.6 mM for 2-octanone and 2-octanol at 20 °C). The growth rates observed in the different assays are indicated in Fig. 6.1. It can be observed that the cell growth is severely inhibited by both substances. While a 2-octanone concentration of 4 mM reduced the specific growth rate by ~ 15 %, a 2-octanone concentration of 5 mM led to a decrease of the growth rate of ~ 30 % in compariosn to the reference. The minimal inhibitory concentrations (MIC) of 2-octanone, i.e. the concentration of 2-octanone at which the cell growth is completely inhibited, is 6 mM. In presence of 2-octanol, the effect is even more severe: the growth rate is reduced by ~ 32 % at only 2 mM. Above this 2-octanol concentration, no growth is observed at all. The observed MIC for 2-octanol is 3 mM.

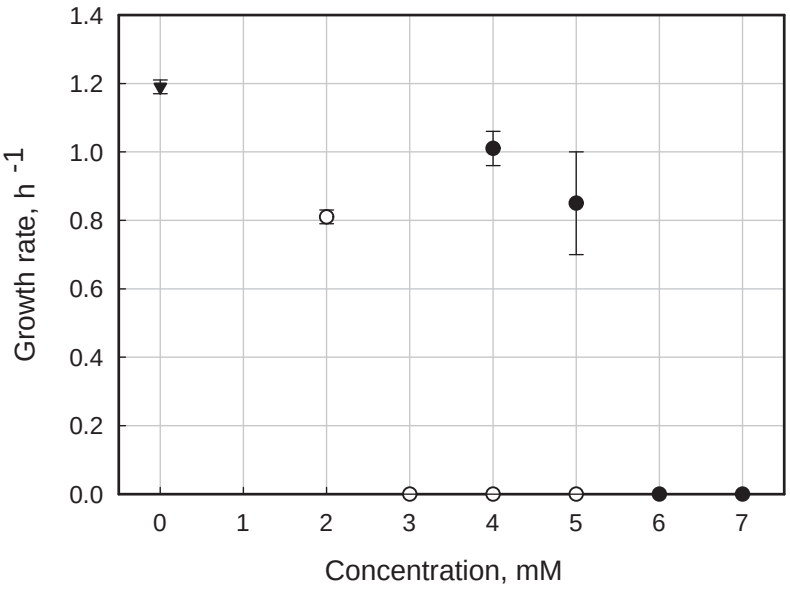

Figure 6.1: Growth rate of *E. coli* LB ADH CB FDH in the presence of varying concentrations of 2-octanone (●) and 2-octanol (○) added to the culture medium in comparison to the growth rate in the reference in pure culture medium (▼). 2-octanone concentrations of 4–7 mM and 2-octanol concentrations of 2–5 mM were evaluated.

Discussion

The growth in presence of varying concentrations of 2-octanone and 2-octanol confirmed the large toxicity of the substrate and the product considered in this process to the biocatalyst used. The experiments performed permitted to determine the minimal inhibitory concentrations (MIC) of 2-octanone and 2-octanol, i.e. the concentrations of 2-octanone and 2-octanol at which the cell growth is completely inhibited (6 mM for 2-octanone and 3 mM for 2-octanol). As a first indication, these values should not be exceeded in the aqueous phase during the biotransformations in order to prevent the biocatalyst from being damaged. Similar low toxic values for 2-octanone and 2-octanol to those observed here were reported for *Saccharomyces cerevisiae* (10 mM for 2-octanone and 9 mM for 2-octanol) (Li *et al.*, 2007) .

These results not only underline the importance of a biphasic reaction mode for this substrate/product pair, but also point out the crucial role of sufficiently large partition coefficients between the solvent and the aqueous phase. As the partition coefficients give the ratio between the concentrations found in the ionic liquid and the aqueous phase, they determine for a given biphasic system how much substrate can be added into the reaction system without risking to damage the biocatalyst. Larger partition coefficients permit

to add more substrate into the reaction system without trespassing the critical values of 2-octanone and 2-octanol than lower partition coefficients. Consequently, the respective partition coefficients are factors of major importance when evaluating the suitability of a given solvent for biphasic whole-cell biocatalyses, as well as when fixing the initial substrate concentration during the process development of a given setup.

6.1.2 Biocompatibility of the ionic liquid

For the application of ionic liquids in whole-cell biocatalysis, it is of great importance that they do not harm the biocatalyst, or at least not more than commonly used organic solvents. To this aim, the biocompatibility of the ionic liquid [HMPL][NTF] was compared to the biocompatibility of common non-water miscible organic solvents (Table 6.1).

After incubation for 5 h in agitated assays containing 20 % solvent, the samples were plated on Agar to determine the number of colony forming units (CFU) (Fig. 6.2). The number of CFUs determined for the assay with ionic liquid was in the same range as the reference not containing any solvent. The long chain alkanes down to heptane showed no significant difference, either. Hexane provoked a decrease in the number of CFUs. The samples from the assays containing toluene, butyl acetate, cyclohexane and chloroform did not show any CFU after incubation for 24 h at 37 °C. According to the method applied (subsection 5.2.4), this means that they contained less than 10^6 CFU per mL sample.

Discussion

The results presented above show that the ionic liquid analysed is generally less damaging for the biocatalyst than most of the organic solvents tested. Only dodecane, decane, and heptane are within the same range than the ionic liquid. Decane and heptane show however a boiling point lower than the boiling point of the product of interest, *R*-2-octanol (174 °C and 97 °C, respectively, vs. 177 °C). If these two solvents were used as second phase in the biotransformation under investigation, the isolation of the product from the solvent phase through distillation would necessitate to evaporate the solvent, present in relatively large quantities. This would constitute a significant investment of energy and consequently increased process costs. In contrast, dodecane has a boiling point larger than the boiling point of the product (216.3 °C vs. 177 °C). With this solvent, the product would be evaporated first during the product isolation. Nevertheless, considering the increased security issues occurring when using this organic solvent, the non-flammable and non-volatile ionic liquid [HMPL][NTF] still constitutes a more attractive alternative.

Table 6.1: Solvents used for the evaluation of their biocompatibility towards *E. coli* LB ADH CB FDH, their corresponding water solubility at 25 °C (source: Merck KGaA, Germany) and partition coefficient in 1-octanol/water systems (log P) (sources: Rajagopal (1996); Sardessai (2002); Zhang *et al.* (2009)).

Solvent	Water solubility, g L^{-1}	log P, -
[HMPL][NTF]	1.9	n.a.
dodecane	non miscible	6.6
decane	$5.0 \cdot 10^{-5}$	5.6
heptane	0.05	4.0
hexane	$9.5 \cdot 10^{-3}$	3.5
cyclohexane	0.055	3.2
toluene	0.52	2.5
chloroform	8	2.0
butyl acetate	7	1.7
MTBE	42	1.0

n.a. = not applicable

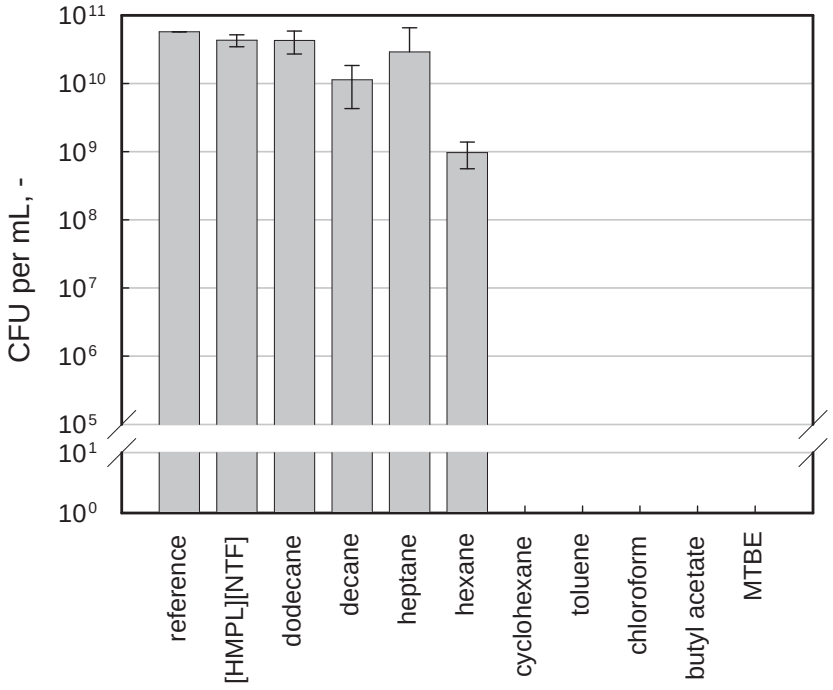

Figure 6.2: Number of colony forming units (CFU) per mL of sample after incubation of *E. coli* LB ADH CB FDH in biphasic assays containing 20 % (v/v) solvent.

The good biocompatibility of the ionic liquid used here is not exceedingly surprising, as the solvent was specifically chosen based on the good conversion reached during biphasic whole-cell biotransformations (Bräutigam *et al.*, 2009). This already indicated that [HMPL][NTF] must be relatively biocompatible to *E. coli*. Other authors presented similarly biocompatible ionic liquids: Cull *et al.* (2000) showed that *Rhodococcus* R312 retained its activity much better in biphasic systems composed of water and [BMIM][PF_6]than in water-toluene systems. The same observation was made by Hussain *et al.* (2007), which also demonstrated the good biocompatibility of [Oc_3MeN][NTF]. Pfruender *et al.* (2006) measured much better viability for *E. coli* and *S. cerevisiae* in assays with [BMIM][PF_6], [BMIM][NTF]and [Oc_3MeN][NTF] than with the organic solvents MTBE, diisopropylether, 1-octanol and 1-decanol.

The organic solvents tested showed a clear dependency between their respective partition coefficient in 1-octanol/water systems (log P), their water-miscibility and the biocompatibility observed. This is a generally known phenomenon: solvents with lower log P show larger water miscibility and larger toxicity because they are polar solvents and therefore partition easily into the aqueous phase and from there into the cell membrane. Common conclusions of experiments evaluating the biocompatibility of organic solvents are that solvents having a log P $<$ 3–4 show severe toxicity towards most cells (Bar, 1988; Rajagopal, 1996; Sardessai, 2002). According to the data in Fig. 6.2, solvents with log P $<$ 3.2 are severely toxic to the recombinant *E. coli* used here.
In contrast to organic solvents, the concept of solvent polarity, represented by the solvent's log P value, cannot be applied to ionic liquids (Dupont *et al.*, 2002). The solvent-solute interactions in ionic liquids have been described as obeying a dual interaction model: ionic liquids act like polar solvents towards polar molecules, but display non polar character towards nonpolar compounds (Armstrong *et al.*, 1999). As only very few consistent structure-activity relationships could be defined for ionic liquids to date, preliminary screening experiments are still necessary to evaluate their biocompatibility.

6.1.3 Enzyme stability in the reaction system

The two enzymes overexpressed in the biocatalyst, *E. coli* LB ADH CB FDH, are the essential driving force behind the biotransformation. In order to gain more information about the reaction system and the effect of varying reaction conditions on the performance of the enzymes, the stability of LB ADH and CB FDH was evaluated in different situations possibly occurring during the reaction. The evaluation of the stability was made on basis

of the half-life of the enzymes. The different sets of experiments were performed in different buffers. Therefore, comparisons are only valid within one set of experiments, and each result presented should not be compared with other results obtained in different sets.

Enzyme stability in presence of ionic liquid

When considering the toxicity of a solvent, two different effects are generally distinguished: the molecular toxicity and the phase toxicity. While the molecular toxicity is caused by the solvent molecules dissolved in the aqueous phase, the phase toxicity is due to the presence of a second phase.

First, the molecular toxicity of the ionic liquid to the enzymes was evaluated. During the biotransformation, this is the toxicity to which the enzymes might be exposed as long as the cell membrane of the biocatalyst is intact. The enzymes should then not come into direct contact with the ionic liquid phase.

For the evaluation of the molecular toxicity of the ionic liquid ([HMPL][NTF]), the hydrophobic ionic liquid was poured into the assay at a volume fraction of 20 %, and the enzymes suspended in phosphate buffer after the cell lysis were added on top, but the phases were not mixed. The only contact between both phases would thus be the naturally forming horizontal interface due to the density difference (buffer phase: ~ 1 g cm^{-3} at 25 °C; [HMPL][NTF]: 1.34 g cm^{-3} at 25 °C). This way, the phases could equilibrate, some ionic liquid dissolving in the aqueous phase (up to 1.9 g_{IL} L^{-1}) and some water dissolving in the ionic liquid (up to 0.9 % wt), but the enzymes would not constantly enter into contact with the solvent phase and there was no emulsion formation between both phases.

The half-life of the LB ADH and the CB FDH while exposed to the molecular toxicity of [HMPL][NTF] are indicated Fig. 6.3. The half-life determined show that neither the LB ADH nor the CB FDH are destabilized by the molecular toxicity of [HMPL][NTF].

When expanding the measurements to other ionic liquids at disposal, it could be shown that the effect observed largely depends on both the solvent and the enzyme considered (Fig. 6.4): while the stability of the LB ADH is hardly affected by the ionic liquids added, the CB FDH shows significant variations of its half-life. However, both enzymes showed the same trend when exposed to the same ionic liquids.

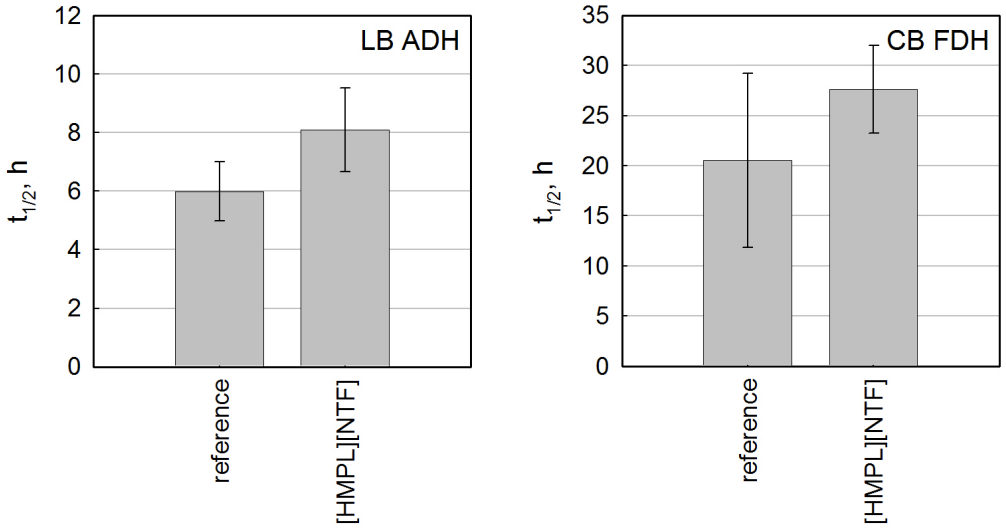

Figure 6.3: Molecular toxicity of [HMPL][NTF]: half-life of the enzymes in ionic liquid saturated phosphate buffer. Half-life of the LB ADH (left) and half-life of the CB FDH (right). The measurements were performed at room temperature and without stirring.

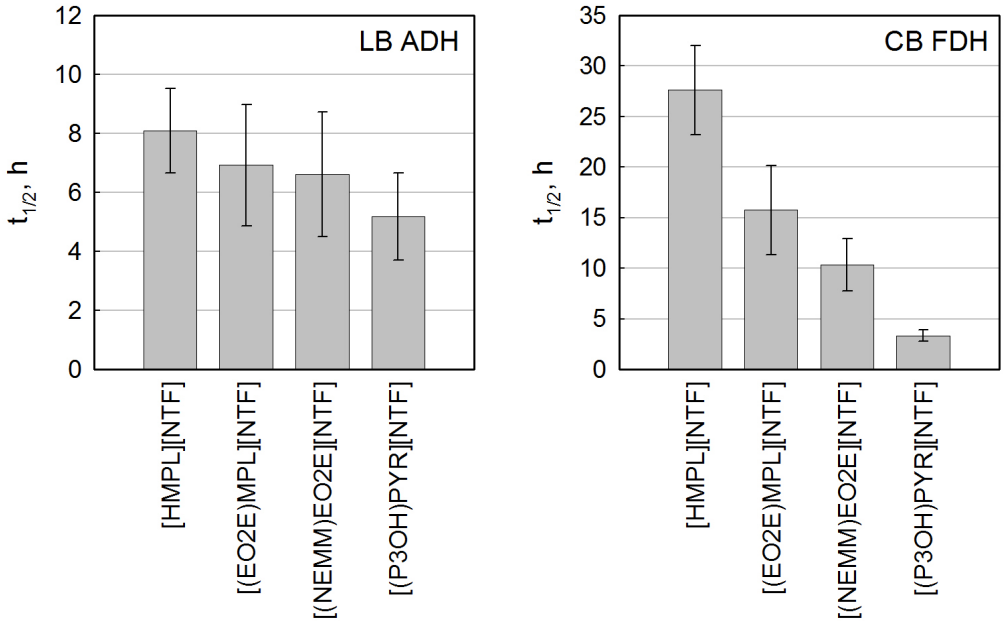

Figure 6.4: Molecular toxicity of various ionic liquids: half-life of the enzymes in ionic liquid saturated phosphate buffer. Half-life of the LB ADH (left) and half-life of the CB FDH (right). The measurements were performed at room temperature and without stirring.

In a second set of experiments, the phase toxicity of the ionic liquid was investigated. The enzymes are only exposed to the phase toxicity when they enter into direct contact with the ionic liquid phase. During the biotransformation, this only occurs if the cell membrane of the biocatalyst has been damaged, so that the enzymes might leak from the cell and are no longer protected by the cell membrane.

For this set of experiments, the hydrophobic ionic liquid was poured into the assay at a volume fraction of 20 %, and the enzymes suspended in phosphate buffer were added on top. This time, however, the assays were mixed. This means that an emulsion was formed between the aqueous phase containing the enzymes and the ionic liquid. The enzymes thus constantly entered into contact with the solvent phase. The half-life of the LB ADH and the CB FDH when exposed to the phase toxicity of [HMPL][NTF] are shown in Fig. 6.5.

While the molecular toxicity of [HMPL][NTF] did not significantly affect neither of the enzymes, the direct interaction of the enzymes with the ionic liquid phase significantly reduced their activity over time. The half-lives determined decreased by ~ 68 % and ~ 52 % for the LB ADH and the CB FDH, respectively, in comparison to the monophasic reference.

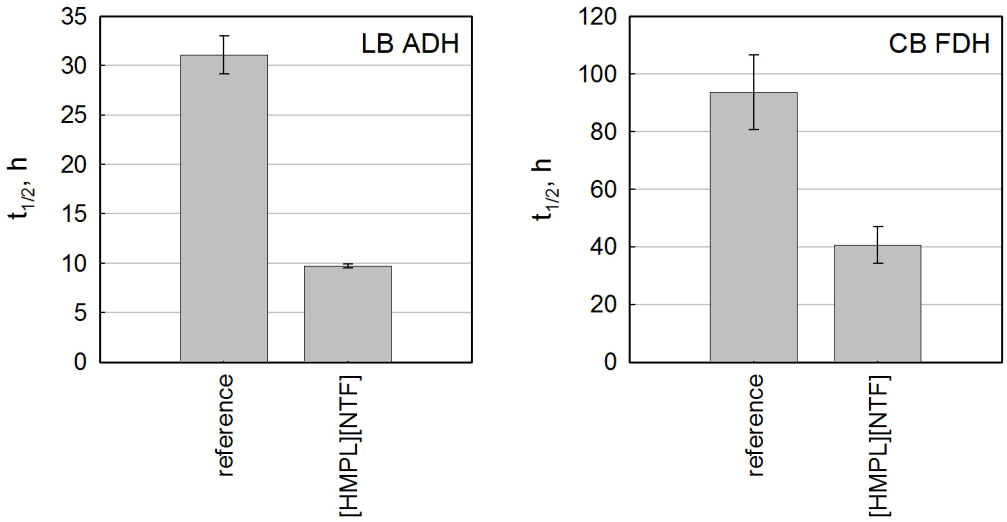

Figure 6.5: Phase toxicity of [HMPL][NTF]: half-life of the enzymes in the emulsion formed by the phosphate buffer with [HMPL][NTF] at a volume fraction of 20 %. Half-life of the LB ADH (left) and half-life of the CB FDH (right). The measurements were performed at room temperature and with stirring at 250 min^{-1}.

Enzyme stability in presence of the substrate and the product

Another factor that might influence the enzyme stability during the biotransformation is the presence of large concentrations of the substrate and the product considered. The enzyme stability was thus also evaluated in presence of theses substances. For these experiments, the concentrations of 2-octanone and 2-octanol in the assays were chosen below their solubility limit in water (8.6 mM for 2-octanone and 2-octanol) and within the range of concentrations expected in the aqueous phase during the biotransformations. The corresponding quantities of 2-octanone or 2-octanol were directly added into the phosphate buffer containing the enzymes. The effect of the substrate and the product was evaluated in separate assays and the assays were not mixed.

When evaluating the half-life of the LB ADH, no significant effect of the presence of 2-octanone and 2-octanol up to concentrations of up to ~ 1 mM or ~ 7 mM, respectively, could be detected (Fig. 6.6). Similarly, no significant loss of activity over time was observed for the CB FDH in comparison to the reference assay without 2-octanone and 2-octanol, either (data not shown).

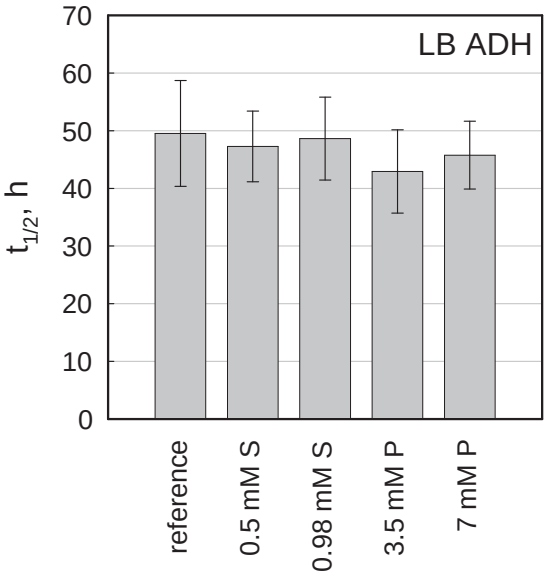

Figure 6.6: Half-life of the LB ADH in pure phosphate buffer and in presence of varying concentrations of the substrate (S), 2-octanone (0.5 mM and 0.98 mM) or the product (P), 2-octanol (3.5 mM and 7 mM). The measurements were performed at room temperature and without stirring.

Discussion

For all the different sets of experiments, the half-lives observed for the LB ADH and the CB FDH were within the expected order of magnitude (Slusarczyk *et al.*, 2000; Felber, 2001; Ansorge-Schumacher *et al.*, 2006; Filho, 2007; Kohlmann *et al.*, 2011b). More precise quantitative comparisons with the published data are difficult because the reaction conditions strongly influence the enzyme stability, but they are rarely identical to those used here. In accordance with the literature data, the stability determined for the LB ADH was generally significantly lower than the stability of the CB FDH in the same conditions.

The experiments involving the ionic liquid [HMPL][NTF] showed that the stabilities of the LB ADH and the CB FDH are not affected by molecular toxicity effects (Fig. 6.3). This means that, if the enzymes are only exposed to low concentrations of ionic liquid dissolved in the aqueous phase, the activity of the enzymes, and thus the process productivity is not negatively affected. This observation is confirmed by the yields ≥ 95 % reached during whole-cell biotransformations with [HMPL][NTF] as second phase (Bräutigam *et al.*, 2009). With these very satisfying outcomes, it was expected that the presence of this solvent would not significantly damage the enzyme inside the cell.

In contrast, the results presented in Fig. 6.5 showed that the enzyme stability was significantly decreased when the phase toxicity was involved, too. When the enzymes entered into direct and repeated contact with the ionic liquid, their activity decreased much more rapidly over time than without the presence of this second phase: while only ~ 7 % of the LB ADH has lost its activity after 3 h in pure aqueous buffer, the intense contact with the ionic liquid deteriorated ~ 20 % of the enzyme initially present in the emulsion over the same period of time.

These results further underline the favourable aspect of whole cells as biocatalyst: while the whole-cell biocatalyst not only permits a cell-internal cofactor regeneration, it also avoids a decrease of the enzyme stability due to the phase toxicity of the solvent. The cell membrane protects the enzymes from the direct interaction with the solvent phase.
Nevertheless, if the biocatalyst is damaged, and the cell membrane is lysed, this is no longer true. The consequences of a lysed cell membrane would not only be a cofactor leakage, but also an increased loss of enzyme activity.

In addition to [HMPL][NTF], the molecular toxicity of a larger set of available ionic liquids was evaluated (Fig. 6.4). This showed that not all the ionic liquids currently available are inoffensive towards the LB ADH and the CB FDH, even if only the molecular toxicity and not the phase toxicity is considered. While very low concentrations of dissolved [HMPL][NTF] do not decrease the stability of the enzymes under consideration, other ionic liquids slightly reduced the stability of the LB ADH, and significantly affected the stability of the CB FDH. The effect an ionic liquid has on the stability of an enzyme both depends on the composition of ionic liquid and on the enzyme. A careful evaluation of the ionic liquid is therefore necessary before its application in biocatalysis.
Interestingly, the ionic liquid that mostly affected the enzyme stability is also the ionic liquid with the largest water solubility, i.e. present in larger quantities in the aqueous medium near the enzyme (water solubility: 78.90 g_{IL} L^{-1} for [(P3OH)PYR][NTF] vs. only 1.9 g_{IL} L^{-1} for [HMPL][NTF]). This property is thus most probably also of influence when enzyme inactivation through molecular effects is observed.

The evaluation of the enzyme stability in presence of 2-octanone or 2-octanol showed that the substrate and the product used here do not harm the enzyme, even if present in concentrations up to ~ 1 mM 2-octanone or 7 mM 2-octanol (Fig. 6.6). In a biphasic setup [HMPL][NTF]-buffer with partition coefficients of 1230 and 172 for 2-octanone and 2-octanol, respectively, this means that biotransformations with substrate (or product) concentrations up to (at least) 1.2 M in the ionic liquid can be performed without harming the enzyme.

6.2 Effects of varying process variables on the biphasic whole-cell biotransformation of 2-octanone

In this part of the project, the impact of two main process variables on the reaction outcome is presented. These variables are the initial substrate concentration in the reaction system and the ionic liquid volume fraction. Both of these variables have a large influence on the evolution of the reaction. Evaluating this effect is important for the process optimisation, but it also permits to gain more information about the entire reaction system. Another process variable of importance is the biocatalyst concentration. The effect of this variable on the reaction outcome is not analysed here. Instead, a biocatalyst concentration of 50 g_{DCW} L^{-1} is fixed. This corresponds to the cell densities commonly reached during high-cell density cultivations.

6.2.1 Effect of varying initial substrate concentrations

An important variable in the process design is the initial substrate concentration. Increased initial substrate concentrations can improve the process productivity, but they might also lead to a substrate or product inhibition of the biocatalyst, or even damage it permanently because both substances are toxic to it (subsection 6.1.1). Therefore, the effect of varying initial substrate concentrations on the evolution of the conversion and the enantiomeric excess was investigated.

Biotransformations with varying initial substrate concentrations

Biotransformations with constant ionic liquid volume fraction (20 %) but with varying initial substrate concentrations were performed at the 200 mL scale. The initial substrate concentrations in the ionic liquid phase were varied from 150 mM to 1200 mM 2-octanone. This corresponds to a range of initially 0.12 mM to 0.97 mM 2-octanone in the aqueous phase after equilibration with the loaded ionic liquid phase (partition coefficient for 2-octanone $D_{IL/aq} = 1230$).

Fig. 6.7 shows the evolution of the quantity of *R*-2-octanol in some of the reaction systems evaluated. Reaction systems initially containing larger concentrations of substrate in the ionic liquid phase show larger initial reaction rates than those with lower initial substrate concentrations. These reaction systems also produce larger final quantities of 2-octanol. In contrast, reaction systems with lower initial substrate concentrations reach larger final conversions, as shown in Fig. 6.8. For reaction systems with initial substrate concentrations between 150 mM and 450 mM, final conversions ≥ 99 % were observed. An initial substrate concentration of 600 mM 2-octanone leads to slightly lower but still satisfying final conversion (97.9 % ± 0.2 %). However, above 600 mM, the final conversion reached shows a significant decrease with increasing substrate concentration. At an initial substrate concentration of 1200 mM, only 81.6 % ± 0.1 % of 2-octanone is converted to 2-octanol after 6 h. The enantiomeric excesses observed did not differ significantly in the different reaction setups. They were ≥ 99.5 % (*R*) over the whole duration of the reaction for each biotransformation performed (data not shown).

The resulting 2-octanone and *R*-2-octanol concentrations in the ionic liquid are shown in Fig. 6.9. This figure illustrates the larger product concentrations found in the ionic liquid of reaction setups with larger initial substrate concentrations, but also the larger 2-octanone concentrations still subsisting in these systems.

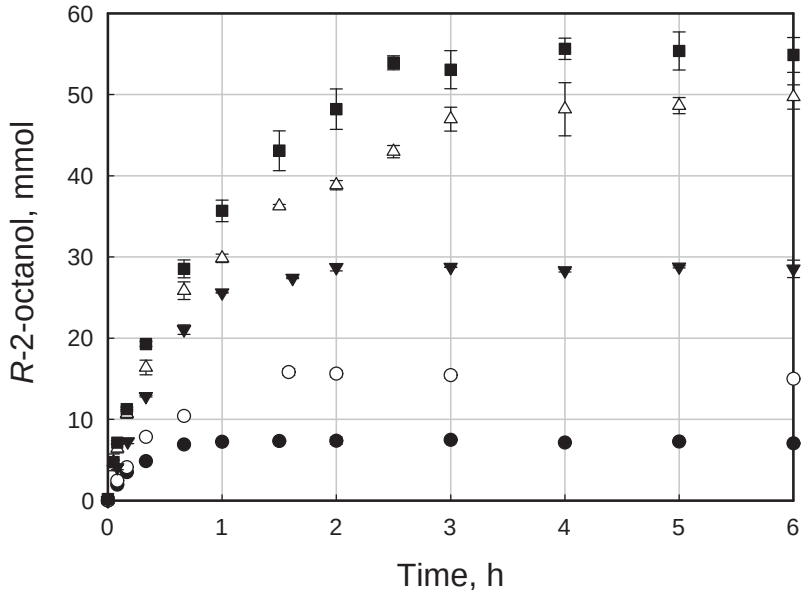

Figure 6.7: *R*-2-octanol production in biphasic reaction systems with 20 % ionic liquid and varying initial substrate concentrations of 150 mM (●), 300 mM (○), 600 mM (▼), 1000 mM (△), and 1200 mM (■) in the ionic liquid. For purposes of clarity not all the setups analysed are shown. The enantiomeric excesses were constantly ≥ 99.5 % (*R*) in each setup.

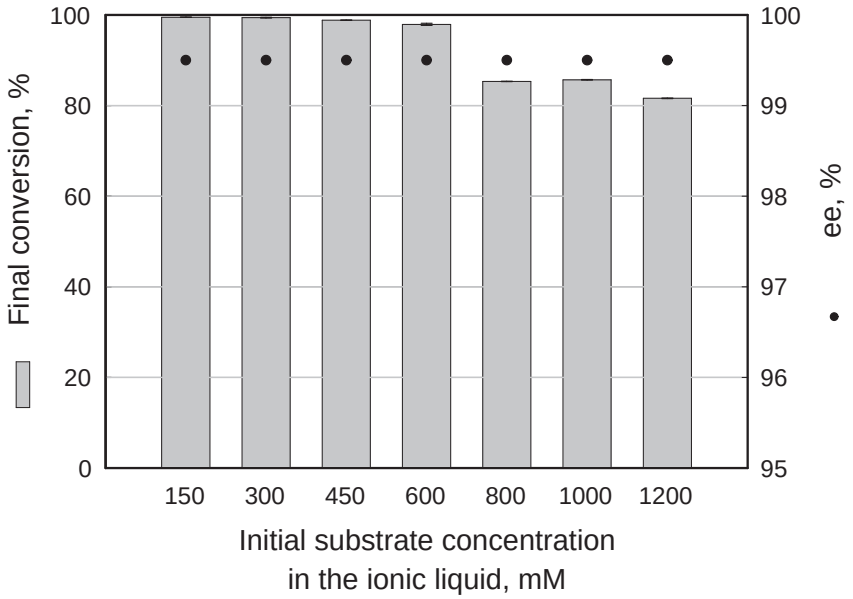

Figure 6.8: Final conversion and enantiomeric excess (ee) for the reduction of 2-octanone in biphasic reaction systems with 20 % ionic liquid and varying initial substrate concentrations.

Fig. 6.10 indicates the resulting space-time yield observed in each of the reaction systems when the final conversion is reached. This value changes largely depending on the

quantities of *R*-2-octanol formed in the different systems and on the time needed to reach the final conversion, which are both larger for reaction systems with larger initial substrate concentrations.

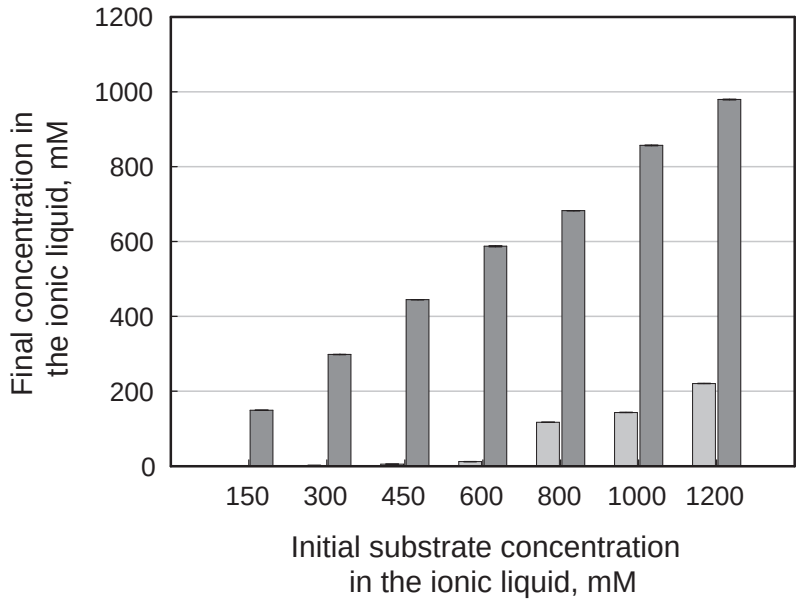

Figure 6.9: Final 2-octanone (▭) and *R*-2-octanol (▬) concentrations in the ionic liquid reached in biphasic reaction systems with 20 % ionic liquid and varying initial substrate concentrations.

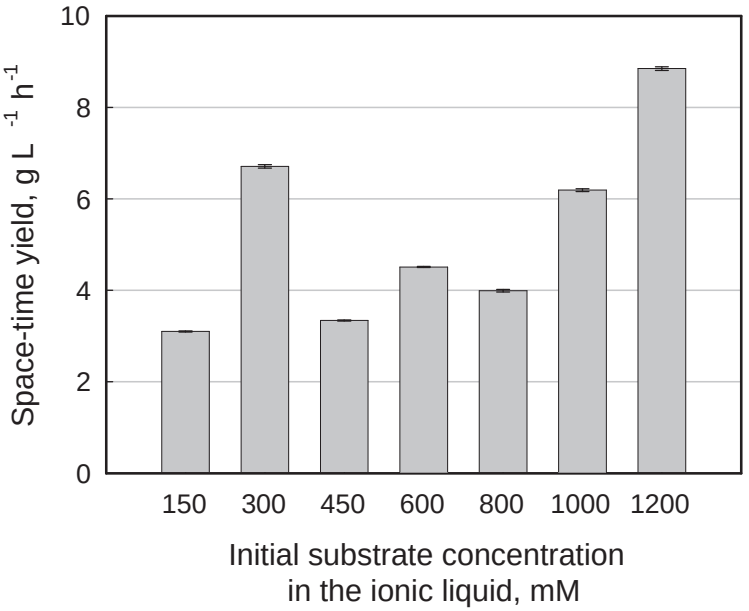

Figure 6.10: Space-time yield in *R*-2-octanol reached in biphasic reaction systems with 20 % ionic liquid and varying initial substrate concentrations. The time period considered in the calculations is the time period necessary to reach the final conversion in each setup.

Investigation of a possible product inhibition

The biotransformations presented above (subsection 6.2.1) showed decreasing conversion at increasing initial substrate concentrations. Possible reasons for these reduced final conversions might be (1) that the enzymes responsible for the biotransformation are inhibited by the large product concentrations present towards the end of these biotransformations, or (2) that the biocatalyst is permanently damaged during the biocatalysis due to the large substrate and/or product concentrations in these setups. Indeed, for reaction systems with an initial substrate concentration of 1200 mM in the ionic liquid, concentrations of up to ~ 1 mM 2-octanone at the beginning of the reaction and up to ~ 6 mM *R*-2-octanol at the end of the reaction are observed in the aqueous phase near the biocatalyst. For the product, these concentrations are above the MIC determined earlier (subsection 6.1.1).

To further investigate these points, the biotransformations with initial substrate concentrations of 1000 mM and 1200 mM were repeated as above, except that the used biocatalyst was replaced with fresh biocatalyst after 6 h reaction time - a duration after which the final conversion was reached in each setup (Fig. 6.7). If the lower conversions were due to a product inhibition of the enzymes, then the conversion should not further increase when fresh biocatalyst is added. However, if the lower conversions observed occurred because the biocatalyst was too damaged to further perform the biotransformation, then the conversion should continue to increase once fresh biocatalyst is added.

Fig. 6.11 shows the conversion reached after the first 6 h of reaction time, as well as 1 h and 5 h after replacing the biocatalyst by fresh cells (‘6 h + 1 h’ and ‘6 h + 5 h’, respectively). A clear increase of the conversion from 90.4 % ± 0.2 % and 88.7 % ± 0.1 % to 97.8 % ± 0.1 % and 96.1 % ± 0.1 % was observed after addition of fresh cells for the 1000 mM and the 1200 mM reaction systems, respectively. The enantiomeric excesses were constant at values ≥ 99.5 % (*R*) in each setup (data not shown).

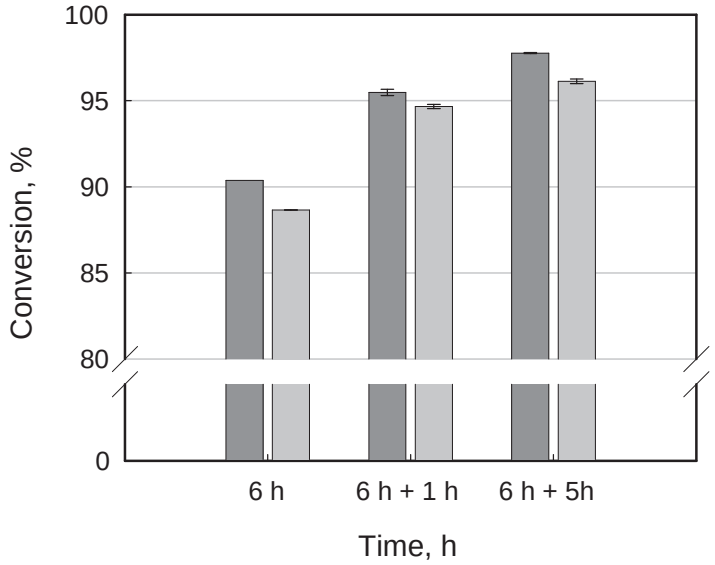

Figure 6.11: Conversion of 2-octanone to *R*-2-octanol in 200 mL biotransformations with 20 % ionic liquid and large initial substrate concentrations in the ionic liquid phase: 1000 mM (▬) and 1200 mM 2-octanone (▭). The conversion was determined after 6 h reaction time, as well as 1 h and 5 h after replacement of the biocatalyst by a fresh charge of cells ('6 h + 1 h' and '6 h + 5 h', respectively).

Investigation of a possible cofactor leakage

If the lower conversion observed for reaction systems with larger initial substrate concentrations are due to the fact that the biocatalyst is damaged by the large substrate and/or product concentrations, then two different scenarios are possible: (1) only the cell membrane is damaged. Then, the cofactor (NAD(H)) might leak through the lysed cell membrane, and the reaction is slowed down or stopped due to the absence of the necessary cofactor. Or (2) not only the cell membrane is damaged, but also the enzymes - now no longer protected by the cell membrane - are denaturated.

To verify which scenario applies in biotransformations with large initial substrate concentrations, a biotransformation with an initial substrate concentration of 1200 mM was performed. After 6 h reaction time, NADH was added to the reaction system to a final concentration of 80 mM in the aqueous phase. If the conversion increases after the addition of NADH, the denaturation of the enzymes responsible for the reduction of 2-octanone to 2-octanol can be excluded. If the conversion does not increase after the addition of NADH, the LB ADH has probably also been permanently damaged during the biotransformation. To reduce the consumption of the costly cofactor, the reaction medium was transferred before the addition of NADH from the 200 mL stirred tank reactor to smaller 10 mL reaction vessels as described in subsection 5.4.4.

Fig. 6.12 shows the conversion reached after 6 h of reaction time, as well as 30 min, 1 h, 2 h and 3 h, respectively, after the addition of NADH ('6 h + x'). A clear increase of the conversion from 77.9 % ± 0.1 % to 93.4 % ± 0.2 % is observed after the addition of cofactor. The enantiomeric excesses were constant at values ≥ 99.5 % (*R*) in each setup (data not shown).

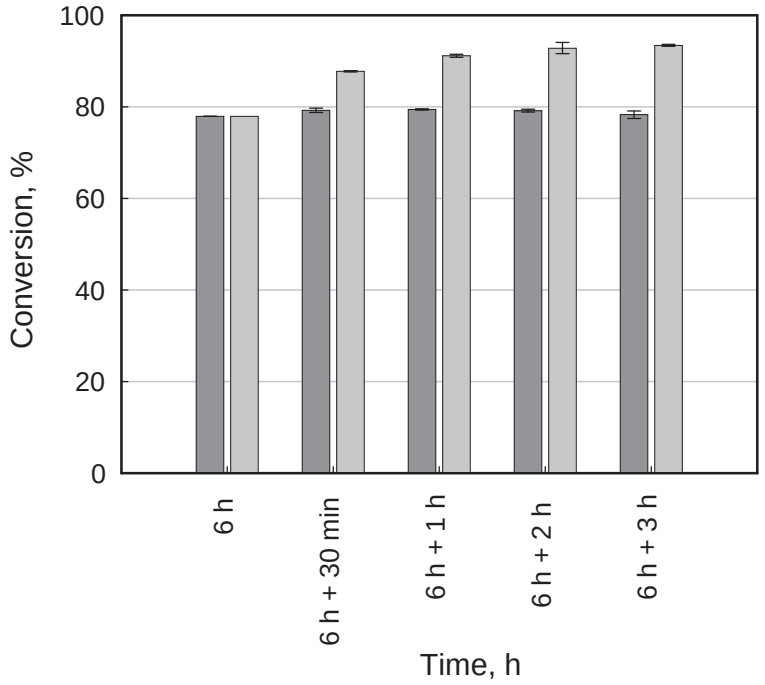

Figure 6.12: Conversion of 2-octanone in 200 mL biotransformations with 20 % ionic liquid and an initial substrate concentration of 1200 mM in the ionic liquid phase. Samples were taken after 6 h reaction time, and 30 min, 1 h, 2 h and 3 h after addition of 80 mM NADH ('6 h + 30 min','6 h + 1 h', '6 h + 2 h' and '6 h + 3 h', respectively): reference assay without addition of NADH (▬) and assay with addition of NADH (▭).

Discussion

The biotransformations with varying initial substrate concentrations showed that reaction systems initially containing larger concentrations of substrate in the ionic liquid phase show larger initial reaction rates than those with lower initial substrate concentrations (Fig. 6.7). The constant equilibrium between both phases means that larger substrate concentrations in the ionic liquid also mean larger substrate concentrations in the aqueous phase containing the biocatalyst. This results in larger initial reaction rates if no substrate inhibition occurs. According to the observations made, an inhibition of the enzymes by 2-octanone can be excluded for the range of substrate concentrations used here (from 0.1

mM 2-octanone to 0.98 mM 2-octanone in the aqueous phase for the concentration range of 150 mM 2-octanone to 1200 mM 2-octanone in the ionic liquid). This is consistent with the data presented by Kohlmann *et al.* (2011a) who only observed a substrate inhibition of the LB ADH at 2-octanone concentrations > 1 mM. Reaction systems with larger initial substrate concentrations also reach larger final *R*-2-octanol contents.
However, considering the final conversion reached, the systems with lower initial substrate concentrations show more satisfying results (Fig. 6.8). While reaction systems with initial substrate concentrations between 150 mM and 450 mM reach final conversions ≥ 99 %, substrate concentrations above 600 mM lead to a pronounced decrease of the final conversion with increasing 2-octanone content.

These two points are reflected in Fig. 6.9: the reaction systems with larger initial substrate concentrations show larger final product concentrations in the ionic liquid - a favourable aspect, because it permits a more efficient downstream processing - but they also show larger contamination by rests of non-converted substrate, which is also present in larger concentrations. To avoid costly purification steps, no substrate should however be present at all. This consideration is thus in favour of reaction systems with lower initial substrate concentrations (up to 450 mM).

In addition to the final product purity, the space-time yield is a variable of major interest. As illustrated by Fig. 6.10, the space-time yield varies largely between the different setups. This is due to the different periods of time necessary to reach the final conversion and to the respective final product content. Not all the reaction systems reaching large space-time yield also present low final substrate concentrations in the ionic liquid. A compromise should thus be made between these two factors. One reaction system showing relatively good space-time yield while still reaching large final conversion and thus low final substrate concentrations in the ionic liquid is the reaction system with an initial substrate concentration of 300 mM 2-octanone in the ionic liquid. The difference to the space-time yield reached in the 1200 mM system (~ 24 %) is probably compensated by the reduced process costs when a subsequent product purification can be avoided, as it is the case for an initial substrate concentration of 300 mM in the ionic liquid.

As the co-substrate necessary for the cofactor regeneration (formate) was always present in large excess, even in the reaction systems with initial substrate concentrations of 1000 mM or 1200 mM, this substance was not limiting the conversion in these systems. Consequently, this cannot have been at the origin of the only moderate final conversion

observed in reaction systems with large initial substrate concentrations. The explanation for the observations made can thus only be a product inhibition of the enzymes or a permanent inactivation of the biocatalyst, damaged by large concentrations of 2-octanone and 2-octanol.

An inhibition of the enzymes by the product formed can be excluded as possible cause for the reduced conversion reached in reaction systems with large initial substrate concentrations. In fact, if the enzymes were inhibited by the product, the conversion would have stopped at the same product concentration in each of the reaction systems evaluated. This was however not the case (Fig. 6.7). This conclusion was confirmed by a subsequent set of experiments, where the biocatalyst was replaced by fresh *E. coli* cells once the conversion stagnated in reaction systems with initial substrate concentrations of 1000 mM and 1200 mM. In both reaction setups, the conversion increased to very satisfying values after replacing the biocatalyst (Fig. 6.11). This permits to conclude that the moderate conversion reached in reaction systems with large initial substrate concentrations is not due to a product inhibition of the biocatalyst, but that it is due to an inactivation of the biocatalyst by the large concentrations of toxic substrate and product.

An addition of NADH to the reaction medium once the conversion has stopped - this time without replacing the biocatalyst - also provoked an increase of conversion (Fig. 6.12). This means that the enzymes responsible for the reduction of 2-octanone have not been deteriorated during the biotransformations, or at least not completely. The stagnation of the conversion previously observed in reaction systems with large initial substrate concentrations is thus probably mainly due to a local lysis of the cell membrane, with limited damage, leading to a cofactor leakage. These observations are in accordance with previous experiments showing that neither the stability of the LB ADH nor the stability of the CB FDH is affected by relatively large 2-octanone or 2-octanol concentrations (subsection 6.1.3). Based on these results, the enzymes should not be more denaturated during biotransformations with large initial 2-octanone concentrations than in reaction systems with initial 2-octanone concentrations of only 150 mM or 300 mM. Consequently, a severe enzyme inactivation could not be at the origin of the different evolutions of conversion observed in the reaction systems evaluated above.
The partial lysis of the membrane probably results from the exposure to relatively large 2-octanone and 2-octanol concentrations. It has indeed been reported that long alkyl chains, as found in 2-octanone and 2-octanol, integrate into the cell membrane, causing imperfections and holes which result in leakage from the cells (Evans, 2006, 2008a).

6.2.2 Effect of varying ionic liquid volume fractions

Another important variable in a biphasic whole-cell biotransformation is the volume ratio of the two phases, i.e. in the present case, the volume ratio of the ionic liquid to the aqueous phase. Due to the given partitioning of the substrate and the product in the ionic liquid-buffer system, an increase of the ionic liquid volume fraction would permit to increase the quantity of substrate added into the reaction system, and thus possibly also the productivity. However, it is not known if and how the ionic liquid will influence the biocatalyst activity if present in very large volume fractions. Therefore, the effect of varying ionic liquid volume fractions on the evolution of the conversion and the enantiomeric excess was evaluated.

Biotransformations with varying ionic liquid volume fractions

Biotransformations with varying ionic liquid volume fractions were performed at the 200 mL scale. Phase ratios ranging from 10 % to 70 % ionic liquid were used, while keeping the initial substrate quantity added into the ionic liquid phase as well as the biocatalyst quantity suspended in the aqueous phase constant. The biocatalyst concentration and the initial substrate concentration in the total reaction system was consequently also constant. The biocatalyst and substrate quantity added to each system, regardless of the ionic liquid volume fraction used, were 8 g_{DCW} and 3.83 mL 2-octanone. This corresponds to a biocatalyst concentration of 50 g_{DCW} L^{-1} in the aqueous phase and a substrate concentration of 600 mM in the ionic liquid phase for a reaction system with an ionic liquid volume fraction of 20 %. Due to the defined partitioning of the substrate between the ionic liquid and the aqueous phase, and to the variation of the phase ratio, this procedure results in different initial substrate and biocatalyst concentrations in the aqueous phases of the various systems (Table 6.2). Consequently, the initial reaction rates will be affected. Still, only this approach permits a convenient comparison of the conversions reached in the different setups.

The spread of compositions of the different reaction setups evaluated here (as indicated in Table 6.2) and in the previous section (Fig. 6.7 and Fig. 6.8) is schematically represented in Fig. 6.13.

Table 6.2: Composition of the different reaction systems evaluated: biocatalyst concentration in the aqueous phase and initial substrate concentrations in the ionic liquid resulting from the variation of the phase ratio while keeping the biocatalyst and substrate quantities constant, and the resulting substrate concentrations in the aqueous phase ($D_{IL/aq,\ 2\text{-octanone}} = 1230$).

Ionic liquid volume fraction, %	Substrate in the ionic liquid, mM	Substrate in the aqueous phase, mM	Biocatalyst in the aqueous phase, g_{DCW} L^{-1}
10	1200	0.98	44
20	600	0.49	50
30	400	0.33	57
40	300	0.24	67
50	240	0.20	80
60	200	0.16	100
70	171	0.14	133

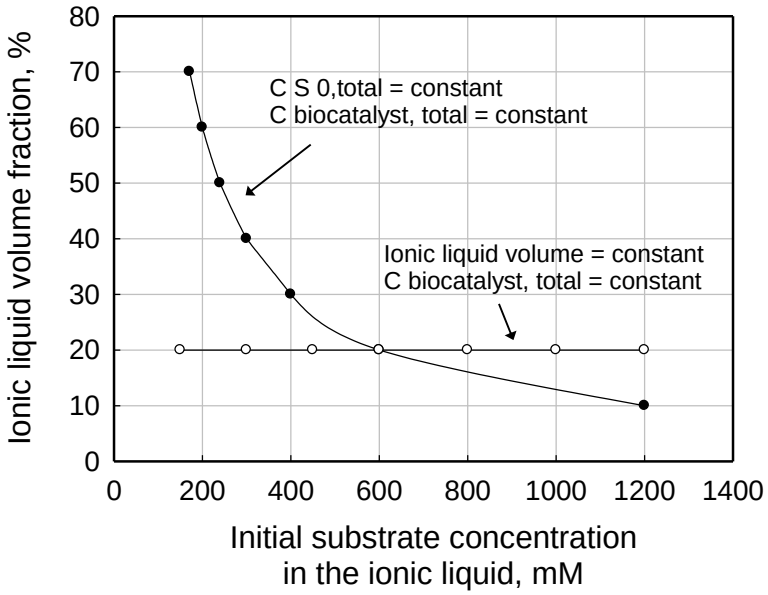

Figure 6.13: Schematic representation of the composition of the different reaction setups evaluated: (1) constant total initial substrate concentration (C S 0, total) and biocatalyst concentration (C biocatalyst, total) at varying ionic liquid volume fractions (●, this section) and (2) constant ionic liquid volume fraction and biocatalyst concentration at varying initial substrate concentrations (○, previous section).

Fig. 6.14 shows the evolution of the conversion in some of the reaction systems evaluated. As mentioned above, the initial reaction rates observed were indeed larger for systems with lower ionic liquid volume fractions than for reaction setups with larger ionic liquid volume fraction: the system with 20 % ionic liquid (600 mM substrate in the ionic liquid)

showed an initial reaction rate of 11.6 μmol s^{-1} ± 0.3 μmol s^{-1}, at 30 % (400 mM substrate in the ionic liquid) an initial reaction rate of 7.5 μmol s^{-1} ± 0.3 μmol s^{-1} was observed, and for 70 % ionic liquid (171 mM substrate in the ionic liquid), 4.3 μmol s^{-1} ± 0.6 μmol s^{-1}.

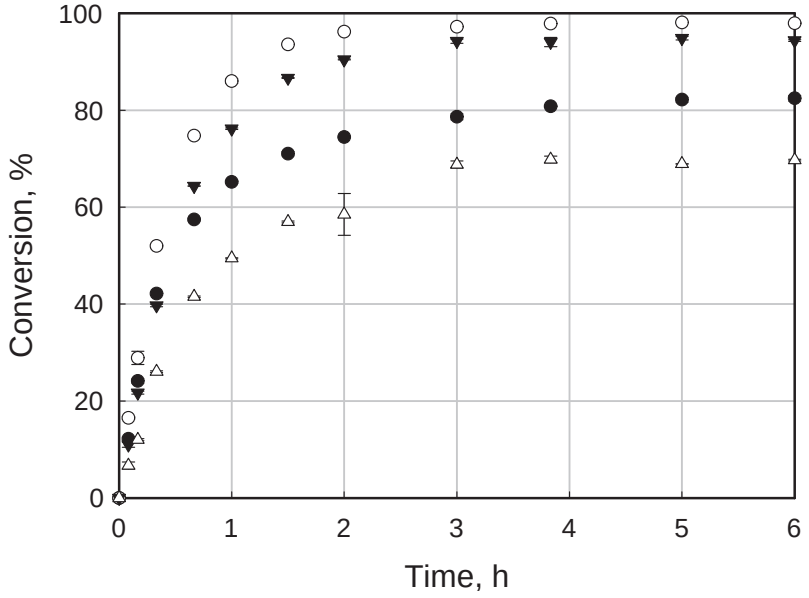

Figure 6.14: Evolution of conversion with time for systems with varying volume fractions of [HMPL][NTF]: 10 %(●), 20 % (○), 50 % (▼), or 70 % (△). For purposes of clarity not all the reaction setups analysed are shown. Enantiomeric excesses were constantly ≥ 99.5 % (*R*) in each setup.

The final conversion reached in each of the reaction systems varies largely with the system composition (Fig. 6.15). In the reaction system containing only 10 % ionic liquid, the final conversion observed is 82.5 % ± 0.6 %. For ionic liquid volume fractions between 20 % and 40 %, the final conversion reached is very similar, between 95.2 % ± 0.2 % and 97.84 % ± 0.08 %. Above 40 % ionic liquid, the conversion decreases again with increasing ionic liquid volume fraction, reaching only 69.70 % ± 0.17 % when using an ionic liquid volume fraction of 70 %. The enantiomeric excesses observed did not differ significantly in the different reaction setups. They were ≥ 99.5 % (*R*) over the whole duration of the reaction for each biotransformation performed (data not shown).

Reaction systems with lower ionic liquid volume fraction reach larger final product concentrations in the ionic liquid than the setups with larger ionic liquid volume fraction (Fig. 6.16). The final substrate concentration in the ionic liquid is largest for the reaction system with only 10 % ionic liquid, low for ionic liquid volume fractions of 20–40 %, and it then increases with increasing ionic liquid content.

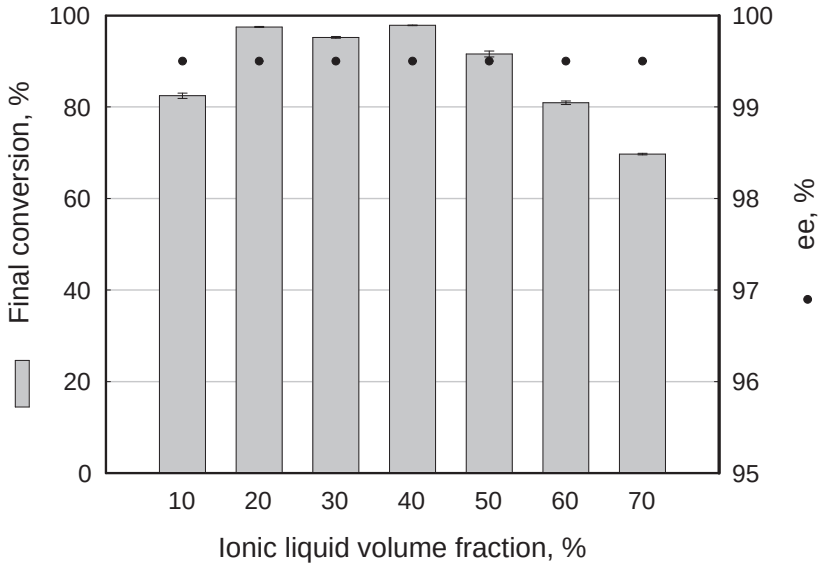

Figure 6.15: Final conversion and enantiomeric excess (ee) reached in biphasic reaction systems with constant initial substrate quantity and varying ionic liquid volume fractions.

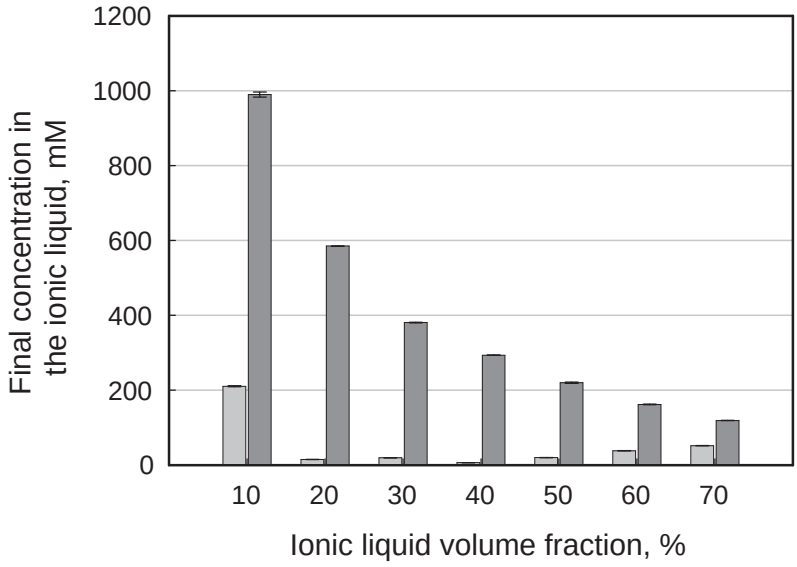

Figure 6.16: Final 2-octanone (▭) and *R*-2-octanol (▬) concentrations in the ionic liquid reached in biphasic reaction systems with constant initial substrate quantity and varying ionic liquid volume fractions.

Fig. 6.17 indicates the space-time yield observed in each of the reaction systems when the final conversion is reached. It varies between 3 and 4.7 g L^{-1} h^{-1}.

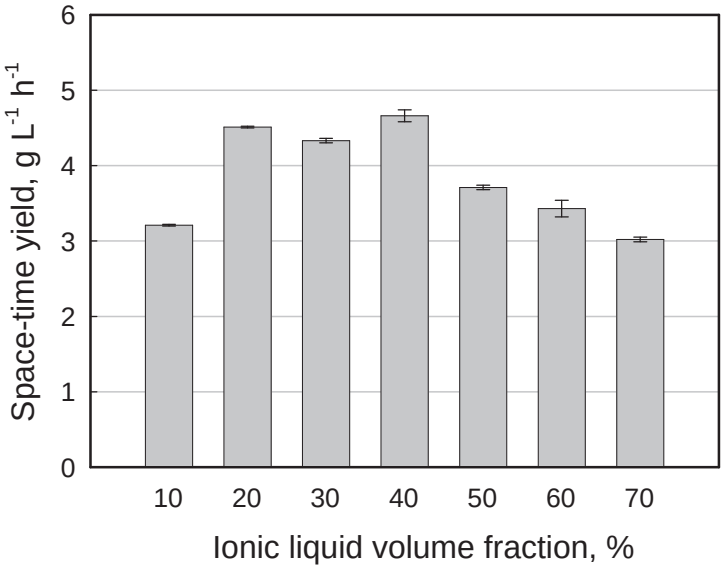

Figure 6.17: Space-time yield in *R*-2-octanol reached in biphasic reaction systems with constant initial substrate quantity and varying ionic liquid volume fractions. The time period considered in the calculations is the time period necessary to reach the final conversion in each setup.

Addition of fresh biocatalyst

To verify if the reduced conversion in reaction systems with large ionic liquid volume fractions is due to an inactivation of the biocatalyst during the biotransformation, the biotransformation with an ionic liquid volume fraction of 70 % was repeated as above, except that the used biocatalyst was replaced with fresh biocatalyst after 6 h reaction time.

Fig. 6.18 shows the conversion reached after 6 h of reaction time, as well as 1 h after replacing the biocatalyst with fresh cells (6 h + 1 h) and 3 h after replacing the biocatalyst with fresh cells (6 h + 3 h). A significant increase of the conversion from 66 % ± 2% to 83.3 % ± 0.3 % is observed after addition of fresh cells. The enantiomeric excesses were constant at values ≥ 99.5 % (*R*) (data not shown).

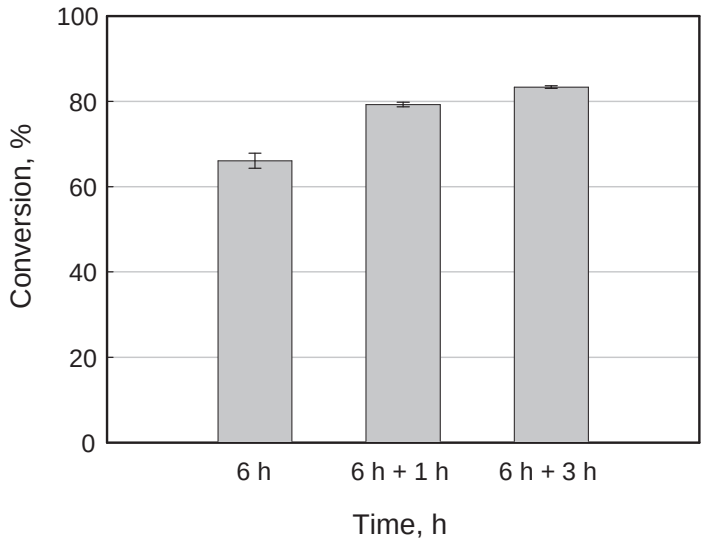

Figure 6.18: Conversion of 2-octanone to *R*-2-octanol in 200 mL biotransformations with an ionic liquid volume fraction of 70 %. The conversion was determined after 6 h reaction time, as well as 1 h and 3 h after replacement of the biocatalyst by a fresh charge of cells ('6 h + 1 h' and '6 h + 3 h', respectively).

Investigation of a possible cofactor leakage and enzyme inactivation

As described in subsection 6.2.1, an addition of NADH once the conversion has stagnated might give an indication if only the cell membrane is damaged, or if the enzymes - now no longer protected by the cell membrane - are also deactivated during the process. To this aim, biotransformations with large ionic liquid volume fractions (50–70 %) were performed, and after 6 h reaction time, NADH was added to the reaction system at a final concentration of 80 mM. To reduce the consumption of the costly cofactor, each reaction was transferred before the addition of NADH from the 200 mL stirred tank reactor to smaller 10 mL reaction vessels mixed by magnetical stirring after 6 h reaction time.

The results showed no significant increase of the conversion for any of the reaction systems analysed. The results for the reaction system with 70 % ionic liquid are shown in Fig. 6.19. The enantiomeric excesses were constant at values ≥ 99.5 % (*R*) (data not shown).

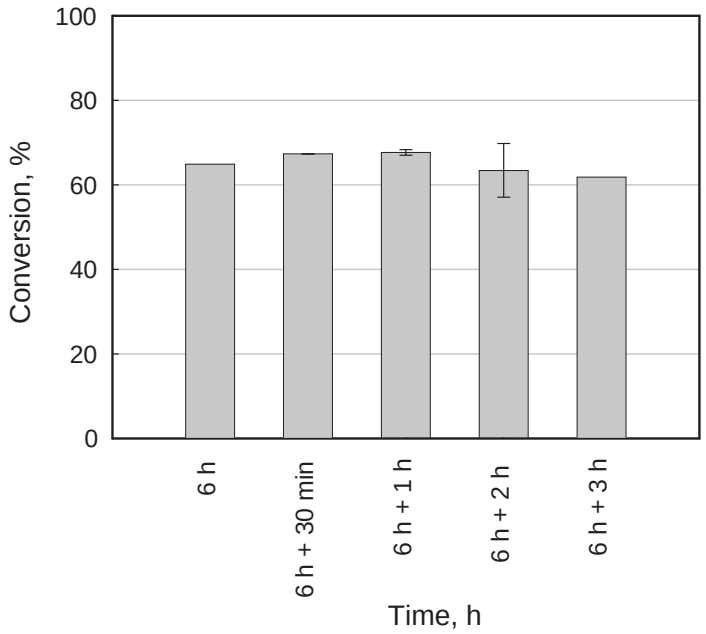

Figure 6.19: Conversion of 2-octanone to *R*-2-octanol in a 200 mL biotransformation with an ionic liquid volume fraction of 70 %. The measurements were made after 6 h reaction time, and 30 min, 1 h, 2 h and 3 h after addition of 80 mM NADH ('6 h + 30 min','6 h + 1 h', '6 h + 2 h' and '6 h + 3 h', respectively).

Discussion

While varying the ionic liquid volume fraction from 10 % to 70 % at constant biocatalyst and substrate quantities, larger initial reaction rates were observed for systems with lower ionic liquid volume fractions, due to the larger substrate concentrations found in their aqueous phase (Fig. 6.14 and Table 6.2). Systems with larger ionic liquid volume fractions on the other hand showed lower initial reaction rates, because the initial substrate concentrations in the aqueous phase were lower. The enzymes were not substrate inhibited within the concentration range applied.

However, it was also observed that reaction systems with very low ionic liquid volume fraction are not only of advantage: the reaction system containing only 10 % [HMPL][NTF] reached only relatively low final conversion (82.5 % ± 0.6 %). At constant substrate quantity in the reaction systems, setups with very low ionic liquid fractions show relatively large substrate and product concentrations in the ionic liquid, and consequently also in the aqueous phase. As was observed in subsection 6.2.1, the relatively large concentrations of of toxic substances (up to ~ 1 mM 2-octanone and ~ 6 mM 2-octanol) found in these systems damage the biocatalyst and reduce its activity.

When comparing the experiments from subsection 6.2.1 (Fig. 6.8) with the experiments performed here (Fig. 6.15), another interesting conclusion can be drawn: at constant substrate concentration in the ionic liquid phase, an increase of the ionic liquid volume fraction from 10 % to 20 % does not negatively affect the productivity of the reaction system. In fact, the reaction system with an ionic liquid volume fraction of 10 % tested here (with an initial substrate concentration of 1200 mM in the ionic liquid phase) reached very similar conversion in comparison to the reaction system with the same initial substrate concentration and an ionic liquid volume fraction of 20 % (81.60 % ± 0.06 %).

Reaction systems with larger ionic liquid volume fraction reach larger final conversions, because the exposure of the biocatalyst to toxic substrate and product is reduced, as was observed for reaction systems with ionic liquid volume fractions of 20–40 %. These three systems reach similar final conversions, indicating that a further increase of the phase ratio above 20 % - and the resulting decrease of substrate and product concentrations in the aqueous phase - does not lead to a considerable improvement of the final conversion.

On the contrary, when a given phase ratio is exceeded, a second effect is observed, which diminishes or even completely removes the advantage created by decreased substrate and product concentrations in systems with larger ionic liquid volume fractions, and leads to reduced final conversions: the large presence of ionic liquid. When comparing the reaction systems evaluated here at ionic liquid volume fractions between 50 % and 70 % with those of varying initial substrate concentrations, the former show much more satisfying final conversions ≥ 99.00 %, while the 2-octanone and 2-octanol concentrations encountered in both sets of experiments are within the same range. The only difference between these two sets of experiments being the ionic liquid content, this factor must be the reason for the less satisfying performance observed here.

Even if some ionic liquids - including the ionic liquid used here ([HMPL][NTF]) - show better biocompatibility than commonly used organic solvents (van Rantwijk *et al.*, 2007 and subsection 5.2.4), it must be concluded here that their large presence does negatively influence the biocatalyst when ionic liquid volume fractions of 40–50 % are exceeded. Above these values, the final conversion decreases with increasing phase ratio.

It should be noted that varying ionic liquid volume fractions induce variations of the size of the dispersed drops, as well as a possible phase inversion. This influences the reaction outcome by increasing (or decreasing) the interfacial areas and provokes a more (or less)

intense interaction of the cells with the solvent phase, exposing the biocatalyst more (or less) to the phase toxicity of the ionic liquid.

For the down stream processing, the final product concentration in the ionic liquid is a point of major interest. The reaction system leading to the largest product concentration among the reaction systems evaluated here (ionic liquid volume fraction of 10 %, Fig. 6.16) however also presents relatively large concentrations of non-converted substrate. This contamination of the product by relatively large quantities of 2-octanone would make a further purification step necessary to obtain enantiopure *R*-2-octanol. Considering the alternatives - larger final product concentrations in the ionic liquid, however also containing relatively large concentrations of non-converted substrate, or lower final product concentrations in the ionic liquid, but with almost no contamination - the latter is surely more favourable from an economic point of view. As the contamination is directly dependent on the conversion reached, reaction systems reaching largest possible conversion would be preferred, even if they present lower final product concentrations in the ionic liquid.

Another variable of interest is the space-time yield: large space-time yield is wanted, but at maximal purity of the product. In the present cases, there is no conflict between these two criteria because the space-time yield varies in parallel to the conversion reached: the setups presenting large final conversion and thus low final concentrations of 2-octanone in the ionic liquid indeed also lead to the largest space-time yield.
Based on these considerations, reaction systems with ionic liquid volume fractions of 20–40 % are clearly favoured, while the reaction systems with 60 % ionic liquid and 70 % ionic liquid are the least attractive.

The replacement of the biocatalyst by fresh cells once the conversion had stopped increasing (Fig. 6.18) confirmed that the low conversion reached in some of the reaction setups was due to the inactivation of the whole-cell biocatalyst during these biotransformations.
In contrast to the biotransformations evaluated in subsection 6.2.1, an addition of NADH at that same point of time did not permit to increase the conversion any further in reaction systems of ionic liquid volume fractions larger than 40 %. This leads to the conclusion that not only the cell membrane was damaged, but that also the enzymes responsible for the transformation of 2-octanone to *R*-2-octanol have been severely harmed in these reaction systems. This conclusion is confirmed by previous analyses concerning the stability of the LB ADH and the CB FDH. Both enzymes retained their stability when exposed to very low concentrations of ionic liquid in the aqueous environment. However, they

showed an accelerated loss of activity when in direct and intense contact with the solvent interface (subsection 6.1.3). At ionic liquid volume fractions larger than 40 %, the contact between the cells and the ionic liquid might indeed be so intense that the cell membrane is deteriorated and the enzymes come into direct contact with the solvent.

6.2.3 Best performing reaction system

Only if the conversion reached during the biotransformation is ≥ 99 % at an enantiomeric excess > 99.5 % (*R*), the product will be sufficiently pure to use it directly as it is recovered at the end of the process, avoiding subsequent costly purification steps. Accordingly, of the different sets of reaction conditions tested above, only those reaching a conversion ≥ 99 % were considered for further applications. The reaction systems satisfying this requirement were setups with 20 % [HMPL][NTF] and an initial substrate concentration of either 150 mM, 300 mM or 450 mM 2-octanone in the ionic liquid phase. Then, the space-time yield of 2-octanol was evaluated for these systems, to determine which reaction system led to the most satisfying results. The results are indicated in Table 6.3. This evaluation showed that the most favourable system was the reaction setup with an initial substrate concentration of 300 mM 2-octanone in the ionic liquid phase and an ionic liquid volume fraction of 20 %, leading to a space-time yield of 33.5 g ± 0.9 g L_{IL}^{-1} h^{-1} after a reaction time of 1 h 30.

Table 6.3: Productivity of the reaction systems reaching a conversion > 99.0 % and an enantiomeric excess > 99.5 % (*R*).

Reaction system	Space-time yield, g *R*-2-octanol L^{-1} h^{-1}	Space-time yield, g *R*-2-octanol L_{IL}^{-1} h^{-1}
20 % ionic liquid at 150 mM 2-octanone	3.10 ± 0.01	15.52 ± 0.01
20 % ionic liquid at 300 mM 2-octanone	6.71 ± 0.04	33.5 ± 0.9
20 % ionic liquid at 450 mM 2-octanone	3.34 ± 0.01	16.72 ± 0.03

Discussion

As mentioned in section 4.2, the production of enantiopure 2-octanol was investigated by several authors. When estimating the success of the process analysed here by comparison with the processes described in literature, it is of importance to consider both the product purity obtained at the end of the process - defined by the combination of the conversion and the enantiomeric excess reached - and the productivity of the process - described by its space-time yield.

Liese (1998), Hu and Xu (2006) and Kohlmann *et al.* (2011a) reached very good conversions between 95 % and 99% at enantiomeric excesses > 99.5 %, but only relatively low space-time yield between 9.4 g L^{-1} d^{-1} (~ 0.4 g L^{-1} h^{-1}) and 21.2 g L^{-1} d^{-1} (~ 0.9 g L^{-1} h^{-1}). Kohlmann *et al.* (2011b) presented more satisfying results in terms of productivity, reaching 45.6 g L^{-1} d^{-1} (~ 1.9 g L^{-1} h^{-1}), at a conversion of 99 % and excellent enantioselectivity. At the same final conversion and enantioselectivity, but with a space-time yield of 6.71 ± 0.04 g L^{-1} h^{-1}, the current process is however still more productive by a factor 3.5. The largest productivity published for the production of 2-octanol was presented by Bräutigam *et al.* (2009): 180 g L^{-1} d^{-1} (~ 7.5 g L^{-1} h^{-1}). The final conversion reached here was however only 95 %, at an enantiomeric excess of 99.7%. The product recovered from that process thus cannot be used without further purification. A subsequent separation of the rests of non-converted substrate from the product of interest is however a time and cost intensive procedure, due to the very similar physical properties of the substrate and the product. In spite of the slightly lower space-time yield reached, the process presented here, not necessitating these supplementary product purification steps, thus constitutes the more attractive option.

6.3 Scale-up to Liter scale

Once satisfying reaction conditions have been found, the next step in the process development is usually the scale-up from lab-scale vessels to larger industrial reactors. In this section, the scale-up from the 200 mL vessel to a standard 1 L stirred tank reactor is investigated. This intermediary step will indicate the feasibility of a scale-up to industrially relevant volumes.

6.3.1 Maximal local energy dissipation

For a robust scale-up of biphasic processes from the small scale to a larger scale, the interfacial area and hence the drop sizes in the emulsion formed should be similar at both scales, because this will guarantee a similar mass transfer in the smaller and the larger scale vessels. As the drop size distribution within a given system is determined by the hydrodynamic forces arising from the stirring (Hinze, 1955; Arai *et al.*, 1977), one strategy is to assure that the same maximal local energy dissipation (ε_{max}) is produced in both reactors.

To this aim, the maximal local energy dissipation was measured as a function of the stirrer speed in the 200 mL reactor. As the Liter scale reactor corresponds to a standard stirred tank reactor, the maximal local energy dissipation can be calculated for different stirrer speeds using the correlation given in equation 5.6. Once the maximal local energy dissipation as a function of the stirring speed is known for both scales, the same drop size and mass transfer conditions can be fixed at the large scale by choosing the stirrer speed leading to the same ε_{max} as observed at the small scale for the stirrer speed used during the biotransformation. In the present case, the stirrer speed used at the 200 mL scale is 600 min^{-1}. According to Fig. 6.20, a stirrer speed of ~ 450 min^{-1} would have to be chosen to reach the same energy dissipation at the Liter scale.

6.3.2 Biotransformation at the Liter scale

According to the calculations presented in subsection 6.2.3, the scale-up experiments were performed at an initial substrate concentration of 300 mM 2-octanone in the ionic liquid phase, 50 g_{DCW} L^{-1} biocatalyst and 0.3 M sodium formate in the aqueous phase, and at an ionic liquid volume fraction of 20 %. To guarantee that the experiments at both scales would be performed in exactly the same conditions, the biotransformations were performed in parallel, using the same biocatalyst batch. Based on the results from subsection 6.3.1, the stirrer speed was fixed to 600 min^{-1} at the 200 mL scale and to 450 min^{-1} at the Liter scale, to guarantee the same maximal local energy dissipation in both setups. The evolution of conversion observed at both scales is depicted in Fig. 6.21.

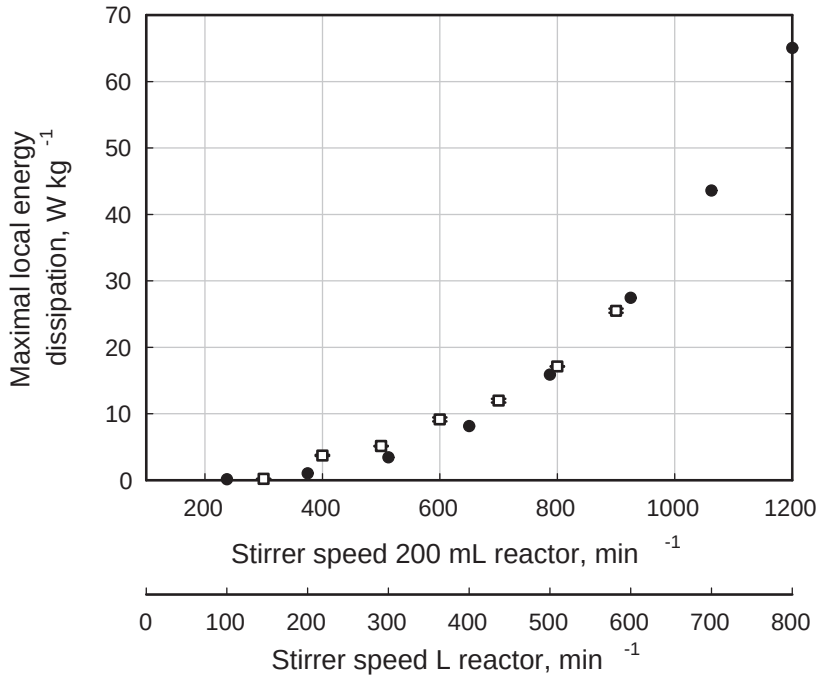

Figure 6.20: Maximal local energy dissipation as a function of the stirrer speed for the 200 mL reactor (□, experimental data) and the Liter reactor (●, calculated data).

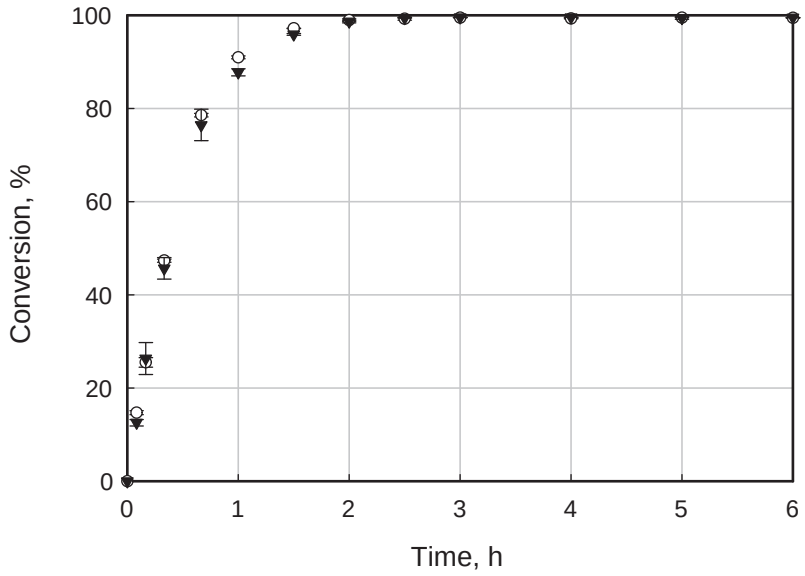

Figure 6.21: Evolution of the conversion during the whole-cell biocatalysis of 2-octanone to *R*-2-octanol: biotransformation at the 200 mL scale (○) and biotransformation at the Liter scale (▼). The enantiomeric excesses were constantly ≥ 99.5 % (*R*) in both setups.

6.3.3 Discussion

As can be seen in Fig. 6.21, not only the final conversion, but also the evolution of conversion over time in the Liter scale reactor is in very good agreement with the data obtained at the 200 mL scale. Both systems led to the same results within the estimation error. The scale-up can thus be considered successful.

These results also mean that the scale-up strategy chosen was correct. Keeping the maximal local energy dissipation constant permitted to avoid mass transfer limitations at the Liter scale. Consequently, a scale-up to even larger volumes should not be problematic either, provided that this condition is still verified.

6.4 Application to a miniaturized stirred tank bioreactor system

The enormous multitude of possible anion/cation combinations - generating according to estimations up to 10^{18} different compounds (Carmichael and Seddon, 2000) - leads to a large choice of possible ionic liquids. In the absence of clear structure-activity relationships, predicting the biocompatibility of the ionic liquid or the partitioning behaviour of given substances in the biphasic reaction setup, the choice for one solvent best suited for a given process is still difficult. Choosing an ionic liquid therefore often makes time intensive preliminary tests and screening procedures necessary.

To date, screening experiments for reaction systems including ionic liquids are mostly performed in shake flasks or other magnetically stirred vials (Cull *et al.*, 2000; Pfruender *et al.*, 2004; Wolfson *et al.*, 2006; Kratzer *et al.*, 2008; He *et al.*, 2009; Arai *et al.*, 2010). However, in such common small-scale reaction systems, sufficient mass transfer is not always assured and the scalability with respect to the larger L-scale stirred tank reactor used subsequently for production purposes is often not given (Hortsch and Weuster-Botz, 2010b).

To overcome the general issue of scalability between small scale and large scale vessels, a miniaturized stirred tank bioreactor system was developed that allows the parallel operation of up to 48 reactors at the mL-scale (Puskeiler *et al.*, 2005; Weuster-Botz *et al.*, 2005). The system is equipped with magnetically driven impellers and shows similar process engineering characteristics as laboratory- and production-scale reactors (Hortsch and Weuster-Botz, 2010c). Through this, a reliable and robust scale-up of the processes

from the small-scale to a larger-scale is assured. Previous studies demonstrated the usefulness of this tool for 'high-throughput bioprocess design' (Kusterer *et al.*, 2008; Vester *et al.*, 2009; Hortsch and Weuster-Botz, 2010a).

Using a small-scale device allowing the parallel evaluation of many different reaction setups as well as the possibility of a reliable scale-up afterwards would be of great interest for the domain of biocatalysis in ionic liquids. Therefore, the suitability of the described high-throughput platform for the process development of reactions involving non-water miscible ionic liquids was investigated.

6.4.1 Maximal local energy dissipation

As mentioned above, a reliable scale-up or a scale-down is only possible if it is assured that the same maximum drop size is reached at both scales. This means that both reactors have to be able to produce the same maximal local energy distribution. To verify if this is possible in the present case, the maximal energy dissipation was measured for the 200 mL system at different stirrer speeds, and compared to the ε_{max} values previously determined for the small-scale reactors (Hortsch and Weuster-Botz, 2010c).

When comparing both sets of data, it can be seen that the maximum local energy dissipation reached in both reaction systems for varying impeller speeds is within the same range of values (Fig. 6.22). This means that the drop size, too, and consequently also the mass transfer can be fixed to very similar values in both reactor types. The good reproducibility of this variable at both scales is thus assured, if the correct stirring speed is chosen.

6.4.2 Biotransformations in the miniaturized stirred tank bioreactor system

The scalability of the small-scale parallel bioreactor system for biphasic whole-cell biotransformations involving ionic liquids was verified by comparing the conversion reached at the 200 mL scale with the results observed in the small-scale reactors. The biotransformations at the 200 mL scale were performed at a stirrer speed of 600 min^{-1}. According to Fig. 6.22, the maximal local energy dissipation provoked would correspond to a stirrer speed of ~ 1100 min^{-1} at the mL scale. At this stirrer speed, the dispersion of the dense ionic liquid- settled at the bottom of the reactor at the beginning of the reaction - was however relatively slow. This is due to the stirrer used, which was not specifically developed for such dense liquids. In order to reach a more rapid homogenisation of the reaction medium, a stirrer speed of 1500 min^{-1} was therefore chosen. This did not influence the evolution of

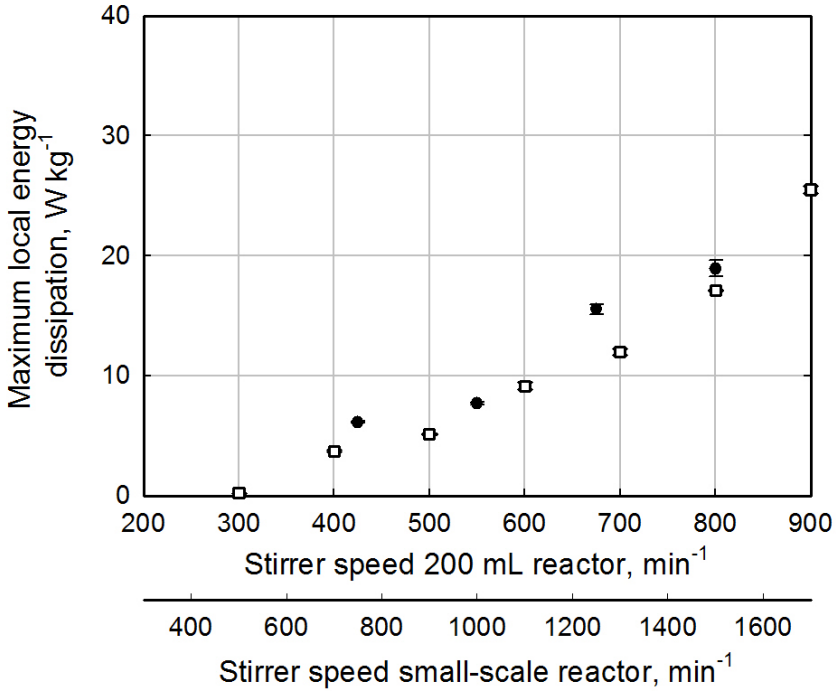

Figure 6.22: Maximal local energy dissipation as a function of the stirrer speed for the 200 mL reactor (□) and the small-scale reactor (●, source Hortsch and Weuster-Botz (2010c)).

the reaction. It was in fact proven that an increase of the stirrer speed from 600 min^{-1} to 900 min^{-1} did not provoke any changes in the reaction evolution at the 200 mL scale (data not shown). This would permit to increase the stirrer speed up to at least 1600 min^{-1} at the small scale without provoking any significant influence of the mass transfer on the biotransformation.

First, four different ionic liquids were used for the biphasic biotransformation of 2-octanone to 2-octanol, at a volume ratio of 20 % ionic liquid: [(EO2E)MPL][NTF], [HMPL][NTF], [HPYR][NTF]and [(NEMM)EO2E][NTF]. The initial substrate concentration was 600 mM 2-octanone in the ionic liquid. The evolution of the conversion in the four different reaction setups at the 200 mL scale and at the smaller scale is depicted in Fig. 6.23 A-D. The reaction kinetics and the final conversion reached at the mL-scale and in the 20-fold larger stirred tank reactor are in good agreement for each of the four different ionic liquids.

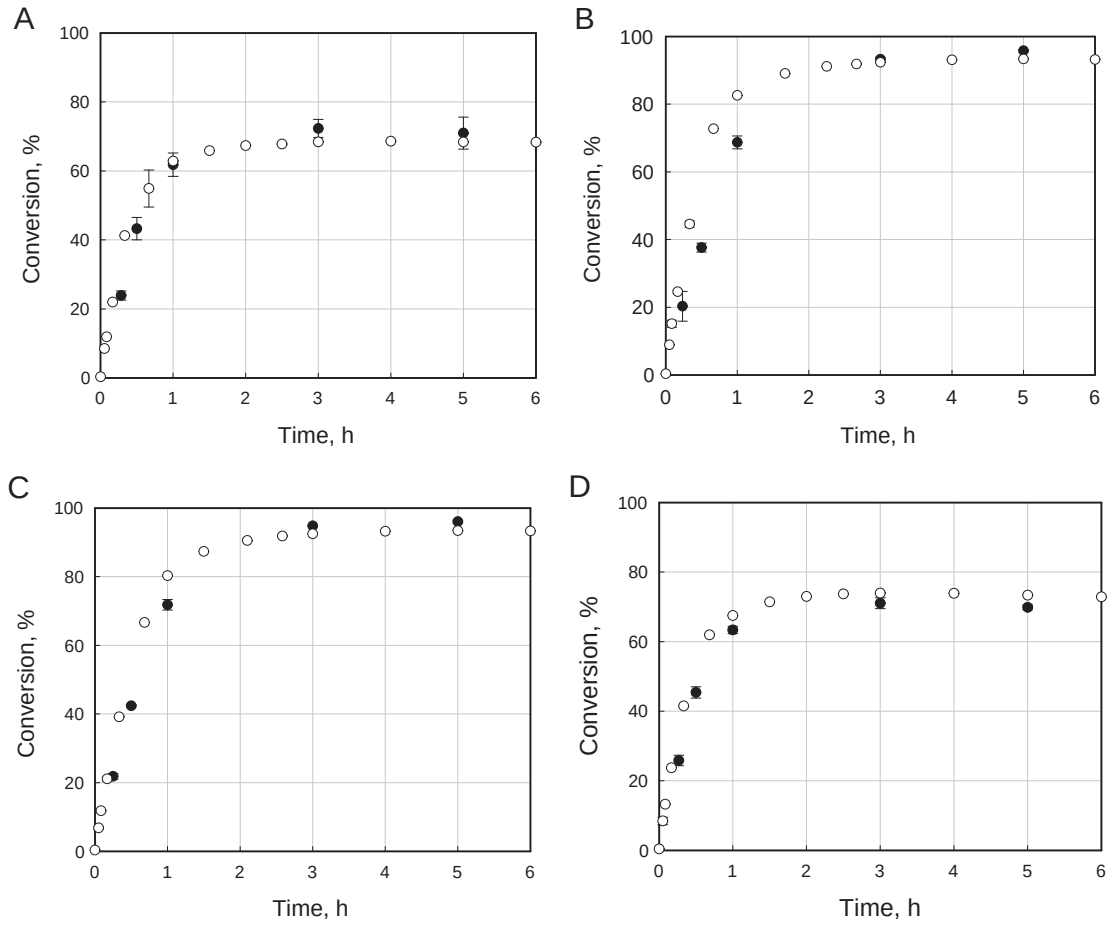

Figure 6.23: Conversion of 2-octanone with time resulting from the biotransformation of 2-octanone in biphasic reaction systems with 20 % ionic liquid at the 200 mL scale (stirrer speed of 600 min^{-1}) (○) and in the mL-scale bioreactor system (stirrer speed of 1500 min^{-1}) (●).A [(EO2E)MPL][NTF], B [HMPL][NTF], C [HPYR][NTF], and D [(NEMM)EO2E][NTF].

Following this, a second set of experiments was performed, varying the phase ratio of the ionic liquid to the aqueous phase. Different reaction systems containing between 20 % and 70 % [HMPL][NTF] were evaluated. The biocatalyst quantity in the aqueous phase and the substrate quantity in the ionic liquid were kept constant (0.56 g_{DCW} and 268 μL 2-octanone). The final conversion of 2-octanone reached after 5 h reaction time is depicted for the experiments at both scales in Fig. 6.24. The conversion in the mL-reaction vessels is in very good agreement with the results achieved at the larger scale for ionic liquid phase fractions up to 40 %. However, at phase fractions larger than 40 %, a deviation of the small scale reaction systems is observed in comparison to the larger scale device, and the difference between the two scales increases with increasing ionic liquid volume fraction.

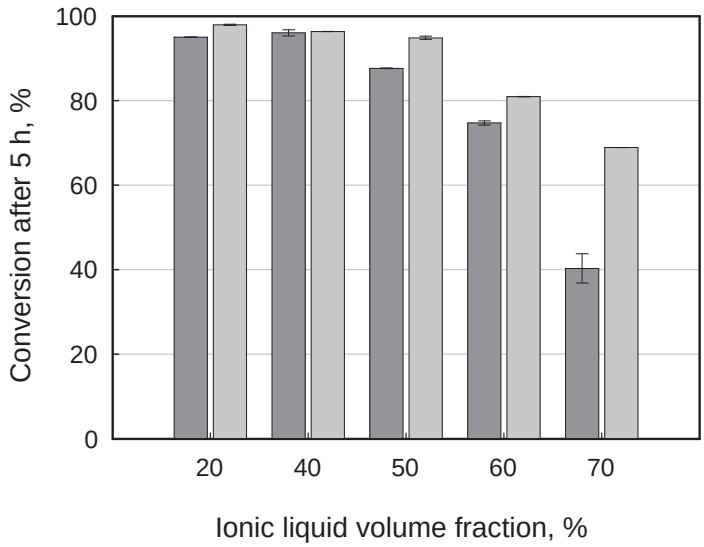

Figure 6.24: Conversion of 2-octanone after 5 h resulting from the biotransformation of 2-octanone in biphasic reaction systems with varying ionic liquid phase fraction (20 %, 40 %, 50 %, 60 % and 70 % [HMPL][NTF]): mL-scale bioreactor system (▬) and 200 mL scale (▭).

6.4.3 Discussion

The first set of experiments, testing different ionic liquids at the small scale, reproduced the results registered at the 200 mL with good precision. The final conversion reached was the same and the evolution of the conversion during the biotransformation was also in good agreement. These results thus prove the usability of the parallel mL-scale reactor system for the process evaluation of different ionic liquids in biphasic setups with an ionic liquid volume fraction of 20 %. While only one biotransformation can be performed at a time at the 200 mL scale - limiting the rate to one experiment per day - up to 48 different setups could be tested during the same period of time using the mL-scale bioreactor system. Moreover, the reaction volume used at the mL-scale was more than 10 times lower than in the 200 mL stirred tank reactor, while still allowing relatively frequent sampling (up to 7 samples over a duration of 5 h). This constitutes an enormous gain of time and ressources, significantly reducing the costs of the process development at this stage.

After this successful demonstration of the applicability of the high-throughput platform for reaction systems containing 20 % ionic liquid, it was evaluated if the parallel mL-bioreactor unit might also be suitable for increased ionic liquid volume fractions. This showed that there was good agreement between the larger scale and the small scale up to an ionic liquid volume fraction of 40 %. However, above this value, a deviation of the small scale was

observed: the conversion reached in the mL-reactors was lower than what was recorded at the 200 mL scale, and the difference between both scales increased with increasing ionic liquid volume fraction. This deviation is due to the fact that the mixing of the dense and viscous liquids becomes more and more difficult at such large ionic liquid volume fractions. As the stirrer used in the milliliter-scale bioreactors is not specifically designed to cope with such large viscosities and density differences as found in these reaction systems, the stirring does not permit to reach a homogeneous emulsion anymore and the ionic liquid (partially) settles at the bottom of the mL-reactor. This leads to mass transfer limitations in these reaction systems and consequently to lower conversion after 5 h.
In contrast, the Rushton turbine used in the 200 mL reactor permits better vertical mixing than the impeller used at small scale and it keeps the more dense ionic liquid from settling to the lower part of the reactor (Fig. 6.25). The inhomogeneity observed at the small scale when an ionic liquid volume fraction of 40 % is exceeded becomes more important with increasing ionic liquid phase fraction. This explains the larger difference between the two scales observed for reaction systems from 50 % ionic liquid to 70 % ionic liquid.
It should be noted that the use of a different stirrer, more specifically designed for the dispersion of relatively dense liquids, might however solve the problems observed.

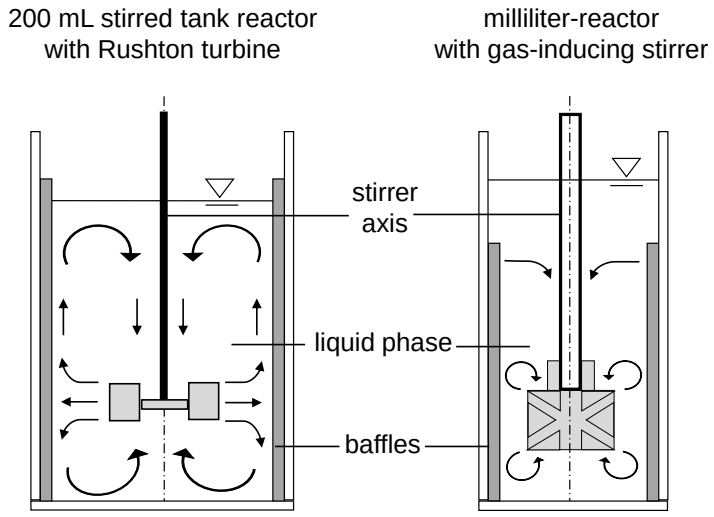

Figure 6.25: Schematic representation of the mixing behaviour in the 200 mL reactor equipped with a Rushton turbine and in the small-scale reactors equipped with a gas-inducing stirrer.

In the current setup, the mL-scale bioreactor unit is thus a tool mostly interesting for reaction setups with ionic liquid volume fractions up to 40 %. This range of volume fractions includes the majority of current applications of ionic liquids in whole-cell biocatalysis presented in literature, which mostly use ionic liquid volume fractions lower than 25 % (Cull *et al.*, 2000; Pfruender *et al.*, 2004; Lenourry *et al.*, 2005; Pfruender *et al.*, 2006; Bräutigam *et al.*, 2007; Hussain *et al.*, 2007; Cornmell *et al.*, 2008a; Shi *et al.*, 2008; Bräutigam *et al.*, 2009; He *et al.*, 2009; Wang *et al.*, 2009). Moreover, reaction systems with only moderate ionic liquid volume fraction might generally be preferred for industrial applications, due to the large volumetric power consumption needed for viscous reaction systems in large scale processes, as well as due to the large cost of the solvent.

However, using a stirrer more specifically designed for biphasic systems in which one phase has relatively large density might permit to expand the domain of applicability also to larger ionic liquid volume fractions. Such a stirrer was e.g. developed by Riedlberger and Weuster-Botz (2010).

It can thus be stated that this high-throughput platform constitutes a very convenient tool for the process development of biphasic reaction systems with moderate ionic liquid volume fractions up to 40 %, and possibly even for reaction systems with larger ionic liquid volume fractions if an appropriate stirrer is used. Its application significantly decreases the time, the effort and the resources necessary to screen different reaction conditions, and even more so when screening such expensive solvents as ionic liquids.

7 Characterisation and modelling of the biphasic whole-cell biotransformation

In the previous chapter, the impact of different system components on the biocatalyst stability and the effect of varying reaction conditions were analysed. This permitted to maximise the conversion reached and to better understand how the reaction outcome is affected when changing the volume ratio or the initial substrate concentration.

In this chapter, the characterisation of the reaction system is taken one step further. Here, the different steps of the reaction - i.e. the different mass transfers and the enzymatic transformation - taking place are characterised (Fig. 5.6). If the corresponding equations and the parameters necessary to describe these steps are available, this will permit to better predict the influence of process characteristics like the stirrer speed or the biocatalyst concentration on the reaction rate. In addition, the equations describing the different steps of the biotransformation can be used to establish a model of the whole-cell biotransformation. If a model was at disposal, this would increase the information available on the reaction system. Parameters that cannot be determined experimentally could be identified, and processes like the evolution of the substrate and the product concentrations within the cell, which cannot be monitored experimentally, could be estimated. Similarly, the biotransformation might be simulated in varying reaction conditions. This would save time and costs because it would not be necessary to perform the corresponding experiments to get to know the outcome of the process in these conditions. Therefore, the characterisation of the different steps, the determination of the corresponding parameters and the identification of a mechanistic model for the biphasic whole-cell biotransformation were the aims of this chapter.

The equations used to describe each reaction step are the differential equations representing the corresponding mass fluxes (equation 5.8 to equation 5.12). The model is formed by simultaneous integration of these differential equations. However, as indicated above, these equations can only be used if all the parameters appearing in these equations are known. Most parameters can be either determined experimentally, or estimated using correlations

which give these parameters as a function of other (known) process characteristics. Some parameters, however, can neither be measured nor estimated. These parameters then have to be identified by fitting the model formed to experimental data and minimizing the error between the simulated data and the experimental data. The identification of unknown parameters is not only necessary to complete the model and to be able to use it thereafter, but it can also be a goal of the modelling procedure.

Each of the mass fluxes taking place during the whole-cell biotransformation can be attributed to one of the following three categories:

- the mass transfer between the ionic liquid and the aqueous phase phase
- the mass transfer between the aqueous phase and the cell
- the enzymatic transformation inside the whole cell

Each of these types of mass transfers is characterized by its own specific type of equations and its own set of relevant parameters. For purpose of clarity, they will therefore be treated separately. Only once all the necessary information has been gathered for each type of transfer, the different sections will be united in the model as final step.

This chapter will thus be structured as follows:

- The first section will focus on the mass transfer between the ionic liquid and the aqueous phase.
- The second section will present the mass transfer between the aqueous phase and the cell.
- The third section will investigate the kinetics of the enzymatic reaction taking place within the cell.
- The fourth section will present a qualitative evaluation of the rate limiting step based on the information gathered during the previous sections.
- The fifth and last part will then present the results related to the model: identification of the unknown parameters, simulations and discussion of the limitations of the current model.

7.1 Characterisation of the mass transfer between the ionic liquid and the aqueous phase

This section will focus on the mass transfer between the ionic liquid and the aqueous phase. As described in subsection 4.5.3, the two-film model is reduced to a one-film model when the transfer resistance in one of the phases can be neglected. This is the case when the ratio of the diffusion coefficients in the respective phases and the partition coefficient of the diffusing substance between the two phases are larger than 1 (Schügerl, 2009) or, according to Brauer (1978a,b), when the product of the square root of the ratio of the diffusion coefficients times the partition coefficient is larger than 30. In the present case, the diffusion coefficients in the respective phases would have to be estimated. However, the partition coefficients of the substrate and the product between the ionic liquid and the aqueous phase are 1230 and 172, respectively. With these values, the threshold values indicated should be exceeded, even if the diffusion coefficient in the ionic liquid was lower than the diffusion coefficient in the aqueous phase by up to two orders of magnitude. It can therefore be considered that the main resistance of the overall mass transfer lies in the aqueous phase. The diffusion from the bulk of the ionic liquid to the ionic liquid-aqueous interface will be neglected and a one-film model is used to characterise the transfer between the ionic liquid and the aqueous phase.

According to the one-film theory, the fluxes of substrate and product between the two phases are given by equation 5.8 and equation 5.12. These equations rely on a number of parameters described in Table 7.1.

Only if all of these parameters are known, equation 5.8 and equation 5.12 can be used to model this part of the reaction process. Most of these parameters can be determined experimentally. The mass transfer coefficient, however, cannot be measured, because the necessary equipment and analytical techniques are not available. It has to be estimated using existing correlations (subsection 4.5.3). These correlations require the knowledge of the corresponding diffusion coefficient in the aqueous phase, as well as of given dimensionless numbers, such as the Reynolds number and the Froude number. The diffusion coefficient itself cannot be measured either, but it can be estimated using correlations based on the viscosity of the aqueous phase, and a.o. on the molecular mass and the molecular volume of the substances considered. The dimensionless numbers can be calculated on basis of the system characteristics. The procedure followed is depicted in Fig. 7.1.

Table 7.1: Parameters involved in the system equations used for modelling the mass transfer between the ionic liquid and the aqueous phase, their respective symbol and determination method.

Parameters	Symbol	Determination
Interfacial area, m^{-1}	a_d	experimental
Mass transfer coefficient, m s^{-1}	β_i	estimation
Diffusion coefficient, m^2 s^{-1}	$D_{i,c}$	estimation
Sauter diameter, m	d_{32}	experimental
Interfacial tension, N m^{-1}	$\sigma_{c,d}$	experimental
Viscosity, Pa s^{-1}	η	experimental
Partition coefficient, -	$D_{IL/aq}$	experimental

c = continuous phase, d = dispersed phase, i = substrate or product

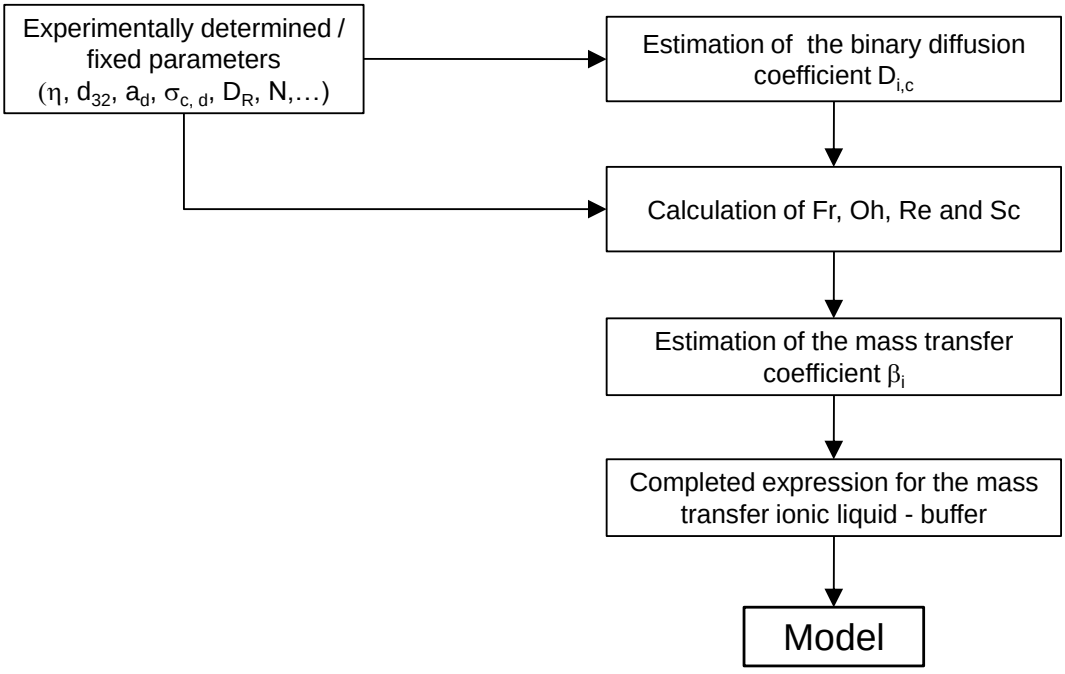

Figure 7.1: Scheme of the different steps towards estimating the mass transfer coefficient and completing the expression used to represent of the mass transfer between the ionic liquid and the aqueous phase in the model.

The first parts of this section will concentrate on the determination of the parameters that can be determined experimentally. The last part will then focus on the estimation of the diffusion coefficients and the mass transfer coefficient.

7.1.1 Viscosity

The viscosity of the liquids present in the reaction system is one of the factors influencing the diffusion of the substrate and the product in the system. These values are needed to estimate the mass transfer coefficient between the ionic liquid and the aqueous phase. Therefore, the viscosities of these liquids (water saturated [HMPL][NTF] and cell suspension of 50 g_{DCW} L^{-1} in phosphate buffer) were determined. For comparison, the viscosities of pure [HMPL][NTF], pure buffer (0.5 M potassium phosphate, 1 M sodium formate, pH 6.5), of buffer saturated with ionic liquid and of a set of other ionic liquids at disposal were also measured. The results are indicated in Table 7.2, Fig. 7.2 and Fig. 7.3.

Table 7.2: Viscosity of various liquids determined at 30 °C.

Liquid	Viscosity, mPa s
Buffer*	1.2 ± 0.5
Buffer* saturated with [HMPL][NTF]	1.18 ± 0.05
Cell suspension (50 g_{DCW} L^{-1} in buffer*)	1.17 ± 0.12
Pure [HMPL][NTF]	77 ± 1
[HMPL][NTF] saturated with buffer*	54 ± 1

* 0.5 M phosphate, 1 M sodium formate, pH 6.5

Discussion

The results indicated in Table 7.2 show that there is no significant difference between the viscosity of the buffer phase used (1 M sodium formate, 0.5 M potassium phosphate) and the viscosity of pure water (0.798 mPa s) (Korson *et al.*, 1969). Saturating the buffer phase with [HMPL][NTF] (solubility 1.92 g L^{-1}) does not lead to a significant change in viscosity. Similarly, the presence of the biocatalyst does not significantly influence the viscosity of the buffer. The large relative error on these very small values is due to the slightly reduced precision of the equipment at such low viscosities.

The viscosity of the ionic liquid [HMPL][NTF] is dramatically larger than the viscosity of water or of organic solvents such as e.g. hexane (~ 0.3 mPa s at 27 °C) or phenol (~ 8 mPa s at 27 °C) (Roth and Scheel, 1923). While the buffer viscosity is not influenced by the presence of low amounts of ionic liquid, the viscosity of the ionic liquid is significantly

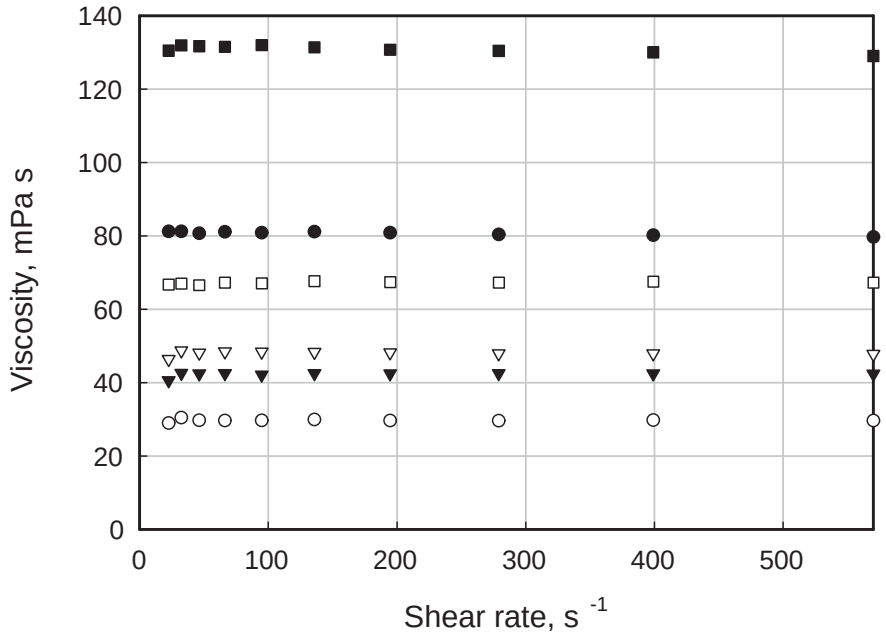

Figure 7.2: Evolution of viscosity with the shear rate applied for various ionic liquids at 30 °C: [BMIM][NTF] (○), [(EO2E)MPL][NTF](●), [HPYR][NTF](▽), [MOE(MPL)][NTF] (▼), [(NEMM)EO2E][NTF] (■) and [(P3OH)PYR][NTF] (□). For purposes of clarity, not all of the liquids evaluated are shown.

decreased when saturated with the buffer phase (0.9 % wt). This is consistent with observations in literature, describing that the presence of low amounts of impurities (i.e. here, water) significantly influences the physico-chemical properties of ionic liquids (Seddon *et al.*, 2000; Jacquemin *et al.*, 2006; Hussain *et al.*, 2007). In the present case, the viscosity is reduced by ~ 30 % by the low amounts of water dissolved in it.

All of the ionic liquids tested above showed Newtonian behaviour, i.e. constant viscosity with increasing shear rate (Fig. 7.2). The viscosities measured for the various ionic liquids were between 28.0 mPa s ± 1.6 mPa s and 181.5 mPa s ± 3.6 mPa s (Fig. 7.3). The viscosities of ionic liquids are generally within a range of 15 mPa s to 500 mPa s (Mantz and Trulove, 2003; Wasserscheid and Welton, 2003). According to these values, the ionic liquids evaluated here show relatively low viscosity in pure state, even if they still constitute viscous liquids in comparison to their commonly used organic counterparts.

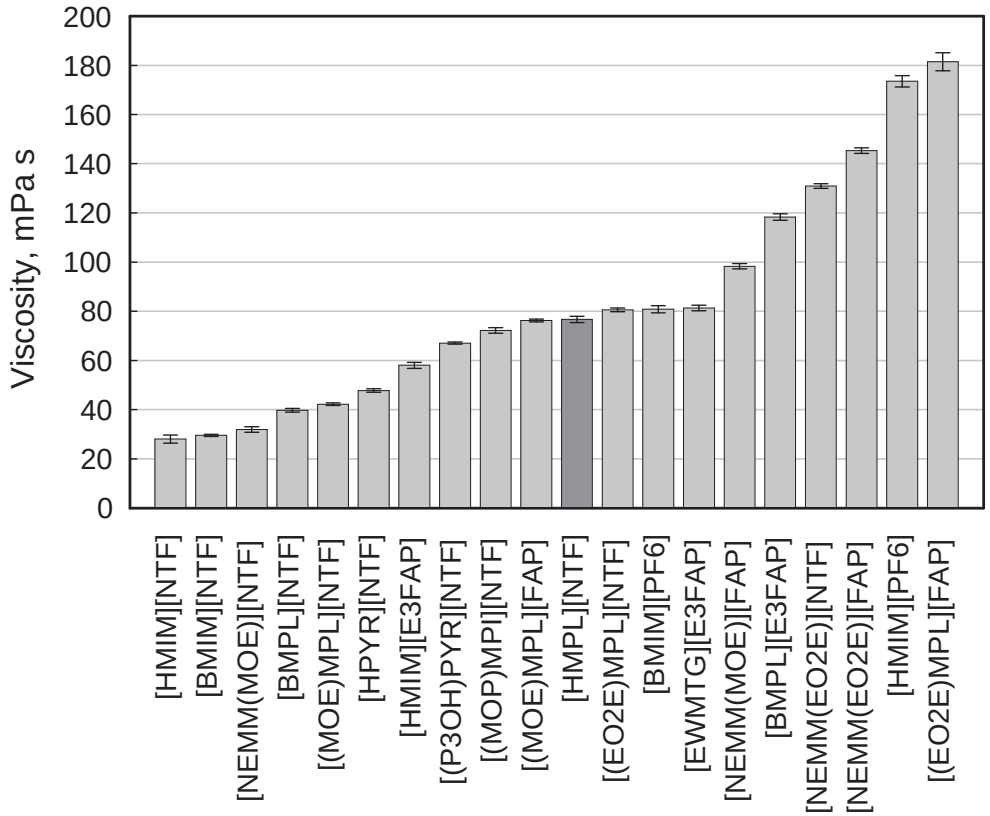

Figure 7.3: Viscosity of various pure ionic liquids determined at 30 °C. The ionic liquid mostly used in this project is [HMPL][NTF] (■).

7.1.2 Surface tension and interfacial tension

The interfacial tension between the ionic liquid and the aqueous phase is also a parameter of influence when considering the diffusion between these two phases. It determines the drop size of the dispersed phase in the emulsion formed and thus the interfacial area through which the transfer occurs. The interfacial tension is consequently also a parameter appearing in the correlation used for the estimation of the mass transfer coefficient of the substrate and the product.

Before measuring the interfacial tension, the surface tension of each of the two liquids had to be determined. In fact, the relative values of the surface tension of each phase determines the method to be applied for the evaluation of the interfacial tension ('standard' De Noüy ring method vs. De Noüy ring 'push' method). Once the surface tension of each liquid is known, the correct method for the measurement of the interfacial tension can be chosen. As the reaction system is not only composed of the pure ionic liquid and the pure aqueous phase, but also contains the substrate (2-octanone) and the product (2-octanol), the influence of these substances on the interfacial tension was evaluated. As both substances are very similar, the investigation of the effect of one of them is considered to be sufficient to estimate the resulting impact. Therefore, only the effect of the product concentration (300 mM and 600 mM) in the ionic liquid on the interfacial tension was analysed.

The values determined for the surface tension of the aqueous phase and [HMPL][NTF] are given in Table 7.3. It can be seen that the surface tension of the ionic liquid is only half of the surface tension determined for the aqueous buffer.

Table 7.3: Surface tension of the two phases used in the biphasic biotransformation. The measurements were performed at 27 °C.

Liquid	Surface tension, mN m^{-1}
buffer*	69.6 ± 0.6
[HMPL][NTF]	32.0 ± 0.1

* 0.5 M potassium phosphate, 1 M sodium formate, pH 6.5

The interfacial tensions of the various biphasic systems analysed are indicated in Table 7.4. A significant decrease of the interfacial tension with increasing product concentration is observed.

Table 7.4: Interfacial tension of different biphasic systems. The measurements were performed at 27 °C.

Biphasic system	Interfacial tension, mN m^{-1}
[HMPL][NTF] / buffer*	17.23 ± 0.02
[HMPL][NTF] (with 300 mM 2-octanol) / buffer*	12.8 ± 0.4
[HMPL][NTF] (with 600 mM 2-octanol) / buffer*	8.5 ± 0.4

* 0.5 M potassium phosphate, 1 M sodium formate, pH 6.5

Discussion

For the aqueous buffer (1 M sodium formate, 0.5 M potassium phosphate), a surface tension of 69.6 mN m^{-1} ± 0.6 mN m^{-1} (27 °C) was determined. This value is very similar to the surface tension determined for pure water at 25°C (71.97 mN m^{-1}) (Speight, 2005). With 32.0 mN m^{-1} ± 0.1 mN m^{-1}, the ionic liquid ([HMPL][NTF]) presents only half the surface tension of the aqueous phase. This lower value is consistent with the observation of a surfactant like behaviour of ionic liquids containing cations with large alkyl chains described in literature (Evans, 2008a).
The most similar ionic liquid that was evaluated in literature is 1-butyl-3-methylimidazolium bis(trifluoromethylsulfonyl)imide ([BMIM][NTF]). For this ionic liquid values between 32.80 mN m^{-1} and 37.5 mN m^{-1} were indicated at room temperature (Huddleston *et al.*, 2001; Freire *et al.*, 2007; Wandschneider *et al.*, 2008; Klomfar *et al.*, 2010). The surface tension determined here for [HMPL][NTF] thus falls within the same range.
In comparison to organic solvents, the value determined for the ionic liquid is slightly larger than the surface tension of *n*-alkanes such as *n*-heptane (20.53 mN m^{-1} ± 0.02 mN m^{-1}) and *n*-decane (24.47 mN m^{-1} ± 0.02 mN m^{-1}), but similar to the surface tension of *n*-hexadecane (28.12 mN m^{-1} ± 0.02 mN m^{-1}) (Rolo *et al.*, 2002).

These measurements also show that in the biphasic system under consideration the liquid with lower density (the aqueous phase, density ~ 1 g cm^{-3} at 25 °C) has larger surface tension than the liquid of larger density ([HMPL][NTF], density of 1.34 g cm^{-3} at 25 °C). This means that the 'standard' De Noüy ring method, where the platinum ring is pulled

from the liquid interface towards the upper phase, cannot be applied to determine the interfacial tension between these two liquids (personal communication, A.KRÜSS Optronic GmbH). Here, the De Noüy ring 'push' method has to be used, where the platinum ring is pushed from the liquid interface towards the lower phase. This consideration is of great importance, as the 'standard' method would not lead to reliable measurements.

The measured interfacial tension between the [HMPL][NTF] and the phosphate buffer is comparable to the interfacial tension determined for esters and water (Demond and Lindner, 1993). It is however significantly lower than the interfacial tension of water with alkanes (around 50 mN m^{-1}), and significantly larger than in water-alcohol mixes (around 5–10 mN m^{-1}).
The interfacial tension between the ionic liquid and the buffer decreases with increasing concentration of 2-octanol in the reaction system. This is a typical behaviour described in literature (Kim and Burgess, 2001): when substances (e.g. here 2-octanol), forming lower interfacial tension with water than the second phase (the ionic liquid) with water, are added into the biphasic system ionic liquid-aqueous phase, the interfacial tension between these two phases (ionic liquid and aqueous phase) decreases.

7.1.3 Drop size distribution and evaluation of the interfacial area

The mass transfer between the ionic liquid and the aqueous phase is a function of the interfacial area between both phases (equation 4.30). The interfacial area can be calculated on basis of the mean Sauter diameter (d_{32}) of the drops of dispersed phase in the emulsion. The Sauter diameter is determined on basis of the corresponding drop size distribution (equation 4.23 and equation 4.24). The drop size distribution in a given emulsion is strongly dependent on the stirrer speed and on the respective volume fractions of the two liquids. In order to estimate the mass transfer between the both liquid phases, the interfacial area needs to be known in the reaction conditions applied, and therefore the drop size distribution was recorded for varying stirrer speeds (from 300 min^{-1} to 900 min^{-1}) and varying volume ratios (from 10 % ionic liquid to 70 % ionic liquid). As the presence of cells might also influence the drop size distribution of the dispersed phase in the emulsion, these measurements were made in abscence as well as in presence of cells.

In addition to the experimental determination of the Sauter diameter, an empirical correlation presented in literature should permit to estimate the Sauter diameter (equation 4.29). The measured data is compared to this estimated value for d_{32}.

During the measurements, the reaction systems with large ionic liquid volume fraction did not allow homogeneous mixing at very low (300 min^{-1}) and very large (900 min^{-1}) stirrer speeds. In addition, at stirrer speeds of 900 min^{-1}, air bubbles were often introduced into the emulsion through the very turbulent surface of the biphasic mixture. These air bubbles - with much larger diameters than the drops of dispersed phase - distorted the actual drop size distribution. The data recorded for stirrer speeds of 300 min^{-1} and 900 min^{-1} are therefore not presented below.
Similarly, the measurements in presence of cells did not permit any conclusions. In fact, the laser in the optical probe used is not strong enough to still detect the drops of dispersed phase when the optical density is as large as in the samples analysed (5 g_{DCW} L^{-1} and 50 g_{DCW} L^{-1}) (personal communication, MTS Sensor Technologie GmbH & Co. KG). A probe with stronger laser was not at disposal. The data presented below will therefore only consider biphasic systems without cells.

On basis of the different drop size distributions recorded at stirrer speeds between 400 min^{-1} and 800 min^{-1} for biphasic reaction system with ionic liquid volume fractions between 10 % and 70 %, the mean Sauter diameter was calculated. The resulting diameters for each set of conditions are depicted in Fig. 7.4. These diameters permit to determine the interfacial area in the emulsion for each set of conditions. Exemplarily, the data for an ionic liquid volume fraction of 20 % at varying stirrer speeds are shown in Fig. 7.5.

For a given stirrer speed, Fig. 7.4 shows an increase of the Sauter diameter with increasing ionic liquid volume fraction until a volume fraction of 50 %. Above a value of 50–60 %, the Sauter diameter decreases again with increasing ionic liquid content. This observation was made at all the stirrer speeds evaluated.
When considering the evolution of the Sauter diameter for one fixed ionic liquid volume fraction, a decrease of the Sauter diameter with increasing stirrer speed is observed. Again, this holds for each ionic liquid volume fraction analysed. The inverse effect is observed on the interfacial area a_d (Fig. 7.5).

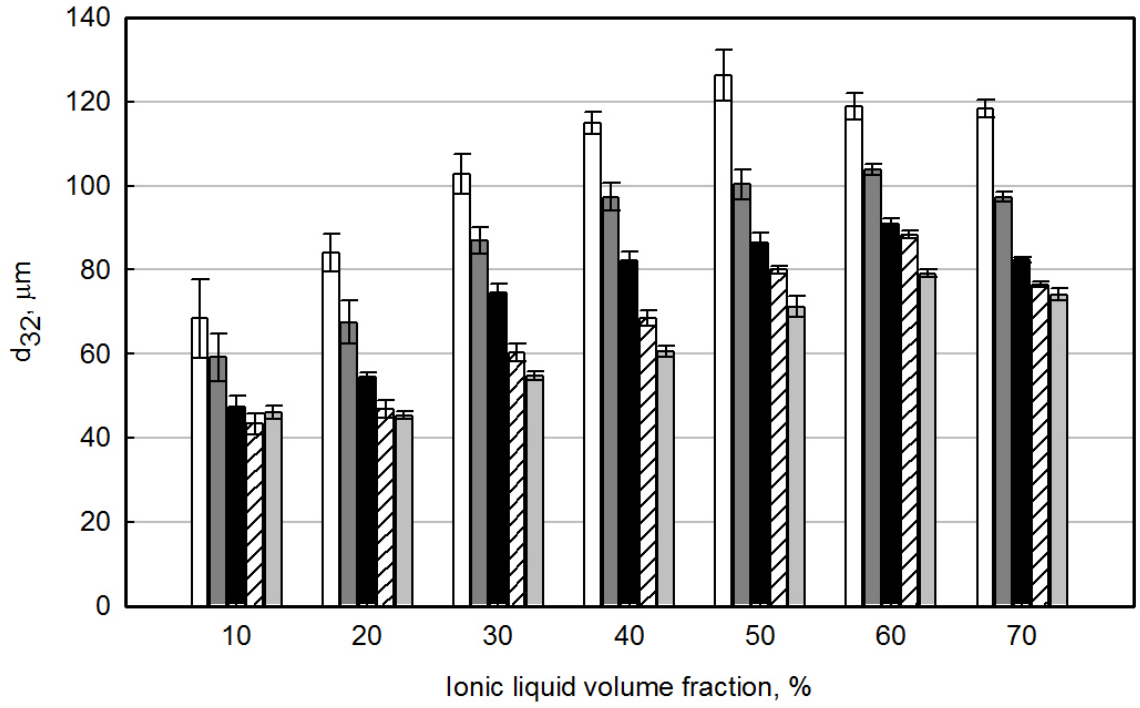

Figure 7.4: Sauter diameter (d_{32}) as a function of the ionic liquid volume fraction for varying stirrer speeds: 400 min^{-1} (▭), 500 min^{-1} (▬), 600 min^{-1} (■), 700 min^{-1} (▨) and 800 min^{-1} (▭).

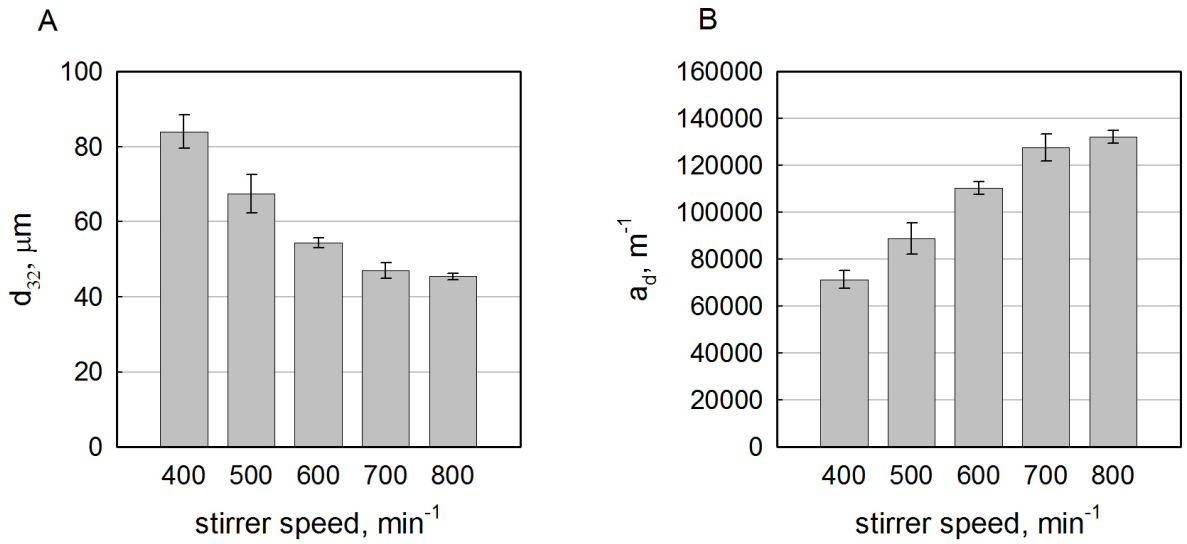

Figure 7.5: Sauter diameter (d_{32}) as a function of the stirrer speed (A) and the corresponding interfacial area per volume of dispersed phase (a_d) (B) for a reaction setup with 20 % ionic liquid.

Comparing the estimated Sauter diameters with the real data recorded for ionic liquid volume fractions of 20 % (Table 7.5), the estimated values are larger by almost a factor 2–2.7. The empirical correlations used significantly overestimate the Sauter diameter for the system under consideration. The same observation was made when estimating the Sauter diameter at varying stirrer speeds for reaction systems with 10 % ionic liquid or 30 % ionic liquid (data not shown).

Table 7.5: Comparison of the estimated and measured Sauter diameter (d_{32}) for a reaction setup with an ionic liquid volume fraction of 20 % and varying stirrer speeds.

Determination method	d_{32}, μm 400 min^{-1}	d_{32}, μm 500 min^{-1}	d_{32}, μm 600 min^{-1}	d_{32}, μm 700 min^{-1}
Experimental	84 ± 4	67 ± 5	54 ± 1	47 ± 2
Estimation*	225.05	169.24	134.20	110.37

* estimation according to Calabrese *et al.* (1986b), equation 4.29

Discussion

For a fixed volume ratio, the mean Sauter diameter decreases with increasing stirrer speed. The decrease in size due to an increase of the stirrer speed is more important at low stirrer speeds, and then increasingly slows down as larger stirrer speeds are considered. This observation was made for each of the different volume ratios tested. It is explained by the increased power input and larger hydrodynamic forces to which the drops are exposed at increasing stirrer speed.

Concerning the different phase ratios tested, the Sauter diameter first increases with increasing ionic liquid content. This is due to the fact that the more dispersed phase is present, the more frequently the drops will collide and coalesce for a small amount of time, before again being dispersed by the hydrodynamic forces induced by the stirrer.
However, starting at a volume fraction between 50–60 % ionic liquid, this tendency is inversed, and the Sauter diameter decreases with increasing ionic liquid content. This change in the system behavior is observed at all stirrer speeds, and it indicates that a change in the system composition is taking place: a shift of roles between the ionic liquid and the aqueous phase. While the ionic liquid constituted the dispersed phase at low ionic liquid volume fraction, the changes in system behavior indicate that this is now no longer

the case. Above a volume fraction of 50–60 %, the ionic liquid becomes the continuous phase and the aqueous phase is now present as drops in the emulsion formed. This phase inversion at an ionic liquid volume fraction 50–60 % is not straightforward, as the volume fraction alone is not sufficient to determine which liquid is the continuous phase and which is the dispersed phase. Other consideration, such as e.g. the interfacial tension and the coalescence influence this phenomenon (Paul *et al.*, 2004).
A visual determination of this phenomenon is not possible here, because the emulsion formed seems very homogeneous at sight, and it is not possible to distinguish the ionic liquid from the aqueous phase. The observation made above is thus a valuable gain of knowledge. This phase inversion has to be taken into account when calculating a_d, the interfacial area per volume of dispersed phase, used to determine the mass transfer between the ionic liquid and the aqueous phase.

The empirical correlation used to estimate the Sauter diameter leads to a large deviation from the real data. It overestimates d_{32} by up to a factor 2.7 (Table 7.5). This might be due to the fact that the empirical correlation was developed on basis of correlations for dilute dispersions. The dependence of d_{32} on the phase fraction of the dispersed phase indicated in this equation was not verified experimentally (Calabrese *et al.*, 1986b). The authors therefore recommend to only use the correlation 'as a first approximation'. In addition, the special characteristics of ionic liquids in comparison to commonly used organic solvents might be part of the reason why this correlation does not permit to make reliable predictions of the Sauter diameter for the biphasic system considered.
While dilute dispersions are relatively well characterised, this correlation was the only correlations presented in literature for viscous phases and non dilute dispersions. It must therefore be concluded that no reliable estimation of the Sauter diameter is available to date for reaction systems with such large volume fraction of the dispersed phase and such viscous dispersed phases as considered here. An estimation of d_{32} on basis of this correlation would lead to a considerable error on this variable, and consequently also on the interfacial area and the estimated mass transfer between the two phases. Currently, a reliable determination of the Sauter diameter for non-dilute reaction systems can consequently only be obtained experimentally.

7.1.4 Mass transfer coefficient of the substrate and the product between the ionic liquid and the aqueous phase

After having determined all the parameters that can be determined experimentally, the still unknown parameters - the mass transfer coefficients of the substrate and the product - can now be determined on basis of existing correlations. As mentioned above, these mass transfer coefficients cannot be determined directly, because they require the knowledge of the corresponding diffusion coefficients. These will be estimated first, and only then the mass transfer coefficients will be evaluated.

The different steps towards the estimation of the mass transfer coefficient will be presented for the set of conditions described in Table 7.6. For other reaction conditions, such as larger stirrer speeds or increased ionic liquid volume fractions, the procedure is identical and it will therefore not be presented here.

Table 7.6: Conditions used to estimate the mass transfer coefficient.

Parameter	Condition fixed
Ionic liquid	[HMPL][NTF]
Buffer	0.5 M potassium phosphate, 1 M sodium formate, pH 6.5
Phase ratio	20 % ionic liquid, 80 % aqueous phase
Stirrer speed	600 min^{-1}
Temperature	30 °C (303.15 K)

Estimation of the diffusion coefficient in the aqueous phase

As described in subsection 4.5.3, five different correlation models are at disposal to estimate the diffusion coefficients of the substrate and the product (equation 4.41 to equation 4.46). As the domain of validity of each of these correlations fits the situation analysed here, a preliminary distinction between these correlations is difficult. Therefore, all the different models were evaluated in parallel. Once the resulting values are known, it might then be possible to first verify if they lead to significantly different results and then exclude those leading to clear outliers or absurd results.

It should be noted that the correlation models used do not permit to distinguish between the substrate (2-octanone) and the product (2-octanol). In fact, the only characteristic specific to the diffusing substance included in the respective models is the molar volume (equation 4.41 to equation 4.46). In the absence of experimental data, this parameter is estimated according to an additive method using the volume increments by Le Bas for the calculation of molar volumes (Reid, 1988). Using this method, the estimated molar volumes of the substrate and the product differ by only 2 %. With such a low relative difference of the molar volume, the difference between the resulting values for the diffusion coefficient for 2-octanone and 2-octanol given by equation 4.41 to equation 4.46 will be insignificant. Consequently, it is unnecessary to consider two different diffusion coefficients. In the following, only one diffusion coefficient will therefore be considered for both the substrate and the product. As the mass transfer coefficients are calculated on basis of the diffusion coefficients, there will also be only one mass transfer coefficient, used for both the substrate (2-octanone) and the product (2-octanol) in the subsequent work.

The different models considered give the diffusion coefficient as a function of various factors, including the viscosity, the molecular volume and the molecular mass. All of the values used in the corresponding calculations are indicated in the appendix (Table G.27).

The correlations applied led to the diffusion coefficients listed in Table 7.7. It can be seen that the different correlation models give diffusion coefficients of the same order of magnitude. However, between the lowest estimation of $D_{i,c}$ (according to Othmer & Thakar) and the largest values (using the correlations by Tyn & Calus and Reddy & Doraiswamy), there is almost a factor two. On average over the 5 different results, a value of $2.65 \cdot 10^{-10}$ m^2 s^{-1} $\pm$ $0.7 \cdot 10^{-10}$ m^2 s^{-1} is obtained. In the absence of other rational criteria permitting to choose one of the diffusion coefficients rather than the others, the diffusion coefficient closest to the average value was chosen for further calculations. This mass transfer coefficient was given by the correlation proposed by Wilke and Chang (1955).

Estimation of the mass transfer coefficient

Three different models are available to estimate the mass transfer coefficient on basis of the diffusion coefficient and other process relevant parameters (equation 4.32, equation 4.33 and equation 4.34). As above, the three models will be evaluated in parallel. No preliminary distinction concerning their reliability can be made, because all the models indicated are valid for the reaction setup considered here.

Table 7.7: Binary diffusion coefficient ($D_{i,c}$) estimated on basis of different correlation models.

Correlation model used	$D_{i,c}$, $m^2\ s^{-1}$
Wilke & Chang	$2.51 \cdot 10^{-10}$
Othmer & Thakar	$1.71 \cdot 10^{-10}$
Reddy & Doraiswamy	$3.41 \cdot 10^{-10}$
Tyn & Calus	$3.40 \cdot 10^{-10}$
Hayduk & Minhas	$2.20 \cdot 10^{-10}$

As the following calculations are based on the diffusion coefficient as only substance specific parameter, the determination of the mass transfer coefficient will also lead to only one value for both the substrate (2-octanone) and the product (2-octanol).

The three correlations considered give the mass transfer coefficient as a function of different dimensionless numbers, as well as various physical and geometric system characteristics, such as the interfacial tension or the impeller diameter. The system specifications used for the calculations of β are given in the appendix (Table G.27). Based on these parameters, and on the diffusion coefficient determined in the previous subsection ($D_{i,c} = 2.51 \cdot 10^{-10}\ m^2\ s^{-1}$), the Schmidt number, the Froude number, the Ohnesorge number and the impeller Reynolds number were determined according to equation 4.35 to equation 4.38. The resulting values are indicated in Table 7.8.

Table 7.8: Schmidt number (Sc), Froude number (Fr), Ohnesorge number (Oh) and Reynolds number (Re) for the biphasic reaction system [HMPL][NTF] - phosphate buffer at a stirrer speed of 600 min^{-1} and an ionic liquid volume fraction of 20 % ($d_{32} = 54\ \mu m$).

Number	Value
Sc_c	9936
Fr	0.29
Oh	0.0042
Re	2088

Using all of the parameters now at disposal, the mass transfer coefficient was then evaluated applying each of the three different correlations available for its estimation. The results are indicated in Table 7.9.

Table 7.9: Mass transfer coefficient (β) of 2-octanone and 2-octanol estimated using three different correlations.

Correlation used	β, m s^{-1}
Skelland & Moeti	$1.516 \cdot 10^{-6}$
Skelland & Tedder	$3.592 \cdot 10^{-7}$
Skelland & Lee	$7.801 \cdot 10^{-7}$

The results in Table 7.9 show that the three correlations for the estimation of the mass transfer coefficient lead to similar values. Based on these mass transfer coefficients, the maximal mass transfer rate from the interface between the ionic liquid and the aqueous phase to the bulk of the aqueous phase can be estimated: supposing that the substrate concentration is 300 mM in the bulk of the ionic liquid, this would lead to a concentration of ~0.24 mM at the interface (partition coefficient of 2-octanone between the ionic liquid and the aqueous phase: 1230). The maximal transfer rate would be observed when no substrate is present in the aqueous phase at all. Based on the mass transfer coefficients determined, this maximal transfer rate between the ionic liquid and the aqueous phase would be between $1.93 \cdot 10^{-6}$ mol L^{-1} s^{-1} and $8.16 \cdot 10^{-6}$ mol L^{-1} s^{-1} (with respect to the total reaction volume and with an ionic liquid volume fraction of 20 %).

Discussion

The different values obtained for the diffusion coefficient are all within the same order of magnitude. In contrast to the diffusion in gas, where diffusion coefficients around 10^{-6}–10^{-5} m^2 s^{-1} are expected, the diffusion in liquids is generally much slower, and characterized by diffusion coefficients of 10^{-10}–10^{-9} m^2 s^{-1} (Welty *et al.*, 2001). Among the different values obtained on basis of the different correlations available, the diffusion coefficient given by the correlation proposed by Wilke and Chang (1955) was chosen for further calculations.

The mass transfer coefficients determined through the three correlation models are within one order of magnitude. A quantitative evaluation by comparison with literature data is not possible because mass transfer coefficients are highly dependent on the process conditions. No such data is available in this case.

It can nevertheless be verified if the estimations lead to absurd values, or if, theoretically, the mass transfer coefficient could correspond to one of these values in the reaction process

considered. Even if there is no information about the rates of the different reaction steps, it can be stated that each step of the reaction has to be, at each point of time, at least as rapid as the 'apparent' rate measured during the biotransformation. This 'apparent' rate is the rate at which the product appears in the ionic liquid, the last step of all the different transfers taking place during the biotransformation. This conclusion also holds true for the mass transfer between the ionic liquid and the aqueous phase.
The experimental data showed that the apparent rate was of the order of $4 \cdot 10^{-5}$ mol L^{-1} s^{-1} at the beginning of the reaction. When comparing the maximal transfer rate possible with the estimated mass transfer coefficients (between $1.93 \cdot 10^{-6}$ mol L^{-1} s^{-1} and $8.16 \cdot 10^{-6}$ mol L^{-1} s^{-1}), the production rate observed during the experiments is larger by at least a factor ~ 5 and at most a factor ~ 20. As there is no doubt concerning the repeated and reproducible experimental observation of the apparent rate, it must be concluded that the correlations used significantly underestimate the actual mass transfer coefficients of the substrate and the product. The same observation was made by Pfründer (2005) using the same correlations in a very similar setup. The author investigated a biphasic reaction system with ionic liquids for the reduction of 4-chloroacetophenone by whole cells of *Lactobacillus kefir*. Estimating the maximal substrate transfer from the ionic liquid to the aqueous phase on basis of equation 4.32, a value significantly lower than the observed reaction rate was obtained.

It is difficult to determine precisely why the correlations used lead to such a bad prediction of the mass transfer coefficient in the reaction system analysed here. Further investigation is necessary to determine what exactly leads to the large deviations observed.
As the correlations at disposal cannot be used to estimate this factor, another means has to be found to give a value to this parameter. Because the mass transfer coefficient cannot be measured with sufficient precision, the last possibility remaining is to leave the parameter unknown and use the finally established model to identify it.

7.2 The mass transfer between the aqueous phase and the cell

The mass transfer between the aqueous phase and the cell is described by equation 5.9 and equation 5.11. The parameters appearing in these equations are indicated in Table 7.10.

For the membrane area of *E. coli* and the specific cell volume literature data was used: a membrane area of 23.7 m^2 g_{DCW}^{-1} and a specific cell volume of $3.25 \cdot 10^{-3}$ L g_{DCW}^{-1} based on the data published by Kubitschek (1990). The total cell mass is given by the

Table 7.10: Parameters involved in the system equations used to model the mass transfer between the aqueous phase and the cell, their respective symbol and determination method.

Parameters	Symbol	Determination
Membrane permeability,m s^{-1}	P_i	identification
Specific cell membrane area of *E. coli*, m^2 g_{DCW} $^{-1}$	a_x	experimental*
Specific cell volume of *E. coli*, L g_{DCW} $^{-1}$	v_x	experimental*
Total cell mass,g_{DCW}	$M_{x,total}$	experimental

i = substrate or product, x = biomass, * = experimental data from literature, source Kubitschek (1990)

cell concentration in the aqueous phase times the volume of the aqueous phase. It is thus fixed by the experimental conditions chosen. The membrane permeability of the substrate (P_S) and the product (P_P) cannot be determined experimentally and no correlations exist giving them as a function of other (known) factors. The only solution is thus to identify these parameters by fitting the model to experimental data recorded during the biotransformations. As the substrate and the product are very similar molecules, the membrane permeability of both substances should be very similar, too. The very small differences in the molecules' polarity and 3-dimensional structure due to the ketone and the alcohol group, respectively, should not be relevant in comparison to the effect of the long alkyl chain, which they have in common. For the identification of these parameters by fitting of the model, it will thus be supposed that they are the same ($P_S = P_P = P$).

7.3 The enzymatic transformation

In this section, the enzymatic transformation of the substrate to the product of interest is analysed in more detail. The aim is to gain more information about the two enzymes of interest in order to be able to find a suitable description of the enzyme kinetics which can be introduced into the model to represent this step of the biotransformation.
The transformation of interest is a function of both enzymes overexpressed in the biocatalyst, the LB ADH and the CB FDH. The LB ADH performs the reduction itself, while the CB FDH is responsible for the cofactor regeneration. The main reaction thus depends not only on the activity of the LB ADH, but also on the performance of the CB FDH.

In a first step, initial reaction rate experiments were performed. Then, the expression representing the enzymatic transformation considered in this project is determined.

7.3.1 Characterisation of the LB ADH and the CB FDH

Initial rate experiments were used to determine the respective half saturation constants (K_m) as well as the maximal reaction rate (v_{max}) for each enzyme according to equation 4.14. These parameters permit to estimate the respective activities of the LB ADH and the CB FDH in the presence of given substrate and cofactor concentrations. As both enzymes have a two-substrate mechanism, the measurement of the initial reaction rate were made in presence of an excess of one substrate while varying the concentration of the other substrate, as described in subsection 5.3.2.

Table 7.11: Half saturation constants (K_m) and maximal reaction rate (v_{max}) of the *Lactobacillus brevis* alcohol dehydrogenase (LB ADH) and the *Candida boidinii* formate dehydrogenase (CB FDH) determined at 30 °C.

Enzyme	Parameter	Value	Unit
CB FDH	$K_{m\ formate}$	4.5 ± 0.2	mM
	$K_{m\ NAD^+}$	30.2 ± 1.1	μM
	v_{max}	1185 ± 9	U g_{DCW}^{-1}
LB ADH	$K_{m\ 2\text{-octanone}}$	5.2 ± 1.3	mM
	$K_{m\ NADH}$	7.4 ± 0.7	mM
	v_{max}	5330 ± 190	U g_{DCW}^{-1}

The results in Table 7.11 show that the CB FDH has a much higher catalytic efficiency with NAD^+ than the LB ADH has with NADH. The half saturation constant of the CB FDH for NAD^+ is indeed almost an order of magnitude lower than the half saturation constant of the LB ADH for NADH. In contrast, the maximal reaction rate reached by the LB ADH when the substrate and the cofactor are present in excess is larger by a factor 4.5 than the maximal reaction rate observed for the CB FDH. These considerations are illustrated by Fig. 7.6 and Fig. 7.7. These figures show the evolution of the enzyme activity with varying initial concentrations of one of the substrates in presence of an excess of the other substrate. The ranges of concentrations considered correspond to the range of 'operational' concentrations used in the biotransformation: the phosphate buffer in which the cells are suspended contains up to 1 M sodium formate, the concentration ranges of substrate in the ionic liquid used in the biotransformations lead to a maximum of ~ 1 mM 2-octanone in the aqueous phase, and the sum of the concentrations of the cofactors NADH and NAD^+ in *E. coli* is usually around ~ 1 mM (Link, 2009).

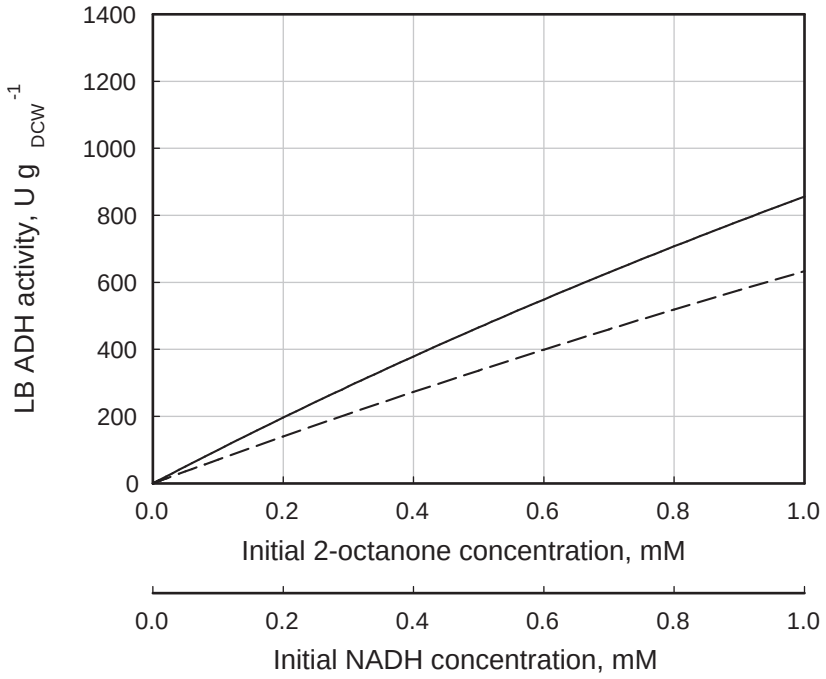

Figure 7.6: Evolution of the LB ADH activity: with varying initial 2-octanone concentrations and in presence of an excess of NADH (—) and with varying initial NADH concentrations and in presence of the maximal solubility concentration of 2-octanone (- - -).

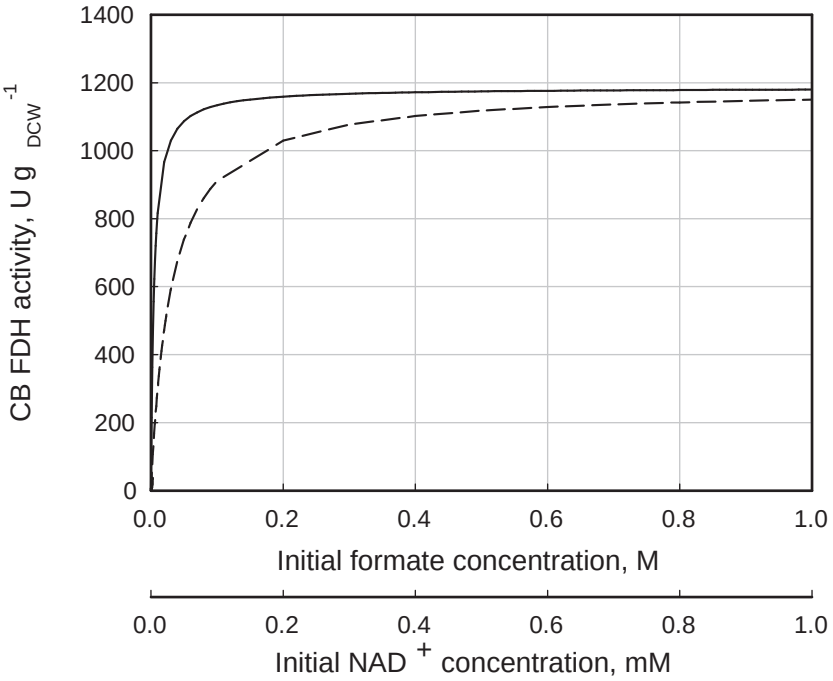

Figure 7.7: Evolution of the CB FDH activity: with varying initial formate concentrations and in presence of an excess of NAD^+ (—) and with varying initial NAD^+ concentrations and in presence of an excess of formate (- - -).

Discussion

The K_m determined for the CB FDH are in accordance with literature data indicating half saturation constants for formate in the range of 5–6 mM at 30 °C and at pH 7 to pH 8.2 (Dijken *et al.*, 1976; Bommarius and Karau, 2005; Ansorge-Schumacher *et al.*, 2006). For NAD^+, a half saturation constant of 50 μM was published (Ansorge-Schumacher *et al.*, 2006). The comparable values with literature data and the low error of the values obtained here permit to suppose that they are of good precision.

Even though the LB ADH is an enzyme frequently used in biocatalysis, only little data was published about the kinetic parameters of this enzyme. The very low catalytic efficiency with NADH observed here - reflected by the large value of the corresponding K_m - was however described previously. In contrast to the large catalytic efficiency with NADPH, the activity of the LB ADH with NADH is so reduced, that it was first supposed that this enzyme did not accept NADH as cofactor at all: during measurements at neutral pH no activity could be detected (Hummel, 1997). This conclusion was contradicted by Machielsen *et al.* (2009), where a K_m for NADH of 130 μM was determined at 30 °C and at pH 5.5. The K_m determined for NADH in the current project is larger by a factor 60 than the data published by Machielsen *et al.* (2009). However, these measurements were made at pH 7, and not at pH 5.5, as in the literature reference. Previous observations made by Hummel (1997) and Machielsen *et al.* (2009) showed a dramatic decrease of the LB ADH activity with increasing pH. The larger pH used in the experiments here is thus most probably the reason for the larger half saturation constant observed.

No data on the K_m for 2-octanone was found for the LB ADH. On a qualitative scale, however, it can be said that the value determined here is relatively high. In fact, a K_m of 0.85 mM was published for LB ADH for acetophenone by Hummel (1997). Acetophenone is one of the preferred *in vitro* substrates of the LB ADH, which favours prochiral ketones, with almost invariably a small methyl group as one substituents and a bulky (often aromatic) moiety as the other (Schlieben *et al.*, 2005). These observations indicate that this substance is most likely not a natural substrate of the LB ADH.

Fig. 7.6 and Fig. 7.7 illustrate how the different values of K_m and v_{max} for both enzymes determine the relative activity of the LB ADH and the CB FDH: the low K_m determined for the CB FDH for the cofactor (NAD^+), as well as the large concentrations of formate that can be added to the buffer permit to reach relatively large activities for the CB FDH. In

contrast, the LB ADH is limited by the large K_m for its cofactor (NADH) and the relatively low maximal concentration of the cofactor in the cell, as well as by the low concentrations of 2-octanone in the aqueous phase during the biotransformation. It consequently reaches only relatively low activities within the range of operational conditions considered. In fact, using a buffer with 0.3 M formate is sufficient to reach saturated conditions for formate for the CB FDH, and in that case already low concentrations of ~ 0.05 mM NAD^+ are sufficient to reach an activity larger than ~ 700 U g_{DCW}^{-1} (Fig. 7.7). This would correspond to a larger activity than the activity the LB ADH could reach if all the cofactor in the cell was present as NADH (corresponding to a concentration of ~ 1 mM NADH) and in presence of 2-octanone at its solubility limit (~ 8.6 mM) (Fig. 7.6), a substrate concentration much larger than the maximal concentration actually present in the aqueous phase during the biotransformations evaluated here (~ 1 mM). Even though the maximal reaction rate of the CB FDH is lower by a factor 4.5 than the maximal reaction rate of the LB ADH, there is thus a large probability to find reaction conditions in which the CB FDH shows larger activity than the LB ADH during the biotransformation. This point is important, because it might permit to significantly reduce the complexity of the equations necessary to represent the enzymatic transformation in the model and it should therefore be verified experimentally.

7.3.2 Expression representing the enzymatic transformation

The respective kinetics of the LB ADH and the CB FDH are both described by an ordered bi-bi mechanism given by equation 4.16 and they are linked by the concentrations of the cofactors NADH and NAD^+. To be able to integrate the correct expression for this enzymatic transformation into the model of the biotransformation, all the parameters intervening in this equation would have to be determined for both enzymes.

However, as discussed above, the large difference between the half saturation constants towards their respective cofactors indicate that the activity of the CB FDH can be larger than the activity of the LB ADH in given reaction conditions. If this was the case, the expression required to reliably describe the enzymatic transformation during the biotransformation could be significantly simplified.

To verify if the CB FDH is more active than the LB ADH in the range of operational conditions illustrated in Fig. 7.6 and Fig. 7.7, the effect of varying substrate concentrations on the apparent rate of the biotransformation was analysed. As the cofactor concentrations

cannot easily be influenced, only the effect of varying concentrations of formate and 2-octanone was investigated. These experiments should permit to determine which of the two enzymes is rate limiting in which reaction conditions.

To evaluate how the formate concentration influences the CB FDH activity in comparison to the LB ADH activity as well as the apparent rate of the biotransformation, biotransformations with varying concentrations of sodium formate in the buffer phase were performed. The 2-octanone concentration was kept constant in all the setups (600 mM 2-octanone in the ionic liquid), and the quantity of sodium formate added was always sufficiently large to avoid a limitation of the conversion of 2-octanone due to this component. The lowest formate concentration in the aqueous phase tested was therefore 0.15 M, which corresponds to an equimolar addition of co-substrate to the reaction system.

Fig. 7.8 shows no significant difference between the initial reaction rate in each of the reaction setups evaluated, independently of the formate concentration used. Nevertheless, the conversion reached in the setup with a formate concentration of 0.15 M in the aqueous phase is significantly lower than the final conversion reached in the other reaction systems. Above an initial formate concentration of 0.3 M in the aqueous phase, increasing formate concentrations do not lead to a different final conversions.

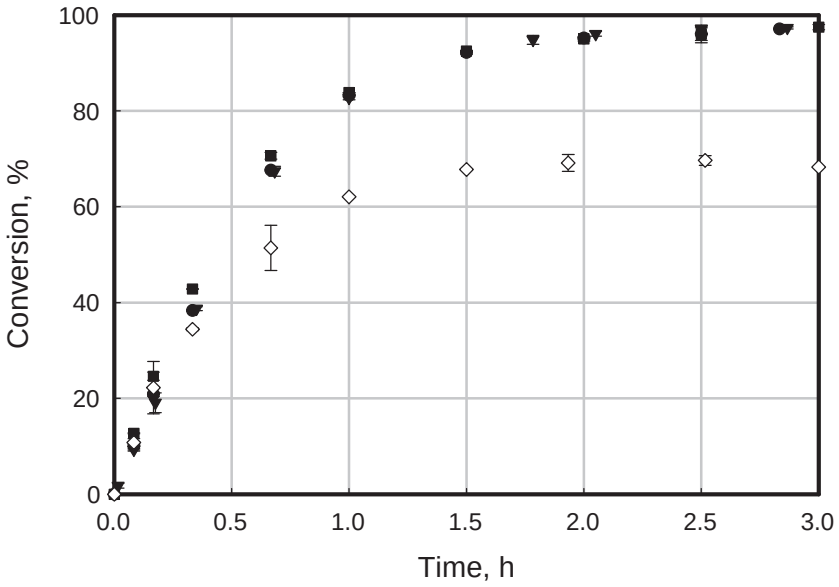

Figure 7.8: Evolution of the conversion of 2-octanone to *R*-2-octanol in 200 mL biotransformations performed with varying initial sodium formate concentrations in the aqueous phase: 0.15 M (◇), 0.3 M (■), 0.5 M (▼) and 1 M (●) sodium formate.

To verify how the 2-octanone concentration influences the LB ADH activity in comparison to the CB FDH activity as well as the apparent rate of the biotransformation, the experiments presented in subsection 6.2.1 were considered: biotransformations with varying concentrations of 2-octanone in the buffer phase were performed. Formate was added in sufficient quantities to avoid a limitation of the conversion of 2-octanone due to this component. These experiments showed an increase of the initial reaction rate with increasing 2-octanone concentration (Fig. 6.7).

Discussion

Biotransformations at varying formate concentrations in the aqueous phase permitted to indirectly observe how the formate concentration in the aqueous phase influences the apparent rate of the biotransformation: independently of the formate concentration chosen, the initial apparent rate of the biotransformation was the same in each setup. This observation can be explained by considering the K_m determined for the CB FDH (Table 7.11). At 0.15 M, the formate concentration found in the aqueous phase corresponds to a value already more than 30 times the K_m. These concentrations thus largely correspond to 'saturated' reaction conditions. Consequently, a further increase of the formate concentration will not lead to an additional increase of the CB FDH reaction rate. Independently if the CB FDH constitutes the rate limiting element or not, the apparent rate is therefore not influenced by varying formate concentrations in this range. To observe an effect on the CB FDH kinetic, the formate concentration would have had to be in a range of ~ 1 mM to 40 mM. These concentrations are however below the minimal formate concentration of at least 0.15 M necessary to avoid a limitation of the reaction by too low quantities of formate present to permit the equimolar regeneration of the cofactor.

Nevertheless, the set of experiments permitted to reach another conclusion: independently of the reaction rates, a minimal formate quantity corresponding to 0.3 M in the aqueous phase is necessary to reach the usual conversions > 95 % in a reaction system with an initial 2-octanone concentration of 600 mM in the ionic liquid. The addition of formate in equimolar quantities is not sufficient. This might be due to thermodynamic reasons (low concentration gradient between the aqueous phase and inside the cell) or due to the partitioning behaviour of formate in the biphasic reaction system.

To determine if the CB FDH is the rate limiting factor of the biotransformation, another set of experiments presented earlier can be used (subsection 6.2.1): when performing

biotransformations at varying initial 2-octanone concentrations, an increase of the apparent rate of the biotransformation with increasing initial 2-octanone concentration was observed (Fig. 6.7). If the cofactor regeneration performed by the CB FDH had been the limiting step, this observation would not have been possible. The apparent reaction rate would have been the same, independently of increasing 2-octanone concentrations. It can thus be confirmed that the CB FDH is not the limiting factor in the current process. In these conditions, its activity can be supposed larger than the activity of the LB ADH.

Based on this conclusion, the following assumptions can be made: (1) the cofactor is regenerated more rapidly by the CB FDH than it is consumed by the LB ADH, and the cofactor will thus be mostly present in its reduced form (NADH) and (2) the influence of the CB FDH kinetic on the overall transformation process can be neglected. This is important for the modelling of the reaction process, because in this case, it will be sufficient to consider the LB ADH kinetic only, instead of the coupled bi-bi mechanism of both enzymes. Moreover, if it is supposed that NADH is constantly regenerated, and at a relatively high rate, it can be supposed that almost no NAD^+ is present during the biotransformation. Similarly, the product of the transformation performed by the LB ADH - *R*-2-octanol - is constantly extracted through the aqueous phase by the ionic liquid. These two considerations indicate that a backward reaction of the LB ADH - the oxidation of the chiral alcohol to the corresponding ketone using NAD^+ as cofactor - is very unlikely and can be neglected. Consequently, the LB ADH kinetic is sufficiently well described by equation 4.17, as presented in subsection 4.4.3. The expression initially planned to be used to describe the enzymatic transformation in the model - the two coupled two-substrate ordered bi-bi mechanisms of the LB ADH and the CB FDH - is thus considerably simplified. In order to be able to use equation 4.17 in the model, the parameters indicated in Table 7.12 have to be determined.

The biocatalyst mass used is given by the biocatalyst concentration in the aqueous phase used for the biotransformation and by the volume of the aqueous phase. The specific cell volume of *E. coli* is indicated in literature (Kubitschek, 1990). The kinetic parameters needed for the simplified expression of the ordered bi-bi mechanism of the LB ADH are determined experimentally.

Table 7.12: Parameters involved in the equation used to model the enzymatic transformation in the cell, their respective symbol and determination method.

Parameters	Symbol	Determination
Biocatalyst mass, g_{DCW}	$M_{x,total}$	experimental
Specific cell volume of *E. coli*, L g_{DCW}^{-1}	v_x	experimental*
Half saturation constant of NADH, M	$K_{m\ NADH}$	experimental
Half saturation constant of 2-octanone, M	$K_{m\ 2\text{-octanone}}$	experimental
Dissociation constant of NADH, M	$K_{i\ NADH}$	experimental
Maximal rate of the forward reaction, U g_{DCW}^{-1}	v_1	experimental

* = experimental data from literature, source Kubitschek (1990)

7.3.3 Determination of the kinetic parameters of the LB ADH

According to the previous analyses, the expression of the enzymatic transformation is reliably represented by equation 4.17 for the LB ADH. To determine the corresponding parameters, initial rate experiments were performed in saturated and in non-saturated conditions. In total, 84 different sets of initial reaction conditions were evaluated and the corresponding initial reaction rates of the LB ADH was recorded. The measurments were either made photometrically or by analysis by gas chromatography, as described in subsection 5.3.2, depending on the NADH content of the assays. The range of 2-octanone and NADH concentrations evaluated were 0–7.4 mM and 0–70 mM, respectively. The kinetic parameters were then determined by non-linear regression. The resulting surface plot is shown in Fig. 7.9. The kinetic parameters obtained are indicated in Table 7.13

Table 7.13: Kinetic parameters of the *Lactobacillus brevis* alcohol dehydrogenase (LB ADH) determined at 30 °C according to equation 4.17.

Parameter	Value	Unit
$K_{i\ NADH}$	1.3 ± 0.4	mM
$K_{m\ NADH}$	5.9 ± 0.9	mM
$K_{m\ 2\text{-octanone}}$	5.7 ± 0.8	mM
v_1	5920 ± 460	U g_{DCW}^{-1}

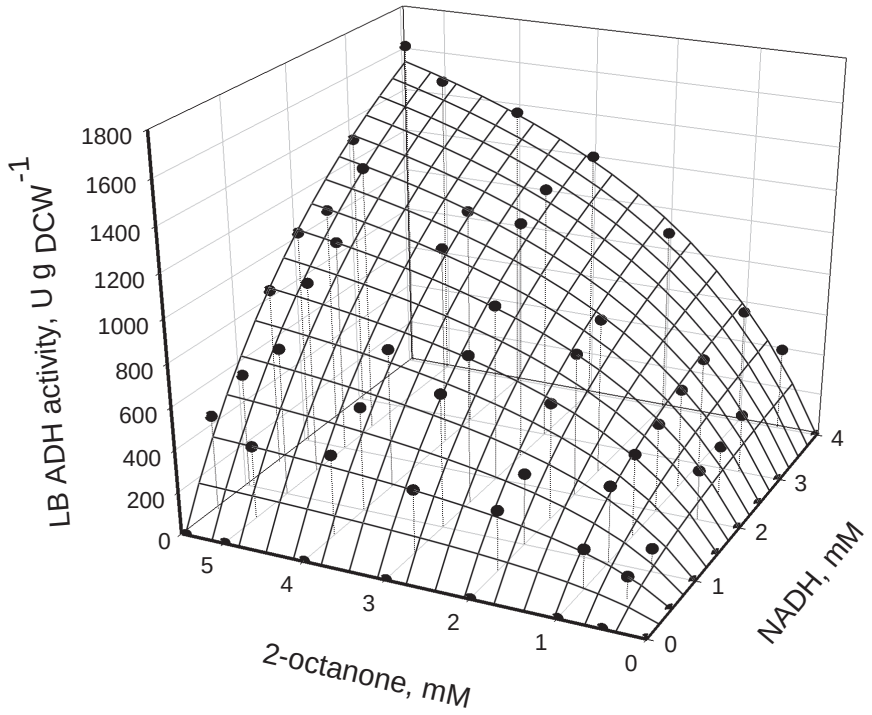

Figure 7.9: Evolution of the initial reaction rate of the LB ADH with varying initial concentrations of NADH and 2-octanone. Excerpt of the data recorded (photometric measurements only).

7.4 Experimental evaluation of the rate limiting step

The biphasic whole-cell biotransformation considered here is a sequence of several consecutive steps going from the ionic liquid to the aqueous phase, from there into the cell, where the transformation takes place, and then again from the cell through the aqueous phase, back into the ionic liquid. If it could be determined which of these steps is rate limiting, then the overall reaction rate of the biotransformation might be increased by finding a way to increase the rate of the corresponding step. Determining which step is rate limiting is therefore of interest for the process development.

For two of the five steps of the biotransformation, a set of experiments can be performed to determine if these steps are rate limiting or not: the transfers between the ionic liquid and the aqueous phase. It was shown that increasing stirrer speeds provoked an increase of the interfacial area (a_d) (Fig. 7.5). As the mass transfer between the ionic liquid and the aqueous phase is directly dependent on a_d (equation 4.30), an increase of the stirrer speed should increase the rate of this transfer, without influencing the rate of the other reaction steps. If this transfer is rate limiting, the apparent rate of the biotransformation should then also increase.

To verify this, two biotransformations were performed in exactly the same reaction conditions (20 % [HMPL][NTF], 50 g_{DCW} L^{-1} biocatalyst in the aqueous phase, 600 mM 2-octanone in the ionic liquid, room temperature), except for the stirrer speed, which was fixed to 300 min^{-1} or 600 min^{-1}. The resulting evolution of the conversion for each of the setups is shown in Fig. 7.10. There are no significant differences between both curves.

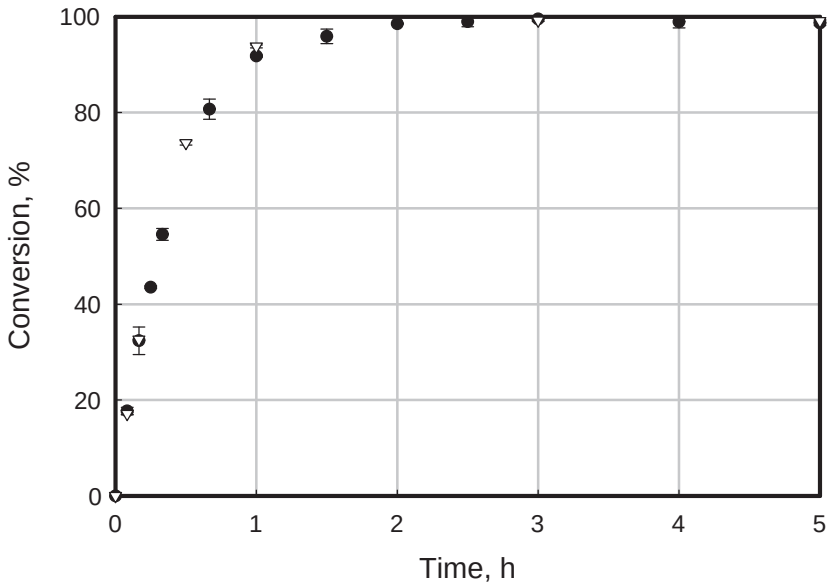

Figure 7.10: Evolution of the conversion of 2-octanone to *R*-2-octanol in 200 mL biotransformations performed at different stirrer speeds: 300 min^{-1} (●) and 600 min^{-1} (▽).

The previous experiments can be completed by another set of experiments, demonstrating a possible limitation by one of the two other mass transfers: the transfer between the aqueous phase and the cell through the cell membrane, and the enzymatic reaction. The mass transfer between the aqueous phase and the cell is dependent on the cell membrane area, and the enzymatic transformation is dependent on the enzyme concentration within the system. Both factors increase proportionally with the biocatalyst concentration. If either of these steps is rate limiting - excluding a limitation by the transfer between the ionic liquid and the aqueous phase - a decrease or an increase of the biocatalyst concentration should then produce an increase or a decrease, respectively, of the apparent rate of the biotransformation.

Three different biotransformations were performed in the same conditions (initial substrate concentration of 600 mM 2-octanone in the ionic liquid, 20 % [HMPL][NTF], stirrer rate of 600 min^{-1}), except for the biocatalyst concentration, which was fixed to 25 g_{DCW} L^{-1}, 50 g_{DCW} L^{-1} or 100 g_{DCW} L^{-1}, respectively.

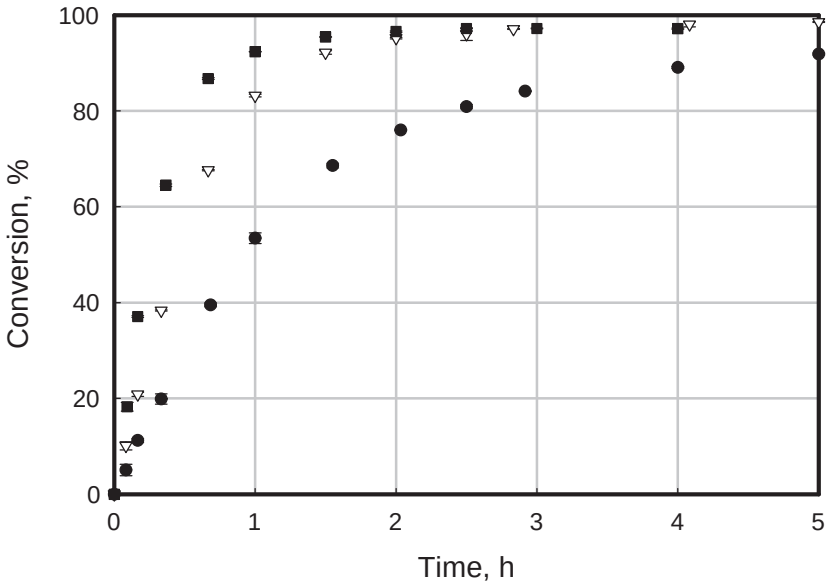

Figure 7.11: Evolution of the conversion of 2-octanone to *R*-2-octanol in biotransformations performed at different biocatalyst concentrations: 25 g_{DCW} L^{-1} (●), 50 g_{DCW} L^{-1} (▽) and 100 g_{DCW} L^{-1} (■).

The results in Fig. 7.11 show that reaction systems with larger biocatalyst concentration present larger reaction rates and reach their final conversion earlier. With an initial reaction rate of $9.4 \cdot 10^{-3}$ mmol *R*-2-octanol s^{-1} ± $0.9 \cdot 10^{-3}$ mmol *R*-2-octanol s^{-1}, the reaction system with 50 g_{DCW} L^{-1} is more rapid by exactly a factor 2 than the reaction system with 25 g_{DCW} L^{-1}, producing $5 \cdot 10^{-3}$ mmol *R*-2-octanol s^{-1} ± $1 \cdot 10^{-3}$ mmol *R*-2-octanol s^{-1}. When comparing the initial reaction rate of the reaction system with a biocatalyst concentration of 100 g_{DCW} L^{-1} to the data of the reaction system with 50 g_{DCW} L^{-1}, the ratio is not exactly identical to the ratio of the respective biocatalyst concentration, but slightly lower (1.75).

7.4.1 Discussion

When performing biotransformations at different stirrer speeds, the evolution of conversion was exactly the same in each of the setups (Fig. 7.10). Even though an increase of the stirrer speed increases the interfacial area and this variable defines the mass transfer between the ionic liquid and the aqueous phase, no increase of the apparent rate of the biotransformation was observed. Consequently, the mass transfer between the ionic liquid and the aqueous phase can be excluded as being rate limiting in the biphasic whole-cell biotransformation considered here.

This conclusion was confirmed by a second set of experiments, performing biotransformations with varying biocatalyst concentrations. Reaction systems with larger biocatalyst concentration showed larger reaction rates and reached their final conversion earlier. More precisely, at the beginning, the initial reaction rates observed in the reaction system with 25 g_{DCW} L^{-1} and 50 g_{DCW} L^{-1} differed by exactly the factor given by their respective biocatalyst concentrations, i.e. a factor of 2. This effect is lost after a short period of time, when the substrate slowly becomes limiting. The consumption of the substrate provokes a more significant decrease of the reaction rate in the more advanced system (50 g_{DCW} L^{-1}) than in the slower reaction system (25 g_{DCW} L^{-1}). The ratio between the respective conversions decreases with time until it finally reaches a value of 1 at the end of the biotransformation.
When comparing the reaction system with 100 g_{DCW} L^{-1} with the reaction system with 50 g_{DCW} L^{-1}, the ratio of their initial reaction rates is slightly lower than the ratio of the biocatalyst concentration (1.75 vs 2). This is probably due to the fact that at 100 g_{DCW} L^{-1}, the biocatalyst concentration is already in a range of values above the domain of linearity between the biocatalyst concentration and the initial reaction rate. An even further increase of the biocatalyst would not provoke a proportional increase of the reaction rate, but a lower increase. At some point, having reached the saturation domain, a still larger quantity of biocatalyst would not increase the reaction rate at all.
These experiments confirm the conclusion drawn by the previous experiments: as the apparent rate of the biotransformation increases with increasing biocatalyst concentration either the mass transfer between the aqueous phase and the cell, or the enzymatic transformation are rate limiting in this biphasic whole-cell process. The transfer between the ionic liquid and the aqueous phase can be excluded as rate limiting step.

If the transfer between the ionic liquid and the aqueous phase is not the rate limiting step, it can be supposed that this transfer occurs much more rapidly than the other reaction steps and that the concentration gradient predicted by the one-film model in the aqueous phase is so small that it can be neglected. The concentration in the bulk of the aqueous phase is then supposed the same than at the interface between both phases, equal to the equilibrium concentration defined by the partition coefficient of the compound between both phases. The one-film model used to represent the mass transfer between the two phases based on the considerations presented in subsection 7.1.4 can then be further simplified as depicted in Fig. 7.12.

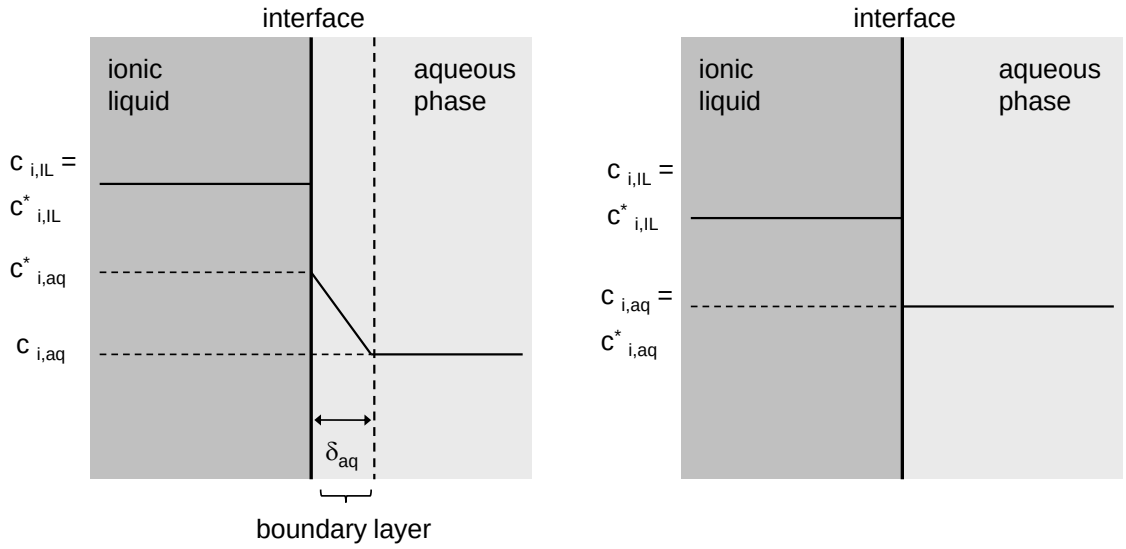

Figure 7.12: Schematic representation of the transfer between the ionic liquid and the aqueous phase: one-film model with homogeneous concentration in the ionic liquid ($c_{i,IL} = c^*_{i,IL}$) and a concentration gradient in the boundary layer formed in the aqueous phase (left) and reduced one-film model when the transfer to the aqueous phase is not rate limiting (right). The concentration gradient in the aqueous phase can then be neglected and the concentration in the bulk is equal to the concentration at the interface defined by the partition coefficient ($D_{i,\,IL/aq}$) ($c_{i,aq} = c^*_{i,aq} = c_{i,IL}/\ D_{i,\,IL/aq}$).

This also simplifies the expressions required to represent the mass transfer in the model of the biotransformation. A simple linear equation linking the concentration in the aqueous phase to the concentration in the ionic liquid by the partition coefficient of the substance will be sufficient instead of the differential equations given by equation 5.18 and equation 5.23.

After these experiments, the next step would be to evaluate whether the mass transfer between the aqueous phase and the cell or the enzymatic transformation is rate limiting. This is only possible if a means is found to observe the effect of each of the fluxes on the apparent rate of the biotransformation separately, but in the reaction conditions encountered during the biotransformation.
A first attempt to gain more information about these fluxes would be to try to uncouple them. One method to do so is by extracting the enzymes from the cell, thereby eliminating the resistances to the fluxes caused by the membrane transfer, and then record the enzyme activity. If the activity observed was larger than the apparent rate of the biotransformation recorded when using the whole-cell biocatalyst, then this step could be excluded as rate limiting step. The drawback of this relatively simple method is that the extraction of

the enzymes from the cell does not permit to reproduce the reaction conditions as they are found within the whole cell during the biotransformation, especially concerning the cofactor concentrations. The reaction conditions would thus not be comparable, and the activities measured for the cell lysate would not permit to draw any reliable conclusions. A second method would be to try to distinguish between both fluxes in the biphasic whole-cell setup by trying to influence one of the two fluxes without influencing the other. A simple increase of the biocatalyst concentration as shown in Fig. 7.11 influences both fluxes and consequently does not lead to additional information. Instead, two different biocatalyst batches with cells of the same membrane area, but with different enzyme concentrations would have to be used. Unfortunately, the task is made more difficult by the presence of two enzymes: the concentration of only one of the two enzymes would have to be varied, while keeping the other constant. Cultivating the biocatalyst to satisfy these strict requirements was not successful in this project. A further distinction between the enzymatic transformation and the mass transfer between the aqueous phase and the cell was therefore not possible here.

7.5 Modelling and simulation

The goal of the previous sections was not only to better understand the reaction process under consideration, but also to identify the correct expression representing each step of the biotransformation to build a model of the biphasic reaction system. In the preceding parts, the considerations relative to each type of mass transfer - i.e. the transfer between the ionic liquid and the aqueous phase, the transfer between the aqueous phase and the cell and the enzymatic transformation - were presented. The most important points were:

1. Concerning the mass transfer between the ionic liquid and the aqueous phase (section 7.1 and section 7.4):
    - The mass transfer coefficient of the substrate and the product (β) appearing in the one-film model used to describe the mass transfer between the ionic liquid and the aqueous phase could not be estimated reliably. The empirical correlations at disposal led to values too low to be consistent with the experimental observations made.
    - It could however be shown experimentally that the mass transfer between these two phases is not rate limiting. The concentration gradient in the aqueous phase can thus be neglected and the concentrations in both the ionic liquid and the aqueous phase can be considered homogeneous. The two phases are consequently supposed to be in constant equilibrium.
2. Concerning the mass transfer between the aqueous phase and the cell (section 7.2):
    - The membrane permeability of the substrate and the product cannot be determined experimentally nor estimated using a correlation. These parameters are thus identified by fitting the model to experimental data. Due to the very similar properties of the substrate and the product, it is supposed that their membrane permeability is the same ($P_S = P_P = P$).
3. Concerning the enzymatic transformation inside the cell (section 7.3):
    - It could be shown that the cofactor regeneration by the CB FDH is not rate limiting when the formate concentration is larger or equal 300 mM in the aqueous phase.

- In these conditions, the kinetic of the biotransformation is sufficiently well described by the LB ADH kinetic alone. Moreover, the ordered bi-bi mechanism of the LB ADH given by equation 4.16 is simplified to equation 4.17. NAD^+ is indeed constantly transformed to NADH and *R*-2-octanol is constantly extracted by the ionic liquid, so that the backward reaction of the LB ADH can be neglected.

On basis of these considerations, the set of equations necessary to describe the reaction system (presented in subsection 5.9.1) is simplified. The fluxes J_1 and J_5 are eliminated, while the fluxes J_2 to J_4 are described by equation 7.1 to equation 7.3.

$$J_2 = P \cdot \frac{A_{x,total}}{V_{x,total}} \cdot 10^3 \cdot \left(\frac{C_{S,IL}}{D_{IL/aq,S}} - C_{S,cell}\right) \tag{7.1}$$

$$J_3 = \frac{M_{x,total}}{V_{x,total}} \cdot \frac{v_{max} C_{NADH} C_{S,cell}}{K_{iNADH} K_{mS} + K_{mS} C_{NADH} + K_{mNADH} C_{S,cell} + C_{NADH} C_{S,cell}} \tag{7.2}$$

$$J_4 = P \cdot \frac{A_{x,total}}{V_{x,total}} \cdot 10^3 \cdot \left(C_{P,cell} - \frac{C_{P,IL}}{D_{IL/aq,P}}\right) \tag{7.3}$$

$$A_{x,total} = a_x \cdot M_{x,total} \tag{7.4}$$

$$V_{x,total} = v_x \cdot M_{x,total} \tag{7.5}$$

$$M_{x,total} = c_x \cdot V_{aq} \tag{7.6}$$

The expressions given by equation 7.1 to equation 7.6 are only valid under the condition that the concentrations in the ionic liquid, in the aqueous phase and within the cells are homogeneous. There are no local concentration gradients.

The mass balances giving the evolution over time of the substrate and the product concentrations in the ionic liquid and inside the cells are then defined by equation 7.7 to equation 7.10. The simultaneous integration of these four differential equations gives the

evolution of $C_{S,IL}$, $C_{S,cell}$,$C_{P,cell}$ and $C_{P,IL}$ with time during the biotransformation. The concentration of the substrate and the product in the aqueous phase ($C_{S,aq}$ and $C_{P,aq}$) are then calculated on basis of $C_{S,IL}$, $C_{P,IL}$ and the partition coefficients of the substrate and the product (equation 7.11 and equation 7.12). These six equations form the new set of equations used to describe the reaction system under investigation.

$$\frac{dC_{S,IL}}{dt} = -J_2 \cdot \frac{V_{x,total}}{V_{IL} + \frac{V_{aq}}{D_{IL/aq,S}}} \tag{7.7}$$

$$\frac{dC_{S,cell}}{dt} = J_2 - J_3 \tag{7.8}$$

$$\frac{dC_{P,cell}}{dt} = J_3 - J_4 \tag{7.9}$$

$$\frac{dC_{P,IL}}{dt} = J_4 \cdot \frac{V_{x,total}}{V_{IL} + \frac{V_{aq}}{D_{IL/aq,P}}} \tag{7.10}$$

$$C_{S,aq} = \frac{C_{S,IL}}{D_{IL/aq,S}} \tag{7.11}$$

$$C_{P,aq} = \frac{C_{P,IL}}{D_{IL/aq,P}} \tag{7.12}$$

7.5.1 Identification of the membrane permeability of 2-octanone and *R*-2-octanol

Using all the parameters determined above, the model of the biphasic whole-cell reaction system is given by the integration of equation 7.7 to equation 7.10. The variables of the model are the concentrations of the substrate and the product in the ionic liquid, in the aqueous phase and in the cell. The integration was made using an ode15s solver in MATLAB (The MathWorks, Inc.). The membrane permeability coefficient (P) of the substrate and the product was determined by fitting the model to experimental data recorded. This data is the evolution of the substrate and the product concentrations in the ionic liquid during the biotransformation.
As the membrane permeability is a biological property, it should be relatively constant independently of the reaction conditions used. Therefore, the membrane permeability should be identified on basis of several different sets of reaction conditions. The aim is to avoid that the identified value only fits one specific biotransformation and make the identification as reliable as possible. However, this not only means that several sets of data should be considered, but also that only those should be considered for which the model established accounts. Otherwise, the result of the identification process will also be flawed. As an inactivation of the biocatalyst is not included in the model, reaction conditions provoking a significant decrease of the biocatalyst activity should not be included. Consequently, only biotransformations with an ionic liquid volume fraction up to 40 % and with initial substrate concentrations up to ~ 600 mM 2-octanone in the ionic liquid were considered. These are the ranges of concentration and phase ratios that showed no or only a very low inactivation of the biocatalyst in comparison to the best performing reaction system (subsection 6.2.1 and subsection 6.2.2).

For the fitting, a global search method was used over the range of 10^{-12} m s^{-1} to 1 m s^{-1} with a step of 80 values per decade. The code used to this aim is presented in the appendix (section H). Nine different sets of biotransformation data were simultaneously fitted, each composed of seven values for the evolution of the substrate concentration and seven values for the evolution of the product concentration in the ionic liquid with time.

While varying the membrane permeability over the range of values indicated above, the resulting sum of the squared errors (SSE, equation 5.24) was calculated for each set of data and over the nine sets of reaction conditions fitted. The evolution of the SSE as a function of P is shown in Fig. 7.13. It shows a global minimum of the SSE recorded, which corresponds to the value of P best fitting all the different data sets simultaneously. The

value of P identified as giving the minimum SSE between the measured and the simulated substrate and product concentrations in the ionic liquid is indicated in Table 7.14.

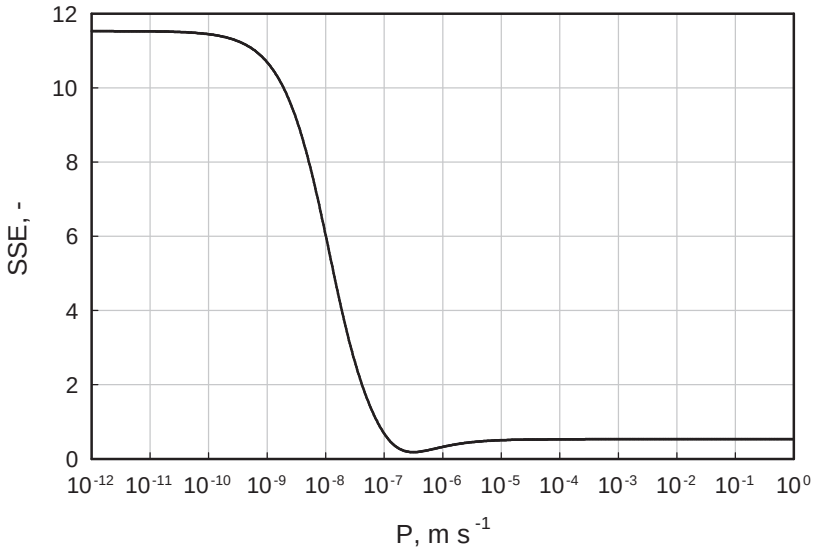

Figure 7.13: Sum of the squared errors (SSE) as a function of the membrane permeability (P).

Table 7.14: Identified value of the membrane permeability (P).

Parameter	Identified value, m s^{-1}
P	$3.16 \cdot 10^{-7}$

Fig. 7.14 shows the simulated *versus* the real evolution of conversion with time for four different biotransformations resulting from the fitting process ($P = 3.16 \cdot 10^{-7}$ m s^{-1}). While the simulated conversion of reaction systems with 20 % ionic liquid and initial substrate concentrations around 300–400 mM are in very good agreement with the experimental data, much larger initial substrate concentrations such as 670 mM and to a larger extent increased ionic liquid volume fractions of 30 % lead to an overestimation of both the reaction rate and the final conversion.

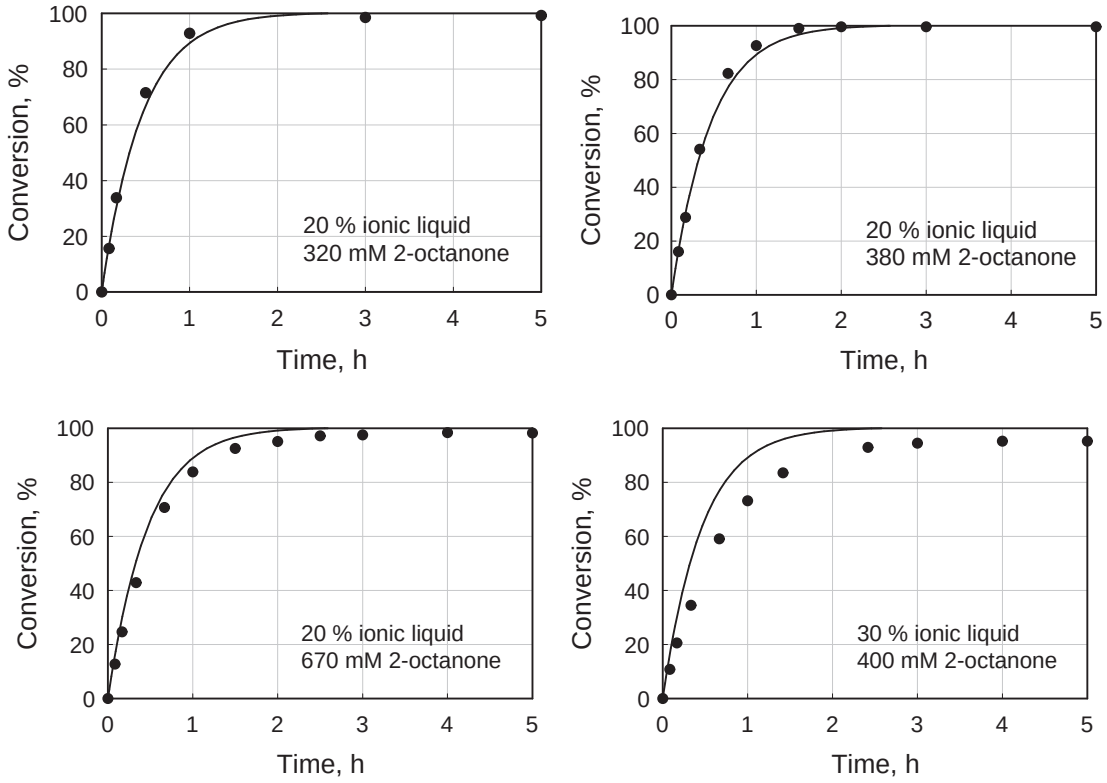

Figure 7.14: Simulated conversion (—) vs. real conversion (●) for biotransformations performed in different reaction conditions: 20 % ionic liquid and initial substrate concentrations of 320 mM, 380 mM and 670 mM 2-octanone in the ionic liquid, and 30 % ionic liquid and an initial substrate concentration of 400 mM 2-octanone in the ionic liquid.

Discussion

The evolution of the SSE as a function of the membrane permeability showed one local minimum, corresponding to the value of P best fitting the model to the sets of experimental data. With a value of $3.16 \cdot 10^{-7}$ m s^{-1}, the identified membrane permeability of 2-octanone and 2-octanol is almost one order of magnitude lower than the values indicated for ethanol ($1.4 \cdot 10^{-6}$ m s^{-1}) by Nielsen and Villadsen (1994). A larger value than for this small molecule was expected, because larger size leads to relatively lower membrane permeability. A more precise quantitative comparison is difficult due to the paucity of available data.

When comparing the real evolution of the conversion to the evolution of the conversion predicted on basis of the identified membrane permeability, most of the simulated data sets were in good to very good agreement with the experimental data. The model predicted the outcome of reaction conditions of 20 % ionic liquid and initial substrate concentrations up to 400 mM very well. When much larger initial substrate concentrations were considered,

a slight deviation was observed: the predicted evolution of conversion is slightly too rapid after 20 min reaction duration, but the final conversion is still predicted with relatively good precision. A more significant difference between the experimental and the simulated data was observed when the ionic liquid volume fraction was increased. Here, the model led to a clear overestimation of both the reaction rate and the final conversion. These observations show the limits of the current model: as it does not include the inactivation of the biocatalyst, reaction conditions provoking such a decrease in the bicoatalyst activity cannot be modelled very reliably. Even though this could not be concluded in the previous experiments (subsection 6.2.2), Fig. 7.14 indicates that an inactivation of the biocatalyst is already taking place at 30 % ionic liquid in significant amounts.

The reason why the inactivation of the biocatalyst by large concentrations of toxic substrate and/or product or by large ionic liquid volume fractions could not be included into the model, here, is that to date no mechanistic expression for this phenomenon exists. The exact mechanism of action of the ionic liquid and the substrate and the product towards the biocatalyst is not yet fully elucidated, nor is a quantitative description of the loss of activity due to these substances at disposal. An attempt to account for these observations by a simple first-order inactivation mechanism was made, but the resulting simulation did not reliably predict the reaction outcome either (data not shown). For these complex interactions, a more sophisticated mechanism is needed.

7.5.2 Simulations with the identified parameters

The identification of the membrane permeability permits to use the model to simulate the biphasic whole-cell biotransformation. Such a simulation is not only of large interest, because it permits to estimate the outcome of a given reaction without having to perform the corresponding experiment, but also because it gives access to information which is not or cannot be accessed experimentally, e.g. the evolution of the substrate and product concentrations within the cell. Using the value identified for P, the results of a simulation for reaction conditions of 20 % ionic liquid and an initial substrate concentration of 380 mM are exemplarily shown in Fig. 7.15.

The 2-octanone concentration in the ionic liquid takes its maximal value at the beginning (t =0), and then decreases exponentially until reaching ~ 0 mM. The simulation of the 2-octanone concentration in the aqueous phase shows a very sharp increase immediately after the start of the reaction. Then, it decreases from its maximal value (~ $3 \cdot 10^{-4}$ M)

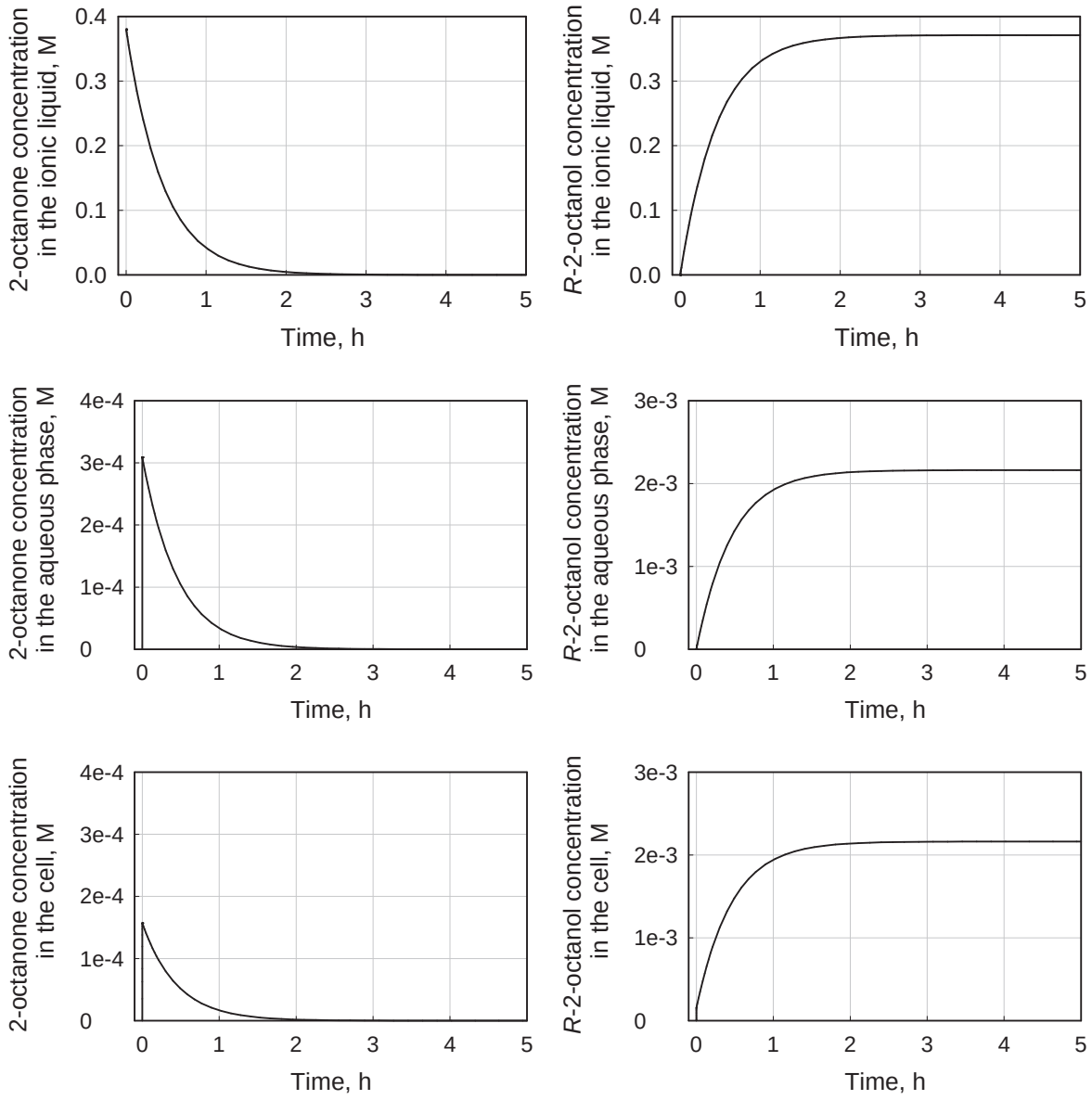

Figure 7.15: Simulated evolution of the substrate (2-octanone, left) and the product (*R*-2-octanol, right) concentrations in the ionic liquid (top), the aqueous phase (middle) and in the cell (bottom) using the identified parameter ($P = 3.16 \cdot 10^{-7}$ m s^{-1}). The biotransformation was simulated in the following reaction conditions: an initial substrate concentration of 380 mM 2-octanone, a biocatalyst concentration of 50 g_{DCW} L^{-1}, and 20 % ionic liquid ([HMPL][NTF]).

exponentially until reaching a value of ~ 0 mM. With a delay of less than 0.1 sec, the same very rapid increase is observed for the cell-internal 2-octanone concentration, followed by an exponential decay. Its maximal value is however slightly lower (~ $1.5 \cdot 10^{-4}$ M).
The simulation of the *R*-2-octanol concentrations within the cell, in the aqueous phase and in the ionic liquid show very similar patterns: only fractions of a second after the beginning, the product concentration starts to increase within the cell, and with a minimal

delay also in the aqueous phase and in the ionic liquid. Over time, the increases of the *R*-2-octanol concentration in the cell, in the aqueous phase and in the ionic liquid slowly reduce until reaching an equilibrium concentration of ~ $2.16 \cdot 10^{-3}$ M inside and outside the cell and of ~ 0.37 M in the ionic liquid.

Discussion

On basis of the identified parameter, the model made it possible to simulate the evolution of the substrate and the product concentrations inside the cell and in the aqueous phase. This is interesting supplemental information, as the techniques available do not permit to monitor the concentrations inside the biocatalyst.

Initially, the substrate is only present in the ionic liquid. The 2-octanone concentration in the ionic liquid is therefore maximal at t = 0, and zero in the aqueous phase and within the cell. The sharp increase of the 2-octanone concentration in the aqueous phase at the beginning of the simulation is what was expected to be observed. In fact, t = 0 corresponds to the moment where the ionic liquid and the aqueous phase are brought into contact, leading to a very rapid establishment of the thermodynamic equilibrium. The maximal value reached by this variable is consequently defined by the partition coefficient of the substrate between the ionic liquid and the aqueous phase ($D_{IL/aq,\ 2\text{-octanone}} = 1230$), corresponding for a 2-octanone concentration of 0.38 M in the ionic liquid to the ~ $3 \cdot 10^{-4}$ M observed in the aqueous phase. From the aqueous phase, the substrate directly diffuses into the cell, where it is transformed to *R*-2-octanol. As a consequence, the 2-octanone concentration in the aqueous phase decreases immediately, and the same sharp increase of the 2-octanone concentration is observed in the cell, with a minimal delay, before it starts decreasing due to the enzymes' activity. Simultaneously, the product concentration inside the cell increases. Some of the product directly diffuses from the cell into the aqueous phase, where the 2-octanol concentration also increases. Finally, the substrate concentration outside and inside the cell fall to ~ 0 mM, whereas the product concentrations reach their maximum in the different compartments of the reaction system. The final values of the product concentrations are defined by the thermodynamic equilibria between the cell and the aqueous phase - leading to identical concentrations of $2.16 \cdot 10^{-3}$ M - and between the aqueous phase and the ionic liquid - leading to a product concentration of 0.37 M in the ionic liquid, as determined by the partition coefficient of the product in these two phases ($D_{IL/aq,\ 2\text{-octanol}} = 172$).

7.5.3 Sensitivity analysis

To determine how sensitive the response of the model is with respect to the value taken by the parameters of interest (P), different scenarios were simulated, varying the membrane permeability by ± 10 % and ± 20 % of the identified value given in Table 7.14. The resulting SSEs were then compared to the SSE obtained in the reference condition (Fig. 7.16).

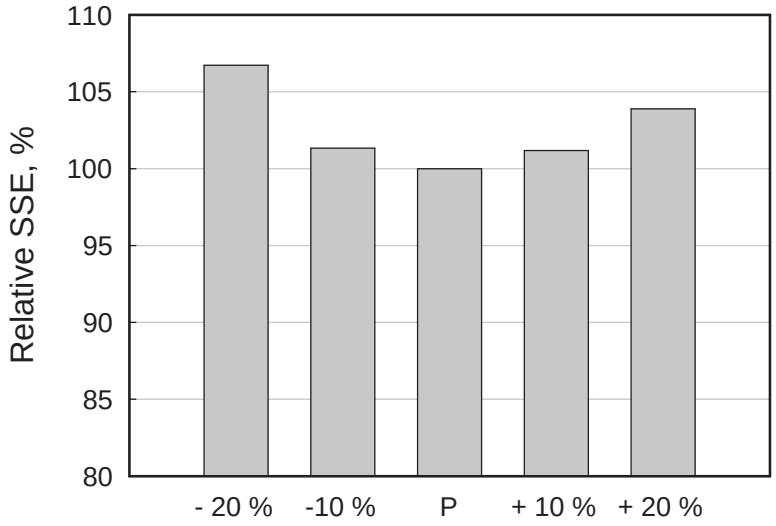

Figure 7.16: Sensitivity analysis: relative sum of the squared errors (SSE) for simulations with varying membrane permeability (P). The error resulting from simulations using values of P ± 10 % and ± 20 % were evaluated and compared to the reference, where $P = 3.16 \cdot 10^{-7}$ m s^{-1}.

When varying the membrane permeability P by up to ± 10 %, the resulting SSE varies by 1.3 % and 1.2 % for a decrease and an increase by 10 %, respectively. A decrease or an increase of P by 20 % provokes a larger deviation of the error. The decrease of P by 20 % leads to an increase of the SSE of 6.7 % and an increase of P by 20 % leads to an increase of 3.9 %.

Discussion

When varying the membrane permeability by 10 % around the value identified, the resulting SSE varies only by little more than 1 %. The model is thus not very sensitive within this range of values. However, a variation of P by 20 % influences the outcome more strongly. Overall, the deviations observed are more significant for decreased values of P than for larger values than the identified value of P. This is in accordance with Fig. 7.13, where the slope of the evolution of the SSE with P is larger towards smaller values than towards larger values of P.

The relatively low sensitivity of the model towards variations as large as 10–20 % is partially due to the large number of data sets on basis of which P was identified. As these are relatively different, the simultaneous fitting of the nine data sets is one of the reasons why the minimum in the SSE observed is within a relatively large 'valley' (Fig. 7.13).

7.5.4 Evaluation of the rate limiting step on basis of the model

The previous sections presented several reasons why the availability of a model of the biotransformation is useful and advantageous: the model permitted to identify the membrane permeability and it can be used to simulate the outcome of the biotransformation over a relatively large range of reaction conditions making time and resource intensive experiments unnecessary. It also confers additional information, such as the evolution of the substrate and product concentrations within the cell, which is data that not available experimentally. In addition to this, however, it also allows to calculate the different mass fluxes because now all the parameters - including the membrane permeability - as well as the evolution of the six variables - the substrate and product concentrations in the ionic liquid, the aqueous phase and in the cell - over time are known.

However, a point of larger interest than the mere evolution of these fluxes would be to determine which is the rate limiting step of the biotransformation. As described in section 7.4, an experimental determination alone was not successful. It only permitted to exclude the mass transfer between the ionic liquid and the aqueous phase, because the parameters determining the transfer between the aqueous phase and the cell (i.e. the membrane area) and the enzymatic transformation (i.e. the enzyme activity within the cell) could not be influenced independently. Using the model, this would be possible by a simple variation of the parameters indicated in the respective equations. Observing the evolution of the apparent rate of the biotransformation while artificially increasing the different fluxes one at a time might then permit to determine which step is rate limiting and which is not.

To this aim, first the membrane area in equation 7.1, then the maximal reaction rate of the enzyme in equation 7.2 and finally the membrane area in equation 7.3 were increased by a factor 4. The effect of these variations on the apparent rate of the biotransformation was determined by observing the resulting conversion, shown in Fig. 7.17.

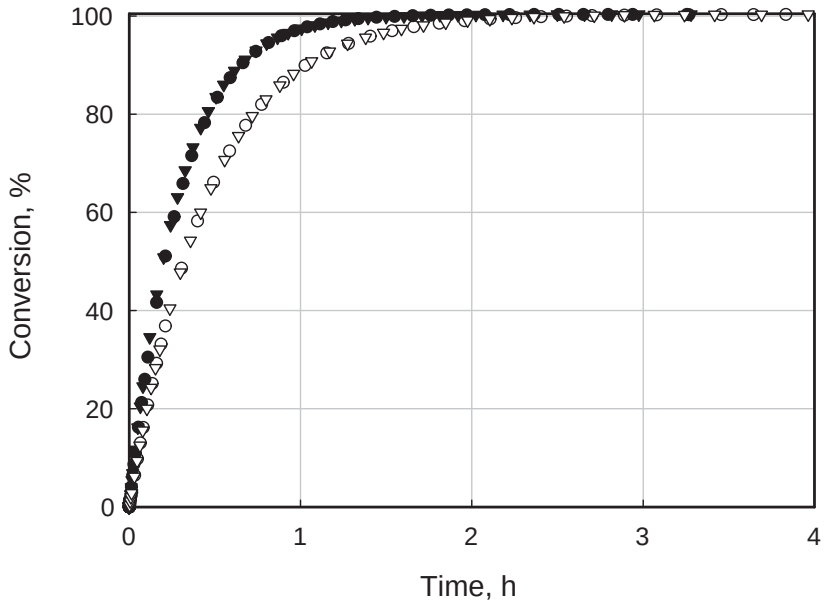

Figure 7.17: Evolution of the conversion when introducing a factor 4 into the equations representing the transfer of the substrate from the aqueous phase to the cell (●), the enzymatic reaction (▼) or the transfer of the product from the cell to the aqueous phase (▽), in comparison to the reference simulation using the real values of the different parameters and the correct expressions for the different fluxes (○).

In comparison to the reference simulation, which was performed using the real values of the membrane area and the maximal reaction rate of the enzymes and which is in accordance with the experimental data, an increased apparent rate of the biotransformation is observed when increasing the membrane area in equation 7.1 and when increasing the maximal reaction rate in equation 7.2. However, when increasing the membrane area in equation 7.3, the apparent rate is the same than in the reference simulation.

Discussion

When increasing the membrane area by a factor 4 in equation 7.3, the apparent rate of the biotransformation did not increase. This artificial initial acceleration of the flux of product from the cell into the aqueous phase did not have any effect on the overall rate, and this step can thus be excluded from being the rate limiting step.

Considering the other two fluxes - the transport of the substrate from the aqueous phase into the cell and the transformation of the substrate to the product - a clear increase of the reaction rate was observed when increasing the membrane area and the maximal reaction rate of the enzymes, respectively, by a factor 4. This would mean that both steps seem

to be rate limiting. Usually it is considered that only one step can be rate limiting, and then the other steps of the reaction are not. However, a further distinction between the effect of an increase of one of these two fluxes on the apparent rate and the effect of an increase of the other is not possible based on these simulations. Indeed, an increase of one of them will always directly influence the other: when the flux of substrate into the cell (J_2, Fig. 5.6) is artificially increased, e.g. by increasing the membrane area, more substrate will be available for the enzymatic transformation, and consequently this flux (J_3) will also increase. Inversely, when the enzymatic transformation (represented by J_3) is accelerated, e.g. by artificially increasing the maximal reaction rate, then the concentration gradient between the substrate outside and inside the cell will be increased because the substrate is consumed more rapidly within the cell, and consequently the flux (J_2) into the cell will also be increased.

The reason why the effect of the transport of the product from the cell to the aqueous phase can be observed separately from the other two fluxes is (1) because the backward reaction of the enzymatic transformation is neglected due to the very rapid regeneration of the cofactor to NADH, and (2) because no product inhibition was observed within the range of concentrations considered here. The product concentration within the cell is supposed to leave the enzymatic reaction unaffected. This variable is thus not intervening in the expression of the enzymatic transformation used in the model, and therefore the enzymatic reaction is not affected by an increase of the transport rate of the product from the cell to the aqueous phase (equation 7.2). This permits to draw the conclusion presented above considering this flux and its non-rate limiting nature.

8 Recycling of the ionic liquid and the biocatalyst

The previous chapters, as well as the constantly increasing number of publications on the subject showed that the use of ionic liquids as second phase in biphasic whole-cell biocatalysis can lead to very satisfying results in terms of conversion and selectivity. In contrast to organic solvents, the use of ionic liquids in processes necessitating a biphasic reaction mode avoids many security issues related to the large volatility and flammability of organic solvents. Nevertheless, there is no industrial application of ionic liquids in whole-cell biocatalysis to date. The main reason for this is the still large cost of these solvents. Estimations indicate that ionic liquids are currently available on average at a price of a few hundred € per kg (Wasserscheid and Welton, 2003). However, even if the costs further decrease to the expected price of 50 € per kg when produced at the ton scale, they will still be significantly more expensive than commonly used organic solvents, such as MTBE (currently ~ 38 € per kg at volumes of 2.5 L, source Carl Roth GmbH). The comparatively large cost of ionic liquids mean that a process involving these solvents is currently only competitive if the ionic liquid is recycled and reused as many times as possible. Similarly, a recycling of the biocatalyst might even further reduce the process costs. These two points are therefore further investigated in this chapter.

8.1 Recycling of the ionic liquid

The recyclability of the ionic liquid [HMPL][NTF] was evaluated by using the same ionic liquid batch during 25 of the following cycles: (1) a biotransformation was performed at the 200 mL scale in the optimised reaction conditions determined in subsection 6.2.3, followed by (2) the phase separation by centrifugation and (3) the product isolation and ionic liquid purification by distillation (Fig. 8.1).

The ionic liquid can only be considered recyclable if two conditions are satisfied during its repeated use:

1. It must be guaranteed that the productivity of the reaction involved is not affected by the recycling procedure.

2. It is therefore essential that no substances harming or inhibiting the biocatalyst are accumulating over time and that the ionic liquid is not degraded during the process.

These points were investigated by monitoring the conversion reached in the biotransformations, as well as the composition of the ionic liquid during 25 subsequent process cycles using the same ionic liquid batch.

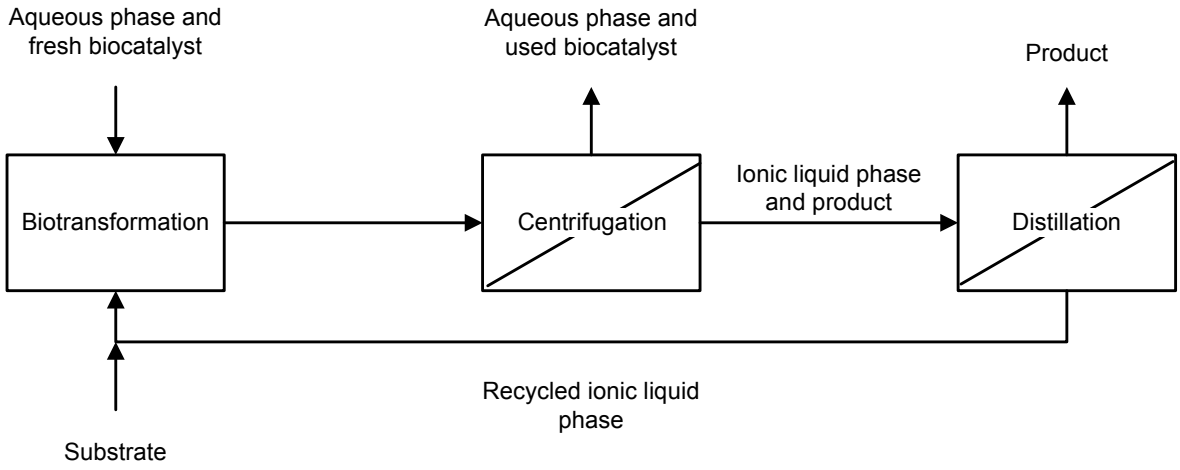

Figure 8.1: Scheme of the process integrated whole-cell biocatalysis in biphasic ionic liquid/water systems with recycling of the ionic liquid phase.

8.1.1 Conversion and selectivity during the recycling process

Based on the previous results (subsection 6.2.3), the reaction conditions were set to a volume fraction of 20 % [HMPL][NTF] and an initial substrate concentration of 300 mM 2-octanone in the ionic liquid phase. Samples were taken before, after and during the biotransformation to monitor the evolution of the conversion and the enantioselectivity during the process.

Fig. 8.2 shows the conversion reached in each of the biotransformations after a reaction time of 5 h, as well as the corresponding enantiomeric excess. It can be seen that there was no significant variation of the final conversion reached over the 25 biotransformations. On average, the conversion reached was 98.5 % ± 0.7 %. In each biotransformation, the enantiomeric excess was constantly ≥ 99.5 % (*R*). Over the 25 cycles, a total of 999 g ± 6 g *R*-2-octanol L_{IL}^{-1} were formed.

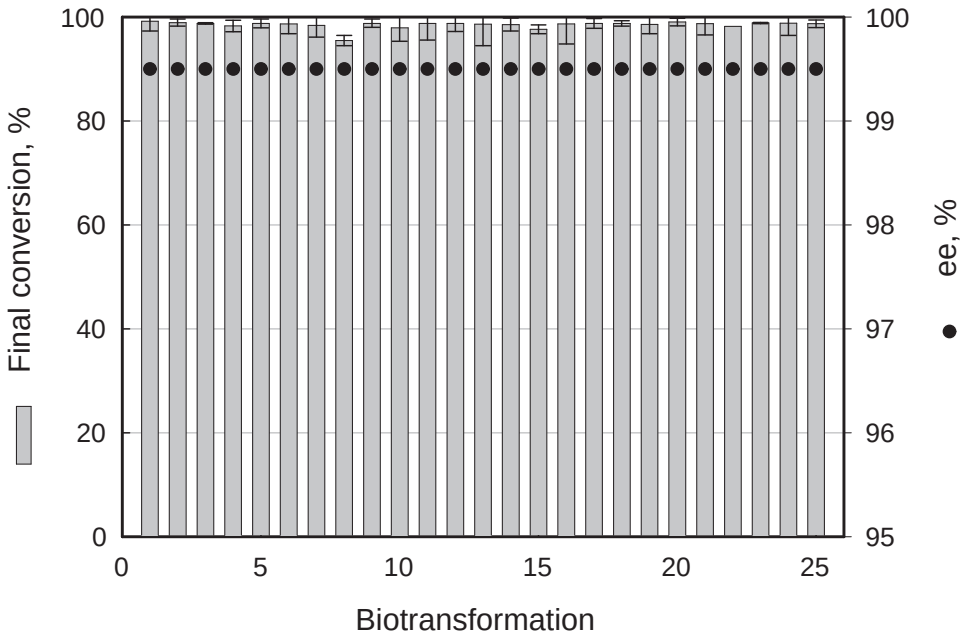

Figure 8.2: Final conversion reached after 5 h reaction time by each biotransformation throughout 25 cycles. The enantiomeric excess was ≥ 99.5 % (*R*) over the whole duration of each biotransformation.

8.1.2 Recovery yield and quality of the recovered ionic liquid

After the biotransformation, the emulsion formed during the reaction was very neatly and efficiently separated into its individual components by centrifugation (5 min, 2500 g, room temperature) (Fig. 8.3).

Figure 8.3: Emulsion before (left) and after (right) the phase separation by centrifugation. The centrifugation permits to completely separate the emulsion into its three composing phases: the aqueous phase (top phase), the cells (middle phase) and the ionic liquid (bottom phase).

The ionic liquid was isolated from the rest of the system components (biocatalyst and aqueous phase) and introduced into the rotary evaporator to isolate the product. After this, the ionic liquid was reused in the next biotransformation. The recovery yield of ionic liquid at each cycle was on average 82.8 % ± 0.8 % .

The quality of the recovered ionic liquid was verified after each process cycle. The analyses made by ion chromatography did not show significant amounts of the considered anions (F^-, Cl^-, Br^- and PO_4^{3-}) and cations (Ca^{2+}, K^+, Mg^{2+}, Na^+, and NH_4^+) in the ionic liquid samples. Throughout all the samples taken over the 25 cycles, the concentrations were generally below 20 ppm (anions) (Table 8.1) and 50 ppm (cations) (Table 8.2).

Table 8.1: Analysis of the ionic liquid samples taken after each process cycle by ion chromatography: bromide (Br^-), chloride (Cl^-), fluoride (F^-) and phosphate (PO_4^{3-}) content (excerpt of the data collected).

Cycle number	Br^-	Cl^-	F^-	PO_4^{3-}
2	< 5 ppm	< 5 ppm	< 5 ppm	n.d.
6	n.d.	< 5 ppm	< 5 ppm	n.d.
10	n.d.	< 5 ppm	< 5 ppm	n.d.
14	< 5 ppm	< 20 ppm	< 5 ppm	n.d.
18	n.d.	< 5 ppm	< 5 ppm	n.d.
22	< 5 ppm	< 20 ppm	< 5 ppm	n.d.

n.d. = not detected

Table 8.2: Analysis of the ionic liquid samples taken after each process cycle by ion chromatography: ammonium (NH_4^+), calcium (Ca^{2+}), magnesium (Mg^{2+}), potassium (K^+) and sodium (Na^+) content (excerpt of the data collected).

Cycle number	NH_4^+	Ca^{2+}	Mg^{2+}	K^+	Na^+
2	< 5 ppm	n.d.	n.d.	< 30 ppm	< 5 ppm
6	< 5 ppm	< 30 ppm	n.d.	< 50 ppm	< 5 ppm
10	n.d.	< 40 ppm	n.d.	n.d.	n.d.
14	n.d.	n.d.	n.d.	n.d.	n.d.
18	n.d.	< 30 ppm	n.d.	< 40 ppm	n.d.
22	n.d.	n.d.	n.d.	n.d.	n.d.

n.d. = not detected

Similarly, the analyses by ^{1}H NMR did not show any significant variations in the spectra recorded (appendix, Fig. I.1 and Fig. I.2).

8.1.3 Product recovery and final product purity

In non-optimized conditions (5 h, 130 °C, < 5 mbar), the distillation enabled on average the recovery of 91 % ± 4 % of the product contained in the ionic liquid phase after the biotransformation at each cycle. The average purity of the recovered product was 97 % ± 3 %.

8.1.4 Discussion

During the 25 subsequent process cycles, no significant loss of productivity occurred due to the repeated use of the same ionic liquid batch. In fact, no substantial variations of the conversion and the selectivity were observed over the 25 biotransformations performed with the same ionic liquid batch (Fig. 8.2). In addition, the analyses of the ionic liquid samples by ion chromatography and ^{1}H NMR did not show any signs of decomposition, neither for the anion nor for the cation constituting the ionic liquid. If there had been a decomposition of the cation, the ^{1}H NMR spectra obtained for different ionic liquid samples would have shown different peaks as the number of process cycles increased. Similarly, if there had been a degradation of the anion, the analyses by ion chromatography would have shown an increasing concentration of fluoride anions gradually accumulating in the ionic liquid phase. A degradation of the ionic liquid during the process can thus be excluded. Considering these two facts, it can be confirmed that [HMPL][NTF] is recyclable over at least 25 cycles.

As the recycling experiments presented are relatively time intensive, the set of experiments was stopped after 25 process cycles. However, as there is no indication of negative consequences of the recycling of this ionic liquid on the process at all, this ionic liquid could most likely be reused during an even larger number of cycles.

With a recovery yield of slightly more than 80 %, not all the ionic liquid could be recovered at each cycle. Considering that the process is in fact almost a closed circuit, except for the aqueous phase and the used biocatalyst being discarded, this loss seems considerable. However, almost half of the loss observed is due to sampling (~ 9.5 % of the total initial ionic liquid volume in a reaction setup with an ionic liquid volume fraction of 20 %), and the rest of it mostly occurs during the transfer of the solvent from one recipient to the other

in between the different process steps (not quantified). The volume lost is consequently greatly dependent on the scale of the process. The recovery yield could therefore most probably be significantly increased at larger scale and at relatively lower sampling volume and frequency.
Due to the large hydrophobicity of the solvent, the ionic liquid effectively lost in the aqueous phase - discarded after each cycle and replaced by fresh buffer - is almost not significant. It constitutes only 0.57 % of the total ionic liquid volume used in a reaction setup with an ionic liquid volume fraction of 20 %.
Some ionic liquid is probably also lost with the biocatalyst. It was indeed shown that ionic liquids containing relatively long alkyl chains on the cation adsorb to the cell membrane or to cell-membrane like structures and that it can accumulate inside cells (Evans, 2006, 2008a,b; Cornmell *et al.*, 2008b; Lou *et al.*, 2009a). This is thus probably also the case with [HMPL][NTF]. As the biocatalyst is eliminated at each cycle, and replaced by a fresh charge of cells, this volume of adsorbed ionic liquid is lost at each cycle. To date, no quantitative estimation is available. Nevertheless, the estimation of the volume lost by sampling and due to the transfer of the ionic liquid from one recipient to the other during the purification step permits to conclude that this accounts for the large part of the ionic liquid volume lost. Hence, the ionic liquid lost by adsorption to the biocatalyst most probably only accounts for a small fraction of it.

The recovery of the product from the ionic liquid through distillation was performed under non-optimized conditions. The recovery yield of this operation could probably be increased further once the temperature and the duration of the distillation have been optimized.

The set of experiments presented above also permitted to demonstrate how simple and effective the recycling process for this solvent is. The separation of the ionic liquid from the emulsion is very straightforward: a short centrifugation step is sufficient to completely separate the different components of the reaction system from another (Fig. 8.3). This is primarily due to the large density difference of the different components (buffer, cells and ionic liquid), as well as due to the ionic liquid's non-miscibility to water. However, these characteristics do not only permit an easy recovery of the ionic liquid, but also of the product, which is dissolved in large part in this phase. Making use of the favourable partition coefficients, the product is isolated from the rest of the reaction components simultaneously with the ionic liquid. Large partition coefficients for the substrate and the product are thus not only favourable for toxicity reasons, but also very accommodating as far as the product isolation is concerned. The final isolation of the organic product and

ionic liquid purification step is also performed in a relatively simple way, by heating under vacuum conditions. Again, it is the favourable characteristics of the ionic liquid that make this step particularly uncomplicated: its non-flammability, its almost negligible vapour pressure and its large thermal stability. The product could thus be isolated and the ionic liquid purified by using simple equipment and without further extraction steps involving other solvents. Considering these points, it seems that non-water miscible ionic liquids are particularly well suited for such a recycling process, and consequently also for application in reaction systems as presented here.

The knowledge gained by this set of experiments is of importance for syntheses based on biphasic catalysis involving ionic liquids. The large cost of this neoteric class of materials has been one of the main arguments inhibiting the implementation of such processes in industry. Showing that the ionic liquid could be recycled over a large number of cycles, the process is now becoming much more attractive from an economic point of view.
When estimating the material costs per reaction batch, the ionic liquid accounts for ~ 90 % of the material costs for the process considered here. Recycling the ionic liquid over 25 cycles would therefore save ~ 86.4 % of the total material costs incurred, whilst performing 100 subsequent biotransformations with reuse of the same ionic liquid phase would potentially reduce the material costs by almost a factor 9. Moreover, the recycling of the ionic liquid is not only favourable from an economic point of view, but also for ecological reasons. The nearly closed system formed when recycling the ionic liquid also means that the solvent phase only has to be replaced and disposed of sporadically, and the volume that needs to be taken care of, as well as the costs related to this procedure, will be significantly reduced.

Finally, the same recyclability as shown for [HMPL][NTF] is expected for any ionic liquid presenting comparable thermal and chemical stability as the ionic liquid used here. The present process setup could then be applied to other asymmetric whole-cell transformations limited by the toxicity of the substrate and/or of the product of interest, and therefore requiring a biphasic setup. The sole condition is that the ionic liquid must present sufficiently large partition coefficients for the substrate and the product, good biocompatibility and non-water miscibility. Limitations are imposed when heat sensitive products are considered, as these would lose their functionality during the separation of the product from the ionic liquid through heating. In such cases, other purification techniques would have to be applied, as e.g. pervaporation.

8.2 Recycling of the biocatalyst

In section 6.1, it could be demonstrated that the enzymes necessary for the biotransformation show good stability in the process conditions as long as there is no intense contact with the solvent interface and that the ionic liquid used is relatively biocompatible to the biocatalyst. A further aspect that should be investigated is therefore the recyclability of the whole-cell biocatalyst during the process. Even though the biocatalyst is not the most expensive component of the reaction system, its recycling would decrease the process costs.

The recyclability of the whole-cell biocatalyst was analysed by reusing the same biocatalyst for several subsequent biotransformations. As it had been shown that the ionic liquid could be recycled without any negative consequences on the process, the ionic liquid was also recycled during these experiments to reduce the consumption of the solvent.
Each biotransformation was followed by a centrifugation step in order to separate the biocatalyst from the other system components (the aqueous phase and the ionic liquid) (Fig. 8.4). The aqueous phase was discarded. The ionic liquid was introduced into the rotary evaporator to isolate the product and purify the solvent. During this time, the biocatalyst was stored at 4 °C in phosphate buffered saline (PBS). The next day, the biocatalyst was resuspended in fresh aqueous phase and added into the 200 mL reactor with the recycled ionic liquid containing new substrate to start a new biotransformation.

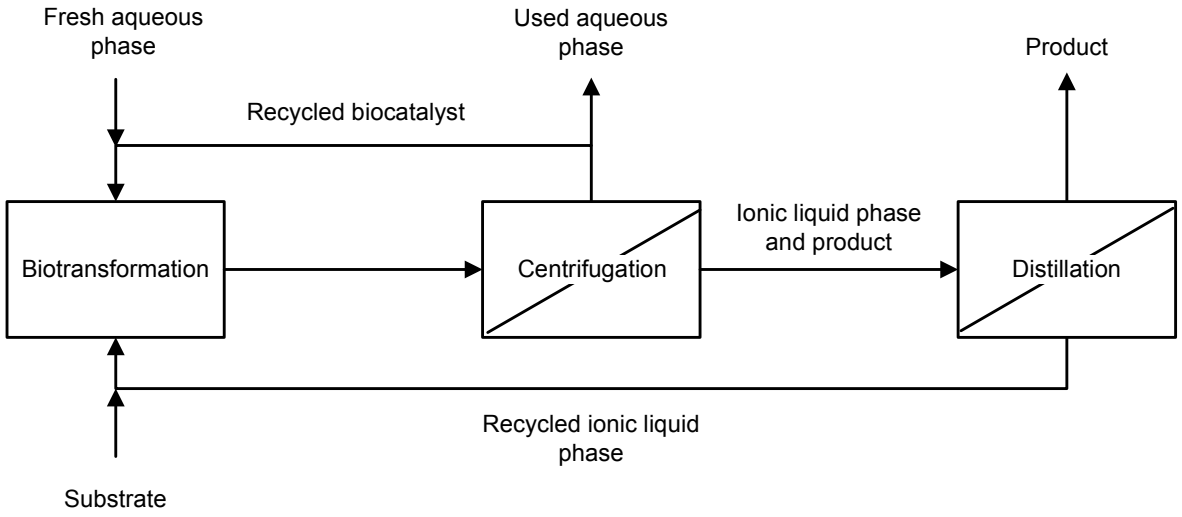

Figure 8.4: Scheme of the process integrated whole-cell biocatalysis in biphasic ionic liquid/water systems with recycling of the ionic liquid phase and of the biocatalyst.

The biotransformations were performed with an initial substrate concentration of 300 mM 2-octanone in the ionic liquid ([HMPL][NTF]), and at an ionic liquid volume fraction of 20 %. The evolution of the conversion with time for three subsequent biotransformations with recycling of the biocatalyst is shown in Fig. 8.5. The conversion reached at each point in time decreases with the number of biocatalyst recyclings. While the first biotransformation showed complete conversion of the substrate after 5 h, the second biotransformation reached ~ 98 % conversion, and the third biotransformation only ~ 92 %. The enantiomeric excess, however, was constantly ≥ 99.5 % (*R*) in each of the biotransformations (data not shown).

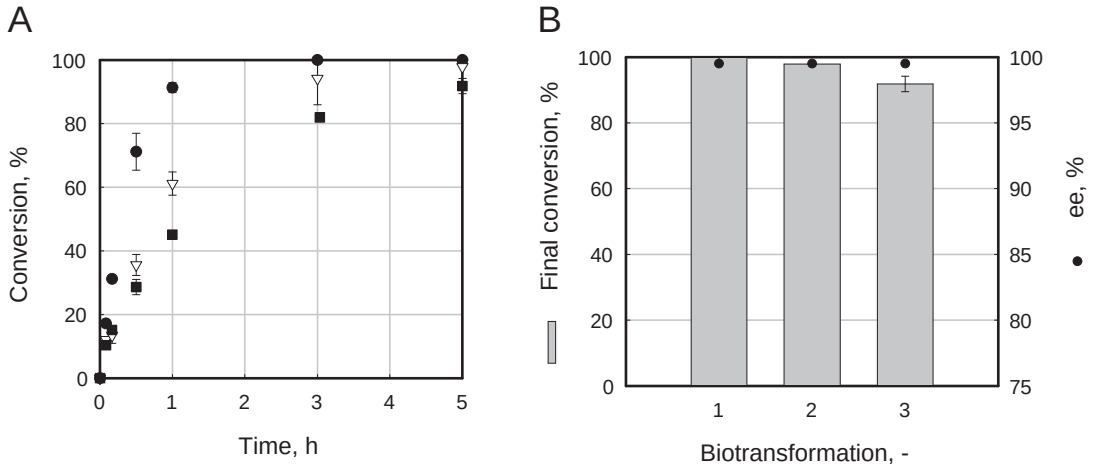

Figure 8.5: Recycling of the biocatalyst: conversion reached in three subsequent biotransformations with an initial substrate concentration of 300 mM 2-octanone in the ionic liquid and an ionic liquid volume fraction of 20 %. A: Evolution of conversion with time for the biotransformation 1 (●), biotransformation 2 (▽) and biotransformation 3 (■). B: Conversion and enantiomeric excess reached in each biotransformation after 5 h reaction time.

To evaluate if the addition of various substances to the aqueous phase could increase the stability of the biocatalyst, this set of experiments was repeated with 5 g L^{-1} glucose or 5 g L^{-1} yeast extract in the aqueous phase, and using a mineral medium according to Bühler *et al.* (2002) instead of the phosphate buffer as aqueous phase. These sets of experiments showed a very similar decrease of the conversion with increasing cycle number of the biocatalyst (data not shown).

8.2.1 Discussion

The recycling of the biocatalyst showed that the biocatalyst used was not stable enough in the reaction conditions considered to reach constant conversion > 99 % after 5 h reaction time in subsequent biotransformations. Still, the decrease of conversion observed with

each cycle was not very large. For applications, which do not necessarily require complete conversion, a reuse of the biocatalyst over two or three cycles might be considered. The slight loss of productivity due to a decrease of conversion of 5–10 % might be acceptable in comparison to the reduced time and cost investment necessary to produce fresh biocatalyst. When a very pure product is required, this will however not be an option. The complete conversion of the substrate is then absolutely necessary during the biotransformation to avoid costly purification steps of the product at the end of the process. The recycling of the biocatalyst in the conditions tested is therefore not an option here if the reaction is stopped after 5 h. If the reaction duration is however increased, it might still be possible to reach the wanted minimal conversion > 99.0 % while recycling the biocatalyst over a small number of cycles. This hypothesis has to be verified experimentally. The resulting decrease of productivity of the process observed in that case might also be partially compensated by the reduced costs due to the biocatalyst recycling. A compromise between the increasing reaction duration and the reduced costs by increasing numbers of biocatalyst recyclings would have to be made.

One explanation to the observed loss of activity is the half life of the enzymes in the conditions encountered during the biotransformation (subsection 6.1.3). Another cause may be a possible degradation of the cell membrane. The cells might get damaged during the centrifugation step or due to the intense contact with the ionic liquid during the transfer from one recipient to another. Even though fresh biocatalyst can be stored over up to three weeks at 4 °C without a significant loss of activity (data not shown), it is not known if this is still true when the biocatalyst has already been used during one biotransformation. The relatively long storage of the biocatalyst between two cycles ($\sim$ 18 h) could thus also negatively influence its activity.
A stabilisation of the biocatalyst would necessitate the reduction of the damage on the cell membrane and the stabilisation of the LB ADH and the CB FDH. Further investigation might permit to determine different process conditions in favour of both, without excessively increasing the process costs or causing mass transfer limitations.
Finally, the stability of the cofactor could also be one reason for the loss of activity. The stability of NADH is indeed known to be significantly reduced at room temperature in comparison to its storage temperature at 4 °C or, preferably, at −20 °C. Consequently, even though it is sufficiently stable to store the biocatalyst up to three week after its cultivation until its use, the cofactor might show significant degradation during the biotransformation at $\sim$ 25 °C. If this is one of the causes for the loss of biocatalyst activity observed, it is not clear if this issue might be solved.

9 Summary and conclusions

Chiral alcohols are frequent building blocks for fine chemicals, agrochemicals and pharmaceuticals and they are used in technical applications. Biocatalysis constitutes a good means to produce them with very high enantioselectivity and under mild reaction conditions by asymmetric reduction of the corresponding ketones. Chiral short chain alcohols and their corresponding ketones constitute however relatively challenging substrate/product pairs for biocatalyses, because many of these substrates and products are toxic to living organisms and show low water solubility. These biotransformations can thus only reach satisfying productivities if they are performed in biphasic setups. An attractive alternative to volatile and flammable organic solvents is the use of ionic liquids as second, non-water miscible phase.

Since the beginning of the century, an increasing number of publications demonstrate the feasibility of such biphasic biotransformations. However, to be able to realize the full potential of these promising reactions, more information on the reaction systems is required. Taking the reaction system presented by Bräutigam *et al.* (2009) as starting point, the aim of this project was to characterise and optimise the biphasic whole-cell biotransformation and to assess its suitability for an industrial application.

In a first step, the biotransformation was characterised concerning the effect of the system components on the reaction outcome. The evaluation of the biocompatibility of the ionic liquid, the substrate and the product showed that the ionic liquid used ([HMPL][NTF]) presented relatively good biocompatibility to the whole-cell biocatalyst and confirmed the large toxicity of 2-octanone and 2-octanol. The evaluation of the enzyme stability showed that the enzymes necessary to perform the biotransformation were not destabilised by the presence of the substrate, the product and low concentrations of ionic liquid. In contrast, an accelerated decrease of the enzyme activity was registered when they were in direct contact with the ionic liquid phase. During a parameter study, the ionic liquid volume fraction and the initial substrate concentrations were varied and the consequences on the conversion and the enantiomeric excess were investigated. These analyses showed that large ionic liquid volume fractions (> 40 %) and large initial substrate concentrations

(> 450 mM) lead to a decrease of the final conversion reached. At such large concentrations, the ionic liquid, as well as the substrate and the product damaged the biocatalyst and thus provoked the early termination of the conversion. The inactivation of the biocatalyst is probably mostly due to a permeabilisation of the cell membrane by the aforementioned substances. The parameter study permitted to determine the reaction setup leading to the largest productivity among those analysed. With an ionic liquid volume fraction of 20 %, 50 g_{DCW} L^{-1} biocatalyst in the aqueous phase and an intial substrate concentration of 300 mM in the ionic liquid, a conversion > 99.0 % at an enantiomeric excess ≥ 99.5 % (*R*) was reached within a reaction duration of 5 h. The space-time yield was 6.71 ± 0.04 g *R*-2-octanol L^{-1} h^{-1}(33.5 ± 0.9 g *R*-2-octanol L_{IL}^{-1} h^{-1}). The scale-up of the biotransformation to Liter scale was performed in these optimised reaction conditions. The evolution of conversion observed at the larger scale was in complete agreement with the smaller scale experiment. The scale-up strategy chosen (constant maximal local energy dissipation) was thus appropriate. Finally, it could be shown that the 'bioreactor unit' developed by Weuster-Botz *et al.* (2005), permitting the parallel operation of 48 miniaturized stirred tank bioreactors, was a suitable tool for the process development of biphasic reaction systems with ionic liquid volume fractions up to 40 %.

The second part of the project was concerned with the characterisation of the different steps of the biotransformation: the mass transfer between the ionic liquid and the aqueous phase, the mass transfer between the aqueous phase and the cell and the enzymatic transformation. This required the determination of different system properties, such as the viscosity of the phases involved, the interfacial tension, the drop size distribution and the kinetic parameters of the enzymes. The estimation of the mass transfer coefficient between the ionic liquid and the aqueous phase led to values considerably too low to fit the experimental observations. The existing correlations could thus not be applied to the present system. The lack of this parameter was resolved by showing that this mass transfer was not the rate limiting step of the biotransformation. A constant equilibrium between the ionic liquid and the aqueous phase could thus be supposed, making the knowledge of this parameter no longer necessary to describe this transfer.
Using the corresponding equations completed by these analyses, a model was established for the biotransformation, permitting to identify the system parameter that could not be measured nor estimated: the membrane permeability for the substrate and the product (P). By fitting the model to experimental data recorded during nine biotransformations performed in different reaction conditions, a value of $3.16 \cdot 10^{-7}$ m s^{-1} was identified for P. With this value, the model permitted to predict the evolution of biotransformations

with an initial substrate concentration up to 400 mM in the ionic liquid with very good precision and showing only a very slight deviation up to initial substrate concentrations of 670 mM 2-octanone in the ionic liquid. For biotransformations with increased ionic liquid volume fractions, the reaction rate and the final conversion were however overestimated. This is probably due to the biocatalyst inactivation provoked by larger ionic liquid volume fractions, a phenomenon not included in the current model.
Another point investigated concerned the rate limiting step of the biotransformation. Biotransformations performed at varying stirrer speeds and biocatalyst concentrations permitted to conclude that the mass transfer between the ionic liquid and the aqueous phase is not the rate limiting step of the biotransformation in the reaction conditions considered. A further distinction between the other reaction steps was not possible experimentally. Here, the model established was used to further elucidate this point: by artificially increasing the different fluxes, the transfer of the product from the cell into the aqueous phase could also be excluded as rate limiting step. Nevertheless, the model did not either permit to completely uncouple the effect of an increased substrate transfer from the aqueous phase into the cell from the effect of an increased enzymatic reaction rate on the apparent rate of the biotransformation. This is due to the fact that both steps are highly dependent on each and an increase of one of them directly provokes an increase of the other, too.

The last part of the project evaluated the recyclability of the ionic liquid and the biocatalyst. These experiments showed that the biocatalyst cannot be recycled without a small, but decisive decrease of the final conversion reached within the same process duration. Considering the very strict requirements imposed (conversion > 99 %), this is not surprising. In fact a slight inactivation of the biocatalyst might be sufficient to decrease the conversion reached after 5 h below this threshhold. More importantly, however, the ionic liquid could be recycled over 25 process cycles including the biotransformation, followed by the product isolation and ionic liquid purification without a loss of productivity during the biotransformation (Fig. 9.1). This last part of the project is of utmost importance for a possible industrial implementation. As ionic liquids are still very expensive materials, processes involving them are only of economic interest if the ionic liquid can be recycled over a large number of cycles.

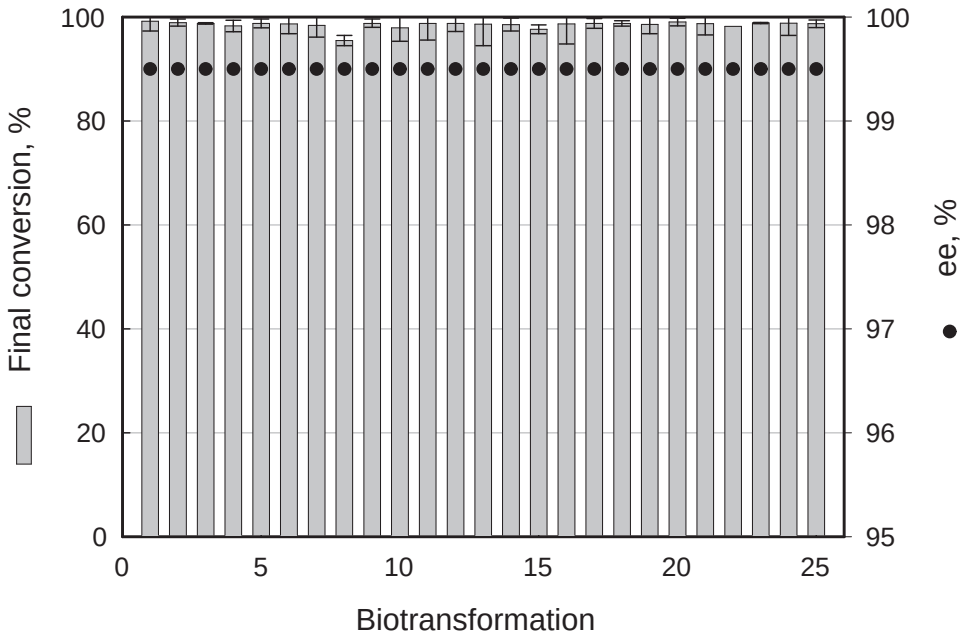

Figure 9.1: Final conversion reached after 5 h reaction time by each biotransformation throughout 25 cycles including the biotransformation, the phases separation and the ionic liquid purification and product isolation. The enantiomeric excess was ≥ 99.5 % (*R*) over the whole duration of each biotransformation.

In conclusion, the results from the experiments above constitute a valuable gain of information for the future design of other biotransformations in biphasic ionic liquid-water systems. The process developed and characterised could be optimised to reach the largest productivity at highest final purity of the product published to date to the authors knowledge. The different process steps are of low complexity and the recycling of the ionic liquid would significantly reduce the material costs of the process, up to a factor 9 if a recycling over 100 cycles is considered. With a conversion > 99.0 % at an enantiomeric excess ≥ 99.5 % (*R*) and with the recycling of the ionic liquid, the process is now ready for industrial application. The use of a non-flammable and non-volatile ionic liquid helps to reduce the security and toxicity issues caused by volatile organic solvents and the simplicity of the process setup - possible due to these properties - showed that non-water miscible ionic liquids are particularly well suited for such an application. The setup presented could be applied to other toxic substrate/product pairs, and to varying organisms and ionic liquids, given a minimal thermal stability of the ionic liquid and the product. This process might thus open the way to a larger number of biphasic processes involving ionic liquids in the domain of white biotechnology.

One issue that deserves further investigation are the biotransformations at large initial substrate concentrations: it could be shown that the low final conversion reached was due to an inactivation of the biocatalyst. When replacing the biocatalyst after 6 h reaction duration, the conversion could be increased to good values > 93 %. It should be verified in which conditions the conversion could be increased to reach final values > 99 %, and if the replacement of the biocatalyst in such reaction systems after a given reaction duration is an attractive solution in terms of productivity and costs.

The model identified for the biphasic biotransformation permitted to predict the evolution of the conversion with good precision for initial substrate concentrations up to 670 mM in the ionic liquid at ionic liquid volume fractions up to 20 %. In future work, the main point of interest would be to expand its domain of validity by including an expression accounting for the (partial) inactivation of the biocatalyst by large ionic liquid volume fractions and large substrate and/or product concentrations. While some authors investigated the interaction of ionic liquids with the cell membrane or with artificial phospholipid bilayers resembling the cell membrane (Evans, 2006, 2008a,b), no mechanistic model is available to date giving the direct relationship between the ionic liquid content of the reaction system and the loss of biocatalyst activity. This is a challenging issue, because it would have to include the cofactor leakage as well as a possible enzyme inactivation. The identification of an empiric model for this process is less demanding. Either approach would permit to apply the model presented to a larger range of varying ionic liquid volume fractions. The same conclusions hold true for the effect of the toxic substrate and product on the biocatalyst.

Finally, the characterisation of the different steps of the reaction showed where the lack of available data made the estimation of given parameters difficult. No reliable correlation model was found for the estimation of the mass transfer coefficient, and generally very little data is available on the diffusion of solutes in systems involving ionic liquids and on the membrane permeability of various substances for different organisms.
Even though, here, the estimation of the diffusion coefficient was not necessary in the end, further investigation on this subject is necessary to be able to describe the mass transfer between an ionic liquid and an aqueous buffer more reliably. As more and more reactions involve ionic liquids, this may become a subject of importance and of interest for other reaction systems, where a correct description of this transfer is required.

References

Abbott, A. P., Boothby, D., Capper, G., Davies, D. L., Rasheed, R. K. (2004). Deep eutectic solvents formed between choline chloride and carboxylic acids: versatile alternatives to ionic liquids. *Journal of the American Chemical Society*, 126(29):9142–9147.

Adlercreutz, P. (1991). Novel biocatalyst for the asymmetric reduction of ketones: Permeabilized cells of gluconobacter oxydans. *Enzyme and Microbial Technology*, 13(1):9–14.

Alberts, B., Bray, D., Lewis, J. (2002). *Molecular Biology of the Cell*. Taylor & Francis, 4th edition.

Ansorge-Schumacher, M. B., Slusarczyk, H., Schumers, J., Hirtz, D. (2006). Directed evolution of formate dehydrogenase from *Candida boidinii* for improved stability during entrapment in polyacrylamide. *FEBS Journal*, 273(17):3938–3945.

Arai, K., Konno, M., Matunaga, Y., Saito, S. (1977). Effect of dispersed-phase viscosity on maximum stable drop size for breakup in turbulent-flow. *Journal of Chemical Engineering Japan*, 10(4):325–330.

Arai, S., Nakashima, K., Tanino, T., Ogino, C., Kondo, A., Fukuda, H. (2010). Production of biodiesel fuel from soybean oil catalyzed by fungus whole-cell biocatalysts in ionic liquids. *Enzyme and Microbial Technology*, 46(1):51–55.

Armstrong, D. W., He, L., Liu, Y. (1999). Examination of ionic liquids and their interaction with molecules, when used as stationary phases in gas chromatography. *Analytical Chemistry*, 71(17):3873–3876.

Awad, W. (2004). Thermal degradation studies of alkyl-imidazolium salts and their application in nanocomposites. *Thermochimica Acta*, 409(1):3–11.

Azcan, N., Demirel, E. (2008). Obtaining 2-octanol, 2-octanone, and sebacic acid from castor oil by microwave-induced alkali fusion. *Industrial & Engineering Chemistry Research*, 47(6):1774–1778.

Bar, R. (1988). Effect of interphase mixing on a water-organic solvent two-liquid phase microbial system: ethanol fermentation. *Journal of Chemical Technology & Biotechnology*, 43(1):49–62.

Baumann, M. D., Daugulis, A. J., Jessop, P. G. (2004). Phosphonium ionic liquids for degradation of phenol in a two-phase partitioning bioreactor. *Applied Microbiology and Biotechnology*, 67(1):131–137.

Bisswanger, H. (2000). *Enzymkinetik: Theorie und Methoden*. Wiley-VCH, Weinheim, 3rd newly revised edition.

Bommarius, A., Karau, A. (2005). Deactivation of formate dehydrogenase (FDH) in solution and at gas-liquid interfaces. *Biotechnology Progress*, 21(6):1663–1672.

Bommarius, A., Riebel-Bommarius, B. R. (2004). *Biocatalysis*. Wiley-VCH, Weinheim.

Bösmann, A., Schulz, P. S., Wasserscheid, P. (2007). Enhancing task specific ionic liquids' thermal stability by structural modification. *Monatshefte für Chemie - Chemical Monthly*, 138(11):1159–1161.

Brauer, H. (1978a). Unsteady state mass transfer through the interface of spherical particles — I physical and mathematical description of the mass-transfer problem. *International Journal of Heat and Mass Transfer*, 21(4):445–453.

Brauer, H. (1978b). Unsteady state mass transfer through the interface of spherical particles — II discussion of results obtained by theoretical methods. *International Journal of Heat and Mass Transfer*, 21(4):455–465.

Bräutigam, S., Bringer-Meyer, S., Weuster-Botz, D. (2007). Asymmetric whole cell biotransformations in biphasic ionic liquid/water-systems by use of recombinant *Escherichia coli* with intracellular cofactor regeneration. *Tetrahedron: Asymmetry*, 18(16):1883–1887.

Bräutigam, S., Dennewald, D., Schürmann, M., Lutje-Spelberg, J., Pitner, W., Weuster-Botz, D. (2009). Whole-cell biocatalysis: Evaluation of new hydrophobic ionic liquids for efficient asymmetric reduction of prochiral ketones. *Enzyme and Microbial Technology*, 45(4):310–316.

Brennecke, J. F., Maginn, E. J. (2001). Ionic liquids: Innovative fluids for chemical processing. *AIChE Journal*, 47(11):2384–2389.

Brodkey, R. (1975). *Turbulence in mixing operations : theory and application to mixing and reaction*. Academic Press, New York.

Bühler, B., Witholt, B., Hauer, B., Schmid, A. (2002). Characterization and application of xylene monooxygenase for multistep biocatalysis. *Applied and Environmental Microbiology*, 68(2):560–568.

Calabrese, R. V., Chang, T. P. K., Dang, P. T. (1986a). Drop breakup in turbulent stirred-tank contactors. Part I: Effect of dispersed-phase viscosity. *AIChE Journal*, 32(4):657–666.

Calabrese, R. V., Wang, C. Y., Bryner, N. P. (1986b). Drop breakup in turbulent stirred-tank contactors. Part III: Correlations for mean size and drop size distribution. *AIChE Journal*, 32(4):677–681.

Carmichael, A. J., Seddon, K. R. (2000). Polarity study of some 1-alkyl-3-methylimidazolium ambient-temperature ionic liquids with the solvatochromic dye, nile red. *Journal of Physical Organic Chemistry*, 13(10):591–595.

Carter, E. B., Culver, S. L., Fox, P. A., Goode, R. D., Ntai, I., Tickell, M. D., Traylor, R. K., Hoffman, N. W., James H. Davis, J. (2004). Sweet success: ionic liquids derived from non-nutritive sweeteners. *Chemical Communications*, 6:630.

Chen, C., Chiou, Y. (1995). Toxicity of binary mixtures of organic chemicals. *Environmental Toxicology & Water Quality*, 10(2):97–106.

Chen, H. T., Middleman, S. (1967). Drop size distribution in agitated liquid-liquid systems. *AIChE Journal*, 13(5):989–995.

Chiappe, C., Pieraccini, D. (2005). Ionic liquids: solvent properties and organic reactivity. *Journal of Physical Organic Chemistry*, 18(4):275–297.

Cleland, W. W. (1963a). The kinetics of enzyme-catalyzed reactions with two or more substrates or products. I. Nomenclature and rate equations. *Biochimica Et Biophysica Acta*, 67:104–137.

Cleland, W. W. (1963b). The kinetics of enzyme-catalyzed reactions with two or more substrates or products. II. Inhibition: nomenclature and theory. *Biochimica Et Biophysica Acta*, 67:173–187.

Cleland, W. W. (1963c). The kinetics of enzyme-catalyzed reactions with two or more substrates or products. III. Prediction of initial velocity and inhibition patterns by inspection. *Biochimica Et Biophysica Acta*, 67:188–196.

Cornmell, R. J., Winder, C. L., Schuler, S., Goodacre, R., Stephens, G. (2008a). Using a biphasic ionic liquid/water reaction system to improve oxygenase-catalysed biotransformation with whole cells. *Green Chemistry*, 10(6):685.

Cornmell, R. J., Winder, C. L., Tiddy, G. J. T., Goodacre, R., Stephens, G. (2008b). Accumulation of ionic liquids in *Escherichia coli* cells. *Green Chemistry*, 10(8):836.

Cromie, S., Popolo, M. G. D., Ballone, P. (2009). Interaction of room temperature ionic liquid solutions with a cholesterol bilayer. *The Journal of Physical Chemistry B*, 113(34):11642–11648.

Cull, S. G., Holbrey, J. D., Vargas-Mora, V., Seddon, K. R., Lye, G. J. (2000). Room-temperature ionic liquids as replacements for organic solvents in multiphase bioprocess operations. *Biotechnology and Bioengineering*, 69(2):227–233.

Danckwerts, P. V. (1951). Significance of liquid-film coefficients in gas absorption. *Industrial & Engineering Chemistry*, 43(6):1460–1467.

de Gonzalo, G., Lavandera, I., Durchschein, K., Wurm, D., Faber, K., Kroutil, W. (2007). Asymmetric biocatalytic reduction of ketones using hydroxy-functionalised water-miscible ionic liquids as solvents. *Tetrahedron: Asymmetry*, 18(21):2541–2546.

Demond, A. H., Lindner, A. S. (1993). Estimation of interfacial tension between organic liquids and water. *Environmental Science & Technology*, 27(12):2318–2331.

Dijken, J. P., Oostra-Demkes, G. J., Otto, R., Harder, W. (1976). S-formylglutathione: the substrate for formate dehydrogenase in methanol-utilizing yeasts. *Archives of Microbiology*, 111(1-2):77–83.

Dipeolu, O., Green, E., Stephens, G. (2009). Effects of water-miscible ionic liquids on cell growth and nitro reduction using clostridium sporogenes. *Green Chemistry*, 11(3):397.

Docherty, K. M., Kulpa, C. F. (2005). Toxicity and antimicrobial activity of imidazolium and pyridinium ionic liquids. *Green Chemistry*, 7(4):185.

Dossat, V. (1999). Continuous enzymatic transesterification of high oleic sunflower oil in a packed bed reactor: influence of the glycerol production. *Enzyme and Microbial Technology*, 25(3-5):194–200.

du Noüy, P. L. (1925). An interfacial tensiometer for universal use. *The Journal of General Physiology*, 7(5):625–631.

Dupont, J., de Souza, R. F., Suarez, P. A. Z. (2002). Ionic liquid (molten salt) phase organometallic catalysis. *Chemical Reviews*, 102(10):3667–3692.

Eckstein, M., Filho, M. V., Liese, A., Kragl, U. (2004). Use of an ionic liquid in a two-phase system to improve an alcohol dehydrogenase catalysed reduction. *Chemical Communications*, 9:1084.

Ernst, M., Kaup, B., MÃ¼ller, M., Bringer-Meyer, S., Sahm, H. (2004). Enantioselective reduction of carbonyl compounds by whole-cell biotransformation, combining a formate dehydrogenase and a (R)-specific alcohol dehydrogenase. *Applied Microbiology and Biotechnology*, 66(6):629–634.

Evans, K. O. (2006). Room-temperature ionic liquid cations act as short-chain surfactants and disintegrate a phospholipid bilayer. *Colloids and Surfaces A: Physicochemical and Engineering Aspects*, 274(1-3):11–17.

Evans, K. O. (2008a). Supported phospholipid bilayer interaction with components found in typical room-temperature ionic liquids - a QCM-D and AFM study. *International Journal of Molecular Sciences*, 9(4):498–511.

Evans, K. O. (2008b). Supported phospholipid membrane interactions with 1-butyl-3-methylimidazolium chloride. *The Journal of Physical Chemistry B*, 112(29):8558–8562.

Faber, K. (1997). *Biotransformations in organic chemistry : a textbook*. Springer Verlag, Berlin; New York, 3rd, completely rev. edition.

Faber, K., Franssen, M. C. R. (1993). Prospects for the increased application of biocatalysts in organic transformations. *Trends in Biotechnology*, 11(11):461–470.

Felber, S. (2001). *Optimierung der NAD-abhängigen Formiatdehydrogenase aus Candida boidinii für den Einsatz in der Biokatalyse*. PhD thesis, Heinrich Heine-Universität Düsseldorf.

Filho, M. V. (2007). *Enantioselective reduction of hydrophobic keto compounds in multiphase bioreactor*. Schriften des Forschnungszentrum Jülich. Reihe Lebenswissenschaften/Life Science. Forschungszentrum Jülich GmbH.

Freire, M. G., Carvalho, P. J., Fernandes, A. M., Marrucho, I. M., Queimada, A. J., Coutinho, J. A. (2007). Surface tensions of imidazolium based ionic liquids: anion, cation, temperature and water effect. *Journal of Colloid and Interface Science*, 314(2):621–630.

Fukumoto, K., Yoshizawa, M., Ohno, H. (2005). Room temperature ionic liquids from 20 natural amino acids. *Journal of the American Chemical Society*, 127(8):2398–2399.

Gale, R. J., Gilbert, B., Osteryoung, R. A. (1978). Raman spectra of molten aluminum chloride: 1-butylpyridinium chloride systems at ambient temperatures. *Inorganic Chemistry*, 17(10):2728–2729.

Galkin, A., Kulakova, L., Yoshimura, T., Soda, K., Esaki, N. (1997). Synthesis of optically active amino acids from α-keto acids with *Escherichia coli* cells expressing heterologous genes. *Appl. Environ. Microbiol.*, 63(12):4651–4656.

Ganske, F., Bornscheuer, U. T. (2006). Growth of *Escherichia coli*, *Pichia pastoris* and *Bacillus cereus* in the presence of the ionic liquids [BMIM][BF4] and [BMIM][PF6] and organic solvents. *Biotechnology Letters*, 28(7):465–469.

Garcia, M. T., Gathergood, N., Scammells, P. J. (2005). Biodegradable ionic liquids : Part II. Effect of the anion and toxicology. *Green Chemistry*, 7(1):9.

Gathergood, N., Garcia, M. T., Scammells, P. J. (2004). Biodegradable ionic liquids: Part I. Concept, preliminary targets and evaluation. *Green Chemistry*, 6(3):166.

Gervais, T., Carta, G., Gainer, J. (2000). Effect of aeration during cell growth on ketone reactions by immobilized yeast. *Biotechnology Progress*, 16(2):208–212.

Ghatee, M. H., Zolghadr, A. R. (2008). Surface tension measurements of imidazolium-based ionic liquids at liquid-vapor equilibrium. *Fluid Phase Equilibria*, 263(2):168–175.

Handy, S. T., Okello, M., Dickenson, G. (2003). Solvents from biorenewable sources: Ionic liquids based on fructose. *Organic Letters*, 5(14):2513–2515.

Harjani, J. R., Singer, R. D., Garcia, M. T., Scammells, P. J. (2008). The design and synthesis of biodegradable pyridinium ionic liquids. *Green Chemistry*, 10(4):436.

Harjani, J. R., Singer, R. D., Garcia, M. T., Scammells, P. J. (2009). Biodegradable pyridinium ionic liquids: design, synthesis and evaluation. *Green Chemistry*, 11(1):83.

Harkins, W. D., Jordan, H. F. (1930a). A method for the determination of the surface and interfacial tension from the maximum pull an on a ring. *Journal of the American Chemical Society*, 52(5):1751–1772.

Harkins, W. D., Jordan, H. F. (1930b). Surface tension by the ring method. *Science*, 72(1855):73–75.

Hayduk, W., Laudie, H. (1974). Prediction of diffusion coefficients for nonelectrolytes in dilute aqueous solutions. *AIChE Journal*, 20(3):611–615.

Hayduk, W., Minhas, B. S. (1982). Correlations for prediction of molecular diffusivities in liquids. *The Canadian Journal of Chemical Engineering*, 60(2):295–299.

He, J., Zhou, L., Wang, P., Zu, L. (2009). Microbial reduction of ethyl acetoacetate to ethyl (R)-3-hydroxybutyrate in an ionic liquid containing system. *Process Biochemistry*, 44(3):316–321.

Heidlas, J., Engel, K., Tressl, R. (1991). Enantioselectivities of enzymes involved in the reduction of methylketones by bakers' yeast. *Enzyme and Microbial Technology*, 13(10):817–821.

Henzler, H. (2000). *Advances in Biochemical Engineering/Biotechnology*, volume 67, chapter : Particle stress in bioreactors, pages 35–82. Springer-Verlag, Berlin, Heidelberg, New York.

Higbie, R. (1935). The rate of absorption of a pure gas into a still liquid during short periods of exposure. *Tram. Am. lnst. Chem. Engrs.*, 31:365.

Hildebrandt, P., Musidlowska, A., Bornscheuer, U., Altenbuchner, J. (2002). Cloning, functional expression and biochemical characterization of a stereoselective alcohol dehydrogenase from *Pseudomonas fluorescens* DSM50106. *Applied Microbiology and Biotechnology*, 59(4-5):483–487.

Hinze, J. O. (1955). Fundamentals of the hydrodynamic mechanism of splitting in dispersion processes. *AIChE Journal*, 1(3):289–295.

Hoffmann, J., Tralles, S., Hempel, D. C. (1992). Testsystem zur Untersuchung der mechanischen Beanspruchung von Partikeln in Bioreaktoren. *Chemie Ingenieur Technik*, 64(10):953–956.

Holbrey, J. D., Rogers, R. D. (2003). Physicochemical properties of ionic liquids. In *Ionic Liquids in Synthesis*, pages 41–55. Wiley VCH, Weinheim, Germany.

Hortsch, R., Weuster-Botz, D. (2010a). Growth and recombinant protein expression with *Escherichia coli* in different batch cultivation media. *Applied Microbiology and Biotechnology*.

Hortsch, R., Weuster-Botz, D. (2010b). Milliliter-Scale stirred tank reactors for the cultivation of microorganisms. In *Advances in Applied Microbiology*, volume 73, pages 61–82. Elsevier.

Hortsch, R., Weuster-Botz, D. (2010c). Power consumption and maximum energy dissipation in a milliliter-scale bioreactor. *Biotechnology Progress*, 26(2):595–599.

Howarth, J., James, P., Dai, J. (2001). Immobilized baker's yeast reduction of ketones in an ionic liquid, [BMIM][PF6] and water mix. *Tetrahedron Letters*, 42(42):7517–7519.

Hu, J., Xu, Y. (2006). Anti-Prelog reduction of prochiral carbonyl compounds by *Oenococcus oeni* in a biphasic system. *Biotechnology Letters*, 28(14):1115–1119.

Huddleston, J. G., Visser, A. E., Reichert, W. M., Willauer, H. D., Broker, G. A., Rogers, R. D. (2001). Characterization and comparison of hydrophilic and hydrophobic room temperature ionic liquids incorporating the imidazolium cation. *Green Chemistry*, 3(4):156–164.

Hummel, W. (1997). New alcohol dehydrogenase for the synthesis of chiral compounds. In *New enzymes for organic synthesis*, volume 58 of *Advances in Biochemical Engineering/Biotechnology*, pages 145–184. Springer Berlin Heidelberg, Berlin Heidelberg.

Hummel, W., Kula, M. (1989). Dehydrogenases for the synthesis of chiral compounds. *European Journal of Biochemistry*, 184(1):1–13.

Hummel, W., Riebel, B. (2000). *US patent 6037158: Alcohol dehydrogenase and its use for the enzymatic production of chiral hydroxyl compounds*.

Hussain, W., Pollard, D. J., Lye, G. J. (2007). The bioreduction of a β-tetralone to its corresponding alcohol by the yeast *Trichosporon capitatum* MY1890 and bacterium *Rhodococcus erythropolis* MA7213 in a range of ionic liquids. *Biocatalysis and Biotransformation*, 25(6):443–452.

Jacquemin, J., Husson, P., Padua, A. A. H., Majer, V. (2006). Density and viscosity of several pure and water-saturated ionic liquids. *Green Chemistry*, 8(2):172.

Jamshidi-Ghaleh, K., Tavassoly, M. T., Mansour, N. (2004). Diffusion coefficient measurements of transparent liquid solutions using moiré deflectometry. *Journal of Physics D: Applied Physics*, 37(14):1993–1997.

Jeromin, G. (2005). *Bioorganikum : Praktikum der Biokatalyse*. Wiley-VCH, Weinheim.

Kagimoto, J., Fukumoto, K., Ohno, H. (2006). Effect of tetrabutylphosphonium cation on the physico-chemical properties of amino-acid ionic liquids. *Chemical Communications*, (21):2254.

Kato, N., Sahm, H., Wagner, F. (1979). Steady-state kinetics of formaldehyde dehydrogenase and formate dehydrogenase from a methanol-utilizing yeast, *Candida boidinii*. *Biochimica Et Biophysica Acta*, 566(1):12–20.

Kavanagh, K. L., Jörnvall, H., Persson, B., Oppermann, U. (2008). Medium- and short-chain dehydrogenase/reductase gene and protein families. *Cellular and Molecular Life Sciences*, 65(24):3895–3906.

Kim, H., Burgess, J. (2001). Prediction of interfacial tension between oil mixtures and water. *Journal of Colloid and Interface Science*, 241(2):509–513.

Klomfar, J., Soucková, M., Pátek, J. (2010). Surface tension measurements with validated accuracy for four 1-alkyl-3-methylimidazolium based ionic liquids. *The Journal of Chemical Thermodynamics*, 42(3):323–329.

Kohlmann, C., Leuchs, S., Greiner, L., Leitner, W. (2011a). Continuous biocatalytic synthesis of (R)-2-octanol with integrated product separation. *Green Chemistry*.

Kohlmann, C., Robertz, N., Leuchs, S., Dogan, Z., Lütz, S., Bitzer, K., Na'amnieh, S., Greiner, L. (2011b). Ionic liquid facilitates biocatalytic conversion of hardly water soluble ketones. *Journal of Molecular Catalysis B: Enzymatic*, 68(2):147–153.

Korson, L., Drost-Hansen, W., Millero, F. J. (1969). Viscosity of water at various temperatures. *The Journal of Physical Chemistry*, 73(1):34–39.

Kosmulski, M., Gustafsson, J., Rosenholm, J. B. (2004). Thermal stability of low temperature ionic liquids revisited. *Thermochimica Acta*, 412(1-2):47–53.

Kragl, U., Kruse, W., Hummel, W., Wandrey, C. (1996). Enzyme engineering aspects of biocatalysis: Cofactor regeneration as example. *Biotechnology and Bioengineering*, 52(2):309–319.

Kratzer, R., Pukl, M., Egger, S., Nidetzky, B. (2008). Whole-cell bioreduction of aromatic α-keto esters using *Candida tenuis* xylose reductase and *Candida boidinii* formate dehydrogenase co-expressed in *Escherichia coli*. *Microbial Cell Factories*, 7(1):37.

Kroutil, W., Mang, H., Edegger, K., Faber, K. (2004). Recent advances in the biocatalytic reduction of ketones and oxidation of sec-alcohols. *Current Opinion in Chemical Biology*, 8(2):120–126.

Kubitschek, H. E. (1990). Cell volume increase in escherichia coli after shifts to richer media. *Journal of Bacteriology*, 172(1):94–101.

Kusterer, A., Krause, C., Kaufmann, K., Arnold, M., Weuster-Botz, D. (2008). Fully automated single-use stirred-tank bioreactors for parallel microbial cultivations. *Bioprocess and Biosystems Engineering*, 31(3):207–215.

Lederberg, J., Bloom, B. R. (2000). *Encyclopedia of microbiology*. Academic Press, San Diego, 2nd ed. edition.

Lee, S., Chang, W., Choi, A., Koo, Y. (2005). Influence of ionic liquids on the growth of *Escherichia coli*. *Korean Journal of Chemical Engineering*, 22(5):687–690.

Lenourry, A., Gardiner, J. M., Stephens, G. (2005). Hydrogenation of C-C double bonds in an ionic liquid reaction system using the obligate anaerobe, *Sporomusa termitida*. *Biotechnology Letters*, 27(3):161–165.

Lewis, W. K., Whitman, W. G. (1924). Principles of gas absorption. *Industrial & Engineering Chemistry*, 16(12):1215–1220.

Li, J. (2006). *Name reactions : a collection of detailed reaction mechanisms*. Springer, Berlin, New York, 3rd expanded edition.

Li, Y., Shi, X., Zong, M., Meng, C., Dong, Y., Guo, Y. (2007). Asymmetric reduction of 2-octanone in water/organic solvent biphasic system with baker's yeast FD-12. *Enzyme and Microbial Technology*, 40(5):1305–1311.

Liese, A. (1998). A novel reactor concept for the enzymatic reduction of poorly soluble ketones. *Journal of Molecular Catalysis B: Enzymatic*, 4(1-2):91–99.

Liese, A., Filho, M. V. (1999). Production of fine chemicals using biocatalysis. *Current Opinion in Biotechnology*, 10(6):595–603.

Link, H. (2009). *Rapid media transition for metabolic control analysis of fed-batch fermentation processes*. PhD thesis, Technische Universität München.

Lou, W., Wang, W., Li, R., Zong, M. (2009a). Efficient enantioselective reduction of 4-methoxyacetophenone with immobilized *Rhodotorula* sp. AS2.2241 cells in a hydrophilic ionic liquid-containing co-solvent system. *Journal of Biotechnology*, 143(3):190–197.

Lou, W., Wang, W., Smith, T. J., Zong, M. (2009b). Biocatalytic anti-Prelog stereoselective reduction of 4-methoxyacetophenone to *R*-1-(4-methoxyphenyl)ethanol with immobilized *Trigonopsis variabilis* AS2.1611 cells using an ionic liquid-containing medium. *Green Chemistry*, 11(9):1377.

Lou, W., Zong, M., Smith, T. J. (2006). Use of ionic liquids to improve whole-cell biocatalytic asymmetric reduction of acetyltrimethylsilane for efficient synthesis of enantiopure *s*-1-trimethylsilylethanol. *Green Chemistry*, 8(2):147.

Lye, G., Woodley, J. (1999). Application of in situ product-removal techniques to biocatalytic processes. *Trends in Biotechnology*, 17(10):395–402.

Machielsen, R., Looger, L. L., Raedts, J., Dijkhuizen, S., Hummel, W., Hennemann, H., Daussmann, T., van der Oost, J. (2009). Cofactor engineering of *Lactobacillus brevis* alcohol dehydrogenase by computational design. *Engineering in Life Sciences*, 9(1):38–44.

Mahnke, E. U., Büscher, K., Hempel, D. C. (2000). A novel approach for the determination of mechanical stresses in Gas-Liquid reactors. *Chemical Engineering & Technology*, 23(6):509–513.

Mantz, R. A., Trulove, P. C. (2003). Viscosity and density of ionic liquids. In *Ionic Liquids in Synthesis*, pages 56–68. Wiley-VCH, Weinheim, Germany.

Marquardt, E. (1997). Adaptive filter algorithms for interference patterns of diffusion measurements. *Optical Engineering*, 36(10):2857.

Marquardt, E. (1998). Digital image holography. *Optical Engineering*, 37(5):1514.

Marsh, K. (2004). Room temperature ionic liquids and their mixtures – a review. *Fluid Phase Equilibria*, 219(1):93–98.

Matsuda, T., Yamagishi, Y., Koguchi, S., Iwai, N., Kitazume, T. (2006). An effective method to use ionic liquids as reaction media for asymmetric reduction by geotrichum candidum. *Tetrahedron Letters*, 47(27):4619–4622.

Matsumoto, M., Mochiduki, K., Kondo, K. (2004). Toxicity of ionic liquids and organic solvents to lactic acid-producing bacteria. *Journal of Bioscience and Bioengineering*, 98(5):344–347.

Mebane, R. C., Holte, K. L., Gross, B. H. (2007). Transfer hydrogenation of ketones with 2-propanol and Raney Nickel. *Synthetic Communications*, 37(16):2787–2791.

Mesentsev, A. V., Lamzin, V. S., Tishkov, V. I., Ustinnikova, T. B., Popov, V. O. (1997). Effect of pH on kinetic parameters of NAD^+-dependent formate dehydrogenase. *The Biochemical Journal*, 321 (Pt 2):475–480.

Moss, G. P. (1996). Basic terminology of stereochemistry (IUPAC recommendations 1996). *Pure and Applied Chemistry*, 68(12):2193–2222.

Müller, J. (2000). *Röntgenstrukturanalyse der R-spezifischen Alkoholdehydrogenase aus Lactobacillus brevis bei 0.99 Å Auflösung und röntgenkristallographische Untersuchung an der D-Aminosäureoxidase aus Trigonopsis variabilis*. PhD thesis, Universität zu Köln.

Nakamura, K., Matsuda, T. (1998). Asymmetric reduction of ketones by the acetone powder of geotrichum candidum. *The Journal of Organic Chemistry*, 63(24):8957–8964.

Nakamura, K., Yamanaka, R., Matsuda, T., Harada, T. (2003). Recent developments in asymmetric reduction of ketones with biocatalysts. *Tetrahedron: Asymmetry*, 14(18):2659–2681.

Nguyen, L. A., He, H., Pham-Huy, C. (2006). Chiral drugs. An overview. *International Journal of Biomedical Science*, 2(2):85–100.

Nie, Y., Xu, Y., Mu, X. Q., Tang, Y., Jiang, J., Sun, Z. H. (2005). High-yield conversion of (R)-2-octanol from the corresponding racemate by stereoinversion using *Candida rugosa*. *Biotechnology Letters*, 27(1):23–26.

Niefind, K., Müller, J., Riebel, B., Hummel, W., Schomburg, D. (2003). The crystal structure of r-specific alcohol dehydrogenase from *Lactobacillus brevis* suggests the structural basis of its metal dependency. *Journal of Molecular Biology*, 327(2):317–328.

Nielsen, J., Villadsen, J. (1994). *Bioreaction engineering principles*. Plenum Press, New York.

Öhrner, N., Orrenius, C., Mattson, A., Norin, T., Hult, K. (1996). Kinetic resolutions of amine and thiol analogues of secondary alcohols catalyzed by the *Candida antarctica* lipase b. *Enzyme and Microbial Technology*, 19(5):328–331.

Ohtani, H., Ishimura, S., Kumai, M. (2008). Thermal decomposition behaviors of imidazolium-type ionic liquids studied by pyrolysis-gas chromatography. *Analytical Sciences*, 24(10):1335–1340.

Osawa, T., Nakagawa, Y., Harada, T., Takayasu, O. (2006). Studies of the effect of pivalic acid on the hydrogenation rate and the enantio-differentiating ability for the hydrogenation of 2-octanone over a tartaric acid-NaBr-modified Nickel catalyst. *Catalysis Letters*, 112(3):163–166.

Osawa, T., Sawada, K., Harada, T., Takayasu, O. (2004). Repeated use of the *in-situ* modified nickel catalyst for the enantio-differentiating hydrogenation of 2-octanone. *Applied Catalysis A: General*, 264(1):33–36.

Othmer, D. F., Thakar, M. (1955). Corrections: "Correlating diffusion coefficients in liquids". *Industrial & Engineering Chemistry*, 47(8):1604.

Ou, G., Zhu, M., She, J., Yuan, Y. (2006). Ionic liquid buffers: a new class of chemicals with potential for controlling pH in non-aqueous media. *Chemical Communications*, (44):4626.

Patel, R. N. (2002). Microbial/enzymatic synthesis of chiral intermediates for pharmaceuticals. *Enzyme and Microbial Technology*, 31(6):804–826.

Paul, E., Atiemo-Obeng, V. A., Kresta, S. M. (2004). *Handbook of industrial mixing science and practice*. Wiley-Interscience, Hoboken, N.J.

Pernak, J. (2001). Synthesis and antimicrobial activities of new pyridinium and benzimidazolium chlorides. *European Journal of Medicinal Chemistry*, 36(4):313–320.

Pernak, J., Goc, I., Mirska, I. (2004). Anti-microbial activities of protic ionic liquids with lactate anion. *Green Chemistry*, 6(7):323.

Pernak, J., Smiglak, M., Griffin, S. T., Hough, W. L., Wilson, T. B., Pernak, A., Zabielska-Matejuk, J., Fojutowski, A., Kita, K., Rogers, R. D. (2006). Long alkyl chain quaternary ammonium-based ionic liquids and potential applications. *Green Chemistry*, 8(9):798.

Pernak, J., Sobaszkiewicz, K., Mirska, I. (2003). Anti-microbial activities of ionic liquids. *Green Chemistry*, 5(1):52–56.

Perry, R. (1999). *Perry's chemical engineer's platinum edition: Perry's chemical engineers' handbook*. McGraww-Hill, New York, 7. edition.

Pfruender, H., Amidjojo, M., Kragl, U., Weuster-Botz, D. (2004). Efficient Whole-Cell biotransformation in a biphasic ionic Liquid/Water system. *Angewandte Chemie International Edition*, 43(34):4529–4531.

Pfruender, H., Jones, R., Weuster-Botz, D. (2006). Water immiscible ionic liquids as solvents for whole cell biocatalysis. *Journal of Biotechnology*, 124(1):182–190.

Pfründer, H. (2005). *Ganzzell-Biokatalyse in Gegenwart ionischer Flüssigkeit*. PhD thesis, Technische Universität München.

Phumathon, P. (1999). Production of toluene cis-glycol using recombinant *Escherichia coli* strains in glucose-limited fed batch culture. *Enzyme and Microbial Technology*, 25(10):810–819.

Prelog, V. (1964). Specification of the stereospecificity of some oxido-reductases by diamond lattice sections. *Pure and Applied Chemistry*, 9(1):119–130.

Puskeiler, R., Kaufmann, K., Weuster-Botz, D. (2005). Development, parallelization, and automation of a gas-inducing milliliter-scale bioreactor for high-throughput bioprocess design (HTBD). *Biotechnology and Bioengineering*, 89(5):512–523.

Rajagopal, A. (1996). Growth of gram-negative bacteria in the presence of organic solvents. *Enzyme and Microbial Technology*, 19(8):606–613.

Ranke, J., Mölter, K., Stock, F., Bottin-Weber, U., Poczobutt, J., Hoffmann, J., Ondruschka, B., Filser, J., Jastorff, B. (2004). Biological effects of imidazolium ionic liquids with varying chain lengths in acute *Vibrio fischeri* and WST-1 cell viability assays. *Ecotoxicology and Environmental Safety*, 58(3):396–404.

Ranke, J., Müller, A., Bottin-Weber, U., Stock, F., Stolte, S., Arning, J., Störmann, R., Jastorff, B. (2007a). Lipophilicity parameters for ionic liquid cations and their correlation to *in vitro* cytotoxicity. *Ecotoxicology and Environmental Safety*, 67(3):430–438.

Ranke, J., Othman, A., Fan, P., Müller, A. (2009). Explaining ionic liquid water solubility in terms of cation and anion hydrophobicity. *International Journal of Molecular Sciences*, 10(3):1271–1289.

Ranke, J., Stolte, S., Störmann, R., Arning, J., Jastorff, B. (2007b). Design of sustainable chemical ProductsThe example of ionic liquids. *Chemical Reviews*, 107(6):2183–2206.

Reddy, K. A., Doraiswamy, L. K. (1967). Estimating liquid diffusivity. *Industrial & Engineering Chemistry Fundamentals*, 6(1):77–79.

Reid, R. (1988). *The properties of gases and liquids*. McGraw-Hill, New York, 4th ed. edition.

Riedlberger, P., Weuster-Botz, D. (2010). *Patent DE 20 2010 011 902.2*.

Rolo, L. I., Caco, A. I., Queimada, A. J., Marrucho, I. M., Coutinho, J. A. P. (2002). Surface tension of heptane, decane, hexadecane, eicosane, and some of their binary mixtures. *Journal of Chemical & Engineering Data*, 47(6):1442–1445.

Roosen, C., Müller, P., Greiner, L. (2008). Ionic liquids in biotechnology: applications and perspectives for biotransformations. *Applied Microbiology and Biotechnology*, 81(4):607–614.

Roth, W., Scheel, K. (1923). *Landolt-Börnstein Physikalisch-Chemische Tabellen*. Springer, Berlin.

Sardessai, Y. (2002). Tolerance of bacteria to organic solvents. *Research in Microbiology*, 153(5):263–268.

Scammells, P. J., Scott, J. L., Singer, R. D. (2005). Ionic liquids: The neglected issues. *Australian Journal of Chemistry*, 58(3):155.

Schlieben, N. H., Niefind, K., Müller, J., Riebel, B., Hummel, W., Schomburg, D. (2005). Atomic resolution structures of R-specific alcohol dehydrogenase from *Lactobacillus brevis* provide the structural bases of its substrate and cosubstrate specificity. *Journal of Molecular Biology*, 349(4):801–813.

Schmid, A., Dordick, J. S., Hauer, B., Kiener, A., Wubbolts, M., Witholt, B. (2001). Industrial biocatalysis today and tomorrow. *Nature*, 409(6817):258–268.

Schroer, K., Tacha, E., Lütz, S. (2007). Process intensification for substrate-coupled whole cell ketone reduction by in situ acetone removal. *Organic Process Research & Development*, 11(5):836–841.

Schügerl, K. (2009). *Solvent extraction in biotechnology: Recovery of primary and secondary metabolites*. Springer Berlin Heidelberg, Berlin Heidelberg.

Schütte, H., Flossdorf, J., Sahm, H., Kula, M. R. (1976). Purification and properties of formaldehyde dehydrogenase and formate dehydrogenase from *Candida boidinii*. *European Journal of Biochemistry / FEBS*, 62(1):151–160.

Seddon, K. R. (1997). Ionic liquids for clean technology. *J. Chem. Technol. Biotechnol.*, 68(4):351–356.

Seddon, K. R., Stark, A., Torres, M. (2000). Influence of chloride, water, and organic solvents on the physical properties of ionic liquids. *Pure and Applied Chemistry*, 72(12):2275–2287.

Segel, I. (1993). *Enzyme kinetics : behavior and analysis of rapid equilibrium and steady state enzyme systems*. Wiley, New York, Wiley classics library edition.

Sherwood, T., Pigford, R., Wilke, C. R. (1975). *Mass transfer*. McGraw-Hill, New York.

Shi, X., Rong, J., Li, Y., Guo, Y., Zong, M. (2008). Effect of surfactant on asymmetric bioreduction of 2-octanone catalyzed by whole cell of *Saccharomyces cerevisiae*. *Journal of Biotechnology*, 136:S383–S383.

Skelland, A., Tedder, D. W. (1987). *Handbook of separation process technology*, chapter : Extraction - Organic chemicals processing, pages 405–466. Wiley.

Skelland, A. H. P., Lee, J. M. (1981). Drop size and continuous-phase mass transfer in agitated vessels. *AIChE Journal*, 27(1):99–111.

Skelland, A. H. P., Lee, J. M. (1982). Errata. *AIChE Journal*, 28(6):1043.

Skelland, A. H. P., Moeti, L. T. (1990). Mechanism of continuous-phase mass transfer in agitated liquid-liquid systems. *Industrial & Engineering Chemistry Research*, 29(11):2258–2267.

Slusarczyk, H., Felber, S., Kula, M., Pohl, M. (2000). Stabilization of NAD-dependent formate dehydrogenase from *Candida boidinii* by site-directed mutagenesis of cysteine residues. *European Journal of Biochemistry*, 267(5):1280–1289.

Speight, J. G. (2005). *Lange's handbook of chemistry*. McGraw-Hill, New York, 16th edition.

Staak, A. (2010). *Glossar*. Helmholtz-Zentrum für Umweltforschung UFZ, http://www.leipziger-kubus.ufz.de/index.php?de=12245.

Stolte, S., Arning, J., Bottin-Weber, U., Müller, A., Pitner, W., Welz-Biermann, U., Jastorff, B., Ranke, J. (2007a). Effects of different head groups and functionalised side chains on the cytotoxicity of ionic liquids. *Green Chemistry*, 9(7):760.

Stolte, S., Matzke, M., Arning, J., Böschen, A., Pitner, W., Welz-Biermann, U., Jastorff, B., Ranke, J. (2007b). Effects of different head groups and functionalised side chains on the aquatic toxicity of ionic liquids. *Green Chemistry*, 9(11):1170.

Straathof, A., Panke, S., Schmid, A. (2002). The production of fine chemicals by biotransformations. *Current Opinion in Biotechnology*, 13(5):548–556.

Swatloski, R. P., Holbrey, J. D., Rogers, R. D. (2003). Ionic liquids are not always green: hydrolysis of 1-butyl-3-methylimidazolium hexafluorophosphate. *Green Chemistry*, 5(4):361.

Tanaka, H., Harada, S., Kurosawa, H., Yajima, M. (1987). A new immobilized cell system with protection against toxic solvents. *Biotechnology and Bioengineering*, 30(1):22–30.

Tanaka, T., Iwai, N., Matsuda, T., Kitazume, T. (2009). Utility of ionic liquid for *Geotrichum candidum*-catalyzed synthesis of optically active alcohols. *Journal of Molecular Catalysis B: Enzymatic*, 57(1-4):317–320.

Taylor, G. (1953). Dispersion of soluble matter in solvent flowing slowly through a tube. *Proceedings of the Royal Society A: Mathematical, Physical and Engineering Sciences*, 219(1137):186–203.

Taylor, G. (1954). Conditions under which dispersion of a solute in a stream of solvent can be used to measure molecular diffusion. *Proceedings of the Royal Society A: Mathematical, Physical and Engineering Sciences*, 225(1163):473–477.

Terashima, T., Ouchi, M., Ando, T., Sawamoto, M. (2010). Thermoregulated phase-transfer catalysis via PEG-armed Ru(II)-bearing microgel core star polymers: Efficient and reusable Ru(II) catalysts for aqueous transfer hydrogenation of ketones. *Journal of Polymer Science Part A: Polymer Chemistry*, 48(2):373–379.

Trincone, A., Lama, L., Lanzotti, V., Nicolaus, B., Rosa, M. D., Rossi, M., Gambacorta, A. (1990). Asymmetric reduction of ketones with resting cells of *Sulfolobus solfataricus*. *Biotechnology and Bioengineering*, 35(6):559–564.

Tsai, J., Wahbi, L., Dervakos, G., Stephens, G. (1996). Production of toluene cis-glycol by a recombinant escherichia coli strain in a two-liquid phase culture system. *Biotechnology Letters*, 18(3).

Tyn, M. T., Calus, W. F. (1975). Diffusion coefficients in dilute binary liquid mixtures. *Journal of Chemical & Engineering Data*, 20(1):106–109.

van Rantwijk, F., Lau, R. M., Sheldon, R. A. (2003). Biocatalytic transformations in ionic liquids. *Trends in Biotechnology*, 21(3):131–138.

van Rantwijk, F., Sheldon, R. A. (2007). Biocatalysis in ionic liquids. *Chemical Reviews*, 107(6):2757–2785.

Vermuë, M., Sikkema, J., Verheul, A., Bakker, R., Tramper, J. (1993). Toxicity of homologous series of organic solvents for the gram-positive bacteria *Arthrobacter* and *Nocardia* sp. and the gram-negative bacteria *Acinetobacter* and *Pseudomonas* sp. *Biotechnology and Bioengineering*, 42(6):747–758.

Vester, A., Hans, M., Hohmann, H., Weuster-Botz, D. (2009). Discrimination of riboflavin producing *Bacillus subtilis* strains based on their fed-batch process performances on a millilitre scale. *Applied Microbiology and Biotechnology*, 84(1):71–76.

Voss, C., Gruber, C., Kroutil, W. (2008). Deracemization of secondary alcohols through a concurrent tandem biocatalytic oxidation and reduction. *Angewandte Chemie International Edition*, 47(4):741–745.

Walden, P. (1914). Molecular weights and electrical conductivity of several fused salts. *Bulletin de l'Académie Impériale des Sciences de St.-Pétersbourg*, pages 405–422.

Wandschneider, A., Lehmann, J. K., Heintz, A. (2008). Surface tension and density of pure ionic liquids and some binary mixtures with 1-Propanol and 1-Butanol. *Journal of Chemical & Engineering Data*, 53(2):596–599.

Wang, C. Y., Calabrese, R. V. (1986). Drop breakup in turbulent stirred-tank contactors. Part II: Relative influence of viscosity and interfacial tension. *AIChE Journal*, 32(4):667–676.

Wang, W., Zong, M., Lou, W. (2009). Use of an ionic liquid to improve asymmetric reduction of 4-methoxyacetophenone catalyzed by immobilized *Rhodotorula* sp. AS2.2241 cells. *Journal of Molecular Catalysis B: Enzymatic*, 56(1):70–76.

Wasserscheid, P., Keim, W. (2000). Ionic liquids - new solutions for transition metal catalysis. *Angewandte Chemie International Edition*, 39(21):3772–3789.

Wasserscheid, P., Welton, T. (2003). *Ionic liquids in synthesis*. Wiley-VCH, Weinheim.

Welty, J. R., Wicks, C. E., Wilson, R. E., Rorrer, G. (2001). *Fundamentals of momentum, heat, and mass transfer*. Wiley, New York, 4th ed. edition.

Weuster-Botz, D. (1999). Die Rolle der Reaktionstechnik in der mikrobiellen Verfahrensentwicklung. Schriften des Forschnungszentrum Jülich. Reihe Lebenswissenschaften/Life Science. Forschungszentrum Jülich GmbH.

Weuster-Botz, D., Puskeiler, R., Kusterer, A., Kaufmann, K., John, G. T., Arnold, M. (2005). Methods and milliliter scale devices for high-throughput bioprocess design. *Bioprocess and Biosystems Engineering*, 28(2):109–119.

Weuster-Botz, D., Stevens, S., Hawrylenko, A. (2002). Parallel-operated stirred-columns for microbial process development. *Biochemical Engineering Journal*, 11(1):69–72.

Wilke, C. R., Chang, P. (1955). Correlation of diffusion coefficients in dilute solutions. *AIChE Journal*, 1(2):264–270.

Wilkes, J. S., Levisky, J. A., Wilson, R. A., Hussey, C. L. (1982). Dialkylimidazolium chloroaluminate melts: a new class of room-temperature ionic liquids for electrochemistry, spectroscopy and synthesis. *Inorganic Chemistry*, 21(3):1263–1264.

Wolfson, A., Dlugy, C., Tavor, D., Blumenfeld, J., Shotland, Y. (2006). Baker's yeast catalyzed asymmetric reduction in glycerol. *Tetrahedron: Asymmetry*, 17(14):2043–2045.

Wooster, T. J., Johanson, K. M., Fraser, K. J., MacFarlane, D. R., Scott, J. L. (2006). Thermal degradation of cyano containing ionic liquids. *Green Chemistry*, 8(8):691.

Yang, Z., Zeng, R., Wang, Y., Li, X., Lv, Z., Lai, B., Yang, S., Liao, J. (2009). Tolerance of immobilized yeast cells in imidazolium-based ionic liquids. *Food Technology and Biotechnology*, 47(1):62–66.

Yu, D., Wang, Z., Chen, P., Jin, L., Cheng, Y., Zhou, J., Cao, S. (2007a). Microwave-assisted resolution of (R,S)-2-octanol by enzymatic transesterification. *Journal of Molecular Catalysis B: Enzymatic*, 48(1-2):51–57.

Yu, D., Wang, Z., Zhao, L., Cheng, Y., Cao, S. (2007b). Resolution of 2-octanol by SBA-15 immobilized *Pseudomonas* sp. lipase. *Journal of Molecular Catalysis B: Enzymatic*, 48(3-4):64–69.

Zhang, F., Ni, Y., Sun, Z., Zheng, P., Lin, W., Zhu, P., Ju, N. (2008). Asymmetric reduction of ethyl 4-chloro-3-oxobutanoate to ethyl (S)-4-chloro-3-hydroxybutanoate catalyzed by *Aureobasidium pullulans* in an aqueous/ionic liquid biphase system. *Chinese Journal of Catalysis*, 29(6):577–582.

Zhang, S., Sun, N., He, X., Lu, X., Zhang, X. (2006). Physical properties of ionic liquids: Database and evaluation. *Journal of Physical and Chemical Reference Data*, 35(4):1475.

Zhang, W., Ni, Y., Sun, Z., Zheng, P., Lin, W., Zhu, P., Ju, N. (2009). Biocatalytic synthesis of ethyl (R)-2-hydroxy-4-phenylbutyrate with *Candida krusei* SW2026: a practical process for high enantiopurity and product titer. *Process Biochemistry*, 44(11):1270–1275.

Zlokarnik, M. (1999). *Rührtechnik : Theorie und Praxis*. Springer, Berlin.

Appendices

A Abbreviations

Table A.1: General abbreviations.

Abbreviation	Signification
ADH	alcohol dehydrogenase
CFU	colony forming units, -
CB FDH	*Candida boidinii* formate dehydrogenase
DCW	dry cell weight, g
DO	dissolved oxygen, %
E. coli	*Escherichia coli*
ee	enantiomeric excess, %
FDH	formate dehydrogenase
IL	ionic liquid
IPTG	Isopropyl β-D-1-thiogalactopyranoside
LB ADH	*Lactobacillus brevis* alcohol dehydrogenase
log $D_{IL/aq}$	decadic logarithm of the partition coefficient of a substance between the ionic liquid and the aqueous phase, -
log $D_{IL/hexane}$	decadic logarithm of the partition coefficient of a substance between the ionic liquid and *n*-hexane, -
log P	decadic logarithm of the partition coefficient of a substance between octanol and water
MTBE	methyl *tert*-butyl ether
MTP	microtiter plate
NAD^+	nicotinamide adenine dinucleotide (oxidized form)
NADH	nicotinamide adenine dinucleotide (reduced form)
OD	optical density, -
PBS	phosphate buffered saline
U	units, unit for the enzyme activity (1 U = 1 μmol s^{-1})

Table A.1: General abbreviations. (continued)

Abbreviation	Signification
vvm	L air (L culture medium)$^{-1}$ min^{-1}
wt	weight, g

Table A.2: General abbreviations: subscripts.

Abbreviation	Signification
subscript c	continuous phase
subscript d	dispersed phase
subscript i	substance i
subscript P	product
subscript S	substrate
subscript x	biomass

Table A.3: Ionic liquid cations and their abbreviation.

Abbreviation	Cation
[BMIM]	1-butyl-3-methylimidazolium
[BMPL]	1-butyl-1-methylpyrrolidinium
[C2OHMIM]	1-(2'-hydroxy)ethyl-3-methylimidazolium
[CABHEM]	PEG-5 cocomonium
[(EO2E)MPL]	1-(ethoxycarbonyl)methyl-1-methylpyrrolidinium
[(EOE)MMO]	4-(2-ethoxyethyl)-4-methylmorpholinium
[EMIM]	1-ethyl-3-methylimidazolium
[EtOHNMe3]	2-hydroxy ethyl trimethylammonium
[EWTMG]	N,N,N,N-tetramethyl-N-ethylguanidinium
[HMIM]	1-hexyl-3-methylimidazolium
[HMPL]	1-hexyl-1-methylpyrrolidinium
[HPYR]	1-hexyl-3-methylpyridinium
[(MOE)MPL]	1-(2-methoxyethyl)-1-methylpyrrolidinium
[(MOP)MPI]	1-(3-methyoxypropyl)-1-methylpiperidinium
[(NEMM)EO2E]	ethyl-dimethyl-(ethoxycarbonyl)methylammonium

Table A.3: Ionic liquid cations and their abbreviation (continued).

Abbreviation	Cation
[(NEMM)MOE]	ethyl-dimethyl-2-methoxyethylammonium
[Oc3MeN]	methyltrioctylammonium
[OMIM]	1-octyl-3-methylimidazolium
[(P3OH)PYR]	N-(3-hydroxypropyl)pyridinium

Table A.4: Ionic liquid anions and their abbreviation.

Abbreviation	Anion
[BF4]	tetrafluoroborate
[Br]	bromide
[CF3SO3]	trifluoromethanesulfonate
[Cl]	chloride
[E3FAP]	tris(pentafluoroethyl)trifluorophosphate
[EtSO4]	ethylsulfate
[MDEGSO4]	ethylenglycolmonomethyl ethersulfate
[ME2PO4]	dimethylphosphate
[MeSO4]	methysulfate
[No3]	nitrate
[NTF]	bis(trifluoromethylsulfonyl)imide
[OcSO4]	octylsulfate
[PF6]	hexafluorophosphate
[SbF6]	hexafluoroantimonate
[TOS]	tosylate

Table A.5: List of symbols.

Symbol	Signification	Unit
A	enzyme activity at time t	U mg^{-1}
A_0	enzyme activity at time t = 0	U mg^{-1}
A_{340}	absorption at 340 nm	-
a_d	interfacial area	m^2
b	path length of the sample	cm
c_D	dissipation constant	-
$C_{i,aq}$	concentration of i in the aqueous phase, mol L^{-1}	
$C_{i,cell}$	concentration of i in the cell, mol L^{-1}	
$C_{i,IL}$	concentration of i in the ionic liquid phase, mol L^{-1}	
C^*_i	equilibrium concentration of i between the aqueous and the ionic liquid phase, mol L^{-1}	
c_{aq}	equilibrium concentration in the aqueous buffer after the extraction	mol L^{-1}
c_{IL}	concentration in the ionic liquid after extraction with *n*-hexane	mol L^{-1}
$c_{hexane,0}$	initial concentration in *n*-hexane	mol L^{-1}
c_{hexane}	equilibrium concentration in *n*-hexane after the extraction	mol L^{-1}
$c_{i,c}$	concentration of i in the bulk of the continuous phase	mol L^{-1}
$c_{i,c}^*$	equilibrium concentration of i at the interface	mol L^{-1}
$c_{i,m}$	concentration of i in the membrane	mol m^{-3}
$c_{i,w}$	concentration of i in the surrounding liquid	mol m^{-3}
c_{NADH}	NADH concentration	g L^{-1}
$c_{S,feed}$	concentration of the limiting substrate in the feed	g L^{-1}
c_S	concentration of the limiting substrates	mol L^{-1}
c_x	cell concentration	g_{DCW} L^{-1}
d	thickness of the membrane	m
d_i	average drop size of the size fraction i	m
$D_{i,c}$	diffusion coefficient of i in the continuous phase	m^2 s^{-1}
$D_{i,m}$	diffusion coefficient of i in the membrane	m^2 s^{-1}
d_{32}	Sauter diameter	m
$D_{IL/aq,\ i}$	partition coefficient of i between the ionic liquid and the aqueous phase	-

Table A.5: List of symbols (continued).

Symbol	Signification	Unit
d_j	average drop size of the size fraction j	m
d_R	stirrer diameter	m
D_R	reactor diameter	m
EA_x	enzyme activity	U g_{DCW}^{-1}
Fr	Froude number	-
h	height of the stirrer blade	m
J_i	mass transfer flux density	mol s^{-1} m^{-2}
J_n	mass flux, m L^{-1} s^{-1}	
K_i	partition coefficient of i between the surrounding liquid and the membrane	-
k_i	inactivation constant	h^{-1}
K_m	half saturation constant	mol L^{-1}
K_S	half-saturation constant	mol L^{-1}
M_c	molar weight of the solvent	g mol^{-1}
$m_{x,total}$	total cell mass, g_{DCW}	
MV_i	molar volume of i at its boiling temperature	cm^3 mol^{-1}
N_R	stirrer speed	s^{-1}
n_i	number of drops in the size fraction i	-
n_j	number of drops in the size fraction j	-
n_S	substrate quantity at time t	mol
$n_{S,0}$	initial substrate quantity	mol
n_R	quantity of *R*-enantiomer	mol
n_S	quantity of *S*-enantiomer	mol
n_P	product quantity at t	mol
Oh	Ohnesorge number	-
p_c	parachor of the solvent	cm^3 $g^{0.25}$ mol^{-1} $s^{-0.5}$
P_i	membrane permeability of i	m s^{-1}
p_i	parachor of the solute	cm^3 $g^{0.25}$ mol^{-1} $s^{-0.5}$
Re	Reynolds number	-
[S]	substrate concentration	mol L^{-1}
Sc_c	Schmidt number of the continuous phase	-

Table A.5: List of symbols (continued).

Symbol	Signification	Unit
Sh	Sherwood number	-
STR	substrate transfer rate	mol L^{-1} s^{-1}
STY	space-time yield	mol L^{-1} h^{-1}
T	temperature	K
t	time	h
$t_{0,feed}$	cultivation time when the feeding is started	h
u_{tip}	stirrer tip speed	m s^{-1}
V_R	reaction volume	L
V	culture volume	L
V_{aq}	volume of the aqueous phase, L	
V_{IL}	volume of the ionic liquid, L	
V_x	sample volume	L
$V_{x,total}$	total cell volume, L	
v	reaction rate	mol s^{-1}
v_{max}	maximal reaction rate	mol s^{-1}
$\dot{V}$	feeding rate	L h^{-1}
Vi	viscosity group	-
We	Weber number	-
X	conversion	%
Y	yield	%
$Y_{X,S}$	biomass to substrate yield	g_{DCW} g_S^{-1}

Table A.6: List of greek symbols.

Symbol	Signification	Unit
β_i	mass transfer coefficient of i	m s^{-1}
ε_{NADH}	molar extinction coefficient of NADH	L mol^{-1} cm^{-1}
ε_{max}	maximum local energy dissipation	W kg^{-1}
$\bar{\eta}$	combined viscosity	Pa s
η_d	viscosity of the dispersed phase	Pa s
μ	specific growth rate	h^{-1}
μ_{max}	growth rate under non-limiting conditions	h^{-1}
μ_{set}	specific growth rate fixed	h^{-1}

Table A.6: List of greek symbols (continued).

Symbol	Signification	Unit
ν_S	stoichiometric factor of the substrate	-
ν_P	stoichiometric factor of the product	-
Φ_c	association coefficient of the solvent	-
φ_d	phase fraction of the dispersed phase	-
φ_{IL}	volume fraction of the ionic liquid in the extraction step	-
$\bar{\rho}$	combined density	kg m^{-3}
ρ_c	density of the continuous phase	kg m^{-3}
ρ_d	density of the dispersed phase	kg m^{-3}
$\sigma_{d,c}$	interfacial tension between the dispersed and the continuous phase	N m^{-1}
τ	half-life	h

B Equipment

Table B.7: General equipment.

Equipment	**Producer**
3D-ORM-probe Typ 6XX	MTS, Düsseldorf, Germany
Analytic scale Explorer E1M213	Ohaus, Gießen, Germany
Analytic scale Extend ED124S	Satorius, Göttingen, Germany
Autoklav Varioklav 500 E	H+P Labortechnik, Oberschleißheim
Bench-top centrifuge Biofuge Stratos	Kendro-Heraeus, Langenselbold, Germany
Bench-top centrifuge Mikro 20	Hettich, Tuttlingen, Germany
Drying oven E28	Binder, Tuttlingen, Germany
Floor-standing centrifuge Rotixa 50 RS	Hettich, Tuttlingen, Germany
Incubator Multitron II	Infors, Einsbach, Germany
Magnetic stirring plate Variomag	H+P Labortechnik, Oberschleißheim
Micropipette 200 μl Transferpipette S	Brand, Wertheim, Germany
Micropipette 20 μl, 1000 μl	Eppendorf, Hamburg, Germany
Microscope Axiolab drb KT	Zeiss, Oberkochen, Germany
Mixer mill MM200	Retsch, Haan, Germany
MTP-photometer EL 808IU	Bio-Tek Instruments, Bad Friedrichshall, Germany
MTP-photometer Software KC Junior v.1.10	Bio-Tek Instruments, Bad Friedrichshall, Germany
Multistirrer plate Multipoint 15	H+P Labortechnik, Oberschleißheim
Multistirrer plate Variomag Poly 15	H+P Labortechnik, Oberschleißheim
pH-electrode BlueLine 24 pH	Schott, Mainz, Germany
pH-meter CG 843	Schott, Mainz, Germany
Photometer Genesys 20	Thermo Spectronic, Neuss, Germany
Tensiometer K10	Krüss, Hamburg, Germany
Tensiometer K100C	Krüss, Hamburg, Germany
Thermomixer comfort	Eppendorf, Hamburg, Germany
Viscosimeter Rheomat 115	Concraves, Zürich, Schweiz
Vortex REAX top	Heidolph, Schwabach, Germany

Table B.8: Gas chromatograph and chromatographic column.

Equipment	Producer/Specification
Gas chromatograph CP-3800	Varian, Darmstadt, Germany
Injector 1079 PTV	temperature programmable
Split control	electronic flow control (EFC)
Chromatographic column BGB-175	BGB Analytik, Germany, length 30 m, internal diameter 0,25 mm, 0,25 μm
Flame ionisation detector	fuel gas: hydrogen and air, carrier gas/make-up-gas: helium
Software Star Version 5.51	Varian, Darmstadt, Germany
Autosampler CombiPal	CTC Analytics, Zwingen, Switzerland
Helium 99.999 % (v/v)	Air Liquide, Krefeld, Germany
Hydrogen 99.999 % (v/v)	Air Liquide, Krefeld, Germany
Synthetic air	house pipe

Table B.9: Stirred tank reactors used for cell cultures and biotransformations.

Equipment	Producer/Specification
Labfors reactor, 7.5 L	Infors HT, Bottmingen-Basel, Switzerland
Labfors reactor, 1.2 L	Infors HT, Bottmingen-Basel, Switzerland
Stirrer	2 six-bladed Rushton impellors
Drive	top, mechanical seal drive coupling
Aeration	mass flow valve sparger
Control station	Infors HT, Bottmingen-Basel, Switzerland
Software Iris-NT Pro Version 4.11	Infors HT, Bottmingen-Basel, Switzerland
pH electrode 405-DPAS-SC-K8S/325	Mettler-Toledo, Gießen, Germany
pH electrode HA405-DPA-SC-S8	Mettler-Toledo, Giessen, Germany
pO_2-probe InPro 6000	Mettler-Toledo, Giessen, Germany
Exhaust gas analyser Easy Line	ABB-Frankfurt, Germany
Exhaust gas filter Sartobran 300 2 μm	Watson-Marlow, Rommerskirchen, Germany
Mass flow controller Advance SCC-F	ABB, Frankfurt, Germany
Pump ISM 444 Ismatec	Glattbrugg, Schweiz

Table B.9: Stirred tank reactors used for cell cultures and biotransformations (continued).

Equipment	**Producer/Specification**
Profors bubble column 400 mL	Infors HT, Bottmingen-Basel, Switzerland
Magnetic drive Microtec AK 120	Infors, Einsbach, Germany
Stirrer	six-bladed Rushton impellor
Drive	bottom, magnetic drive

Table B.10: Rotary evaporator.

Equipment	**Producer/Specification**
Rotary evaporator LABOROTA 4003	Heidolph, Schwabach, Germany
Vacuum pump ROTAVAC vario control	Heidolph, Schwabach, Germany

C Consumables

In addition to the standard consumables, the consumables listed in Table C.11 were used.

Table C.11: Special consumables.

Consumable	**Producer**	**Article number**
Aluminium crimp caps ND11	VRW	548-0010
Crimp vials ND9	VRW	548-0029
Filters, Ø 0,22 μm	Roth	KH54
Glas beads, Ø 0,25-0,50 mm	Roth	A553
Magnetic stirrers, Ø 10 mm	VWR	442-0075
Rotilabo®glas vials, Ø 15 mm	Roth	H306.1
Screw caps N9 blau	Macherey-Nagel	702 285
Screw vials N9-1	Macherey-Nagel	702 283

D Chemicals

Table D.12: General chemicals.

Chemical	Purity	Producer	Article number
Agar-Agar	n.a.	Roth	5210
Acetophenon	≥ 98 %	Merck	800028
Ammonia, 25 %	puriss.	Roth	5460
Ammonium chloride	≥ 99 %	Roth	5470
Boric acid	≥ 99 %	Merck	100165
Calcium chloride*2H_2O	≥ 99 %	Merck	102382
Clerol FBA 265	n.a.	Cognis	n.a.
Cobalt(II) chloride·6H_2O	≥ 99.0 %	Merck	102539
Copper(II) chloride·2H_2O	≥ 99.0 %	Merck	102733
Ethanol	≥ 99.5 %	Merck	100986
Ethyl acetate	≥ 99.5 %	Roth	6784.4
D-Glucose·H_2O	≥ 98.5 %	Roth	6780
Glycerol	≥ 98.0 %	Roth	7530
2-heptanone	≥ 98.0 %	Merck	818711
n-hexane	≥ 98.0 %	Roth	7339
Iron(III) chloride·6H_2O	≥ 99.0 %	Merck	103943
IPTG	≥ 99.0 %	Roth	CN08
Potassium carbonate	≥ 99.5 %	Merck	104924
Kanamycin sulfate	n.a.	Roth	T832
Magnesium sulfate·7H_2O	≥ 99.5 %	Merck	105886
Manganese(II) chloride·4H_2O	≥ 99.0 %	Merck	105927
NADH-Na_2	≥ 98.0%	Roth	AE12
NAD^+	≥ 97.5 %	Roth	AE11
Nickel(II) chloride·6H_2O	≥ 98.0 %	Merck	106717
2-octanol	≥ 97.0 %	Sigma-Aldrich	O4504
R-2octanol	≥ 99.0 %	Sigma Aldrich	147990
S-2-octanol	≥ 99.0 %	Sigma Aldrich	147982
2-octanone	≥ 98.0 %	Roth	O4709
Pepton from casein	n.a.	Roth	8986.1
Monopotassium phosphate	≥ 99.0 %	Roth	3907
Dipotassium phosphat	≥ 99.0 %	Roth	P749

Table D.12: General chemicals (continued).

Chemical	Purity	Producer	Article number
2-propanol	≥ 99.5 %	Merck	818766
Sodium chlorid	≥ 99.5 %	Roth	3957
Sodium dodecylsulfat	≥ 85 %	Merck	817034
Sodium dihydrogenphosphate·H_2O	≥ 99.0 %	Merck	106346
Sodium formate	≥ 98.0 %	Fluka	71540
Sodium hydroxide	≥ 99.0 %	Roth	9356
Sodium molybdat-Dihydrat	≥ 99.5 %	Merck	106521
Sodium selenit	≥ 99.0 %	Sigma-Aldrich	214485
Sodium sulfate	≥ 99.0 %	Merck	822286
Yeast extract OHLY KAT	n.a.	Dt. Hefewerke	n.a.

n.a. = not applicable

Table D.13: Ionic liquids used (the signification of the abbreviations are given in Table A.3 and Table A.4).

Ionic liquid	Producer	Article number
[BMIM][NTF]	Merck	490092
[BMIM][PF6]	Merck	490050
[BMPL][FAP]	Merck	490084
[BMPL][NTF]	Merck	490046
[(E2OH)MIM][NTF]	Merck	490263
[(EOE)MMO][NTF]	Merck	490261
[(EO2E)MPL][FAP]	Merck	IOLI-JE-784
[(EO2E)MPL][NTF]	Merck	IOLI-JE-783
[EWTMG][FAP]	Merck	490129
[HMIM][FAP]	Merck	490078
[HMIM][NTF]	Merck	490031
[HMIM][PF6]	Merck	490065
[HMPL][NTF]	Merck	490100
[HPYR][NTF]	Merck	490124
[(MOE)MPL][FAP]	Merck	IOLI-JE-793
[(MOE)MPL][NTF]	Merck	IOLI-JE-313

Table D.13: Ionic liquids used (the signification of the abbreviations are given in Table A.3 and Table A.4)(continued).

Ionic liquid	Producer	Article number
[(MOP)MPI][NTF]	Merck	490265
[(NEMM)EO2E][FAP]	Merck	IOLI-JE-796
[(NEMM)EO2E][NTF]	Merck	IOLI-JE-782
[(NEMM)MOE][FAP]	Merck	IOLI-JE-772
[(NEMM)MOE][NTF]	Merck	490262
[(P3OH)PYR][NTF]	Merck	490264

E Buffers

Table E.14: Phosphate buffer used for the biotransformations: 0.5 M phosphate, 1 M formate, pH 6.5.

Component	Concentration, g L^{-1}
KH_2PO_4	38.8
K_2HPO_4	38.3
Sodium formate	69.4

Table E.15: Phosphate buffer used for the biotransformations: 0.5 M phosphate, 0.3 M formate, pH 6.5.

Component	Concentration, g L^{-1}
KH_2PO_4	38.8
K_2HPO_4	38.3
Sodium formate	20.8

Table E.16: Buffer used for the activity measurements of the LB ADH.

Component	Concentration, g L^{-1}
KH_2PO_4	5.29
K_2HPO_4	10.82

Table E.17: Buffer used for the activity measurements of the CB FDH.

Component	Concentration, g L^{-1}
KH_2PO_4	1.17
K_2HPO_4	16.1

Table E.18: Phosphate buffered saline (PBS).

Component	Concentration, g L^{-1}
KCl	0.2
KH_2PO_4	0.24
NaCl	8
Na_2HPO_4	1.15

F Culture media

The Agar plates used for the evaluation of the cell viability after incubation in various conditions were prepared as follows: all the components indicated in Table F.19 were combined and autoclaved, except for the antibiotic (Kanamycin). The antibiotic was added under sterile conditions once the autoclaved medium had cooled down sufficiently to avoid a degradation of the antibiotic. It was introduced through a sterile filter. Then, the Agar plates were poured, with a volume of ~ 15-20 mL per plate.

Table F.19: Medium for Agar plates (based on Luria broth).

Component	Concentration	
Peptone	10.0	g L^{-1}
Yeast extract	5.0	g L^{-1}
NaCl	5.0	g L^{-1}
Agar	12.0	g L^{-1}
Kanamycin	100	mg L^{-1}

For the culture media, the trace element solution, the magnesium sulfate solution and the phosphate buffer were prepared as concentrated stock solutions, autoclaved and added in the required amounts under sterile conditions to the other components of the culture medium. For the culture media and feed solutions, the carbon source was autoclaved separately and added to the rest of the components under sterile conditions. The antibiotic used (Kanamycin) was not autoclaved, but added through a sterile filter to the required concentration.

Table F.20: Phosphate buffer (25 x conc.).

Component	Concentration, g L^{-1}
KH_2PO_4	98.0
K_2HPO_4	93.5
NH_4Cl	134.0

Table F.21: Magnesium sulfate solution (500 x conc.).

Component	Concentration, g L^{-1}
$MgSO_4 \cdot 6H_2O$	247.7

Table F.22: Trace element solution (1000 x conc.).

Component	Concentration, g L^{-1}
$FeCl_3 \cdot 6H_2O$	13.653
$CaCl_2 \cdot 2H_2O$	2.466
$MnCl_2 \cdot 4H_2O$	1.999
$ZnSO_4 \cdot 7H_2O$	2.890
$CoCl_2 \cdot 6H_2O$	0.481
$CuCl_2 \cdot 2H_2O$	0.344
$NiCl_2 \cdot 6H_2O$	0.485
$Na_2MoO_4 \cdot 2H_2O$	0.486
Na_2SeO_3	0.349
H_3BO_3	0.124

Table F.23: Preculture medium (based on Luria broth).

Component	Concentration	
Peptone	10.0	g L^{-1}
Yeast extract	5.0	g L^{-1}
NaCl	5.0	g L^{-1}
Glucose	6.0	g L^{-1}
Phosphate buffer (25 x conc.)	20	mL L^{-1}
Kanamycin	100	mg L^{-1}

Table F.24: Culture: batch medium (based on Luria broth).

Component	Concentration	
Peptone	10.0	g L^{-1}
Yeast extract	5.0	g L^{-1}
NaCl	5.0	g L^{-1}
Glucose·$1H_2O$	6.0	g L^{-1}
Phosphate buffer (25 x conc.)	20.0	mL L^{-1}
Magnesium sulfate solution (500 x conc.)	5.0	mL L^{-1}
Trace element solution (1000 x conc.)	1.0	mL L^{-1}
Kanamycin	100	mg L^{-1}

Table F.25: Culture: glucose feed (based on Luria broth).

Component	Concentration	
Peptone	10.0	g L^{-1}
Yeast extract	20.0	g L^{-1}
NaCl	5.0	g L^{-1}
Glucose·$1H_2O$	400.0	g L^{-1}
Phosphate buffer (25 x conc.)	30.0	mL L^{-1}
Magnesium sulfate solution (500 x conc.)	10.0	mL L^{-1}
Trace element solution (1000 x conc.)	2.0	mL L^{-1}
Kanamycin	100	mg L^{-1}

Table F.26: Culture: glycerol feed (based on Luria broth).

Component	Concentration	
Peptone	10.0	g L^{-1}
Yeast extract	20.0	g L^{-1}
NaCl	5.0	g L^{-1}
Glycerol	400.0	g L^{-1}
Phosphate buffer (25 x conc.)	30.0	mL L^{-1}
Magnesium sulfate solution (500 x conc.)	10.0	mL L^{-1}
Trace element solution (1000 x conc.)	2.0	mL L^{-1}
Kanamycin	100	mg L^{-1}

G Specifications used for the modelling

In the conditions considered (Table 7.6), the aqueous phase constitutes the continuous phase, while the ionic liquid constitutes the dispersed phase. The subscript 'i' stands for either the substrate or the product. As both substances are considered equal in the estimation of the mass transfer coefficient, no distinction is necessary. The properties of 2-octanone were used. For the continuous phase, the properties of pure water were used.

Table G.27: Specifications used to estimate the mass transfer coefficient.

Symbol	Parameter	Value	Unit
a_x	specific cell membrane area of *E. coli*	23.7	m^2 g_{DCW} $^{-1}$
d_R	stirrer diameter	0.028	m
D_R	reactor diameter	0.06	m
d_{32}	Sauter diameter	54	μm
g	gravity	9.81	m s^2
MM_c	molecular weight of the continuous phase	18.016	g mol^{-1}
MV^c	molar volume of the continuous phase	18.9	cm^3 mol^{-1}
MV^i	molar volume of the diffusing substance (2-octanone)	185	cm^3 mol^{-1}

Table G.27: Specifications used to estimate the mass transfer coefficient (continued).

Symbol	Parameter	Value	Unit
N_R	stirrer speed	10	s^{-1}
T	temperature	303.15	K
V_{aq}	volume of the aqueous phase	0.00016	m^3
V_{IL}	volume of the ionic liquid	0.00004	m^3
v_x	specific cell volume of *E. coli*	$3.25 \cdot 10^{-3}$	L g_{DCW}^{-1}
η_c	dynamic viscosity of the buffer	2.48	mPa s
η_d	dynamic viscosity of the ionic liquid	54.23	mPa s
φ_d	volume fraction of the dispersed phase	0.2	-
Φ_c	association coefficient of the continuous phase	2.26	-
σ_c	surface tension the continuous phase	71.22	mN m^{-1}
$\sigma_{d,c}$	interfacial tension	12.78	mN m^{-1}
σ_i	surface tension of 2-octanone	25.96	mN m^{-1}
ρ_c	density of the buffer	997	kg m^{-3}
ρ_d	density of the ionic liquid	1340	kg m^{-3}

Table G.28: Intermediate parameters calculated on basis of the specifications in Table G.27.

Symbol	Parameter	Value	Unit
P_i	parachor of the diffusing substance (2-octanone)	417.59	cm^3 $g^{0.25}$ $s^{-0.5}$
P_c	parachor of the continuous phase	54.91	cm^3 $g^{0.25}$ $s^{-0.5}$
Vi	viscosity group	1.03	-
We	Weber number	171.26	-
$\bar{\eta}$	combined viscosity	4	Pa s
$\bar{\rho}$	combined density	1066	kg m^{-3}

H MATLAB code

MATLAB code used for the identification of the membrane permeability.

```
%% Data set

time =[0 300 600 1800 3600 10800 18000]';

exempCils = [0.2144 0.1500 0.1071 0.0342 0.0048 0.0011 0.0009
             0.3233 0.2489 0.2115 0.0891 0.0234 0.0051 0.0027
             0.3557 0.2857 0.2266 0.1069 0.0327 0.0041 0.0045
             0.3604 0.2628 0.1965 0.0692 0.0188 0.0032 0.0043
             0.3800 0.3188 0.2530 0.0559 0.0326 0.0039 0.0015
             0.7498 0.5399 0.3971 0.1347 0.0318 0.0124 0.0114
             0.6677 0.5448 0.4950 0.2969 0.0168 0.0159 0.0113
             0.4601 0.4160 0.3788 0.1774 0.1292 0.0260 0.0224
             0.2994 0.2762 0.2481 0.1583 0.0939 0.0182 0.01297]';

exempCilp = [0 0.0474 0.0852 0.1434 0.1766 0.1823 0.1774
             0 0.0450 0.1058 0.2193 0.2962 0.3271 0.3290
             0 0.0562 0.1068 0.2513 0.3199 0.3529 0.3343
             0 0.0729 0.1391 0.2738 0.3268 0.3412 0.3466
             0 0.0597 0.1001 0.1912 0.2844 0.3424 0.3812
             0 0.1339 0.2384 0.4383 0.6289 0.5933 0.6047
             0 0.0778 0.1584 0.3792 0.4946 0.6039 0.6003
             0 0.0496 0.0968 0.2127 0.3480 0.4371 0.4386
             0 0.0238 0.0537 0.1362 0.2414 0.3053 0.3169]';

exempX =[0   24.41 44.77 80.59 97.41 99.41 99.50
         0   15.56 33.78 71.49 92.83 98.49 99.19
         0   16.69 32.46 70.57 90.90 98.88 98.70
         0   22.05 41.93 80.13 94.66 99.09 98.78
         0   16.03 28.76 82.27 92.60 99.01 99.61
         0   27.55 46.72 80.77 95.38 98.78 98.22
         0   12.71 24.63 56.72 83.81 97.48 98.18
         0   10.77 20.55 46.78 73.15 94.44 95.19
         0   7.99 17.92 46.12 72.16 94.41 95.63]';

C =  [0.2144 0.3233 0.3557 0.36041 0.3800 0.7498 0.6677 0.4601  0.2994
      0      0      0      0       0      0      0      0       0
      0      0      0      0       0      0      0      0       0
      0      0      0      0       0      0      0      0       0 ];

%%  Solve and loop

SSEsave = 1000;
ii=10.^[-12:1/80:-0];
errM=zeros(length(ii));

for i = 1:length(ii)

    a=ii(i);
```

```
49      t  = 60*60*6;
50
51      %constants
52      Ds = 1229.30;
53      Ps = a;
54      vmax = 9.86188E-05;
55      KmA = 0.0063374;
56      KmB = 0.0057368;
57      KiA = 0.0011729;
58      Pp = a;
59      Dp = 171.67;
60      ax = 23.7;
61      Vx = 3.25E-03;
62
63      %reaction system specifications chosen
64      Cx = 50;
65      Vil = 0.04;
66      Vaq = 0.16;
67      Cnadh = 0.001;
68
69      %calculated parameters
70      mxtotal = Cx * Vaq;
71      axtotal = ax * mxtotal;
72      Vxtotal = Vx * Cx * Vaq;
73
74      %parameter vector
75      par = [Ds Ps vmax KmA KmB KiA Pp Dp Vxtotal Vil Vaq axtotal mxtotal Cnadh]';
76
77      %solve DE system
78
79      for k = 1:9
80
81          options=odeset('RelTol',1e-8,'AbsTol',1e-8);
82          [xaxis,Y]=ode15s(@(t,y) syseq_newall(t,y,par),time,C(:, k),options);
83
84          %conversion
85          Cils = Y(:,1);
86          Cilp = Y(:,4);
87          X = 100*(Vil*Y(:,4)+ Vaq* (Y(:,4)/Dp) + Vxtotal*Y(:,3))/(C(1,k)*Vil);
88
89          %compare real vs simulated
90          errorCilp = Cilp - exempCilp(:,k);
91          errorCilp2 = errorCilp.^2;
92          SSECilp = sum (errorCilp2);
93          errorCils = Cils - exempCils(:,k);
94          errorCils2 = errorCils.^2;
95          SSECils = sum (errorCils2);
96          SSE(k) = SSECilp + SSECils;
97
98      end
99
100     sumSSEk= sum(SSE);
101     errM(i) = sumSSEk;
102
```

```
103         if  sumSSEk < SSEsave
104             SSEsave = sumSSEk;
105             asave = a;
106             Xsave = X;
107             Ysave = Y;
108         end
109     end
110
111     Caqs = Ysave(:,1)/Ds;
112     Caqp = Ysave(:,4)/Dp;
113     asave
114     SSEsave
```

MATLAB code used for the simulation of varying reaction conditions.

```
1
2   %% experimental dat
3
4   time =[0 300 600 1800 3600 10800 18000]';
5
6   exempCils = [0.2144 0.1500 0.1071 0.0342 0.0048 0.0011 0.0009
7                0.3233 0.2489 0.2115 0.0891 0.0234 0.0051 0.0027
8                0.3557 0.2857 0.2266 0.1069 0.0327 0.0041 0.0045
9                0.3604 0.2628 0.1965 0.0692 0.0188 0.0032 0.0043
10               0.3800 0.3188 0.2530 0.0559 0.0326 0.0039 0.0015
11               0.7498 0.5399 0.3971 0.1347 0.0318 0.0124 0.0114
12               0.6677 0.5448 0.4950 0.2969 0.0168 0.0159 0.0113
13               0.4601 0.4160 0.3788 0.1774 0.1292 0.0260 0.0224
14               0.2994 0.2762 0.2481 0.1583 0.0939 0.0182 0.01297]';
15
16  exempCilp = [0 0.0474 0.0852 0.1434 0.1766 0.1823 0.1774
17               0 0.0450 0.1058 0.2193 0.2962 0.3271 0.3290
18               0 0.0562 0.1068 0.2513 0.3199 0.3529 0.3343
19               0 0.0729 0.1391 0.2738 0.3268 0.3412 0.3466
20               0 0.0597 0.1001 0.1912 0.2844 0.3424 0.3812
21               0 0.1339 0.2384 0.4383 0.6289 0.5933 0.6047
22               0 0.0778 0.1584 0.3792 0.4946 0.6039 0.6003
23               0 0.0496 0.0968 0.2127 0.3480 0.4371 0.4386
24               0 0.0238 0.0537 0.1362 0.2414 0.3053 0.3169]';
25
26  exempX =[0  24.41 44.77 80.59 97.41 99.41 99.50
27           0  15.56 33.78 71.49 92.83 98.49 99.19
28           0  16.69 32.46 70.57 90.90 98.88 98.70
29           0  22.05 41.93 80.13 94.66 99.09 98.78
30           0  16.03 28.76 82.27 92.60 99.01 99.61
31           0  27.55 46.72 80.77 95.38 98.78 98.22
32           0  12.71 24.63 56.72 83.81 97.48 98.18
33           0  10.77 20.55 46.78 73.15 94.44 95.19
34           0  7.99 17.92 46.12 72.16 94.41 95.63]';
35
```

```
C =  [0.2144  0.3233  0.3557  0.36041  0.3800  0.7498  0.6677  0.4601   0.2994
        0       0       0       0       0       0       0       0        0
        0       0       0       0       0       0       0       0        0
        0       0       0       0       0       0       0       0        0 ];

%% Reading of important parameters

t  = 60*60*6;

%constants
Ds = 1229.30;
Ps = 3.79473E-07;
vmax = 9.86188E-05;
KmA = 0.0063374;
KmB = 0.0057368;
KiA = 0.0011729;
Pp = 3.79473E-07;
Dp = 171.67;
ax = 23.7;
Vx = 3.25E-03;

%reaction system specifications chosen
Cx = 50;
Vil = 0.04;
Vaq = 0.16;
Cnadh = 0.001;

%calculated parameters
mxtotal = Cx * Vaq;
axtotal = ax * mxtotal;
Vxtotal = Vx * Cx * Vaq;

%parameter vector
par = [Ds Ps vmax KmA KmB KiA Pp Dp Vxtotal Vil Vaq axtotal mxtotal Cnadh]';


%% Solve DE system

for k = 1:9

    options=odeset('RelTol',1e-4,'AbsTol',1e-5);
    [xaxis,Y]=ode15s(@(t,y) syseq_newall(t,y,par),time, C(:, k),options);

    %% Conversion, Cils and Cilp
    Cils = Y(:,1);
    Cilp = Y(:,4);
    X = 100*(Vil*Y(:,4)+ Vaq* (Y(:,4)/Dp) + Vxtotal*Y(:,3))/(C(1,k)*Vil);
    Caqs = Y(:,1)/Ds;
    Caqp = Y(:,4)/Dp;

    %% Error
    errorCils = Cils - exempCils(:,k);
    errorCils2 = errorCils.^2;
    SSECils = sum (errorCils2);
```

```
90      errorCilp = Cilp - exempCilp(:,k);
91      errorCilp2 = errorCilp.^2;
92      SSECilp = sum (errorCilp2);
93      SSE(k) = SSECils + SSECilp;
94
95  end
96
97  sumSSEk= sum(SSE)
```

MATLAB code containing the system equations on which the identification and the simulation processes rely.

```
1   function dy = syseq_newall(t,y,p)
2   dy = zeros(4,1);
3
4   Ds       = p(1);
5   Ps       = p(2);
6   vmax     = p(3);
7   KmA      = p(4);
8   KmB      = p(5);
9   KiA      = p(6);
10  Pp       = p(7);
11  Dp       = p(8);
12  Vxtotal  = p(9);
13  Vil      = p(10);
14  Vaq      = p(11);
15  axtotal  = p(12);
16  mxtotal  = p(13);
17  Cnadh    = p(14);
18
19  J2 = Ps * (axtotal / Vxtotal) * 1000 * ((y(1)/Ds)-y(2));
20  J3 = (mxtotal/Vxtotal)*((vmax * Cnadh * y(2)) / ((KiA * KmB) + (KmB * Cnadh) + (KmA *
        y(2)) + (Cnadh * y(2)) ));
21  J4 = Pp * (axtotal / Vxtotal) * 1000 * (y(3)-(y(4)/Dp));
22
23  dy(1)= - J2 * (Vxtotal/(Vil + (Vaq/Ds)));
24  dy(2)= J2 - J3;
25  dy(3)= J3 - J4;
26  dy(4)= J4 * (Vxtotal/(Vil + (Vaq/Dp)));
```

I Recycling of the ionic liquid

After each process cycle, samples of ionic liquid were taken to verify the quality of the solvent, i.e. to verify if there had been degradation of the anion or the cation during the recycling process or if other substances were accumulating in the ionic liquid. The results of the analyses by ion chromatography can be found in Table 8.1 and Table 8.2. For the analyses by ^{1}H NMR, two spectra are exemplarily included below (Fig. I.1 and Fig. I.2).

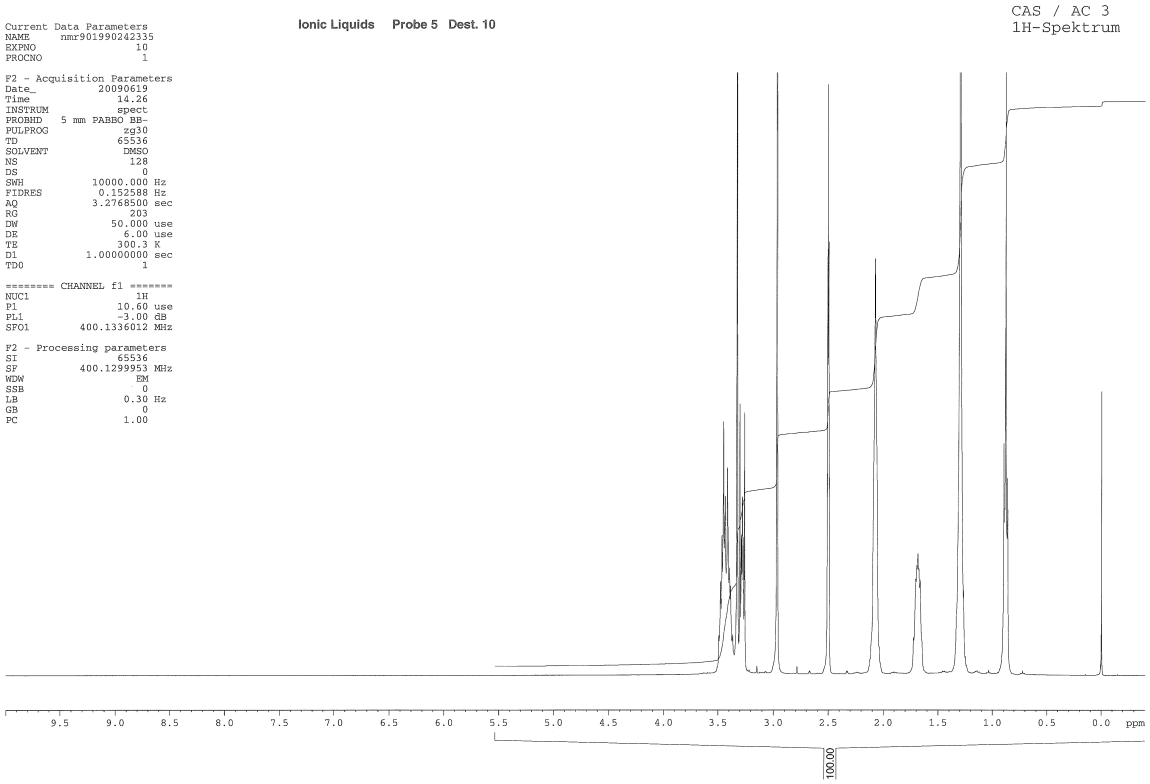

Figure I.1: ^{1}H NMR spectrum of the ionic liquid sample after process cycle number 10.

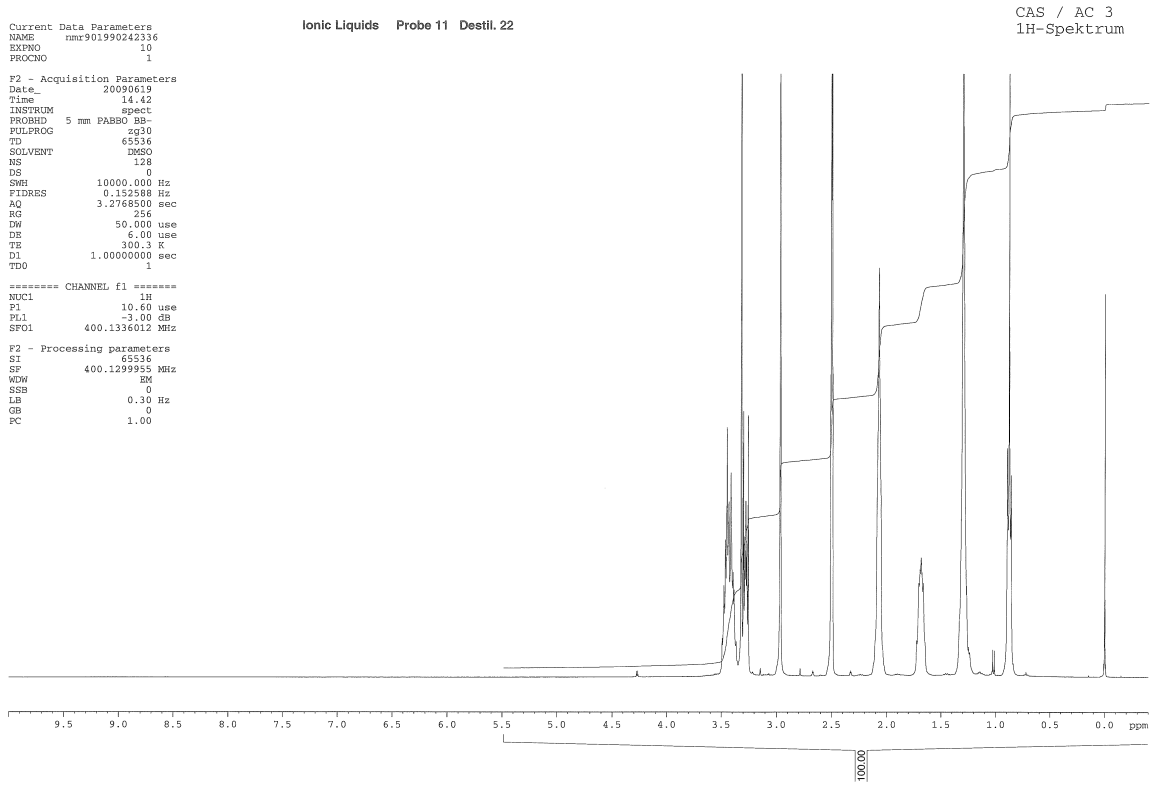

Figure I.2: ^{1}H NMR spectrum of the ionic liquid sample after process cycle number 22.